Adaptation of the South-Eastern drainage system under a changing climate

Groundwater and wetland modelling

Amin Gholami, Adrian D. Werner, Ehsan Kamali Maskooni, Hongxiang Fan, Amir Jazayeri, and Cristina Solórzano-Rivas

Goyder Institute for Water Research
Technical Report Series No. 25/4

www.goyderinstitute.org

Goyder Institute for Water Research Technical Report Series ISSN: 1839-2725

The Goyder Institute for Water Research is a research alliance between the South Australian Government through the Department for Environment and Water, CSIRO, Flinders University, the University of Adelaide and the University of South Australia. The Institute facilitates governments, industries, and leading researchers to collaboratively identify, develop and adopt innovative solutions for complex water management challenges to ensure a sustainable future.

This *Adaptation of the SE drainage system to a changing climate* project has been jointly funded by the Australian Government through the National Water Grid Fund, the Limestone Coast Landscape Board, and the South Australian Government. The project was delivered by the Goyder Institute for Water Research partners: CSIRO, the University of South Australia, Flinders University and the University of Adelaide in collaboration with the Limestone Coast Landscape Board, South Eastern Water Conservation and Drainage Board (SEWCD Board) and the Department for Environment and Water. This report was prepared by Amin Gholami, Adrian Werner, Ehsan Kamali Maskooni, Hongxiang Fan, Amir Jazayeri and Cristina Solórzano-Rivas.

Enquires should be addressed to: Goyder Institute for Water Research
The University of Adelaide (Manager)
209A, Level 2 Darling Building, North Terrace,
Adelaide, SA 5000
tel: (08) 8313 5020
e-mail: enquiries@goyderinstitute.org

Citation

Gholami A, Werner AD, Maskooni EK, Fan H, Jazayeri A, and Solórzano-Rivas C (2025) *Adaptation of the South-Eastern drainage system under a changing climate. Groundwater and wetland modelling*. Goyder Institute for Water Research Technical Report Series No. 25/6.

Disclaimer

Contents

Figures

Tables

First Nations Respect and Reconciliation

The Goyder Institute for Water Research and Limestone Coast Landscape Board, acknowledges the Traditional Custodians of the lands and waters of the Limestone Coast and South East region, where this project took place. Together we pay our respects to their Elders—past, present, and emerging—and recognise Aboriginal people as the First Peoples and Nations of South Australia, possessing and caring for these lands under their own laws and customs.

We respect the enduring cultural, spiritual, physical, and emotional connections that Aboriginal peoples maintain with their lands and waters. We recognise the diverse rights, interests, and obligations of First Nations and the deep cultural connections that exist between different First Nations communities. We seek to support their meaningful engagement and honour the continuation of their cultural heritage, economies, languages, and laws, which remain of ongoing importance.

We walk together with the First Nations of the South East and the Ngarrindjeri peoples through organisations such as Burrandies Aboriginal Corporation, Ngarrindjeri Aboriginal Corporation, the Ngarrindjeri Lands & Progress Aboriginal Corporation and South East Aboriginal Focus Group. For the work of generations past, and the benefit of generations future, we seek to be a voice for reconciliation in all that we do.

Project Summary

The Limestone Coast of South Australia is a highly modified landscape with an extensive cross-catchment drainage system converting what was once a wetland dominated landscape into one dominated by agricultural production. The region now has a diverse agricultural sector and extensive forestry plantations which are highly dependent on reliable rainfall and easy access to the region's substantial groundwater resources. However, as climatic conditions become hotter and drier it's important to understand impacts on ground and surface water resources and consequent risks to primary production and the environment to build a water secure future.

Achieving water security in the Limestone Coast region under a changing climate requires a more integrated and holistic approach to water resource management. In particular, the interactions between surface water and groundwater must be better understood, quantified, and managed to balance the seasonal demands—removing excess water from productive lands during winter while safeguarding groundwater-dependent agriculture and ecosystems during summer.

The "Adaptation of the South Eastern Drainage Network under a changing climate" project aims to inform opportunities to improve water management in the region - including potential use of water in the drainage network - to address risks to primary industries and groundwater dependent ecosystems. Delivered through the Goyder Institute for Water Research, research teams from the CSIRO, Flinders University and the University of South Australia have completed five separate but inter-connected tasks:

1. Quantifying the value of consumptive and non-consumptive uses of water
   This task assessed the value of additional water for key primary industries in the region, while also estimating the value of water for non-consumptive uses aimed at achieving ecological outcomes. Together, these valuations provide important context to the project's hydrological tasks, informing options to manage additional available water in the region.

2. Current and future water availability
   A water balance model for the region has been developed using the Bureau of Meteorology's Australian Water Resources Assessment – Landscape (AWRA-L) model. It integrates national and regional datasets to capture surface runoff, recharge, and soil moisture, while accounting for seasonal dynamics and regional variability. The model enables analysis of climate change impacts on the full water balance, providing insight into future water availability, supporting both short- and long-term water management decisions.

3. Groundwater and wetland modelling
   Site-specific models representing three-dimensional aquifer-wetland interactions have been developed for two key groundwater dependent sites. The models test the feasibility of changing the water distribution in the local landscape to improve ecosystem health and mitigate impacts of groundwater extraction. Options included redirecting / holding water back in drains, altering surface water inflows and reducing the extent of the wetland basin with levees. The learnings from modelling these two disparate sites will assist decisions to manage additional available water in the region.

4. Sea water intrusion risk
   The coastal area south of Mount Gambier is an area of high value irrigated agriculture and significant karst springs where the risk of seawater intrusion is of concern for both irrigators and environmental assets. This task set out to understand the extent and hydrodynamics of seawater intrusion in the region with an airborne electromagnetic survey of the south coast area, undertaken in October 2022, and construction of cross-sectional models to simulate seawater intrusion under different scenarios at different regional locations. This work provides the evidential basis to build on previous projects where reinstating wetlands by retaining water in drains appeared to effect some control over the seawater interface.

5. Groundwater, Ecology, Surface water and Wetland Assessment Tool (GESWAT)
   To enable opportunities to improve water management to be easily identified and investigated - including the potential use of water in the drainage network –a dynamic GIS tool (GESWAT) was built. GESWAT brings together outputs from the other project tasks integrating them in a tool with a range of other critical data (e.g. surface water flows, groundwater levels, and rainfall data, annual water use and allocation data, ecological information and other standard datasets). GESWAT provides the LC Landscape Board and its partner agencies a single platform with which to view, compare and interrogate the diversity of hydrological and ecological information available to inform policy and management decisions.

This report details results from Task 3 of the project.

Further results from this project are presented in the following reports:

Task 1

Cooper, C., Crase, L., Kandulu, J., and Subroy, V. (2025) *Adaptation of the South-Eastern drainage system under a changing climate – Quantifying the value of different water uses and future demands*. Goyder Institute for Water Research Technical Report Series No. 25/2

Task 2

Gibbs, M.S., Montazeri, M., Wang, B., Crosbie, R., Yang, A. (2025) *Adaptation of the South-Eastern drainage system under a changing climate - Water Availability for South East Drainage Adaptation*. Goyder Institute for Water Research Technical Report Series No. 25/3

Task 3

Gholami, A., Werner, A.D., Maskooni, E.K., Fan, H., Jazayeri, A., and Solórzano-Rivas, C. (2025) *Adaptation of the South-Eastern drainage system under a changing climate - Groundwater and wetland modelling*. Goyder Institute for Water Research Technical Report Series No. 25/4

Task 4

Davis A, Munday TJ, and Ibrahimi T (2025) *Adaptation of the South-Eastern drainage system under a changing climate - Limestone Coast Airborne Electromagnetic Survey: Acquisition, Processing and Modelling*. Goyder Institute for Water Research Technical Report Series No. 25/5.1

Davis A, Munday TJ, and Ibrahimi T (2025) *Adaptation of the South-Eastern drainage system under a changing climate - Limestone Coast Airborne Electromagnetic Survey: Conductivity-Depth Sections*. Goyder Institute for Water Research Technical Report Series No. 25/5.2

Gholami, A., Werner, A.D., Solórzano-Rivas, C., Jazayeri, A., Maskooni, E.K., and Fan, H. (2025) *Adaptation of the South-Eastern drainage system under a changing climate - Seawater intrusion risk*. Goyder Institute for Water Research Technical Report Series No. 25/5.3

Task 5

Gonzalez, D., Werner, A., Jazayeri, A., Pritchard, J., Fan, H., Botting, S., Judd, R. (2025) *Adaptation of the South-Eastern drainage system under a changing climate - Groundwater, Ecology, Surface water and Wetland Assessment Tool (GESWAT) Spatial Data Dictionary*. Goyder Institute for Water Research Technical Report Series No. 25/6

Executive Summary

This report describes the methodology and key findings of hydrological modelling undertaken as part of Task 3 (*Groundwater and wetland modelling*) of the Goyder project: *Adaptation of the South-Eastern drainage system under a changing climate*. The primary goal of this investigation is to develop and apply numerical models of two important ecohydrological systems, Bool Lagoon and the Limestone Coast Landscape Board's Karst Springs and Peat Fen restoration project ("Karst Springs Restoration site"), located in the South East of South Australia.

The models developed in this study are used to examine various intervention measures aimed at improving ecosystem health at the two sites, primarily through enhanced environmental water availability. Exchanges between surface systems and underlying aquifers are important to the hydrology of these regions, and therefore, models were designed to simulate both surface and subsurface water movements and the interdependencies thereof. This required novel surface water-groundwater interaction modelling techniques, and as such, a significant part of the current investigation is the development and refinement of a new workflow, which produced a modelling methodology for the simulation of wetland-aquifer interactions in the South East.

The modelling was preceded by an extensive literature review, which summarised the existing knowledge of conditions in the study area, as well as engineering methods for intervening in the hydrology of wetlands to improve ecological conditions. The results of that review, combined with discussions with the Limestone Coast Landscape Board, led to a series of potential remedial options that were considered in the design of scenarios, focussed on improving the hydrological conditions of two case study sites in the South East. The review of remedial measures and conditions in the study area informed the modelling workflow to explore potential engineering interventions.

The modelling methodology involved the extraction of sub-models from existing regional-scale three-dimensional (3D) groundwater flow models of the study area that were developed by the Department for Environment and Water (DEW) in 2023. The regional models that include Bool Lagoon and the Karst Springs Restoration site (near Deep Creek) within their study areas simulate the periods 1970–2021 and 1970–2022, respectively. Initially, the regional-scale models were converted from MODFLOW 2005 to a more recent version, MODFLOW 6. This allowed the advanced surface water modelling capabilities of MODFLOW 6 to be accessed, in addition to other MODFLOW upgrades, such as adaptive time-stepping. A comparison of groundwater levels between MODFLOW 2005 and MODFLOW 6 demonstrated adequate correlation between the two versions of MODFLOW, affirming the successful transition to MODFLOW 6. There were discrepancies between one of the *parent* models developed by DEW and the corresponding MODFLOW 6 model because the parent model used the Seawater Intrusion (SWI2) package of MODFLOW, whereas the MODFLOW 6 model did not. Justifications for those differences are offered.

Sub-models of the two target areas were then extracted from the MODFLOW 6 regional-scale models, which were derived from MODFLOW 2005 models developed by DEW. The use of sub-models reduced the spatial extent, lowering model run times and allowing for surface systems to be simulated with reasonable run times. Comparisons between the MODFLOW 6 sub-models and the *parent* MODFLOW 2005 regional-scale models validated the sub-model construction methodology.

The sub-models were subsequently augmented to simulate wetland hydrology, requiring a larger computational burden than the simulation of only groundwater flow. This explicit representation of wetlands is an advance on their implicit representation in the parent regional models, where the latter (implicit approach) is standard practice in the construction of regional-scale groundwater management models. Wetlands were simulated using the Lake package and the Water Mover package of MODFLOW 6. The Lake package allows for the dynamic simulation of surface water bodies, whereby surface water levels are affected by open-water evaporation, direct rainfall, groundwater inflows/outflows, stream inputs, and discharge to downstream surface water systems. The Lake package of MODFLOW 6 allows the water body to change in its spatial extent, depth and volume, including a complete drying out and rewetting of the surface water footprint. This is particularly critical for the simulation of wetlands in the study area. Each water body simulated by the Lake package has a uniform (horizontal) water surface elevation, and therefore, wetlands

were represented by multiple water bodies where spatial differences in the wetland water surface elevation are known to occur, as observed in field data.

The Water Mover package of MODFLOW 6 was applied to connect each surface water body (simulated with the Lake package), thereby treating wetlands as multiple, connected bodies of water and providing water surface differences between the upstream and downstream limits of these systems (where water level gradients in wetlands are known to exist). Other adjustments were needed to the sub-models to allow for the explicit simulation of wetlands, including parameterisation of the Lake package conductance, which controls the interaction between wetlands and the underlying aquifer. Direct rainfall and evaporation were also added to the model as inputs/outputs to/from wetlands. Inflows to Bool Lagoon from Mosquito Creek were added to the north-eastern end of the wetland, while inflows into the Karst Springs Restoration site from the Deep Creek Branch 1 Drain were included.

Of the two case studies, Bool Lagoon has an existing wetland whereas the Karst Springs Restoration model was developed to examine the proposed remediation of a drained wetland. Field measurements of wetland water levels and outflows to Drain M were available to assess the Bool Lagoon sub-model. Additionally, existing remote sensing data were compiled and analysed to evaluate the inundated area of Bool Lagoon during the period of simulation. High-resolution satellite images were collected from Digital Earth Australia (DEA) using the Water Observations from Space (WOfS) dataset and processed to allow for inundated and dry areas to be differentiated. Temporal variations in the Bool Lagoon inundated area from remote sensing data and from the MODFLOW 6 simulations were then compared, albeit without seeking quantitative measures of goodness-of-fit. Adjustments to MODFLOW 6 input parameters (outlet invert elevation, slope of the outlet channel, width of the outlet, and hydraulic conductivity and thickness of wetland sediments) were undertaken (manually), based on a subjective assessment of consistency, to improve the match between model outputs and observation data (surface water levels, groundwater heads, and outflow to Drain M).

The match between MODFLOW 6 and field data (remote sensing imagery, groundwater and surface water levels, and stream flow data from the downstream outflow) was found to be reasonable for Bool Lagoon. This builds confidence that the wetland hydrology has been approximately reproduced in the models. There are limited data available to assess the surface hydrology of the Karst Springs Restoration site, and we are simulating a new development where a wetland is being introduced, so it was not possible to undertake a model-field data comparison of surface conditions at that site. Although the model of Bool Lagoon was deemed to have adequately reproduced the measured hydrology of the region, the match to field data could be improved through additional comparisons and a more rigorous calibration methodology. For the Karst Springs Restoration site, we were able to reproduce the hydrogeological conditions of the regional model for only part of the model domain because of challenges in reproducing the heads of the SWI2 model. The lack of field data in areas where the models disagree makes it difficult to ascertain which of the errors in the original regional model and in our sub-model ought to be corrected through calibration.

Once a reasonable match between field data and MODFLOW 6 was achieved, several scenarios were tested to explore the potential for engineering modifications to increase the inundated areas and depths of Bool Lagoon. Scenario testing at Bool Lagoon focused on seven predictive scenarios aimed at exploring ecosystem health improvements through changes in water management practices. These included assessing the effects of inflow modifications, groundwater pumping restrictions, levee elevation adjustments, and downstream regulator modification. Specifically, the following scenarios were run: (a) testing a 20% increase or decrease in the discharge from Mosquito Creek to assess the impact of modified inflows; (b) modifying downstream gates to reduce flows into Drain M (i.e., a simple scenario was assessed whereby the outlet was effectively blocked); (c) reducing groundwater pumping around Bool Lagoon, using buffer zones of 2 km and 5 km in which groundwater pumping is halted; (d) increasing the elevation of the levee between the Main Basin (including Little Bool Lagoon) and the Central Basin (including Western Basin) by 0.20 m and 0.40 m.

The results showed that inflow modifications and groundwater pumping restrictions caused only small changes in groundwater heads and surface water levels in and around Bool Lagoon. The analysis of the influence of pumping neglected wells outside the model domain, which may affect wetland–aquifer interactions in ways that have not been assessed. Blocking the downstream regulator led to significant

increases in water levels, improved groundwater conditions, and an expansion of the area of inundation, demonstrating the importance of this structure. It should be recognised that blocking the downstream regulator of Bool Lagoon is not a realistic condition, because of the flood mitigation provision that Bool Lagoon provides.

An increase in the elevation of the levee separating the Main Basin (upstream of the levee) from the downstream Central Basin (including Western Basin) (by 0.20 m and 0.40 m) led to higher surface water levels in the Main Basin (including Little Bool Lagoon)—by up to 0.20 m and 0.40 m, respectively. The water levels of Hacks Lagoon, upstream of the Main Basin (including Little Bool Lagoon), also rose with the increased height of the levee between Main and Central Basins. Water levels in Hacks Lagoon increased during dry periods by up to 0.11 m and 0.20 m for the 0.20 m and 0.40 m levee elevation increase scenarios, respectively. Surprisingly, the increased levee elevation enhanced wetness in the Central Basin (including Western Basin) during dry conditions, with higher surface water levels by as much as 0.68 m and 1.12 m for the 0.20 m and 0.40 m levee elevation increases, respectively. This was a surprising outcome because it was anticipated that the levee would cause drier conditions downstream of it. The increase in the water levels of the Central Basin (including Western Basin) during dry periods is attributed to the rise in groundwater levels caused by the extra ponded water in the Main Basin (including Little Bool Lagoon), which, in turn, enhanced groundwater inputs into Central Basin (including Western Basin) during dry conditions. This is observed in the groundwater levels at ROB25, located in the Central Basin (including Western Basin), which rose by as much as 0.24 m and 0.38 m for the 0.20 m and 0.40 m levee elevation increase scenarios, respectively. Raising the levee produced surface water levels in the Central Basin that were lower during wet conditions, by up to 0.21 m for the 0.20 m levee elevation increase and 0.28 m for the 0.40 m levee elevation increase, as a consequence of the reduced outflows from Main Basin (including Little Bool Lagoon). The levees caused a reduction in the outflows to Drain M, by up to 1.52×10^5 m³/d and 4.74×10^5 m³/d for the 0.20 m and 0.40 m levee-rise scenarios, respectively.

For the wetland at the Karst Springs Restoration site, the scenarios were simpler. That is, different elevations of the outlet structure were tested to examine the resulting effects on surface water and groundwater levels in this area. This was examined in conjunction with the addition of levees to create ponded water over the region designated for rehabilitation. Additionally, we assessed the impact of modified inflows by testing a 20% decrease in discharge from Deep Creek and a 20% reduction in rainfall into the wetland, in lieu of advice on the impacts of climate change on inflow.

Altogether, six scenarios were conducted for the Karst Springs Restoration site to examine the hydrological effects of modifying the downstream control weir crest and reducing water inputs. Raising the weir crest from 2.0 m AHD to 2.5 m AHD significantly increased surface water levels, water volume, and the inundated area, whereas lowering the crest to 1.5 m AHD almost eliminated the wetland. In contrast, reductions in rainfall and inflows had minimal impacts on the wetland surface extent and no observable effects on groundwater heads. The outcomes showed that groundwater heads remained largely unchanged across all scenarios, highlighting the limited sensitivity of the groundwater system to these interventions.

We recommend undertaking additional simulations to further explore the potential to enhance the hydrology of the Bool Lagoon Complex, including: (a) levee construction scenarios in Bool Lagoon, such as modifications to the existing connection between Hacks Lagoon and Bool Lagoon, the construction of a levee through the middle of Bool Lagoon, and a third levee within the lower part of Bool Lagoon; (b) pumping of groundwater into Bool Lagoon; (c) implementation of Aquifer Storage and Recovery schemes; and (d) land-surface lowering scenarios. These scenarios may be undertaken as part of continuing research on this topic through PhD studies at Flinders University, with relevant outcomes to be described in subsequent short reports/memos to the Limestone Coast Landscape Board.

Acknowledgements

This Adaptation of the SE drainage system to a changing climate project has been jointly funded by the Australian Government through the National Water Grid Fund, the Limestone Coast Landscape Board, and the South Australian Government. The project was delivered by the Goyder Institute for Water Research partners: CSIRO, the University of South Australia, Flinders University and the University of Adelaide in collaboration with the Limestone Coast Landscape Board, South Eastern Water Conservation and Drainage Board (SEWCD Board) and the Department for Environment and Water.

The authors wish to express their gratitude to several individuals whose contributions have been invaluable to this project. Special thanks are extended to Sue Botting and Ryan Judd from the Limestone Coast Landscape Board for their many contributions to this work, including the provision of data, feedback on the methodology and reports, and a variety of other areas of assistance. We are also grateful for discussions with Peter Cook, who assisted in defining the scope of this work, and for Fiona Adamson's contributions to project management. Technical assistance from James Lassaline (Honours student) is also recognised.

1 Introduction

1.1 Background

The Limestone Coast of South Australia is a significantly altered landscape (Gehrig et al., 2015). Historically, wetlands occupied the interdunal swales and flats with up to 53% of the region submerged during winter and early spring in wet years (Holmes and Waterhouse, 1983). The construction of drainage channels, beginning in 1863, has altered the landscape, so that only about 6% of the original wetland area remain, of which 10% are regarded as intact (Gehrig et al., 2015). Nevertheless, the region hosts wetlands of international significance under the Ramsar Convention, including Bool and Hacks Lagoons, Piccaninnie Ponds, Lakes Albert and Alexandrina, and the Coorong. A long list of other wetlands in the Limestone Coast are classified as nationally significant according to the Directory of Important Wetlands in Australia (ANCA, 2001; Taylor, 2006). The majority of wetlands in the region (77% of wetlands and 96% of the total wetland area) are highly dependent on groundwater, which therefore plays a crucial role in maintaining the biodiversity of the Limestone Coast (SKM, 2009a).

The wetland ecosystems of the Limestone Coast face ongoing threats from declining groundwater levels, which are caused by combination effects of the extensive drainage network, groundwater extraction and other land-use activities that affect the hydrogeology of the region (Smith et al., 2015). Groundwater is the dominant source of freshwater for agriculture and urban water supply in the Limestone Coast (Mustafa et al., 2012), leading to considerable extraction. The fall in groundwater levels caused by this has changed the hydrology of most wetlands throughout the Limestone Coast substantially. Climate change is expected to exacerbate the decline in wetlands of the region (Gehrig et al., 2015). Projections indicate that a reduction of up to 42% (for the driest climate-change scenarios) in groundwater recharge may occur by 2050. This adds to water availability challenges for both ecosystems and agriculture (Crosbie et al., 2013).

1.2 Aims

The primary objective of this project is to apply numerical modelling to investigate management options to improve water availability for a selection of groundwater-dependent ecosystems in the Limestone Coast region. Various water management interventions and hydrological conditions are assessed in examining the availability of environmental water, with the principal aim of informing targeted strategies to protect the region's wetlands and groundwater-dependent ecosystems while balancing the use of groundwater resources for agriculture and other purposes. It is expected that the conclusions about intervention measures for the case studies adopted herein will inform the potential for intervention measures to improve wetland health in other parts of study area. The project also develops a modelling methodology for wetland investigation that can be applied to other examples where data are sufficient to parameterise the type of model that is applied here. This project draws extensively on the advice of partner investigators from the Limestone Coast Landscape Board who engaged with the research team in devising water management and modelling scenarios and assessing the results. These exchanges led to significant knowledge gains related to available data, potential methods for modifying management practices, and the research direction of the current study, which is constrained by the limits and capabilities of the models used to investigate the two field sites described herein.

The first objective of the current study was to review the physiography of the study area and possible methods for wetland remediation that might be considered in this project. Efforts to achieve this were provided by an extensive Literature Review, which is briefly summarised in the current report.

2 Literature review summary

Keddy (2010) defines a wetland as a distinct ecosystem that is flooded or saturated by water (fresh, brackish, or salt water), either permanently or seasonally. Wetlands provide crucial habitat for many important species of fauna and flora (Colvin et al., 2019). The wetlands that occur within modified landscapes are particularly susceptible to impacts from human activities, given their dependence on catchment hydrological processes and the associated discharge of water, nutrient and sediments from the surrounding landscape (Leibowitz et al., 2018). Wetlands also serve as buffers between developed areas (e.g., populated and agricultural areas) and natural ecosystems, and are commonly considered key indicators of regional ecosystem health (US EPA, 2021).

As wetlands occur under a wide range of hydro-geomorphological conditions, it is important to understand the key controlling factors in their behaviour in any attempt to improve their ecological functions. To this end, several wetland classification systems have been developed. For example, Brinson and Malvárez (2002) grouped wetlands into seven classes, including depressional, riverine, mineral soil wet flats, organic soil wet flats, estuarine (or tidal fringe), lacustrine (or lacustrine fringe), and slopes. They differentiate wetlands based on the geomorphic setting, dominant water source and the flow patterns within and surrounding the wetland. The US Fish and Wildlife Service use the Cowardin classification system FGDC (2013), which uses the wetland's landscape position, vegetation cover and hydrologic regime, producing five wetland types (marine, tidal, lacustrine, palustrine and riverine). In Australia, wetlands are classified based largely on the Ramsar Convention (DCCEEW, 2021a), leading to three categories of wetlands and 40 different wetland types. These depend on such factors as the water source and hydrological regime, vegetation, water characteristics (e.g., salinity), landscape position and geomorphology.

The main causes of wetland degradation across the globe are development pressures, invasive species, pollution, climate change, and changes to the natural flow regimes of catchments (Valnet Inc., 2022). DEH and DWLB (2003) identified the root causes, major threats, and management issues facing wetlands across South Australia, as: (a) Failure to value the functions, services and benefits of wetlands, primarily due to a lack of societal knowledge of wetlands, (b) Lack of baseline information and integration approaches, (c) Destruction of wetlands due to the conversion to alternative uses (most commonly due to landscape drainage or reclamation), (d) Changes to water regimes (e.g., drainage schemes, groundwater extraction, river diversions, etc.), (e) Introduced plant and animal species, (f) Pollution impacts, (g) Inappropriate land use practices, (h) Salinity, and (i) Over-exploitation of wetland resources (e.g., recreational activities, aquaculture, etc.).

Substantial wetland losses have occurred in the study area (Limestone Coast of South Australia). According to DEH and DWLB (2003), less than 2% of the permanent wetlands and 8% of the temporary wetlands that occurred at the time of European settlement remain in the region. The main cause is thought to be reductions in flooding events (i.e. flood extent and duration) due to the large-scale drainage scheme that redirects water to the sea (DEH and DWLB, 2003). The remaining wetlands in the Limestone Coast are located primarily within grazing regions (64%), with 4% in cropping regions, 16% in forestry areas, and 4.5% in conservation and native forest reserves. Other wetlands (11.5%) occur within non-agricultural private land, urban areas, golf courses, industrial land, and other crown lands (GSA, 2000). The variety of wetland types and settings leads to a wide range of threats to wetland extent and condition in the Limestone Coast, including (GSA, 2000): (a) Changes in water availability, (b) Physical disturbance, including direct drainage and conversion to other land uses, (c) Interception of local flows, (d) Changes in the salinity regime, (e) Increasing nutrients, (f) Loss of species (plants and animals), (g) Loss of connectivity to other ecosystems, (h) Climate change and reduced rainfall, and (i) Aquatic pest plants and animals.

There are two forms of interventions described in the literature for improving wetland ecosystem conditions (MBWSR, 2019): (a) Engineering design and construction, and (b) Natural system enhancements. Perhaps the most common form of engineering interventions adopted in wetland restoration are related to the modification of drainage systems. These include:

(a) Surface drainage systems (drains, channels, levees, etc.): Installation, modification and/or removal of surface drainage systems may target the cross-sectional area, grade, vegetation conditions,

inlet/outlet controls, pumping infrastructure (e.g., lift stations), in-channel structures, and drain-groundwater connectivity.

(b) Subsurface drainage schemes: Most common are tile-drain schemes, which can be manipulated to control near-surface groundwater conditions. Tile drains are perforated pipes (typically made of clay, concrete, or plastic) installed below the ground to collect and convey excess water away from agricultural or wetland areas. These systems have the potential to lower the water table, which may prevent natural groundwater flow from reaching wetlands. Therefore, the removal of tile drains in the Limestone Coast may allow wetlands to receive higher groundwater inflow rates, or the discharge from any existing tile drains may perhaps be redirected to serve as inputs to adjacent wetlands (MGA, 2018).

(c) Wetland geomorphological changes: These include the construction of levees and outlet structures to direct and control hydrologic outflows and to capture inflows (e.g., from springs, overland flow, flooding events, etc.). Excavation of wetland soils is also common to remove accumulated sediment in the wetland, to enhance wetland depths, amongst various other restoration purposes (e.g., removing undesired vegetation or contaminated soil, etc.).

The natural enhancement of wetlands most commonly targets plant communities, aimed at maximising habitat benefits for native wildlife species, improving water quality and soil conditions, and increasing the diversity of flora and combatting invasive species. This is achieved by maximising the use of native seedbanks and controlling wetland weed species, while accounting local conditions.

3 Overview of the study area

This section provides a brief overview of key hydrogeological features of the Lower Limestone Coast region. We focus on aspects of relevance to wetland-aquifer interaction and the construction of wetland-aquifer models, notwithstanding that the model parameters adopted in this project were taken almost exclusively from the regional models upon which they were based. Brief descriptions of the target sites for wetland-aquifer interaction modelling are also provided.

3.1 Geology

The Lower Limestone Coast is underlain by the Gambier Embayment (GE), which is the most westerly embayment of the Otway Basin. The GE is bounded in the north by the Padthaway Ridge and in the east by the Dundas Plateau, as shown in Figure 1. Cobb and Barnett (1994) indicate that the GE is bounded in the north east by the Kanawinka Monocline, although a more recent investigation by Lawson et al. (2009) concluded that the northern boundary of the GE lies approximately along the Kingston-to-Naracoorte line, associated with a magnetic high located between Lucindale and Struan (Lawson et al., 2009). The GE extends offshore to the Continental Shelf (Barnett et al., 2015; Knight et al., 2019).

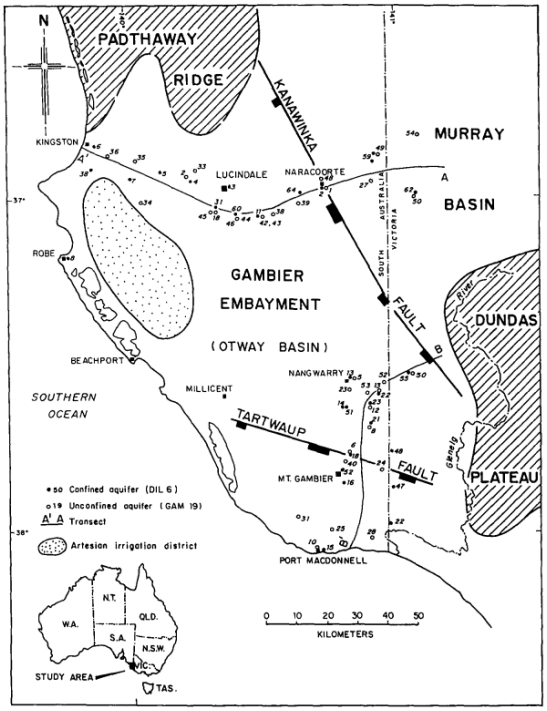

Figure 1. Location of the Gambier Embayment (taken from Love et al., 1993).

The sedimentation of the GE commenced in the Palaeocene to Early Eocene, forming the Wangerrip Group, which contains the Pember Mudstone and the Dilwyn Formation (Barnett et al., 2015). The latter includes the Tertiary Confined Sands Aquifer and the Dilwyn Clay aquitard. Marine influences increased in the Middle to Late Eocene periods, during which the Mepunga Formation and Narrawaturk Marl were deposited (Barnett et al., 2015). The Gambier Limestone, which forms part of the regional unconfined aquifer, is part of the marine Heytesbury Group, which formed in the Late Eocene to Middle Miocene.

Volcanic activity during the Pleistocene epoch led to remnant volcanic cores of Mt Gambier, Mt Shank and Mt Burr (Barnett et al., 2015). Eustatic sea level changes caused marine transgressions as far inland as the Kanawinka Fault and the reworking of sediments during the Pleistocene. Interglacial periods during the

Pleistocene led to the formation of the Bridgewater Formation, which consists of aeolian calcarenite deposited as coastal dunes (Brown and Stephenson, 1991). These formed in strand lines sub-parallel to the coastline (Barnett e al., 2015) that are evident in the modern topography. Inter-dunal areas filled with shallow marine limestone of the Padthaway Formation, which occur on top of the karstic Gambier Limestone and, with the Bridgewater Formation, add to the regional unconfined aquifer system (Barnett et al., 2015).

Groundwater flow within GE aquifers is influenced by significant structural features, including the northwest-trending Kanawinka Fault and the south-trending Tartwaup Fault (Figure 1).

3.2 Hydrogeology

Previous hydrogeological investigations of the study area have subdivided the stratigraphic units into two primary groundwater flow systems: (1) Tertiary Confined Sand Aquifer (TCSA), and (2) Tertiary Limestone Aquifer (TLA). Both systems were deposited in the Cainozoic period (66 mya to present), and contain a mixture of fresh and saline groundwaters. The TCSA and the TLA are separated by the Upper Tertiary Aquitard (UTA). Morgan et al. (2015) tabulated the known hydraulic properties of the TSCA, the TLA and the UTA.

The TCSA consists primarily of Dilwyn sand and clay units, generally increasing in thickness (up to 800 m south of Mt Gambier) towards the south. The TCSA wedges out near the Padthaway Ridge and the Dundas Plateau. It comprises multiple sub-aquifers, although it is treated as a single unit for management purposes. Most wells only penetrate the uppermost sand unit. The occurrence and extensiveness of clay layers increases towards the south (Barnett et al., 2015).

The unconfined TLA aquifers encompasses the Tertiary Gambier and Murray Group Limestones, as well as the overlaying Quaternary Padthaway and Bridgewater Formations. It varies in thickness from being absent to 300 m (Barnett et al., 2015). Groundwater flow occurs mainly in the secondary porosity caused by karstification, leading to highly variable aquifer properties. Despite the karstic nature of the TLA, it is believed that karst features do not form a significant interconnected system of conduits, and rather, groundwater flow behaviour is more comparable to intergranular flow processes (Barnett et al., 2015; Herczeg et al., 1997).

Although the UTA is thought to be a regionally extensive sequence, Harrington and Lamontagne (2013) identified several areas where leakage occurs between the TLA and TCSA. These include the Nangwarry/Tarpeena region, a location south of Strathdownie (approximately 33 km northeast of Mount Gambier), and the Lake Mundi area (approximately 21 km east of Nangwarry). Love et al. (1993) and Harrington et al. (1999) also interpreted significant upward and downward leakage between the TLA and the TCSA at various other locations.

3.3 Wetlands

The Limestone Coast region has over 17,000 mapped wetlands, most of which have been substantially altered due to the conversion of their natural state for grazing, cropping or forestry, and because of changes to their hydrology from drainage, groundwater decline, and reduced rainfall. The wetlands of the Limestone Coast vary widely in size, depth, permanence, water source, salinity and connectivity with other hydrological features of the landscape. Although Fass and Cook (2005) concluded that groundwater input is generally low in terms of the overall water balance of Limestone Coast wetlands, Cook et al. (2008) found that groundwater inputs to Honan's Wetland, some 16 km west-north-west of Mount Gambier, could be highly variable over space and time. Other studies have shown a wide range of groundwater dependency in Limestone Coast wetlands (e.g., Harding and O'Connor, 2012; Keppel et al., 2017; Smith et al., 2015).

Figure 2 shows the wetlands of the Limestone Coast categorised according to the groundwater dependence, as reported by Morgan et al. (2015) from their review of information on the South Australian Wetland Inventory Database. The dependency of wetlands on groundwater depicted in Figure 2 was based on a comparison of the wetland topography versus regional groundwater heads. However, a subsequent analysis

of wetland connectivity by Taylor et al. (2015) and others found that the presence or absence of clogging layers (i.e., low-hydraulic conductivity layers) plays a major role in wetland-aquifer connectivity in the Limestone Coast. Additionally, several wetlands are known to depend on the discharge of springs from the underlying limestone aquifers, including Piccaninnie Ponds, Ewens Ponds and the Karst Springs Restoration site, which are described by Harrington and Lamontagne (2013).

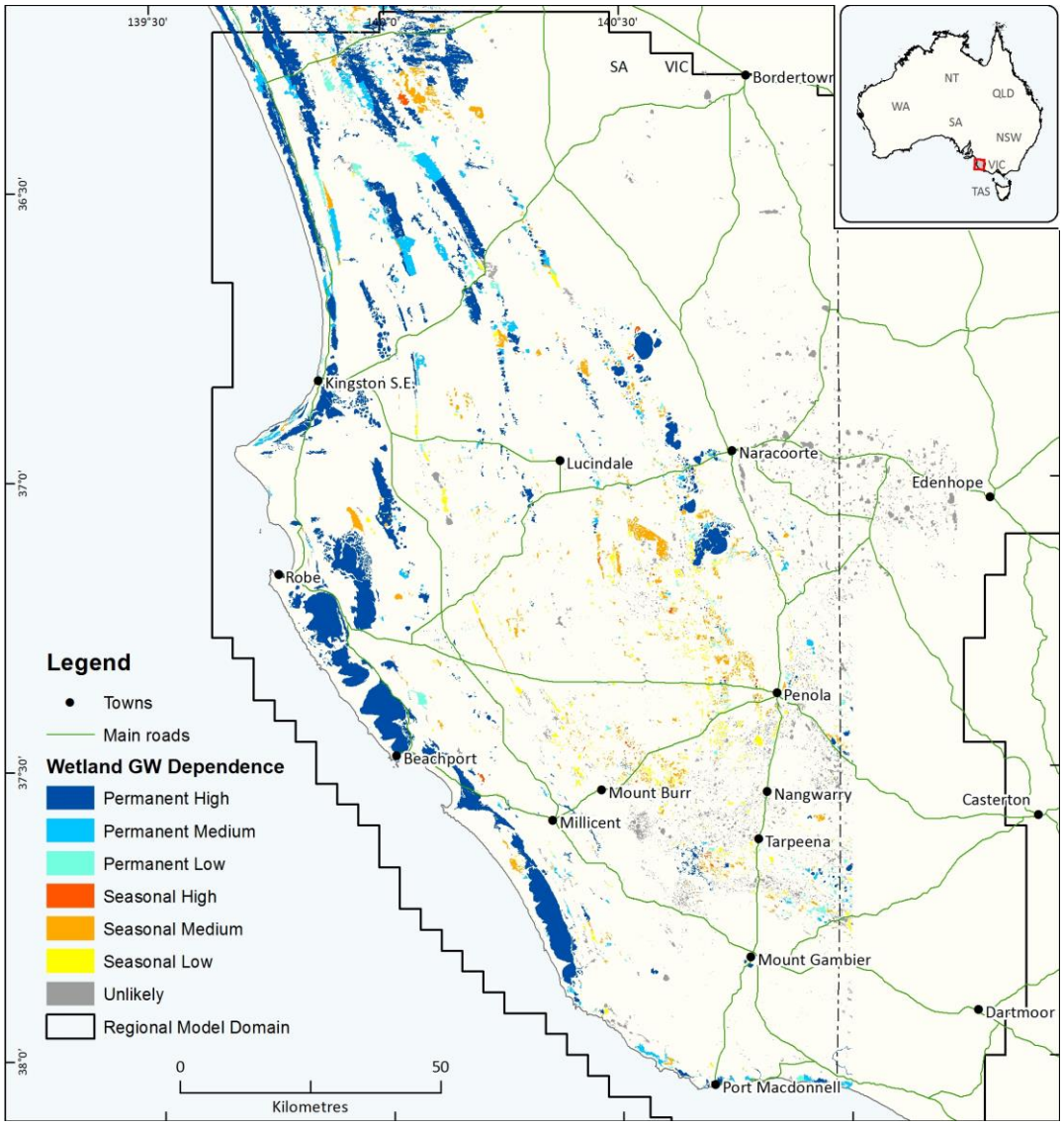

Figure 2. Wetlands in the South East of South Australia, showing groundwater dependence (taken from Morgan et al., 2015).

3.4 Case study sites

Following a series of interactions with research partners at the Limestone Coast Landscape Board, two sites (Bool Lagoon and the Karst Springs Restoration site) were selected for targeted wetland-aquifer interaction modelling, aimed at assessing various engineering strategies for improving the conditions of wetlands in those areas. The former is a renowned Ramsar-listed ecosystem while the latter is a proposed site for wetland rehabilitation. The two sites require different types of guidance from the current modelling investigation, in terms of wetland-groundwater interactions and the effects of potential engineering modifications on the hydrology of the respective systems. Figure 3 provides a locality map for the two sites.

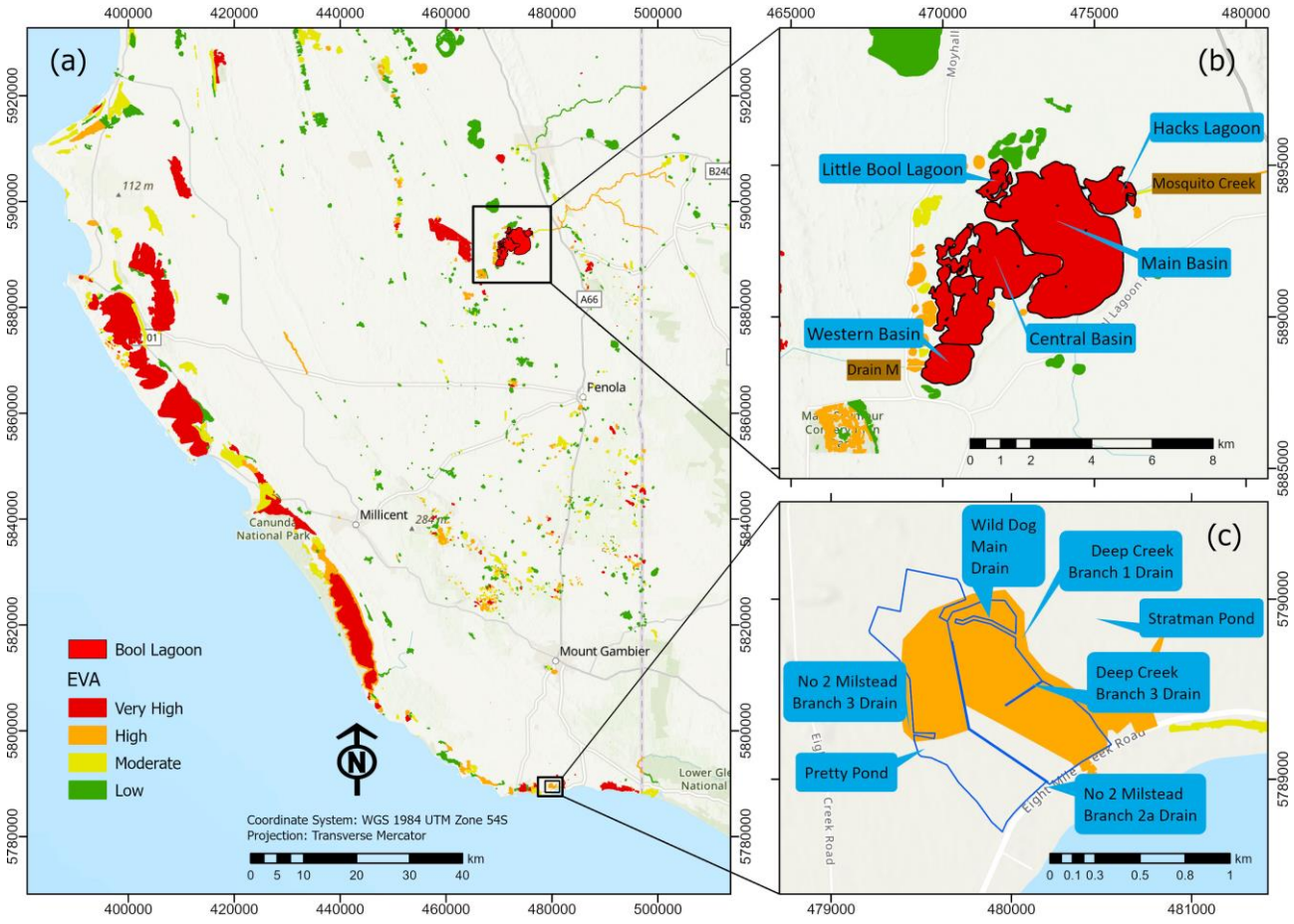

Figure 3. (a) Locality map for two wetland sites in the Lower Limestone Coast of South Australia, showing wetlands with EVA (Environmental Value Assessment) scores ranging from "Low" to "Very high", according to Taylor (2006). (b) Close-up of Bool Lagoon, with five sub-basins identified. (c) Close-up of the proposed wetland in the Karst Springs Restoration area, where the blue region is the proposed wetland extent and the orange area reflects the original wetland boundary impacted by drainage, which corresponds to a zone of High EVA.

3.4.1 Bool and Hacks Lagoons

Bool Lagoon is situated approximately 77 km north of Mount Gambier, while Hacks Lagoon is immediately upstream (to the north east) of Bool Lagoon (Figure 3). Bool and Hacks Lagoons (referred to as the "Bool Lagoon Complex" in the remainder; Brownlow, 1997) together provide important seasonal wetland habitat to a wide range of threatened species. For example, the Bool Lagoon Complex includes a wide variety of aquatic and semi-aquatic vegetation, including floating-leaved species, reeds, sedges, tussock vegetation, tall shrubland and native grasses of high conservation value (DEH, 2006). The ecosystem provides habitat for 22 species of internationally important migratory birds, as well as vulnerable fish, the Striped Legless Lizard and the Southern Bell Frog (DEH, 2006). For this reason, the Bool Lagoon complex has been designated a Ramsar site that is arguably the most renowned system of its type in South Australia, and is considered an important remnant wetland within a region that is otherwise highly modified (DEH, 2006).

The Bool Lagoon complex is located on an interdunal flat, in a landscape characterised by lunettes, which are crescent-shaped ridges that form on the leeward side of shallow lakes and depressions (DEH, 2006). Brownlow (1997) described the Bool Lagoon Complex as four interlinked basins, as: Hacks Lagoon, Main Basin, Central Basin and Western Basin (Figure 3b). Others additionally recognise "Little Bool", a wetland located to the immediate north west of the Main Basin (Figure 3b), as part of the Bool Lagoon Complex (LCLB, 2021). When full, the inundated area of the Bool Lagoon Complex is around 2,530 ha (DEH, 2006), and the

depth is 1.6–2.1 m (Brownlow, 1997), although Nitschke (1984) recommended limiting the water level depth to 0.8 m to avoid inundating bird breeding areas.

The temperate climate of Bool and Hacks Lagoons causes strong seasonality, with annual average rainfall of 550–600 mm and annual potential evaporation of 1400 mm (DEH, 2006). Stream inputs occur into Hacks Lagoon from the north via Mosquito Creek (Figure 3b), which has a catchment area of about 1215 km^2 that is mostly located in Victoria (Heneker, 2006). Hacks Lagoon flows into Bool Lagoon, which discharges in the south to Drain M via a regulator. Prior to European settlement, Hacks and Bool Lagoons were part of the Mosquito Creek floodplain (LCLB, 2021). Hacks Lagoon previously discharged to the north into the waterway that now becomes Drain E, which flows NNE to Jip Jip Waterhole near Marcollat, after receiving inflows also from Naracoorte Creek, which is north of the Bool Lagoon Complex (Heneker, 2006; DEH, 2006). In the early 1960s, Bool Lagoon's potential to mitigate Mosquito Creek floods was recognised, regulator gates and flood levees were added, and flood waters ponded in the lagoons for the first time in 1968. Mosquito Creek discharge, directed into the Bool Lagoon Complex via Hacks Lagoon, is stored within the Bool Lagoon Complex to levels that are controlled through the operation of a regulator gate connected to Drain M, in the south (3b) (Brownlow, 1997). Hacks Lagoon is a semi-permanent wetland that discharges through a spillway installed between Bool Lagoon and Hacks Lagoon, and is influenced by the manipulation of Bool Lagoon water levels via the outlet regulator, albeit depending on the inputs from Mosquito Creek. Bool Lagoon remains a seasonal water body (LCLB, 2021).

Declines in both the base flow and mean flow of Mosquito Creek threaten the current hydrological regime of the Bool Lagoon Complex (SAVBGARC, 2023). Mosquito Creek had permanent flows from 1971 to 2001, but has since become seasonal (SENRMB, 2019). These declines are linked to lower groundwater level in the Mosquito Creek catchment (SAVBGARC, 2023).

The Bool Lagoon Complex is considered a groundwater-dependent ecosystem, although wetland-groundwater interactions are spatially and temporally variable, creating complex hydrogeological relationships. DEH (2006) showed that groundwater level fluctuations create gaining (inflows from groundwater into the Bool Lagoon Complex) and losing (losses to groundwater) conditions during the year, subject to the seasonality of groundwater inputs. A transect of monitoring sites across Bool Lagoon Complex by DEH (2006) showed inflows from groundwater on the eastern side, and losses to groundwater in the west, indicating that the system is potentially a flow-through wetland. Turnadge and Lamontagne (2015) subsequently treated Bool Lagoon as a flow-through system in their cross-sectional modelling to examine wetland-groundwater interactions. DEH (2006) conclude that the characteristics of Mosquito Creek inputs and groundwater-surface water interactions are critical factors in the floristic composition and habitat diversity of Bool Lagoon.

Groundwater-wetland interactions are influenced by a clogging layer of clay present within the bed sediments of the Bool Lagoon Complex that was assessed through field testing by Taylor et al. (2015). DEH (2006) describes the bed sediments as black, poorly drained organic soils with a high pH. The mean saturated hydraulic conductivity of the wetland clogging layer was found to be 0.227 m/d from the testing of 15 samples distributed across the wetland using an Eijkelkamp soil water permeameter. Lithological logging indicated that the clogging layer has a mean thickness of ~8 m, although Turnadge and Lamontagne (2015) used a clogging layer thickness of 1 m in their analysis of the hydrology of Bool Lagoon. The value of the clogging layer thickness used in the current models is described in Section 4.4.1. The thickness of the clogging layer is used in the simulation to determine the lakebed leakance parameters, which control rates of surface water-groundwater interactions along with groundwater-wetland water level differences (Langevin et al., 2017).

3.4.2 Proposed Karst Springs Restoration site

The proposed wetland in the Karst Springs Restoration area (the site is associated with Deep Creek, to the west of Eight Mile Creek) is approximately 22 km south of Mount Gambier (Figure 3). Deep Creek borders the eastern margin, the Wild Dog Drain occurs at the northern border of the site, while the No 2 Milstead Branch 3 Drain occurs at the western boundary (Figure 3c). An ecological survey of Deep Creek found Variegated Pygmy Perch, Spotted Galaxias, and River Blackfish (Hammer et al. 2009), although in low

abundance. Hammer et al. (2009) recommend riparian habitat restoration of Deep Creek to conserve other threatened and endangered species, such as the Australian Grayling.

DEW (2024) produced depth-volume relationships for the proposed wetland area, which they subdivided into eastern and western halves. They determined that the average stream flow in Deep Creek during 1970–1991 was ~67 ML/d, which has fallen to 57 ML/d (on average) during 2004–2023. DEW (2021) suggest that Deep Creek has shown stronger seasonality in flow since 2005, similar to groundwater level trends, which have shown declines of up to 4 m since the 1970s within the wider region south of Mount Gambier (DEW, 2021). The soil conditions of the site are similar to other parts of the coastal Limestone Coast of South Australia, which are dominated by calcareous sands and peat soils overlying the limestone deposits of the TLA (e.g., Bachmann et al., 2015).

The average rainfall at the study area is around 730 mm/y (1970–2022; the period of the model simulation), and the mean potential evapotranspiration is approximately 1317 mm/y (1970–2022). Deep Creek is fed by a spring (Stratman Pond) that has relatively stable salinities (760–910 μS/cm) (DEW, 2021). Deep Creek previously flowed east, behind the coastal dunes of Riddoch Bay, to connect with Eight Mile Creek near the mouth (Slater and Farrington, 2010). However, through drainage works for land productivity, Deep Creek now discharges directly to the sea.

4 Methods

4.1 Overview

The methodology of the current study aims to develop localised models of two important wetland sites within the Limestone Coast: the Bool Lagoon Complex and the Karst Springs Restoration site (near Deep Creek). The former is an important Ramsar site, while the latter is an area where increased inundation is proposed through engineering modifications with the aim of reinstating wetland conditions to a former agricultural site. These two sites were selected through consultation with team members from the Limestone Coast Landscape Board.

The two localised models or *sub-models* of the Bool Lagoon Complex and the Karst Springs Restoration site were based on two existing, sub-regional models developed by the Department of Environment and Water (DEW, 2023a, 2023b). The groundwater parameters of the sub-models were based almost exclusively on the models of DEW (2023a, 2023b). The methodology adopted here has not been applied previously to wetland simulation in Australia, to the author's knowledge. Thus, the techniques described below needed to be developed and tested for the purposes of this investigation. This involved considerable trial and error and extensive analysis to assess the validity of each phase of the workflow, which represents a novel approach to wetland analysis. A summary of the methodology is provided in Table 1.

Table 1. Overview of modelling methodology for wetland simulation.

Step	Description
1	Obtain existing groundwater flow models of the study area (DEW, 2023a, 2023b). Validate model input files by re-running relevant models and comparing results to those provided in accompanying reports.
2	Convert the input files of existing models into Python scripts.
3	Convert existing models from MODFLOW 2005 to MODFLOW 6.
4	Extract sub-models from existing models using Python.
5	Run the Bool Lagoon Complex and the Karst Springs Restoration sub-models for the transient cases of the existing (*parent*) models and compare results to the parent models to validate the method of sub-model construction.
6	Add the Lake package of MODFLOW 6 to the sub-models, run the sub-models, and compare the results to available field data. This was undertaken only for the Bool Lagoon Complex sub-model, because the Karst Springs Restoration sub-model does not simulate historical wetland behaviour.
7	Modify the Lake package of the sub-models to have multiple "Lakes" and add the Water Mover Package to move water between lakes.
8	Run the model and compare the results to the available data (Bool Lagoon Complex model only).
9	Undertake sensitivity analysis of wetland-aquifer connectivity.
10	Run models for various Bool Lagoon scenarios, including changes in discharge, levee construction, adjustments to downstream gates, reduction of groundwater pumping, and land-surface lowering.
11	Run models of various Karst Springs Restoration scenarios, focussing on the elevation of the outlet structure.
12	Make interpretations, draw conclusions and complete reporting.

4.2 Summary of existing models

Here, we summarise the two existing models that were used to extract wetland-aquifer sub-models. The two existing models are: (a) the mid-south east sub-regional model (DEW, 2023a) (see Figure 3b), and (b) the coastal areas south sub-regional model (DEW, 2023b) (see Figure 3c). These were used to build wetland-aquifer sub-models of the Bool Lagoon Complex and the Karst Springs Restoration site, respectively.

4.2.1 Mid-south east sub-regional model

The mid-south east sub-regional model (DEW, 2023a) was constructed in MODFLOW 2005 using the Groundwater Vistas graphical user interface. The model comprises one layer, representing the TLA (described in Section 3.2). The horizontal extent is about 100 km east-west by 70 km north-south (model-corner coordinates are E433507 N5842369; GDA 2020 MGA Zone 54), discretised into square cells of side dimension 100 m (DEW, 2023a). No-flow boundaries have been placed along the northern and southern parts of the model domain, while a general-head boundary is used in the west and part of the eastern edge of the model. Figure 4 illustrates the existing sub-regional model and the extracted sub-model that was subsequently adapted for wetland-aquifer simulation.

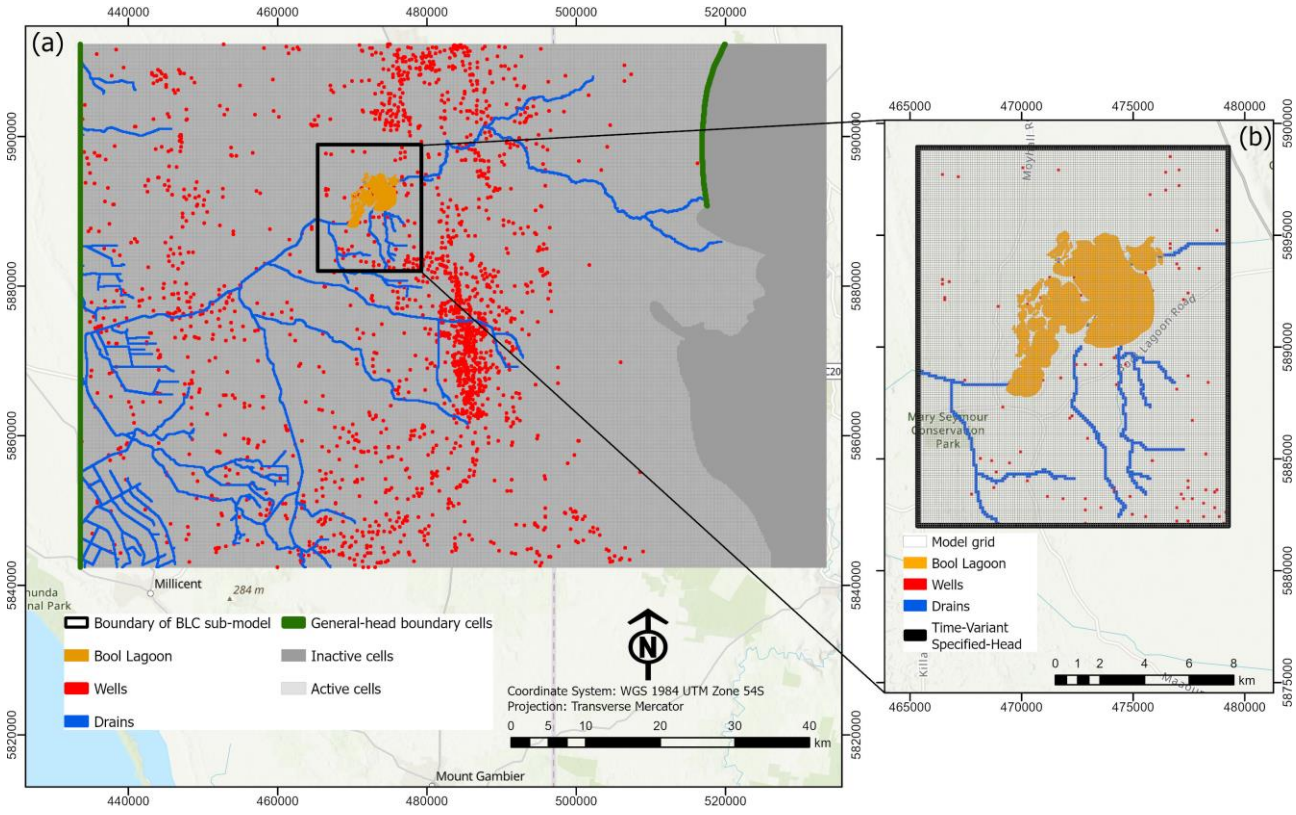

Figure 4. (a) The mid-south east sub-regional model (DEW, 2023a), and (b) the Bool Lagoon Complex (BLC) sub-model.

The top of the sub-regional model (land surface) was derived from a regional LiDAR digital elevation model (DEW, 2020), ranging from 12 m AHD in the western plains to 212 m AHD in the elevated eastern areas. The base of the model (the TLA bottom) was determined from drillhole data and the hydrostratigraphic model of Barnett et al. (2015), with elevations ranging from −248 m AHD in the central and western part of the domain to 75 m AHD in the uplifted east.

The transient period of simulation (1 Aug 1970 to 31 Jan 2021) was discretised into 202 quarterly stress periods (each being 89–92 days), such that seasonal variability observed in the principal stresses of rainfall and pumping are represented only approximately (DEW, 2023a). Winter-spring rainfall generates recharge during May–October, while irrigation, pumping and evapotranspiration cause seasonal falls in the groundwater levels during the dry season of November to April (during which time, recharge in the model is set to zero). DEW (2023a) derived recharge estimates using the water table fluctuation method over the observation period 1970 to 2020. Nine recharge areas were adopted, representing different geological properties, soil types and land uses. Additional zones were included to simulate point source recharge through sinkholes in the Naracoorte Ranges, based on Cramer's (1990) work. Within each zone, time-varying recharge rates represent the spatial average for that year from wells within each zone. Areas of plantation forest were also accounted for, with recharge rates reduced based on plantation dates using the forest water accounting method (DEW, 2023a). In cases where plantation dates were unavailable, recharge was assumed to be zero for the entire simulation, while zones covered by native vegetation were also assigned no recharge, consistent with SENRM (2013). This method for applying recharge to the model is recognised by DEW (2023a) as a simplified approach.

Groundwater evapotranspiration within pasture areas, which incorporates most of the model area, adopts a maximum rate (i.e., for the situation where the water table reaches the land surface) of 450 mm/y, with an extinction depth (i.e., the water table depth below the land surface at which groundwater evapotranspiration ceases) of 2 m (DEW, 2023a). In plantation forest areas, groundwater evapotranspiration rates were determined using forest water accounting models (Harvey, 2009), with consideration given to plantation establishment dates. Groundwater evapotranspiration was modelled in plantation areas using the ETS package (Banta, 2000) with two segments, setting the parameters 'proportion of extinction depth' (PXDP) and 'proportion of maximum extinction depth' (PETM) to 0.95, and an extinction depth of 6 m (DEW, 2023a). Management areas and plantation dates were used to group and categorize 36 zones for implementing time-varying rates of potential groundwater evapotranspiration.

Groundwater pumping was based on estimates by Harrington and Li (2015) for pre–2007 rates, and on metered pumping data thereafter. Pumping (and irrigation) outside of summer months isn't considered in the model, and rather, the metered pumping volumes are distributed over the spring to autumn stress periods. In the Victorian parts of the model domain, pumping is based on previous models (Morgan et al., 2015; CDM Smith, 2017) and annual reports from the Border Groundwater Review Committee (e.g., DELWP, 2020).

Surface drainage within the model domain, including Mosquito Creek, is simulated only as groundwater losses to gaining sections of streams, without considering the transfer of water along waterways. That is, surface water features are represented using MODFLOW's Drain package, which allows for groundwater discharge but not inputs to groundwater from surface features. Drain bed elevations were set to 1 m below the land surface. Drain conductance values (representing drain-groundwater connectivity) were calculated from the drain dimensions, bed thickness (assumed to be 1 m) and hydraulic conductivity (assumed to be 1 m/d) of the drain bed material (DEW, 2023a). Drain conductances were modified during model calibration, leading to values ranging from 2 to 6375 m^2/d. The absence of surface runoff within the model of DEW (2023a) precludes the comparison of drain fluxes with measured drain flow rates.

The aquifer hydraulic conductivity and specific yield in the model were determined using PEST (Doherty et al., 2010), with initial values adopted from historical aquifer testing. The geometric mean of hydraulic conductivity values in the model is 23.7 m/d, which is similar to the average of the available pump test results of 22 m/d. The geometric mean of specific yield values in the model is 0.095.

4.2.2 Coastal-areas south sub-regional model

The coastal-areas south sub-regional model (DEW, 2023b) is also a MODFLOW 2005 model created using Groundwater Vistas. The model represents only the TLA, with the TCSA not considered. The aquifer is subdivided into three layers to reflect vertical differences in heads within the TLA, which tends to be thicker near the coast. The model is approximately 65 km east-west by 35 km north-south, again discretised using

100 m square cells (DEW, 2023b) – see Figure 5. This includes an offshore component of the aquifer that extends ~2 km out to sea.

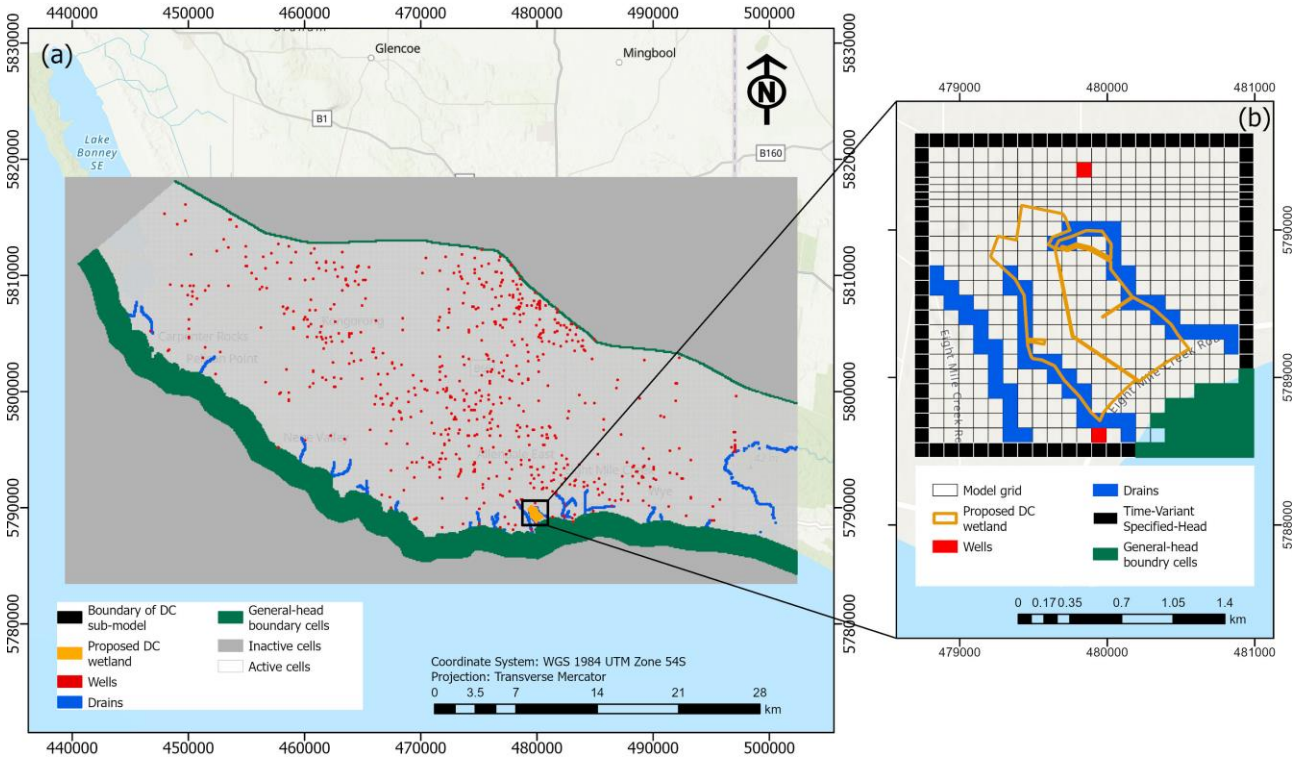

Figure 5. (a) The coastal-areas south sub-regional model, and (b) The Karst Springs Restoration (i.e., Deep Creek; DC) sub-model.

To simulate the hydraulic influence of the freshwater-seawater interaction at the coastal boundary, DEW (2023b) applied the MODFLOW Seawater Intrusion Package, SWI2 (Bakker et al., 2013). SWI2 neglects vertical flow and assumes a sharp interface between freshwater and seawater by neglecting dispersion effects, allowing for an approximation of the location of the freshwater-seawater interface. When the SWI2 package is invoked, the heads that are output from MODFLOW are equivalent freshwater heads, accounting for the density of seawater and taken from the top of the layer from which the head is reported (Bakker et al., 2013). As MODFLOW adopts block-centred representation of the subsurface, the coastal boundary in sub-models has a different equivalent freshwater head, because the centre of model cells was adopted for this calculation.

The northern boundary assumes a general-head condition to simulate groundwater inflows, albeit with declining heads consistent with historical trends since the 1970s. The eastern and western limits of the model are assigned no-flow conditions (DEW, 2023b). The seafloor was modelled as a general-head boundary, with head values representing the equivalent freshwater head at the ocean bottom. Sea level was assumed to be 0 m AHD, and tidal and seasonal sea level variations were not simulated.

The model top is coincident with the land surface, which was set to LiDAR data (DEW, 2020) for onshore areas and the seafloor elevation in offshore areas (Whiteway, 2009). Layer elevations were otherwise set according to lithological logs and interpretations thereof by Harrington et al. (2007), Lawson (2013) and DEW (2021).

The model has a transient simulation period of 1 Aug 1970 to the 31 Jan 2022, represented using 206 quarterly stress periods. Rainfall recharge is presumed to occur during May to October, while irrigation pumping is taken to occur from November to April. Although the quarterly stress periods are thought to be coarse (DEW, 2023b), groundwater level data are generally available only quarterly and extraction data annually, and hence the temporal discretization is considered to be consistent with the available dataset.

DEW (2023b) estimate recharge in pasture areas using the water table fluctuation method (Crosbie and Davies, 2013; Fu et al., 2019), while recharge in plantation forest areas was set to 17% of the pasture recharge rate, as an approximation of the lower recharge in plantation forests (Benyon and Doody, 2004). This aligns with the Lower Limestone Coast Water Allocation Plan, in which the recharge in softwood plantations is 83% lower than in adjacent pasture. Recharge is again set to zero in native vegetation areas, consistent with SENRM (2013).

In pasture areas, the rate of groundwater evapotranspiration when the water table reaches the land surface was set to 450 mm/y and the extinction depth is 2 m, based on Wood (2017). For plantation forests, groundwater evapotranspiration is assumed to be zero because groundwater levels are typically more than 6 m below the land surface under plantations in the study area, although some groundwater evapotranspiration from plantation forests is likely (DEW, 2023b).

Groundwater pumping is based on metered data from 2007 onwards, and on the estimates of Harrington and Li (2015) for earlier years. In most cases, there was sufficient information to assign wells to the model layers from which they are expected to extract groundwater, although wells are typically open to all the TLA sub-units that they penetrate (DEW, 2023b).

Surface drainage (constructed drains and the Glenelg River) and spring discharge were represented by DEW (2023b) using the Drain package, with drain bed elevations set to 1 m below the land surface. At spring locations, the conductance (C_d) values were set very high for sites such as Piccaninnie Ponds (C_d = 100,755 m^2/d), reflecting the general notion that the springs are freely discharging. Piccaninnie Ponds is up to 120 m deep with groundwater inputs to the spring vent occurring at all depths of open limestone (DEW, 2023b).

Within the model domain, 35 hydraulic conductivity (K) values are reported from aquifer tests at 16 locations (DEW, 2021), producing values ranging from 0.1 to 10,780 m/d, reflecting the strong heterogeneity of the study area. The geometric mean K of pump test values in the study area is 11.6 m/d. The corresponding K value for the broader Limestone Coast region is 22.7 m/d (n = 374) (DEW, 2023b).

Hydraulic conductivity was again estimated by DEW (2023b) through model calibration using PEST (Doherty et al., 2010). Calibration led to geometric mean horizontal hydraulic conductivity values of 34.5 m/d, 19.5 m/d, and 10.5 m/d in layers 1, 2 and 3, respectively, aligning reasonably well with field-based estimates. The vertical hydraulic conductivity (K_z) was coupled to the horizontal hydraulic conductivity such that the ratio between the two was sought through model calibration. Storage parameters, calibrated using pilot points, produced a geometric mean specific yield of 0.102 in layer 1, while layers 2 and 3 were treated as confined, with geometric mean storativity values of 9.2×10^{-6} and 1.5×10^{-6}, respectively.

4.2.3 Converting existing models to MODFLOW 6

The existing models were converted to MODFLOW 6 (from MODFLOW 2005) in anticipation of the need to access the advanced capability of MODFLOW 6 to simulate surface water features. MODFLOW 6 does not support input parameters in the same way they are used in MODFLOW 2005 (Langevin et al., 2017), and as such, MODFLOW 2005 files needed to be converted into a new set of files compatible with MODFLOW 6. Our initial attempts to do this used the USGS code *Mf5to6* to convert MODFLOW 2005 files to the MODFLOW 6 format. Attempts to use Mf5to6 revealed some missing stress periods in the well file created for MODFLOW 6, due to formatting issues in the original well input file. Another issue arose when converting the ETS file to an EVT file, in that Mf5to6 created an excessively large EVT file (>100 GB), which significantly increased the MODFLOW 6 run time. As a result, instead of using the Mf5to6 code, Python scripts were developed to extract all the required parameters from the MODFLOW 2005 input files for reconstructing the MODFLOW 6 input files. The flowchart in Figure 6 illustrates the relationship between MODFLOW 2005 and MODFLOW 6 packages, where each link required Python coding to execute the necessary conversion.

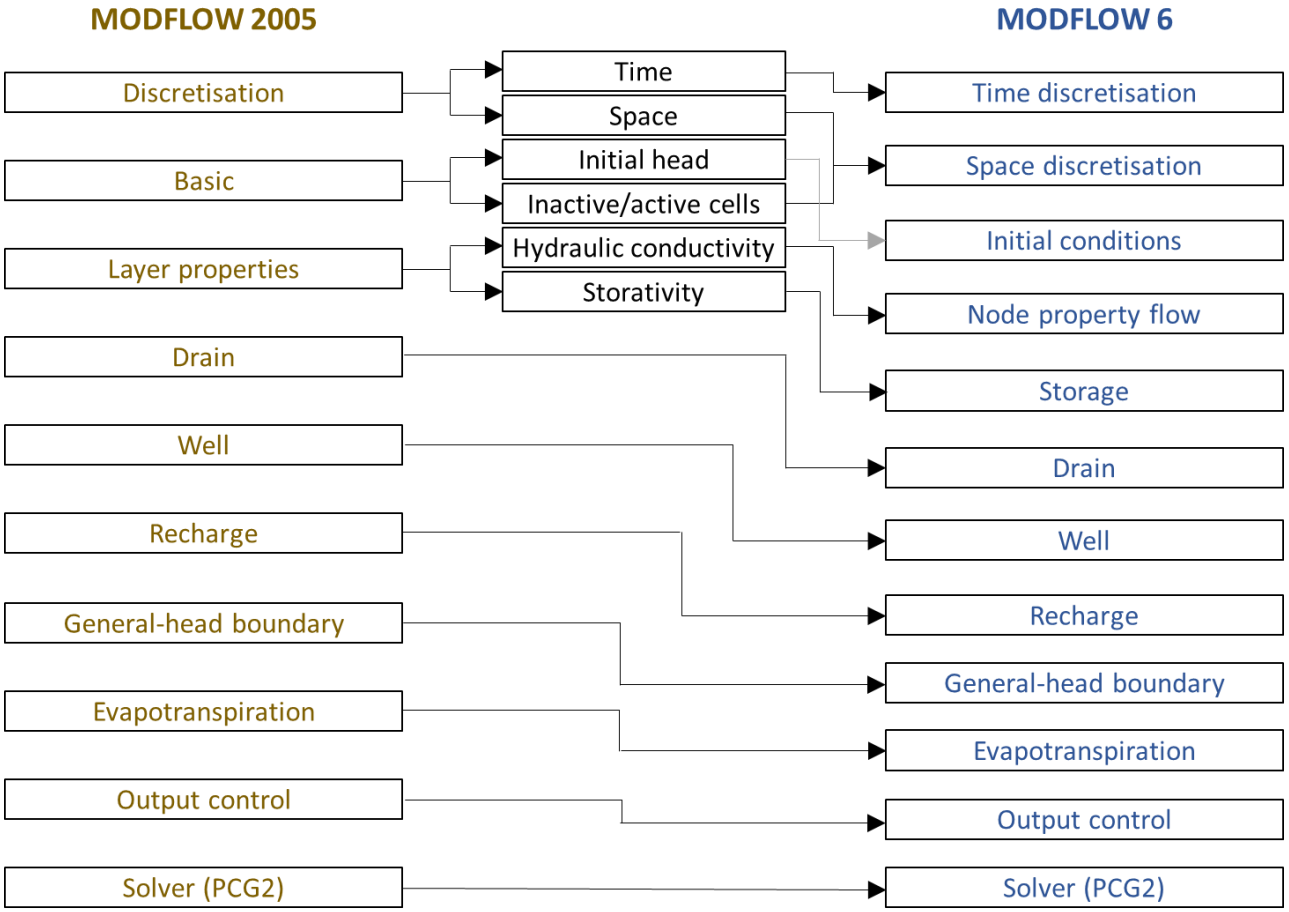

Figure 6. Flowchart for the conversion of MODFLOW 2005 to MODFLOW 6 using Python scripts.

As shown in Figure 6, the datasets of the MODFLOW 2005 model needed to be extracted and reconstituted into input packages to MODFLOW 6, including information relating to time discretisation, spatial data, the occurrence of active and inactive cells, initial head values, hydraulic conductivity and storativity. The Well, Drain, General-Head Boundary, Evapotranspiration and Output Control packages were incorporated directly into their corresponding packages in MODFLOW 6, whereas other packages required the data from the original models to be significantly rearranged. Additionally, information from the Preconditioned Conjugate-Gradient package in MODFLOW 2005 was used to generate the MODFLOW 6 solver (Iterative Model Solution package).

4.3 Extracting sub-models from existing models

The extraction of sub-models from the larger existing models of DEW (2023a, 2023b) was intended to reduce the spatial extent and therefore the model run times when wetland simulation was added to the computational demand – namely to represent the Bool Lagoon Complex and the proposed wetland at the Karst Springs Restoration site. The extent of sub-models was intended to ensure that the entire wetland area of interest was captured, plus regions surrounding the wetland that might be relevant to engineering scenarios (e.g., reduced groundwater pumping). Otherwise, the size of the sub-models was minimised to reduce the computational demand and runtimes. Figures 4a and 5a display the extent of the existing models produced by DEW (2023a, 2023b), while Figures 4b and 5b show the sub-models extracted as part of this investigation, including the locations of drains, wells and general-head boundaries. The original structured grid was retained to maintain consistency and allow direct comparison with the sub-regional model developed by DEW (2023a, 2023b). Although unstructured grids offer advantages for simulating irregular

domains such as lakes, their integration would require a completely new model due to challenges in aligning hydraulic properties and boundary conditions across differing grid geometries.

In order to obtain consistency between existing models and the Bool Lagoon Complex and the Karst Springs Restoration sub-models, groundwater heads were extracted from existing models and applied as time-variant specified-head boundaries in the corresponding sub-models, except where an existing head-dependent boundary condition occurred at the sub-model boundary, in which case, the latter was retained. Because the cell sizes and the grid orientation of the sub-models are the same as those adopted in the original (parent) models, model stresses (drains, recharge, pumping, evapotranspiration, etc.) could be directly translated from the original model to the sub-model (see Figure 4 and 5) without the need for cell subdivision or amalgamation.

4.4 Wetland simulation

Following the extraction of the two sub-models from existing sub-regional models, the Lake package of MODFLOW 6 was added. As the two case studies (Bool Lagoon Complex and Karst Springs Restoration) have significantly different hydrogeological conditions and engineering design objectives, the application of the Lake package also differs between the two models. As such, we describe the construction of each sub-model separately in the following sub-sections.

4.4.1 Bool Lagoon Complex

The methodology for applying the Lake package of MODFLOW 6 (Langevin et al., 2017) to the simulation of the Bool Lagoon Complex was developed after considerable trial-and-error. The techniques described in the remainder are without precedent in Australian groundwater modelling investigations (to the authors' knowledge), and therefore, the following provides a new workflow for wetland-modelling interaction analysis that advances on prior hydrogeological investigations of wetlands.

The introduction of the Lake package to a groundwater model requires the addition of a new top model layer. This layer hosts the Lake of the Bool Lagoon Complex, including Bool, Hacks and Little Bool Lagoons. In our application, the top of the *Lake layer* was assigned an elevation of 67 m AHD, which is 3 m higher than the maximum topographical elevation of the Bool Lagoon Complex sub-model. The top elevation of 67 m AHD was effectively an arbitrary choice, although it needed to be higher than the maximum topographical elevation of the lake area. The base of the Lake layer was set to match the elevation of the top of the sub-model (i.e., the lake bathymetric elevation distribution). The addition of the Lake layer increased the number of layers in the sub-model from one (from the parent model) to two. The cells within the additional Lake layer were set to "inactive" (IDOMAIN = 0 in MODFLOW 6) to signify that these cells are Lake cells but are otherwise not incorporated into groundwater flow calculations. The distribution of these cells was determined from a shape file of the maximum inundated area of the Bool Lagoon Complex provided by the Limestone Coast Landscape Board. The remaining cells in this top layer, located outside the lake area, were initially treated as dry cells. This was achieved by setting the initial head to lower than the base of the layer. The model's wetting feature was configured to prevent these dry cells from becoming wet (WETDRY = 0) and thereby becoming part of the groundwater flow system calculations.

Figure 7 shows the spatial configuration of the Bool Lagoon Complex model, highlighting the vertical configuration of the model for simulating the Bool Lagoon Complex.

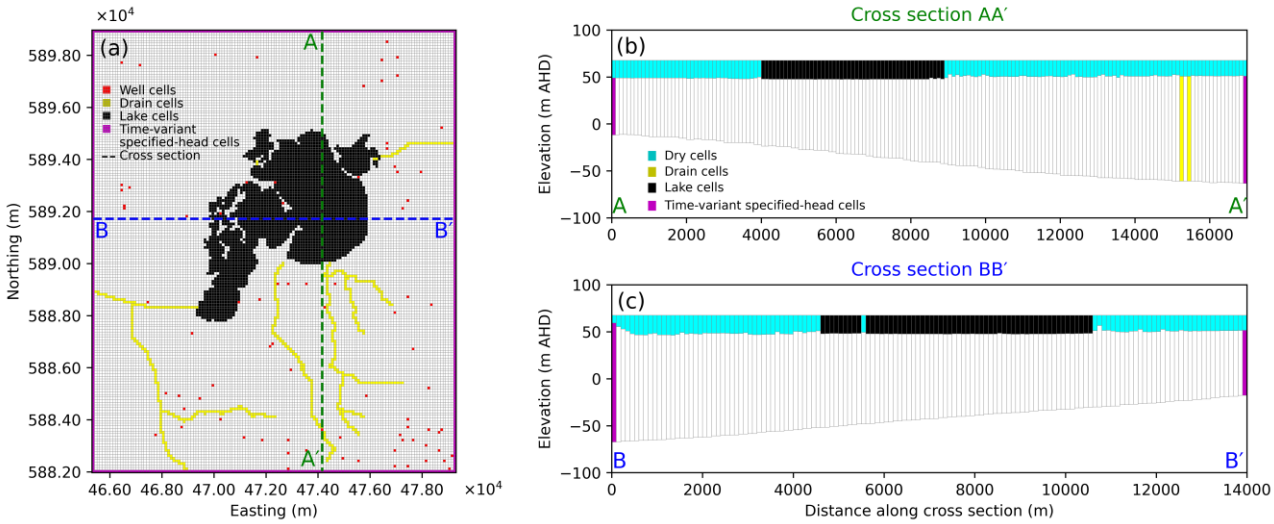

Figure 7. Spatial and vertical structure of the Bool Lagoon Complex model. (a) Map view showing the locations of well, drain, lake, and time-variant specified-head cells, along with the positions of two cross sections. The vertical arrangement of model layers and boundary conditions used to simulate the Bool Lagoon Complex are shown in: (b) Cross section AA' and (c) cross section BB'.

Rainfall and potential evaporation data (class A pan evaporation) were integrated into the lake model, sourced from the SILO climate database (https://www.longpaddock.qld.gov.au/silo/point-data). Figure 8 shows the rainfall and potential evaporation rates applied during the simulation period (1 Aug 1970 to 31 Jan 2021). The average rainfall for the period was ~555 mm/y (1970–2021; the period of the model simulation), while the average potential evaporation was ~1452 mm/y (1970–2021; the period of the model simulation). The initial lake stage was set to 49 m AHD, which is high relative to Bool Lagoon Complex water levels presented by Harding (2018). This is meant to be only a rough initial value, and given this, the first 3–6 months of the model simulation should be a considered a "warm-up" period.

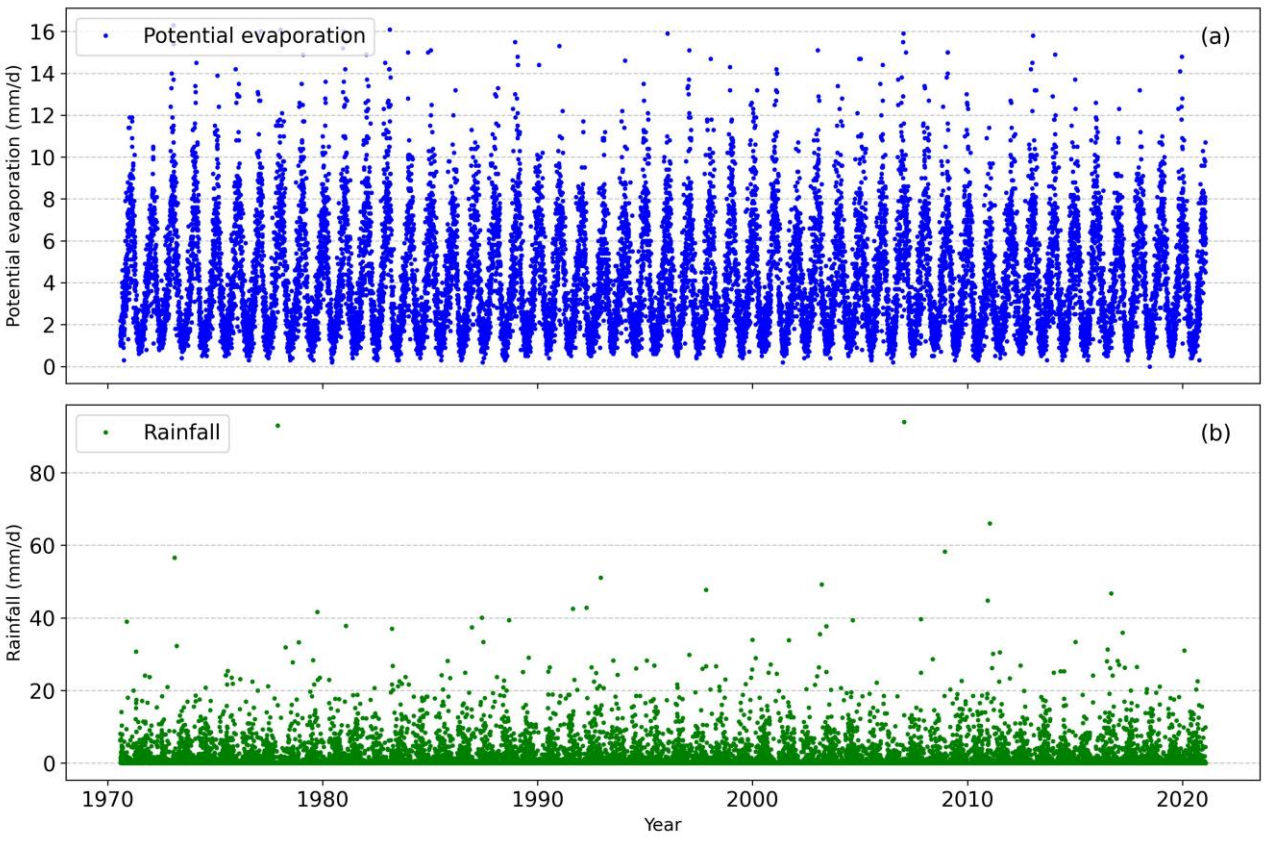

Figure 8. (a) Rainfall and (b) potential evaporation during the simulation period (1970–2021) for Bool Lagoon.

The lakebed leakance, representing the ratio of the hydraulic conductivity to the thickness of the lakebed, is an important control on lake-groundwater interaction. According to Taylor et al. (2015), the lakebed's hydraulic conductivity ranges from 4 x 10^{-8} m/s (0.0035 m/d) to 9 x 10^{-6} m/s (0.78 m/d), with an average of 0.39 m/d. The lakebed thickness varies between 4 to 11 m, averaging 7.5 m, although this is based on limited lake sediment testing (Taylor et al., 2015). An initial lakebed leakance of 0.052 d^{-1} was adopted (i.e., 0.39 m/d ÷ 7.5 m), based on the data of Taylor et al. (2015). Taking the cell size of 100 m by 100 m, this leakance is equivalent to a conductance of 520 m^2/d, which falls within the range used for the drain conductance in simulating the effect of surface water bodies on the groundwater system in the parent model (see Section 4.2.2). A sensitivity analysis was undertaken to explore the role of the lakebed leakance on the surface and subsurface hydrology of the system.

The model incorporates inflows from Mosquito Creek as a specified-flux input boundary condition in the Lake package. Figure 9 shows gauged flows in Mosquito Creek for the period 1971 to 2024. Outflow from the Bool Lagoon Complex via Drain M is recorded at the A2390541 gauging station (Figure 9a), which is immediately downstream of the Bool Lagoon outlet regulator. Figure 9b shows the historical flow data (1985–2024) at this gauging station.

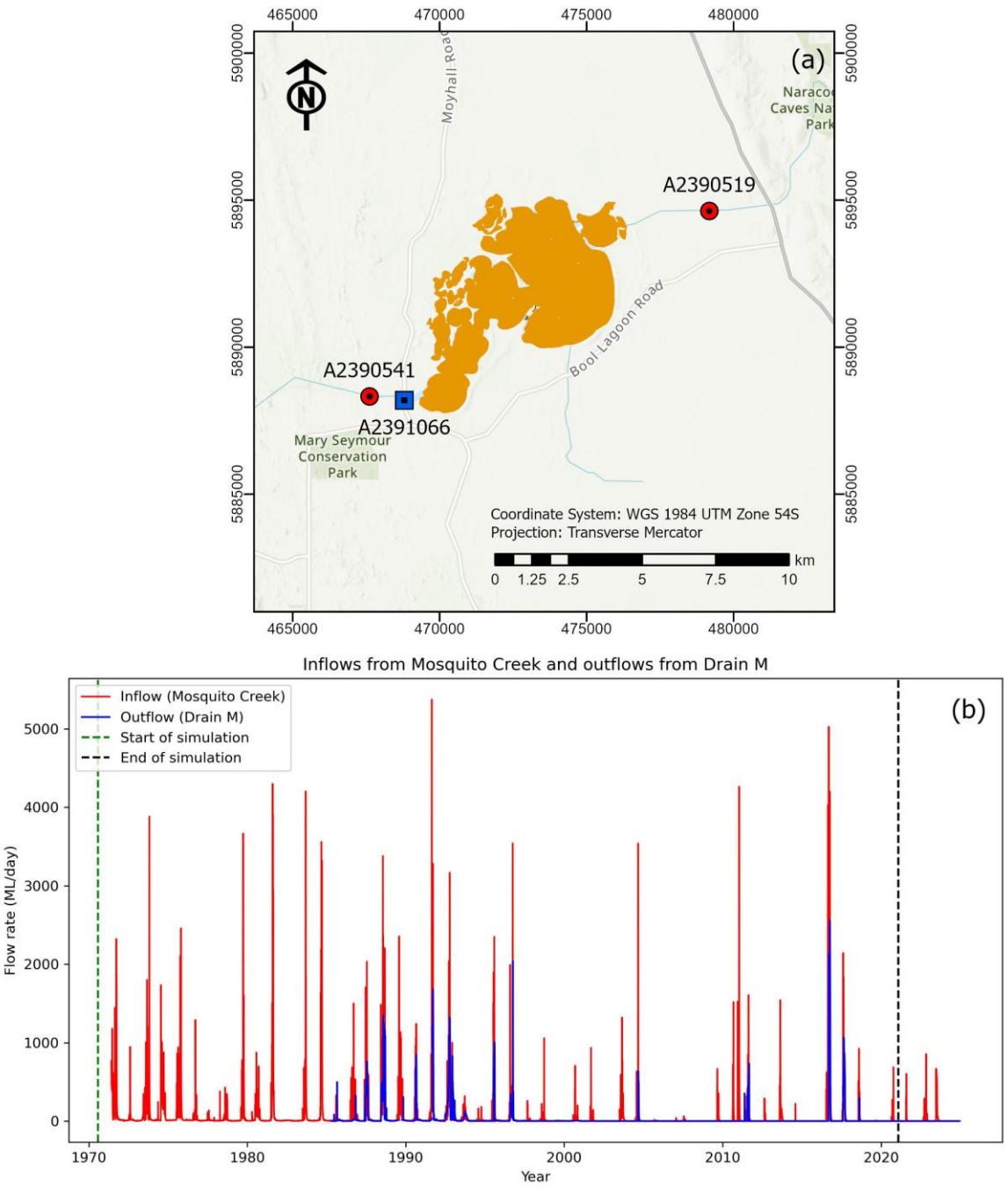

Figure 9. (a) Locality map of Bool Lagoon showing hydrographic stations near the inlet and outlet, where the red circles represent gauging stations that measure inflow from Mosquito Creek (A2390519) and outflow from Drain M (A2390541), while the blue square marks the station recording water levels at the Bool Lagoon regulator. (b) Hydrographs of Mosquito Creek (Gauging Station: A23950519) for the period 1971–2024 and Drain M (Gauging Station: A2390541) immediately downstream of the Bool Lagoon regulator, for the period 1985–2024.

The history of inflows and outflows to/from the Bool Lagoon Complex show considerable variability. Flows during the Millenium Drought (1996–2010) were substantially reduced, including almost 10 years without significant discharge from the Bool Lagoon Complex. Flows have been lower since the Millenium Drought, compared to prior. Only two outflow events are evident since 2017.

Figure 10 shows the water levels recorded at the Bool Lagoon regulator, i.e., station A239166 (see Figure 9 for its location) and the corresponding outflow from Bool Lagoon into Drain M (captured at station A2390541) for the period during which both data sets were available, i.e., from June 2017 to October 2024. There has been a lack of outflow from the Bool Lagoon Complex since 2018. Figure 11 shows a close up of the period

during which both flows and water levels were available, and when flows occurred in Drain M (June 2017 to December 2018).

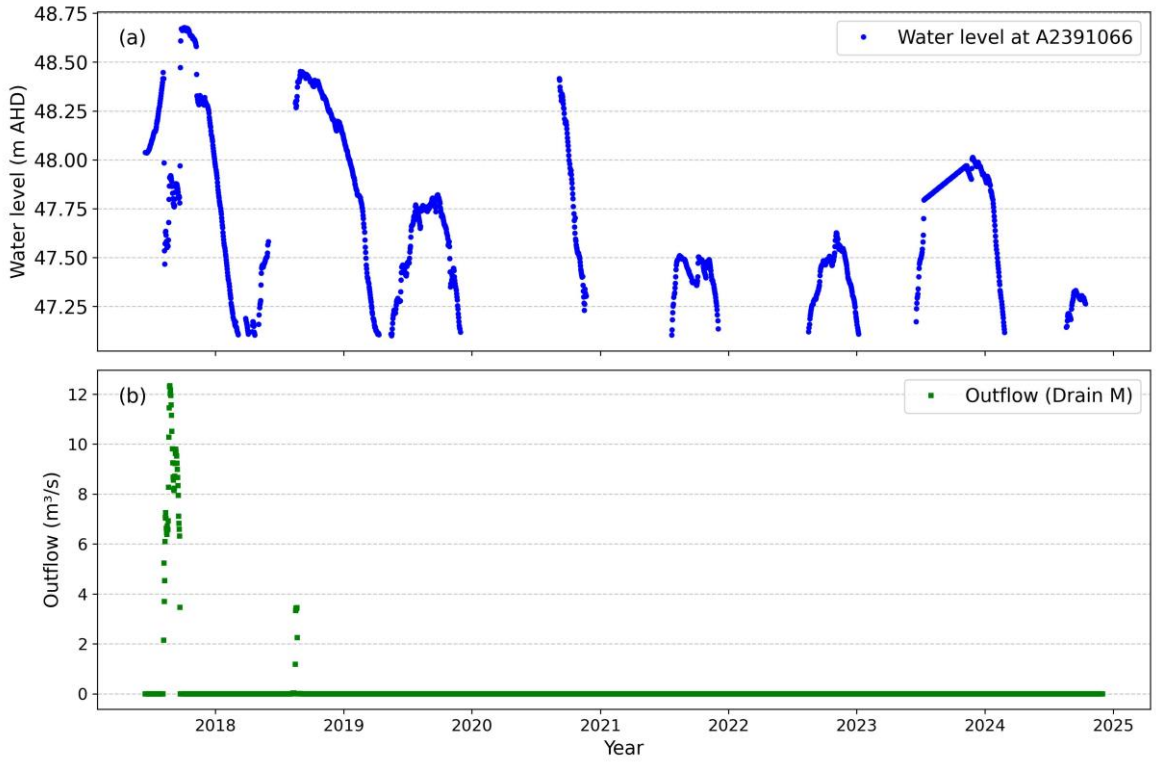

Figure 10. (a) Surface water levels recorded at gauging station A239166 (Bool Lagoon regulator), and (b) corresponding outflow into Drain M (immediately downstream of the Bool Lagoon regulator, measured at station A2390541) for the period June 2017 to October 2024.

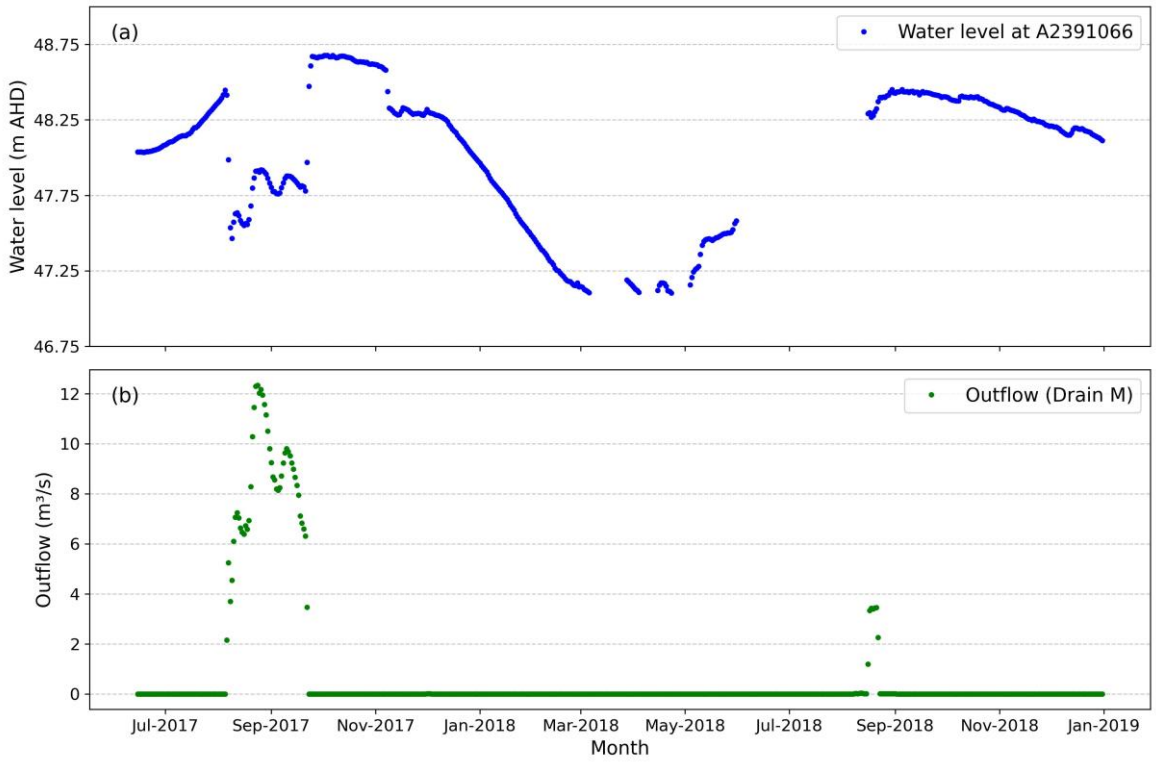

Figure 11. (a) Surface water levels recorded at gauging station A239166 (Bool Lagoon regulator), and (b) corresponding outflow into Drain M (immediately downstream of the Bool Lagoon regulator) for the period June 2017 to December 2018. Other periods of recorded flows without corresponding water levels are not shown.

Figure 11 indicates that the occurrence of flow into Drain M in 2017 caused a lowering of water levels in the Bool Lagoon Complex, with higher water levels when the regulator was closed at other times. Although this is intuitive, it makes the simulation of the downstream regulator challenging, because there does not appear to be an easily reproducible procedure for operating the regulator (e.g., a predictable flow into Drain M occurs at a known Bool Lagoon Complex water level elevation) that can be simulated in MODFLOW 6. This is because the operation of the regulator has depended on the decisions of personnel taking into account a wide range of other factors that are not easily captured within MODFLOW 6. As a consequence, it appears that flow into Drain M occurred at lower water level elevations than at other times, when the regulator was closed but the Bool Lagoon Complex water levels were higher. Nevertheless, we sought a relationship between water level and discharge to Drain M because this is required in the model to control the outflow from the Bool Lagoon Complex. An investigation into other options for simulating outflow from the Bool Lagoon Complex into Drain M should be sought in the future.

Figure 12 shows the relationship between the water level recorded at the Bool Lagoon regulator and the corresponding outflow from the Bool Lagoon Complex into Drain M. The green circles indicate the data from the most recent gate opening (August 2018; Figure 11). We assume that this relationship represents the most recent (and continuing) approach to the operation of the gate, although there are few data points. The blue circles in Figure 12 correspond to data from an earlier operation (August–September 2017; Figure 11). Although the recorded water levels during this period were lower than those in August 2018, the outflow was significantly higher. This may have been caused by opening a different number of gates, and/or adopting alternative gate opening heights between the two outflow events. In any case, it appears that the operational strategy of the regulator changed during the intervening period. It's also clear that the Bool Lagoon Complex water levels do not dictate the operation of the downstream regulator. This is apparent from the difference in the slopes of the head-flow relationships for the two periods (Figure 12). For the purposes of running modelling simulations, a gate operation strategy needs to be created, and therefore, both the August–September 2017 and August 2018 data were used to define rating curves for the regulator, and both were tested through simulation of the Lake package sub-model of the Bool Lagoon Complex.

An explanation for regulator operation, rather the application of observed water levels and heads to define the regulator operation as we have attempted in the current study, is given by Gibbs et al. (2015). According to Gibbs et al. (2015), water is released from the Bool Lagoon Complex each day at a rate considered necessary to maintain the water level as follows:

(a) 48.15 m AHD during June;
(b) 48.24 m AHD during July;
(c) 48.30 m AHD at the end of the first week in August;
(d) 48.40 m AHD during the third week of August;
(e) 48.55 m AHD at the end of August; and
(f) 48.61 m AHD for as long as possible from the second week in September.
(g) No release occurs if the water level in the wetland is below the maximum level for the relevant time of year.
(h) The maximum release rate is 1000 ML/d.

Nitschke (1984) adds further details of relevance to the understanding of how the Bool Lagoon Complex regulator is operated. Nitschke (1984) reports that the top of the gates has an elevation 49.22 m AHD when the gates are closed, while the invert level of the channel is 46.93 m AHD. Nitschke (1984) also reports that the regulator discharges at around 10 m^3/s when the water level is 48.24 m AHD (July target level). Obviously, this requires that the gates are open. DEH (2006) adds further information relevant to the hydrology of the regulator, although the situations they describe are rare events that are beyond the scope of the current study. They suggest that Bool Lagoon Complex water levels equalling or exceeding the spillway level at Hacks Lagoon and the top of the closed regulator gates can be expected on average once every 20 years, while levels exceeding the 'stoplogs' at Hacks Lagoon are expected to occur on average once every 50 years. However, operation of the regulator would no doubt occur to avoid this type of event, given the catastrophic flooding that would accompany it. DEH (2006) also recommends that when water levels exceed 49.52 m AHD (presumably this is referring to the water level near the downstream end of the Bool Lagoon Complex), stopbanks are threatened, and the flow of water over the top of the regulator gates becomes uncontrollable. It is challenging to incorporate these details in entirety into the parameters of the Lake package that control discharge, and we presently have insufficient information to know the precise mechanisms for outflows to Drain M from the Bool Lagoon Complex. Relevant data to better define the operation of the Bool Lagoon Complex regulator will be useful for future modelling efforts. Another complication in simulating the regulator is the discharge (leakage) that occurs through the gates even when these are closed. In summary, additional work is needed to parameterise the downstream outlet of the Bool Lagoon Complex, because it isn't clear whether the current parameters accurately define the water level-discharge relationship. This includes uncertainty in the gate operating rules, any leakage through the gates, or other outlet mechanisms that are not clearly defined in existing documentation. Although a rating curve (flow versus water level) is needed to control outflows from the Lake package of MODFLOW 6, the operational rules given above are only partially helpful in creating the outflow rating curve. That is, without knowing the flows associated with a given water level in the downstream part of the Bool Lagoon Complex, the head-discharge function that the Lake package requires contains significant uncertainties.

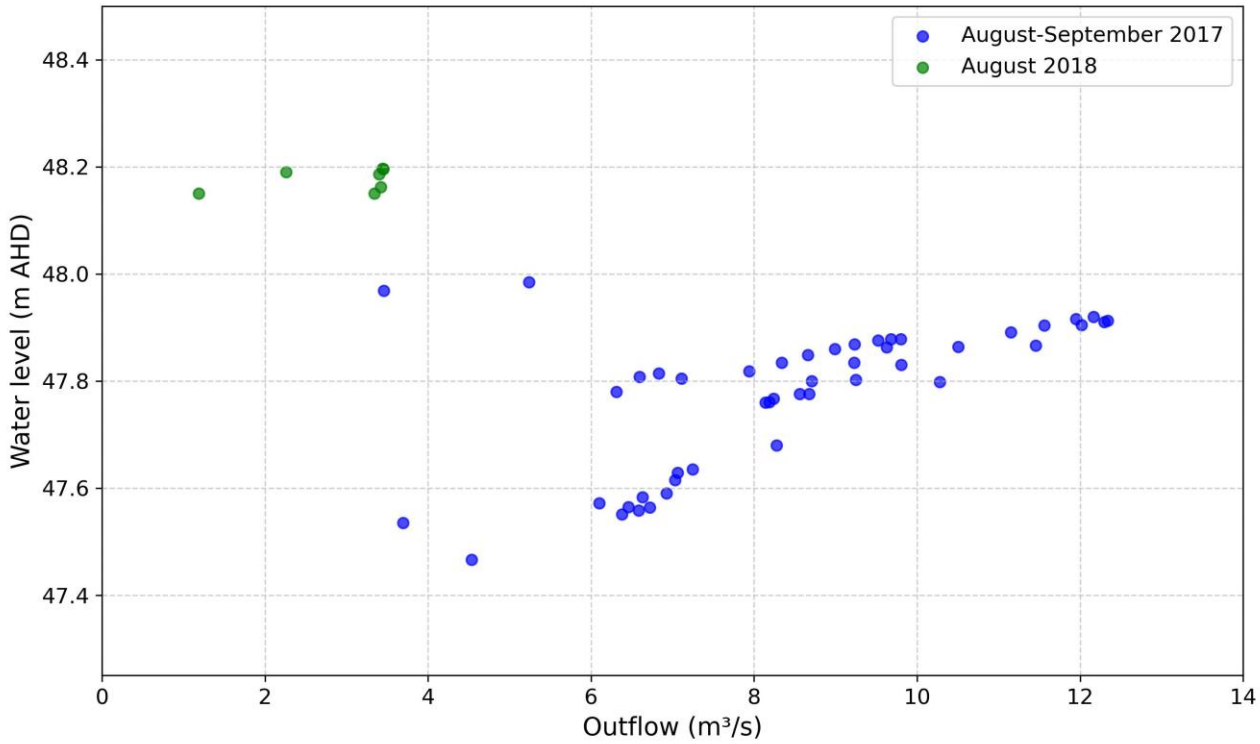

Figure 12. Relationship between water levels at gauging station A239166 and outflow into Drain M, for the period 2017–2024. Green circles indicate data from more recent operation of the regulator (August 2018), while blue circles indicate data from earlier operations (August–September 2017).

The Lake package of MODFLOW 6 provides three options to simulate lake outlets: (a) specified outflow, (b) Manning's equation, and (c) the sharp-crested weir equation (Langevin et al., 2017). The latter two options are rating-curve types of controls, of the type discussed above (i.e., water level versus discharge relationships). In this study, the specified outflow option (i.e., (a)) could not be applied because outflow data are available only for a portion of the simulation period (1970–2021). Additionally, the outflow cannot be specified in modelling scenarios, and rather, the outflow should be a function (i.e., a natural response) of the stresses applied to the model and a prediction variable for simulations. Therefore, the other two outflow options were tested.

According to Langevin et al. (2017), the discharge out of a lake can be calculated using Manning's equation for a channel with a rectangular cross section, given as:

$$Q_o = \frac{1}{n} W D^{\frac{5}{3}} S^{\frac{1}{2}} \quad (1)$$

where Q_o is the outflow rate of discharge (L^3T^{-1}); n is the Manning's roughness coefficient of the outlet channel ($TL^{-1/3}$); W is the width of the outlet channel (L); D is the water depth above the outlet invert elevation (L); and S is the slope of the outlet channel (unitless). The water depth above the outlet invert elevation is calculated as:

$$D = H_L - z \quad (2)$$

where H_L is the lake stage (m AHD), and z is the channel invert elevation (m AHD).

Alternatively, lake discharge can be represented using a sharp-crested weir equation, given by:

$$Q_o = \frac{2}{3} C_d W D^{\frac{3}{2}} (2g)^{\frac{1}{2}} \quad (3)$$

where C_d is a discharge coefficient (unitless), W is the width of the weir outlet (L), D is the water depth above the outlet weir invert elevation (L), which is calculated using Eq. (2) except with z set to the weir crest elevation, and g is gravitational acceleration (LT^{-2}).

The outlet regulator of the Bool Lagoon Complex operates in a more complicated way than an ungated weir or an open channel, for which flow is defined by Equations (1) and (3). As discussed above, the outlet of the Bool Lagoon Complex is a channel equipped with gates, which are operated according to (DEH, 2006; Gibbs et al., 2015, Nitschke, 1984): (a) the design capacity of Drain M, (b) the water levels in Bool Lagoon, (c) the elevation of levees, and (d) the time of year, although DEH (2006) report only occasional, historical operation of the gates. Nevertheless, we define a discharge-water level relationship for simulating the regulator in the Lake package. Figure 13 shows the fitted rating curves for the two different times and using the two alternative equations (Equations (1) and (3)). Note that we have added three artificial points: (1) 62.5 m^3/s at a water level of 49.52 m AHD, where the former reflects the maximum inflow from Mosquito Creek, and the latter is the extreme maximum water level in Bool Lagoon; (2) 29.25 m^3/s, corresponding to the maximum outflow recorded at Drain M, which is assumed to be associated with the maximum level (49.22 m AHD) as indicated by the top elevation of the gate when closed; and (3) a water level below which the gate remains closed (and the discharge is zero) to maintain water levels in the lake. For the two rating curves obtained from the 2017 and 2018 data, the water level elevations below which there is no discharge were taken to be 46.93 m AHD and 47.8 m AHD, respectively. The above-mentioned artificial points extended the rating curves to allow for the simulation of a wider range of conditions relative to those encountered during the 2017 and 2018 flow events.

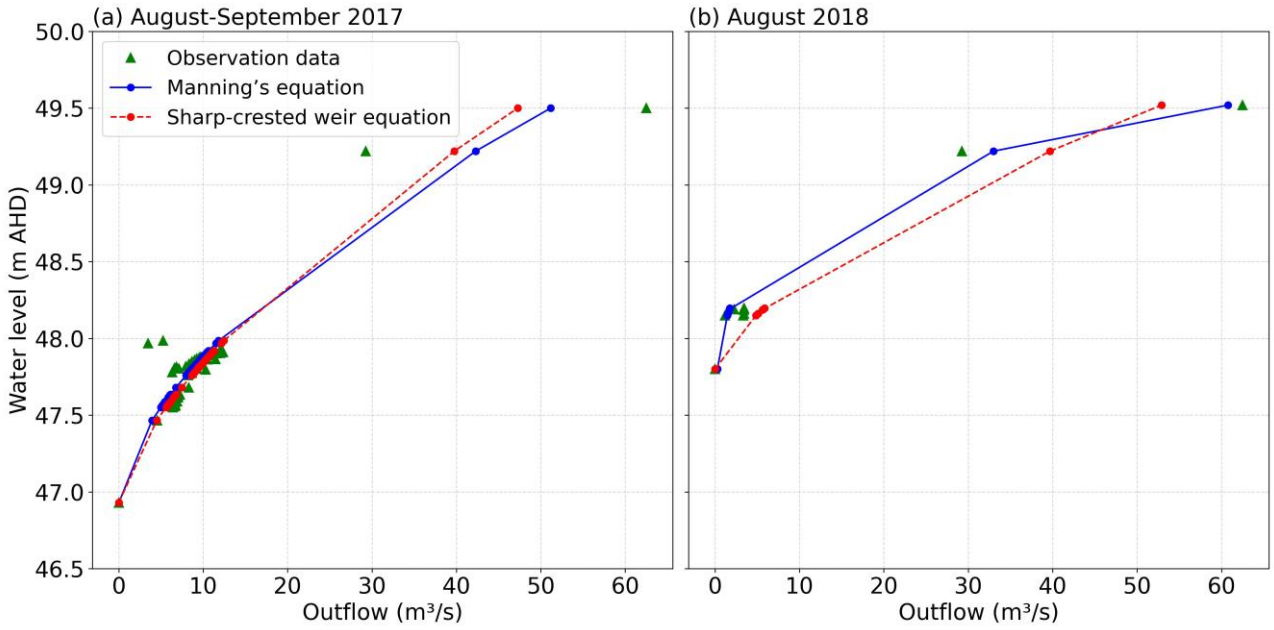

Figure 13. Rating curve data (water level versus discharge) for the downstream regulator of the Bool Lagoon Complex. Two periods are represented: (a) August–September 2017, and (b) August 2018. Fitting curves are provided, corresponding to the two options in the Lake package for assigning downstream boundary conditions, as described above (Equations (1) to (3)). Here, "Observation data" also includes flow-water level points added artificially to extend the range of the available dataset.

The fitted rating curve functions shown in Figure 13 are defined by the parameters provided in Table 2. Note that the parameters *W*, *n* and *S* were obtained through curve-fitting the above-mentioned functions (Equations (1) and (3)), while *z* was assigned directly given knowledge of the regulator. The value of C_d is a fixed value (0.61) in MODFLOW 6 (Langevin et al., 2017). This value is typical of conditions where the water level is only a small height above the weir crest (e.g., Henderson, 1966).

Table 2. Hydraulic parameters of the outlet boundary condition for the Bool Lagoon Complex, for defining flow into Drain M using Manning's or the sharp-crested weir equations. Rating curves were calibrated to water level and discharge data for two different periods: August–September 2017 and August 2018.

Parameters	August–September 2017		August 2018	
	Manning	**Sharp-crested weir**	**Manning**	**Sharp-crested weir**
W (m)	12.55	6.36	14.27	13.1
z (m AHD)	46.93	46.93	47.8	47.8
n ($sm^{-1/3}$)	0.031	-	0.032	-
S (unitless)	0.007	-	0.0008	-
C_d (unitless)	-	0.61	-	0.61

The first attempt to simulate the Bool Lagoon Complex adopted a single "Lake" to represent the entire water body. In doing so, the entire Bool Lagoon Complex was represented by a flat water surface (i.e., a single water level across the whole Bool Lagoon Complex). This is because the Lake package presumes a uniform, horizontal water surface for each "Lake". However, we anticipate that the Bool Lagoon Complex wetland system has a water surface slope that is important for proper representation of wetland-groundwater interactions. As shown in Figure 14, the head difference between Bool Lagoon Complex surface water levels at the different observation points (e.g., between stations A2391070 and A2391067) is around 30 cm (as an approximate average over time) over a distance of roughly 7.6 km along the Bool Lagoon Complex axis (i.e., along the direction of flow in the Bool Lagoon Complex).

Despite the absence of a water level gradient in the single-lake version of the Bool Lagoon Complex sub-model, it nevertheless provided important, initial insights into the performance of MODFLOW 6 (applying the Lake package), and therefore, we have included it in the current report. Appendix A shows the results of single-lake simulations, including groundwater levels, surface water levels and discharge rates.

Following the simulation of the Bool Lagoon Complex using a single-lake representation, the Bool Lagoon Complex was subdivided into three *sub-lakes*, identified within the Lake package using "1", "2" and "3" within the respective sub-lake areas. This was intended to better capture the water surface gradient of the Bool Lagoon Complex observed in field data. The three sub-lakes were: (1) Hacks Lagoon, (2) Main Basin (plus Little Bool Lagoon), and (3) Central Basin (plus Western Basin). This allowed for three distinct water bodies (sub-lakes), each with different water level elevations, as an approximation of the water surface slope of the Bool Lagoon Complex. Figure 14 depicts the geometry of the sub-lakes that together represent the Bool Lagoon Complex wetland area.

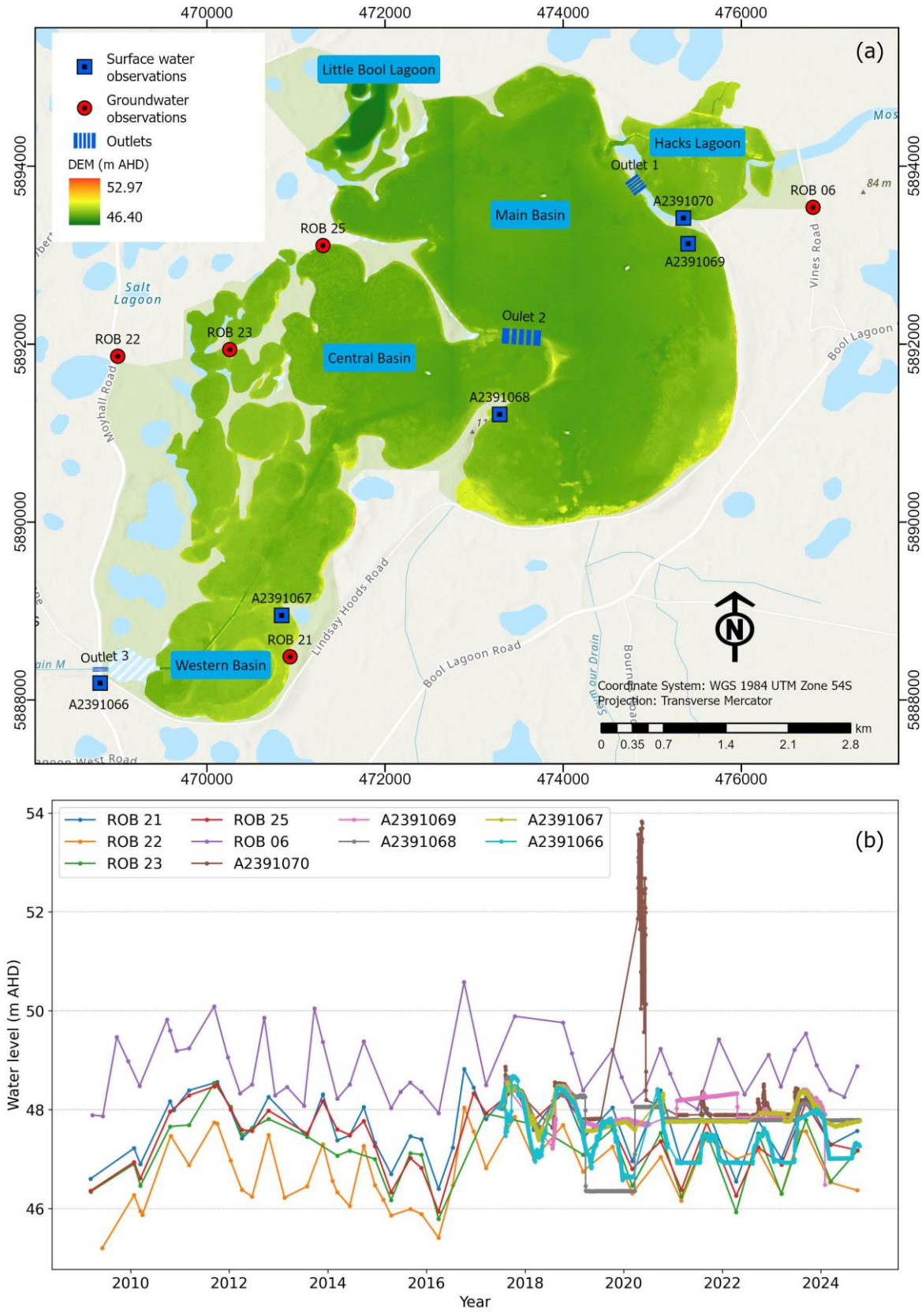

Figure 14. (a) Depiction of the sub-basins of the Bool Lagoon Complex, showing surface water monitoring sites, local groundwater monitoring wells (those with extended record periods), and the lake bathymetry. "Outlets" represent controls in the model, where water is passed from one sub-lake to the other or is discharged from the Bool Lagoon Complex. (b) Groundwater and surface water levels around/in the Bool Lagoon Complex for the period 2009–2024 ("ROB" indicates groundwater hydrographs, while labels starting with "A" are surface water hydrographs). The location of monitoring sites is shown in (a).

Water is transferred between the sub-lakes of the three-lake version of the model using the Water Mover package of MODFLOW 6 (Langevin et al., 2017). This facilitates water movement between different "packages" within the MODFLOW 6 model. Specifically, water is channelled from the outlet of Hacks Lagoon to Main Basin (including Little Bool Lagoon) and subsequently from Main Basin to Central Basin (which also includes Western Basin). The sharp-crested weir equation was employed to calculate outflows from the Bool Lagoon Complex (as discussed below) and exchange fluxes between the sub-lakes. Although Manning's equation was another option for calculating exchange fluxes between the sub-lakes, both methods produced similar head-flux relationships, and therefore, the sharp-crested weir equation was adopted to be consistent with the method for determining flows into Drain M. The Water Mover package then takes the calculated time-varying discharge (calculated using Equation (3) and the upstream lake water level) and adds them as input fluxes to the downstream sub-lake. The parameters for estimating outlet flows from Hacks Lagoon (to Main Basin (including Little Bool Lagoon)) and Main Basin (to Central Basin (including Western Basin)) are detailed in Table 3.

Table 3. Hydraulic parameters of modelled outlet weirs: from the outlet of Hacks Lagoon to Main Basin (including Little Bool Lagoon) and from Main Basin to Central Basin (including Western Basin).

Discharge from sub-lakes:	**Discharge coefficient (C_d, unitless)**	**Width of the outlet (m)**	**Invert elevation (m)**
Hacks Lagoon (Outlet 1)	0.61	90	48.2
Main Basin (including Little Bool Lagoon) (Outlet 2)	0.61	500	48.0

Bool Lagoon Complex surface water levels calculated in MODFLOW 6 were compared to field measurements, as were local groundwater levels and the rates of discharge into Drain M. This was undertaken for several variations of the base case Bool Lagoon Complex sub-model to explore the effects of alternative parameterisation of the Bool Lagoon Complex. The model configuration was varied based on: (a) the use of a single lake or three sub-lakes to represent the Bool Lagoon Complex, and (b) the equation used (sharp-crested weir or Manning's equation) to calculate flows into Drain M. Eight of the model configurations are outlined in Table 4.

Table 4. Eight configurations of the Bool Lagoon Complex sub-model.

Representation of the Bool Lagoon Complex in the Lake package	**Discharge equation**	**Discharge equation fitting period**
Single lake	Sharp-crested weir equation	August–September 2017
		August 2018
	Manning's equation	August–September 2017
		August 2018
Three sub-lakes	Sharp-crested weir equation	August–September 2017
		August 2018
	Manning's equation	August–September 2017
		August 2018

Model-field data comparisons were undertaken using observations of groundwater heads at five observation wells (ROB06, ROB21, ROB22, ROB23 and ROB25) and surface water levels at five gauging stations (A2391066, A2391067, A2391068, A2391069 and A2391070). Appendix A presents those comparisons. The results demonstrate that the three sub-lake model using the sharp-crested weir equation, fitted with August 2018 data, outperformed the other configurations in terms of model performance, particularly for the

discharge into Drain M. Consequently, this configuration was adopted for the Bool Lagoon Complex sub-model in subsequent analyses, including sensitivity analysis and scenario simulations.

Sensitivity analysis was undertaken to test the lakebed leakance. This involved two additional simulations where the lakebed hydraulic conductivity was varied. The subsequent modelling scenarios to assess are described in Section 4.4.3.

4.4.2 Karst Springs Restoration site

Similar to the Bool Lagoon Complex model, adding the Lake package to the Karst Springs Restoration sub-model involved the addition of a new top model layer, in which the region occupied by the wetland was designated as the Lake package. The top of this layer was set to 7 m AHD, which is roughly 3 m higher than the highest topographical elevation of the Karst Springs Restoration sub-model to ensure that water levels don't reach the top of the layer. The bottom of the Lake layer matches the top elevation (land surface) of the groundwater domain of the sub-model, reflecting the proposed wetland's bathymetry. This addition increases the sub-model's layers from three to four. Within this new Lake layer, cells are marked as "inactive" (IDOMAIN = 0 in MODFLOW 6) to indicate that they are Lake cells not involved in groundwater flow calculations. The wetland footprint represents the maximum inundated area of the proposed wetland at the Karst Springs Restoration site, as provided by the Limestone Coast Landscape Board.

Figure 15 illustrates the spatial layout and vertical structure of the proposed wetland at the Karst Springs Restoration site.

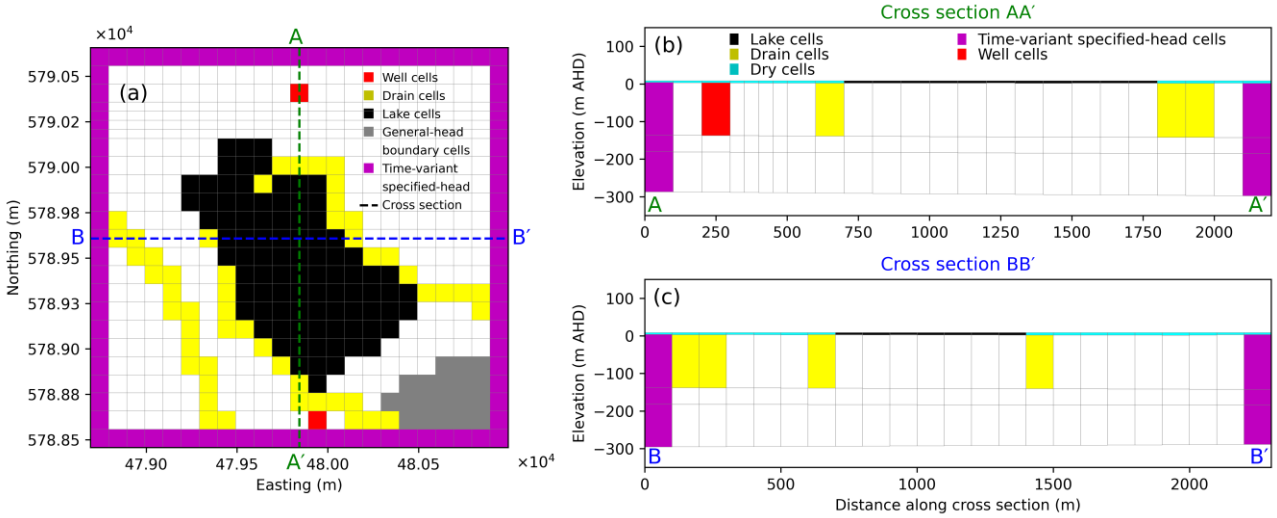

Figure 15. Spatial layout and vertical structure of the proposed wetland at the Karst Springs Restoration site. (a) Map view showing the distribution of well, drain, lake, and time-variant specified-head cells, along with the locations of two cross sections. (b) Cross section AA' and (c) cross section BB' depict the vertical arrangement of model layers and boundary conditions used in the simulation of the proposed wetland.

Outside of the lake area, the top layer cells were assigned water levels to cause them to be dry, which was achieved by setting the initial head below the layer's base. With the re-wetting package of MODFLOW 6 turned off (WETDRY = 0), this ensured that these cells are not part of the groundwater flow simulation. Rainfall and potential evaporation inputs for the lake model were obtained from the SILO climate database. Figure 16 shows the rainfall and potential evaporation rates applied during the simulation period (1 Aug 1970 to 31 Jan 2022). The average rainfall for the period was ~730 mm/y (1970–2022; the period of the model simulation), while the average potential evaporation was ~1317 mm/y (1970–2022; the period of the model simulation). The initial lake stage was set to 0 m AHD (mean sea level), indicating an initially dry lake.

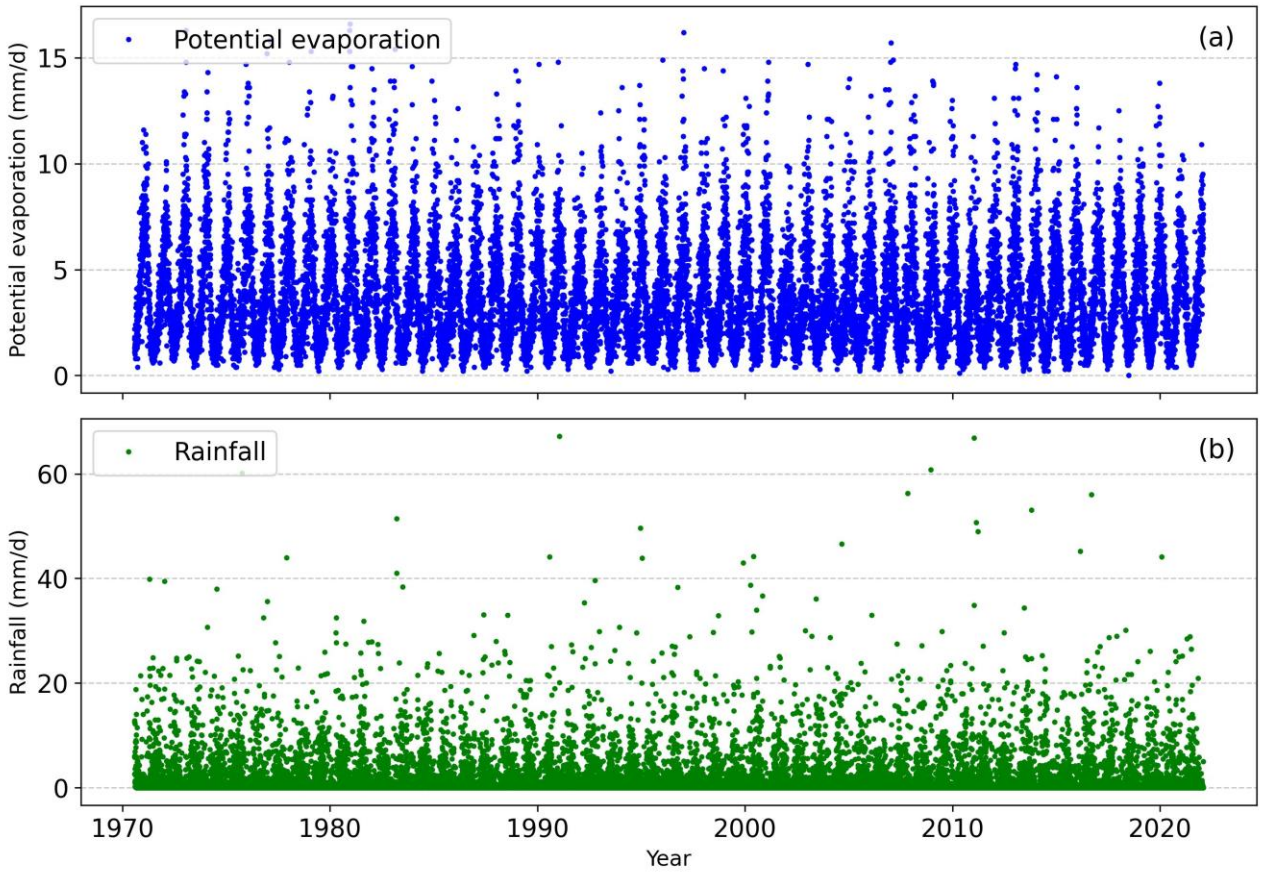

Figure 16. (a) Rainfall and (b) potential evaporation during the simulation period (1970–2022) for the Karst Springs Restoration site.

An initial lakebed leakance value of 5 d^{-1}, was adopted for the Karst Springs Restoration site in the absence of information on the soils of the area to the contrary. Taking into account the cell size, this equates to a lakebed conductance of 50,000 m^2/d. This conductance, as well as the groundwater heads and the wetland water level, dictate the upward and downward leakage of water between the wetland and the underlying aquifer. A sensitivity analysis was conducted to explore the influence of lakebed leakance on the system's surface and subsurface hydrology (see Section 5.3.2). The conductance of the Drain package that was used to simulate the current footprint of the wetland area at the Karst Springs Restoration site (or at least groundwater discharge to it) ranged from 2 to 27750 m^2/d in the parent model of DEW (2023b).

The Lake package received inputs from the Deep Creek drain. Those flows are measured at gauging station A2390507 (see Figure 17 for its location). Inflows to the Karst Springs Restoration wetland were assigned as a specified-flux boundary condition into the Lake package. Figure 17 displays recorded flows in Deep Creek from 1970 to 2024. Although there are clearly data gaps in the measurements of Deep Creek discharge, the current study adopted simple linear interpolation of the available measurements. Infilling methods, similar to those used by Peterson and Western (2018) for groundwater hydrographs, could be used to enhance the resolution of the Deep Creek hydrograph in future iterations.

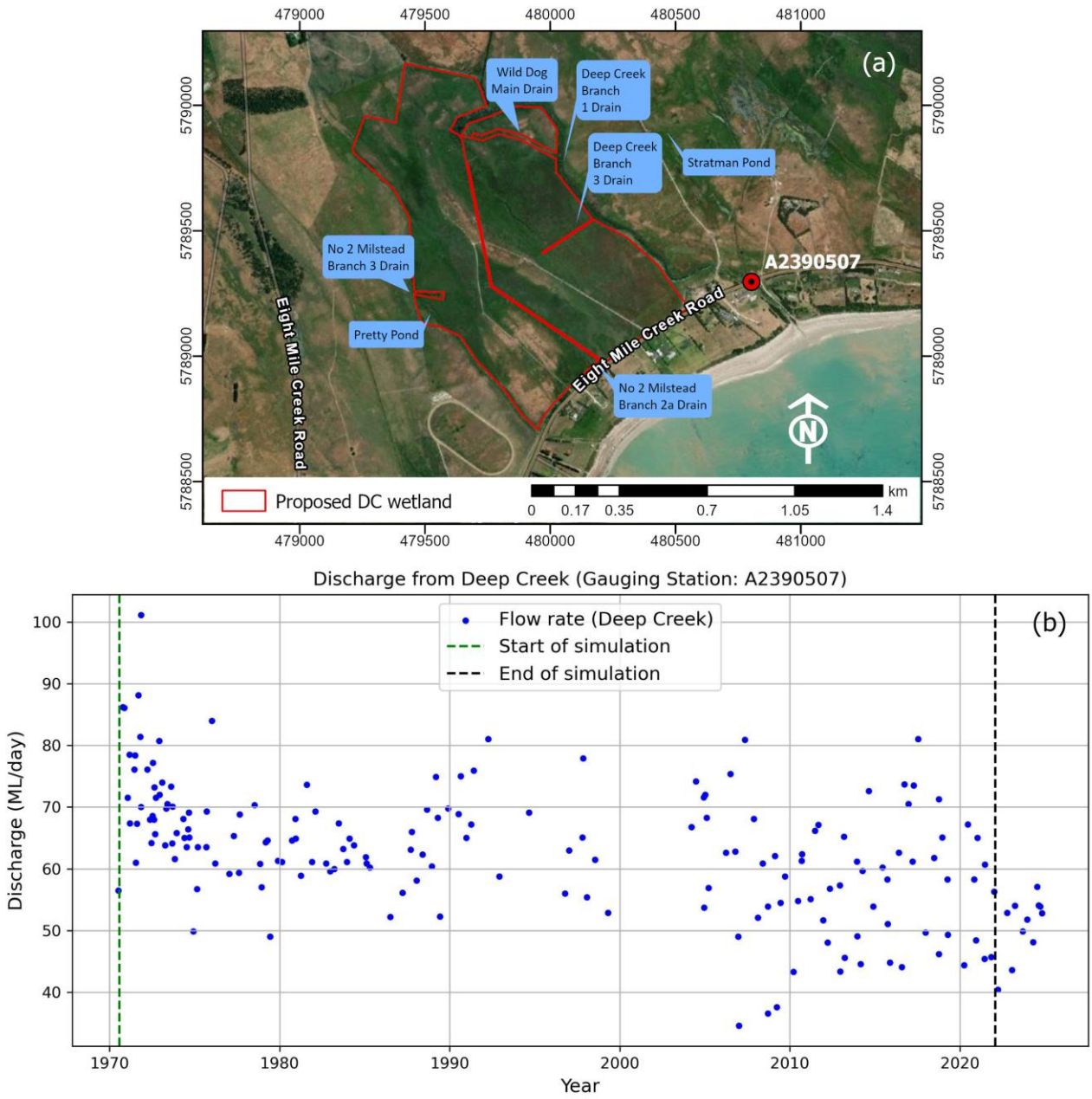

Figure 17. (a) Locality map of the proposed Karst Springs Restoration (i.e., Deep Creek; DC) wetland showing the hydrographic station of Deep Creek, and (b) Hydrograph of Deep Creek discharge (Gauging Station: A2390507) for the period 1970–2024.

The sharp-crested weir equation (Equations (2) and (3)) was used to calculate the outflows from the proposed Karst Springs Restoration wetland in MODFLOW 6. The discharge coefficient (C_d) was 0.61, which is the fixed value of MODFLOW 6 (Langevin et al., 2017). The outlet width (W) and invert elevation (z) were set to 17 m and 2 m AHD, respectively, based on the provided information from the Limestone Coast Landscape Board.

Nguyen and Plush (2024) undertook an assessment of the topography of the Karst Springs Restoration study area. They assessed the inundated area at various water level elevations to create water level-volume and water level-area curves for the wetland water body. These were determined for water level increments of 0.25 m, from 1.5 m AHD to 4 m AHD. Figure 18 illustrates the topographical map of the area, used by Nguyen and Plush (2024) for their analysis. An example of the inundated area is shown for an elevation of 2.5 m AHD in Figure 19. At this elevation, 69% of the total wetland area is open water, and the volume of stored water in the wetland is approximately 390 ML.

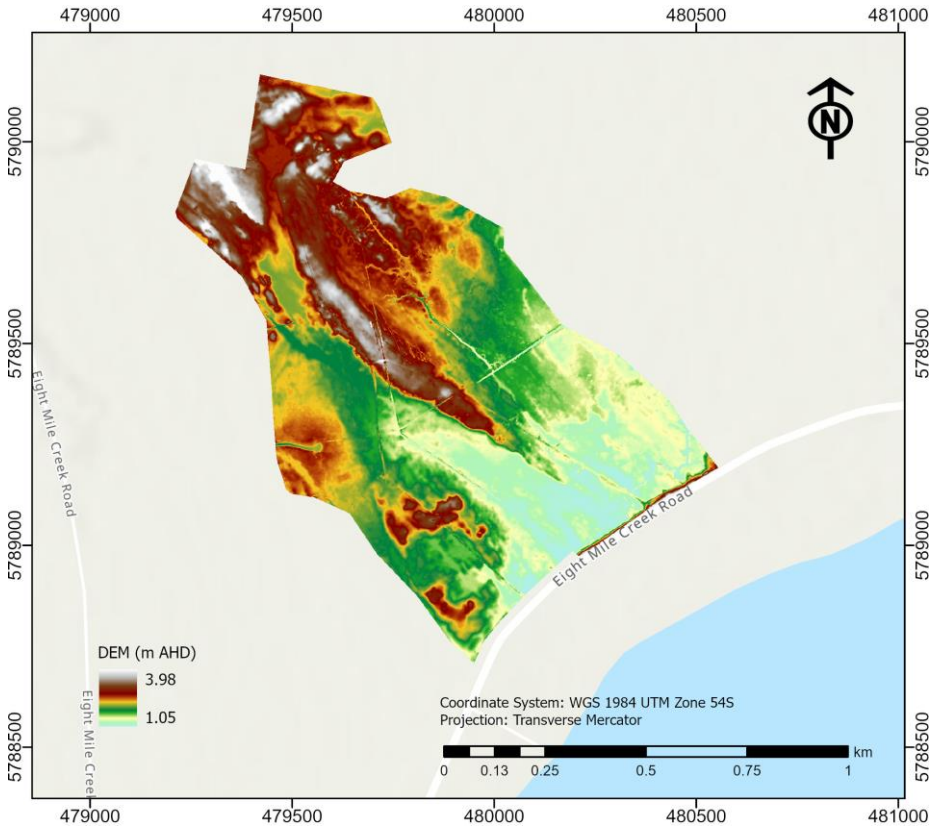

Figure 18. Topographic map of the Karst Springs Restoration study area, based on Nguyen and Plush (2024).

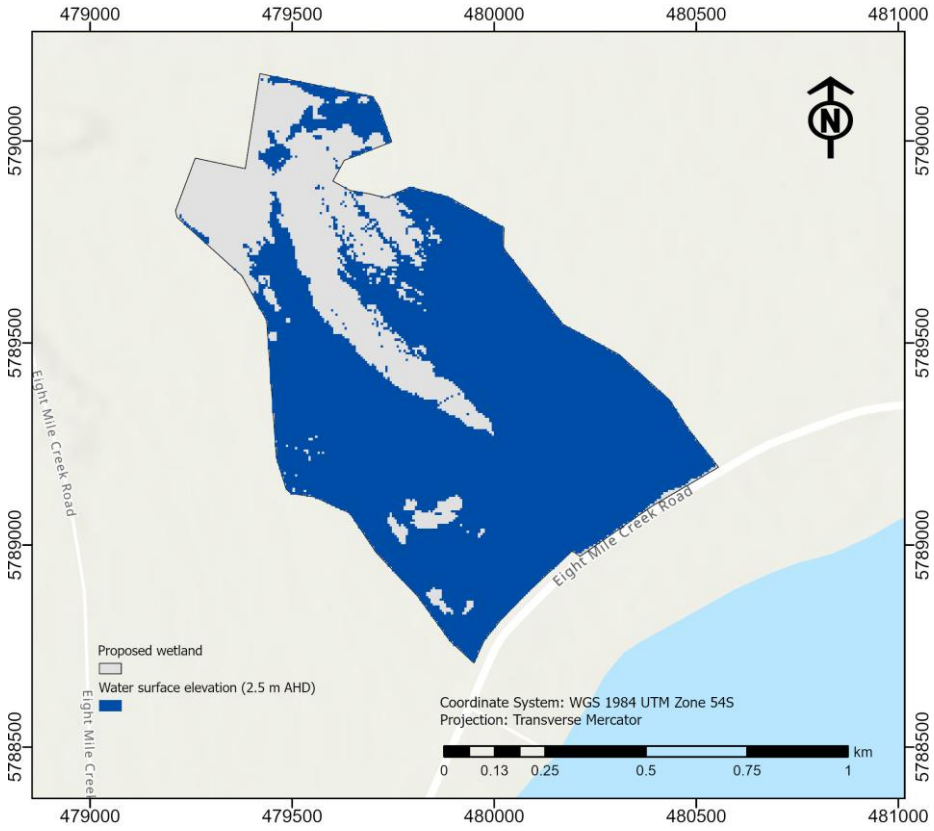

Figure 19. Example of the inundated area of the Karst Springs Restoration study area for a water surface elevation of 2.5 m AHD.

4.4.3 Modelling scenarios

Bool Lagoon Complex: Scenarios were designed to explore options for improving ecosystem health in Bool Lagoon through hydrological changes, mainly increased wetness. Initial scenarios were based on discussions with the Limestone Coast Landscape Board. Further scenarios may be undertaken following the completion of this report through engagement with the project stakeholders. Table 5 lists the scenarios completed to date.

Table 5. Scenarios for analysing the hydrology of the Bool Lagoon Complex under modified conditions.

Scenarios	Description
BLC-S1	Decrease inflow from Mosquito Creek by 20%
BLC-S2	Increase inflow from Mosquito Creek by 20%
BLC-S3	Turn off all groundwater pumping within 2 km of the Bool Lagoon Complex
BLC-S4	Turn off all groundwater pumping within 5 km of the Bool Lagoon Complex
BLC-S5	Block the downstream Bool Lagoon Complex regulator to Drain M
BLC-S6	Increase the elevation of the levee between the Main Basin (including Little Bool Lagoon) and the Central Basin (including Western Basin) by 0.20 m
BLC-S7	Increase the elevation of the levee between the Main Basin (including Little Bool Lagoon) and the Central Basin (including Western Basin) by 0.40 m

Karst Springs Restoration site: Scenarios for the Karst Springs Restoration sub-model were limited because wetland modifications are proposed for the site that have already been designed. Scenarios for the Karst Springs Restoration site are listed in Table 6.

Table 6. Scenarios for analysis the hydrology of the Karst Springs Restoration site.

Scenarios	Description
DC-S1	Decrease the crest of the downstream control weir at this site to 1.5 m AHD
DC-S2	Decrease the crest of the downstream control weir at this site to 1.7 m AHD
DC-S3	Increase the crest of the downstream control weir at this site to 2.2 m AHD
DC-S4	Increase the crest of the downstream control weir at this site to 2.5 m AHD
DC-S5	Decrease the rainfall to the wetland by 20%
DC-S6	Decrease the surface water inflow to this site by 20%

4.5 Water surface identification with remote sensing

The following describes efforts to use remotely sensed observations to check the predictions of wetland area from the Bool Lagoon Complex modelling. This investigation is further to the body of work that is described in the original project brief. The remotely sensed estimates of the inundated of the Bool Lagoon Complex are intended to provide a check on the results obtained from MODFLOW 6 modelling within the current study.

4.5.1 Satellite Imagery

Digital Earth Australia (DEA), a data platform developed by Geoscience Australia, delivers analysis-ready satellite data for monitoring temporal changes in Australia's land surface (Lewis et al., 2017). DEA offers free and open access to earth observation data from the Landsat (Loveland et al., 2012) and Sentinel-2 (ESA, 2015) satellite programs. The Landsat program, managed by the United States Geological Survey and NASA, includes three multi-spectral satellites: Landsat 5 TM (1984–2013), Landsat 7 ETM+ (1999–present), and Landsat 8 OLI (2013–present). These satellites capture imagery with a 30 m resolution and revisit the Earth approximately every 16 days. Landsat 5 TM, while operational from 1984, consistently collected data between 1987 and 2011, and was decommissioned in 2013. The Landsat 7 ETM+ and Landsat 8 OLI missions remain active; however, a scan-line corrector failure in Landsat 7 ETM+ in May 2003 introduced striping in the imagery due to missing data. Although no gap-fill algorithm is applied, the remaining data still provide valuable insights, especially when combined with imagery from Landsat 8 OLI (Andrefouet et al., 2003). Raw data from the Landsat missions have undergone corrections, standardisation, and orthorectification to create a 25-m resolution analysis-ready dataset (Dhu et al., 2017). This archive is accessible through DEA via the Open Data Cube API, enabling automated extraction and processing of Earth observation data.

4.5.2 Water Observations from Space (WOfS)

The Water Observations from Space (WOfS) algorithm identifies water presence by classifying cloud-masked pixels into three categories: wet, dry or invalid (e.g., where the latter is cloud-covered or on steep slopes) across all temporal observations (Mueller et al., 2016). It employs a decision-tree model informed by Landsat band ratios and supplementary datasets, such as valley bottom flatness and pixel quality, which enhance validation compared to simpler classifiers like the normalised difference water index (NDWI). WOfS is operationalised by Digital Earth Australia (DEA) to process the Landsat archive, offering a 34-year dataset of water classifications across Australia (1986 to 2020). Utilising this extensive archive, we extract pixels classified as wet to generate a series of maps depicting surface water bodies within the study area. While the WOfS classifier achieves a high overall accuracy of 97% in detecting water, its performance diminishes when water coexists with other features, particularly vegetation, within the same pixel. This limitation is pronounced in environments like wetlands and riparian zones, where mixed-pixel misclassifications commonly label wet areas as dry. The classifier performs optimally when analysing clear, unobstructed water surfaces captured by satellites (Mueller et al., 2016). Water surface maps derived from WOfS were used to compare and validate the modelled lake area. Notably, the failure of the scan-line corrector in Landsat 7 ETM+ in May 2003 resulted in imagery acquired post-failure containing stripes of missing data, as no gap-fill algorithm has been applied (Mueller et al., 2016). These data gaps adversely affect the overall quality of the satellite imagery. Moreover, the Bool Lagoon area is often cloud-covered, complicating the comparison between WOfS-derived and modelled water surface extents. To mitigate this issue, a cloud filter was applied, selecting images with less than 10% cloud coverage. This integration of remote sensing data with MODFLOW 6 offers a rare combination of these techniques for wetland analysis, and is expected to enhance confidence in the reliability of modelling outputs.

5 Results

5.1 Convert existing models: MODFLOW 2005 to MODFLOW 6

The wetland simulation models used in the current study apply MODFLOW 6, and have smaller spatial extents relative to existing models that are intended to assess the wider groundwater system. The first step in the methodology was to convert the parent, larger-scale models, developed in MODFLOW 2005, to MODFLOW 6. Subsequently, sub-models were extracted from the parent models, with the target wetlands centred within the resulting sub-models.

The Bool Lagoon Complex sub-model was extracted from the mid-south east sub-regional model (DEW, 2023a). A comparison of the original MODFLOW 2005 version of the model and a MODFLOW 6 version of the model is shown in Figure 20.

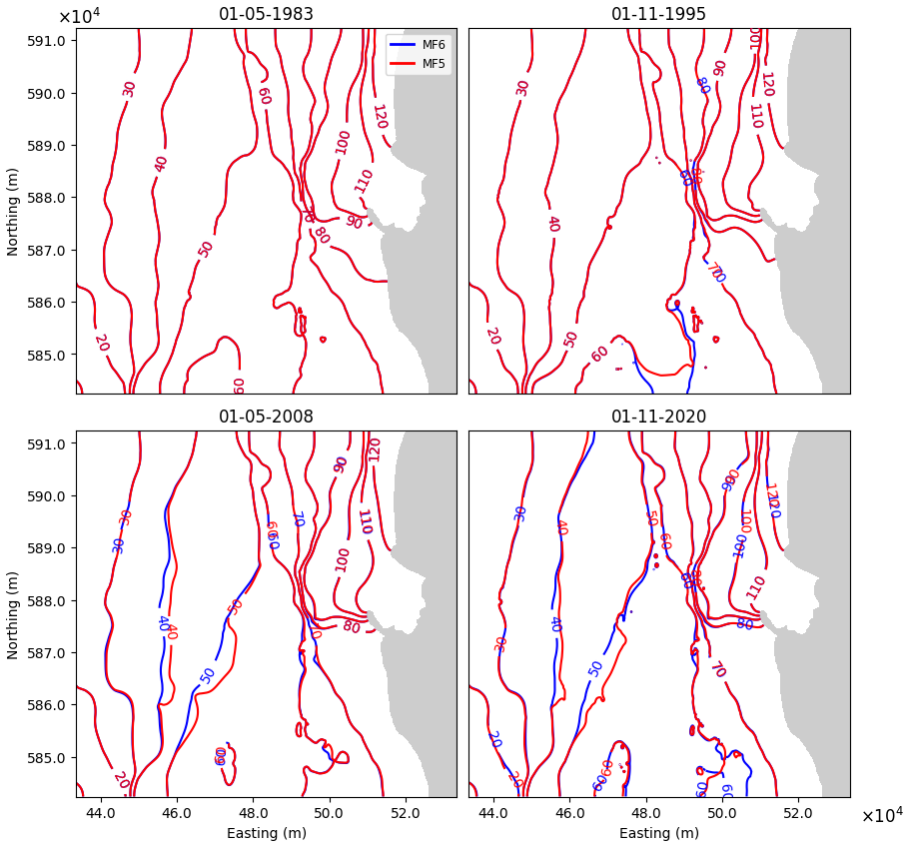

Figure 20. Comparison of head contours between MODFLOW 2005 (MF5; DEW, 2023a) and MODFLOW 6 (MF6) for the mid-south east sub-regional model at four different times.

The results in Figure 20 demonstrate reasonable similarity in head distributions between the MODFLOW 2005 and MODFLOW 6 models, which we consider indicates that the conversion between the two codes occurred correctly.

The Karst Springs Restoration sub-model was extracted from the coastal-areas south sub-regional model (DEW, 2023b). A comparison of the original model and a MODFLOW 6 version of the model is provided in Figures 21 to 23, for layers 1 to 3, respectively.

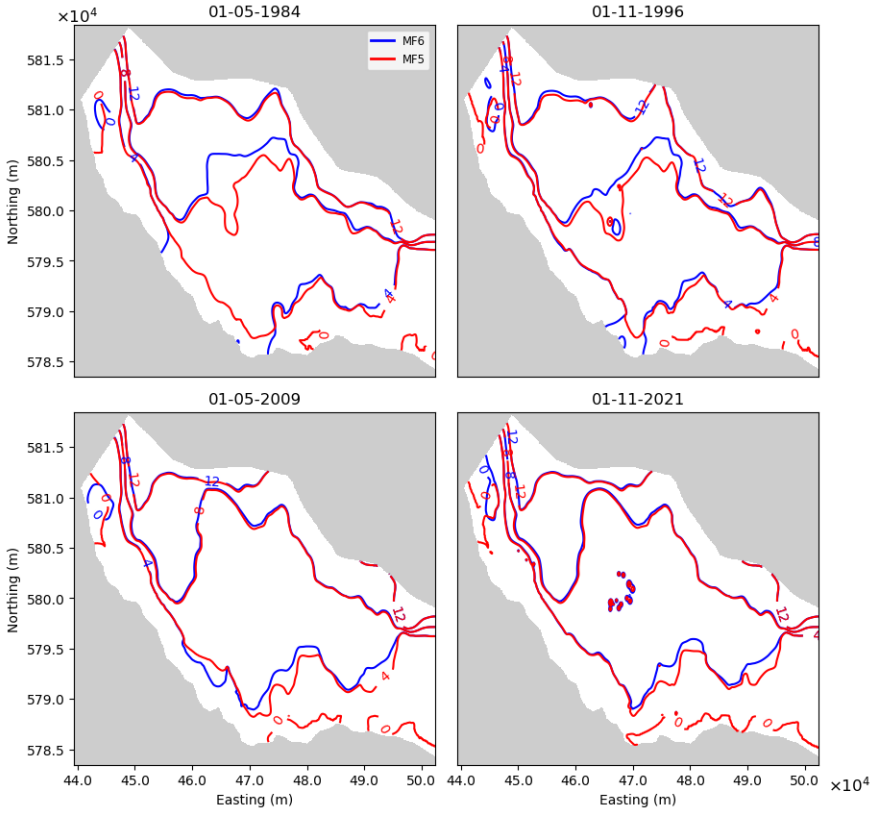

Figure 21. Comparison of head contours between MODFLOW 2005 (MF5; DEW, 2023b) and MODFLOW 6 (MF6) for the coastal-areas south sub-regional model at four different times (layer 1).

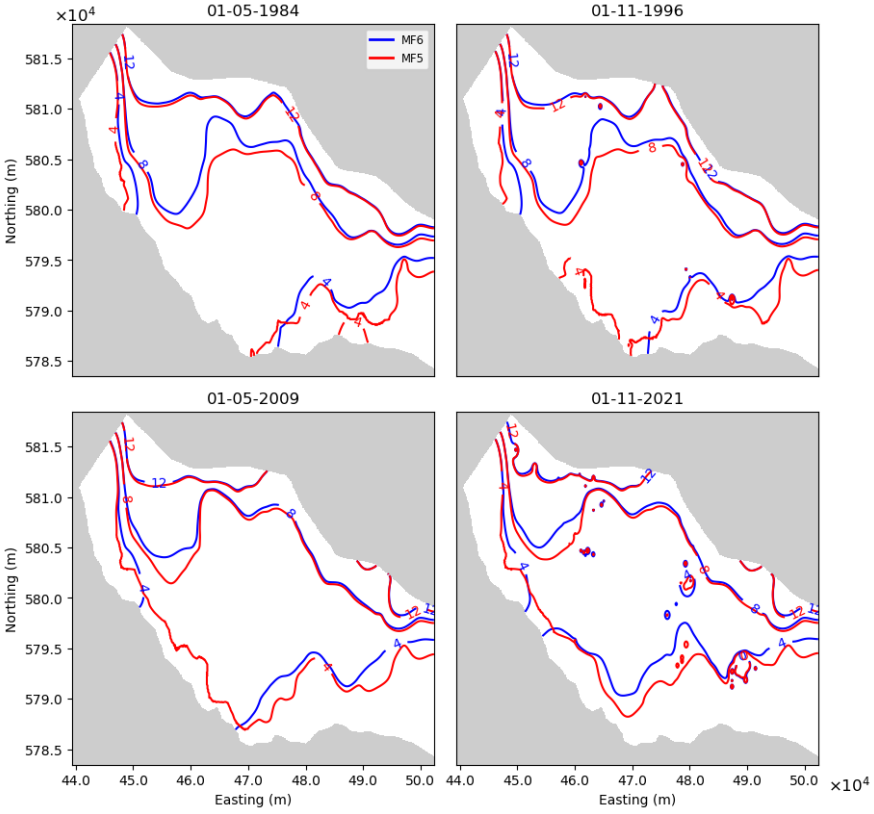

Figure 22. Comparison of head contours between MODFLOW 2005 (MF5; DEW, 2023b) and MODFLOW 6 (MF6) for the coastal-areas south sub-regional model at four different times (layer 2).

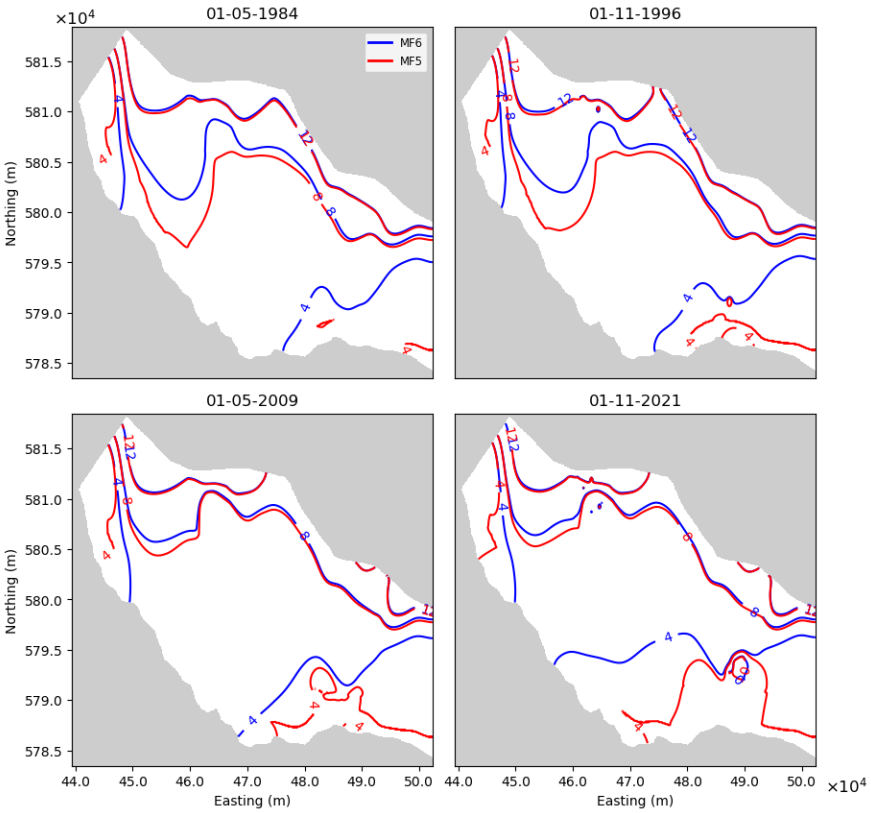

Figure 23. Comparison of head contours between MODFLOW 2005 (MF5; DEW, 2023b) and MODFLOW 6 (MF6) for the coastal-areas south sub-regional model at four different times (layer 3).

Figures 21-23 indicate reasonable overlap in the heads of the MODFLOW 2005 and MODFLOW 6 models in the northern part of those models. Near the coast, there are problems with the match between MODFLOW 2005 and MODFLOW 6. Our investigation into this discrepancy concluded that these differences are related to the approach to the ocean boundary condition adopted in the MODFLOW 2005 and MODFLOW 6 models. The MODFLOW 2005 model (DEW, 2023b) applies the SWI2 package, whereas the MODFLOW 6 uses a freshwater-only approach. The SWI2 model outputs equivalent freshwater heads (EFHs) in regions where seawater is predicted to occur, whereby the EFHs are calculated based on a density correction (for the higher density of seawater relative to freshwater) taken at the top of each model cell (Bakker et al., 2013). MODFLOW 6 outputs heads at the centre of the cell (Langevin et al., 2017), while density corrections for seawater in the aquifer are applied only at the seafloor, rather than within the groundwater system, as occurs within the SWI2 model.

Our previous research into the treatment of subsea boundary conditions (Solórzano-Rivas and Werner, 2018) found that assumptions about the salinity of offshore aquifers may significantly influence the extent of seawater. We contend also, following from this earlier work, that MODFLOW heads need to be assessed at cell centres given its formulation. Thus, heads reported by the SWI2 model may not be reliable. For this reason, we have neglected the mismatch between MODFLOW 2005 (with the SWI2 code enacted) and MODFLOW 6 (freshwater only). In general, the results shown in Figures 20 to 23 indicate that MODFLOW 2005 models were successfully converted to MODFLOW 6, notwithstanding challenges in reproducing the coastal boundary in the Karst Springs Restoration sub-model. Figure 24 shows the locality map of the proposed Karst Springs Restoration wetland along with observation wells, and compares groundwater levels around the Karst Springs Restoration wetland using the respective sub-model (in MODFLOW 6), the corresponding parent model (in MODFLOW 2005) over the period 1970–2022, and available field measured data from wells CAR066, MAC097 and MAC098 for layer 2, and CAR004 for layer 1.

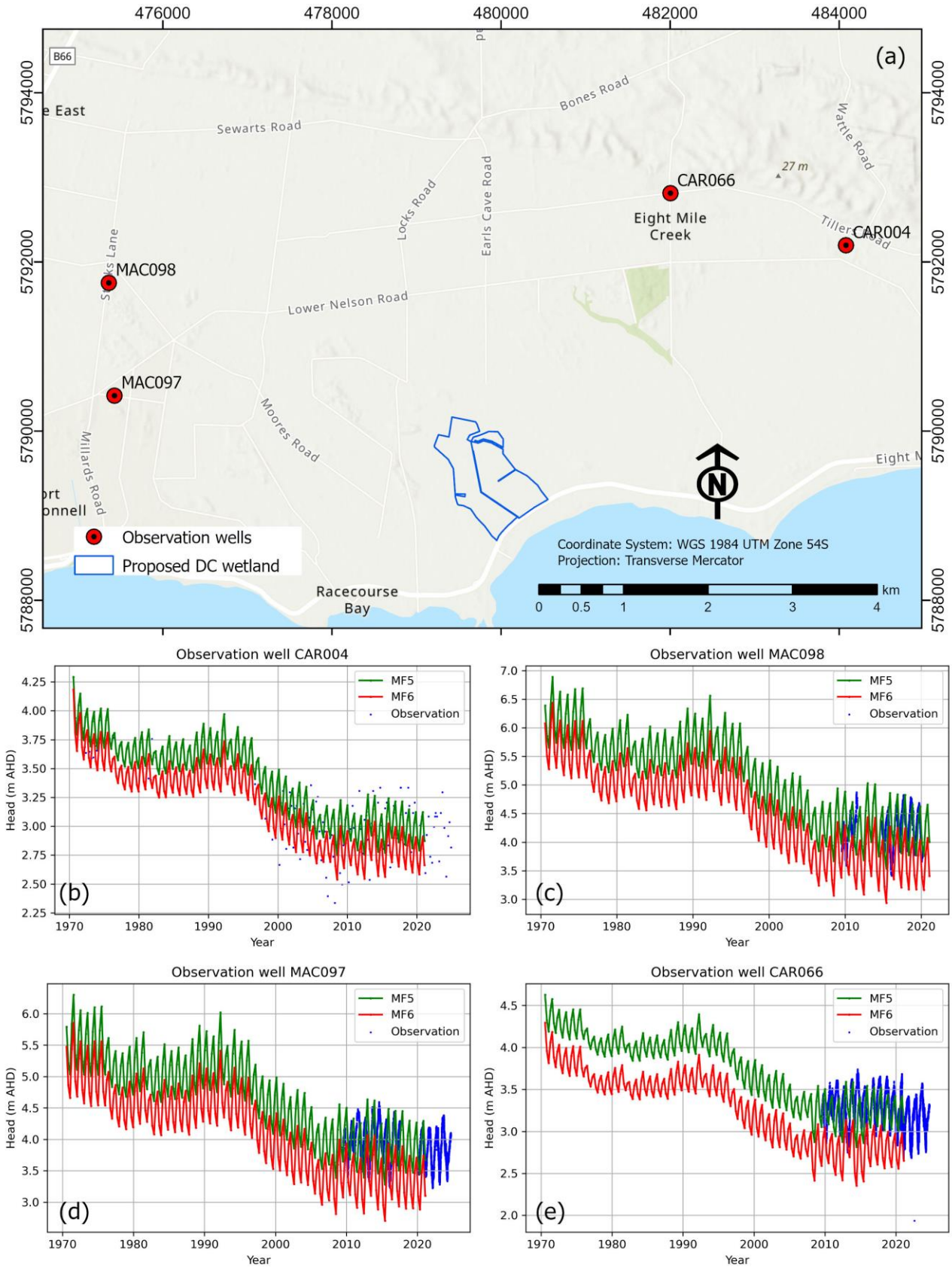

Figure 24. (a) Locality map of the proposed Karst Springs Restoration (i.e., Deep Creek; DC) wetland showing observation wells. (b) to (e) Comparison of groundwater water levels around the proposed DC wetland, showing the results from MODFLOW 2005 (MF5; DEW, 2023b) and MODFLOW 6 (MF6) for the period 1970–2024, and available field measured data (CAR066, MAC097 and MAC098 for layer 2 and CAR004 for layer 1).

Figure 24 illustrates that the groundwater levels simulated by the parent model (in MODFLOW 2005) and the Karst Springs Restoration sub-model (in MODFLOW 6) show reasonable similarity in groundwater level and similar trends, including long-term declines and seasonal variations. However, the water levels simulated by MODFLOW 6 are consistently lower than those simulated by MODFLOW 2005 over the simulation period. We attribute this to the aforementioned issues with consistency between MODFLOW 2005 (with SWI2) and MODFLOW 6, although other factors (such as differences in the numerical methods applied in the two versions of MODFLOW) may also have contributed to these discrepancies.

It is noteworthy that MODFLOW 2005 appears to produce a better match to the field data than the MODFLOW 6 model, especially at observation wells MAC098, MAC097, and CAR066. As can be seen in Figure 24, both models show the same general trend, but the MODFLOW 6 model underestimates the groundwater head values compared to MODFLOW 2005 by up to 0.7 m in some locations. As mentioned earlier, this is most likely related to differences in the coastal boundary condition. Re-calibration of the MODFLOW 6 model would likely achieve a better match, but this was not considered feasible given the timeframes of the current project.

5.2 Extracting sub-models from existing models

Sub-models were extracted from the MODFLOW 6 versions of the sub-regional models developed by DEW (2023a, 2023b). Figure 25 compares the Bool Lagoon Complex sub-model (in MODFLOW 6) with the corresponding parent model (in MODFLOW 2005) at four different times. This comparison was undertaken to test the validity of the sub-model extraction methodology.

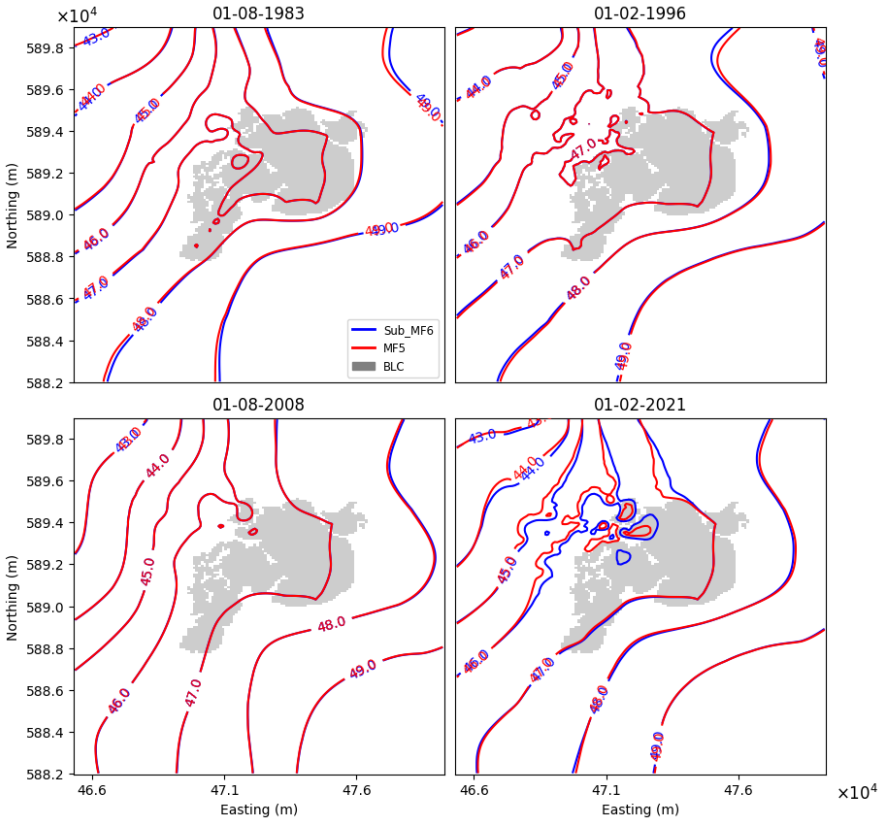

Figure 25. Comparison of head contours between the MODFLOW 2005 parent model (MF5) and the sub-model of the Bool Lagoon Complex ("Sub_MF6") developed in MODFLOW 6, at four different times. The grey area represents the location of Bool Lagoon Complex (BLC).

The groundwater heads from the extracted sub-model of the Bool Lagoon Complex (in MODFLOW 6) appear to be closely matched to those of the original MODFLOW 2005 parent model (DEW, 2023a). This alignment confirms that the sub-model extraction process and conversion to MODFLOW 6 was valid.

Figures 26 to 28 present comparisons between the MODFLOW 6 Karst Springs Restoration sub-model (shown for layers 1 to 3, respectively) and the MODFLOW 2005 parent model (DEW, 2023b).

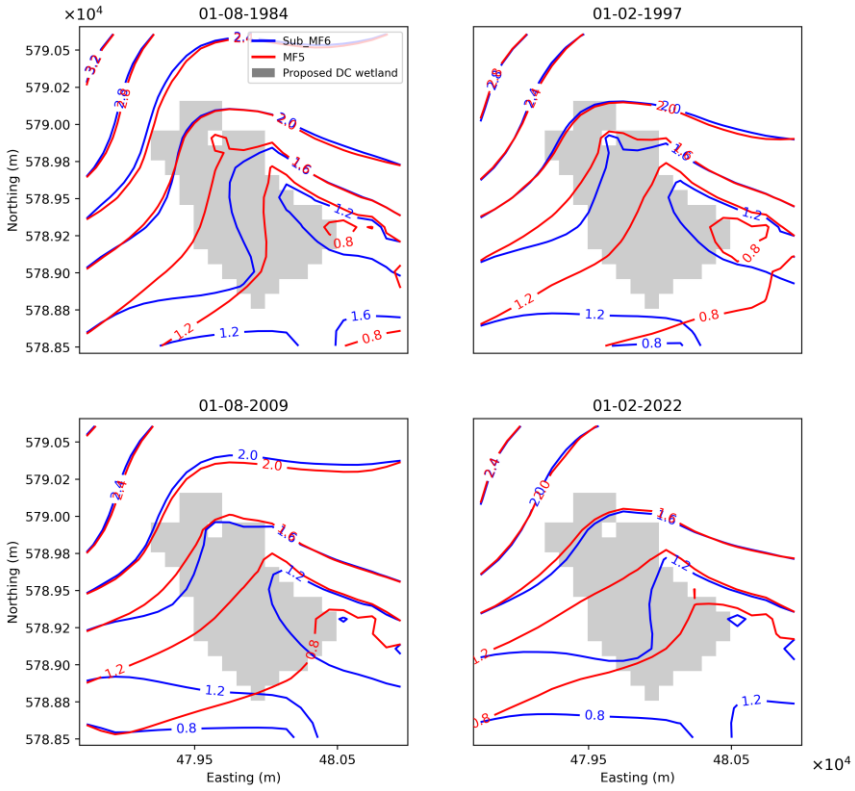

Figure 26. Comparison of head contours between the MODFLOW 2005 parent model ("MF5") and the sub-model of the Karst Springs Restoration site ("Sub_MF6"), developed in MODFLOW 6, at four different times (layer 1). The grey area indicates the location of the Karst Springs Restoration (i.e., Deep Creek; DC) site.

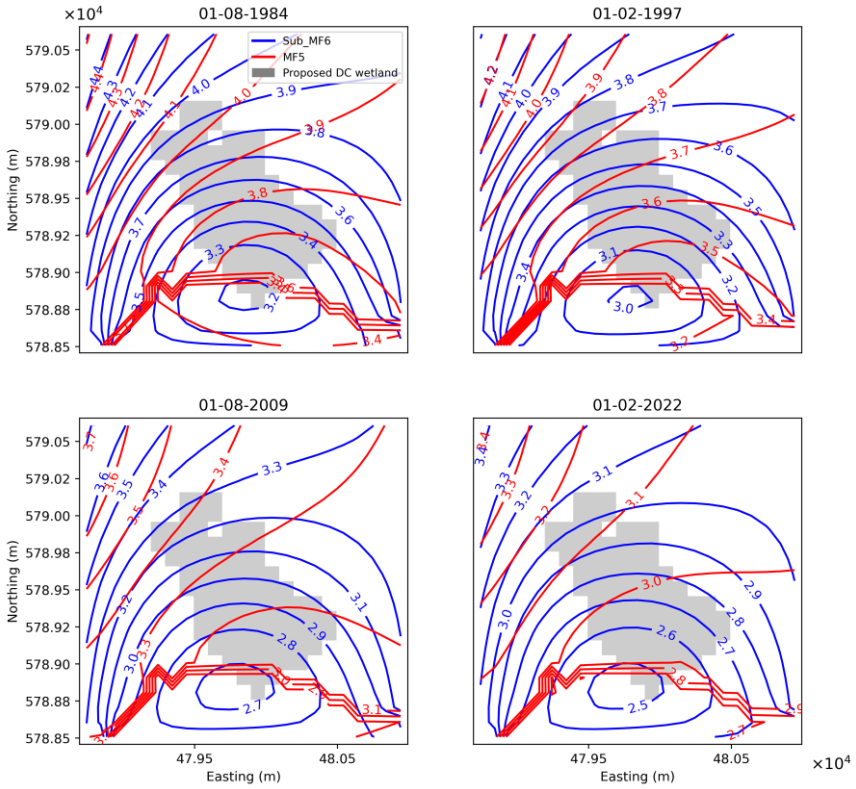

Figure 27. Comparison of head contours between the MODFLOW 2005 parent model ("MF5") and the sub-model of the Karst Springs Restoration site ("Sub_MF6"), developed in MODFLOW 6, at four different times (layer 2). The grey area indicates the location of the Karst Springs Restoration (i.e., Deep Creek; DC) site.

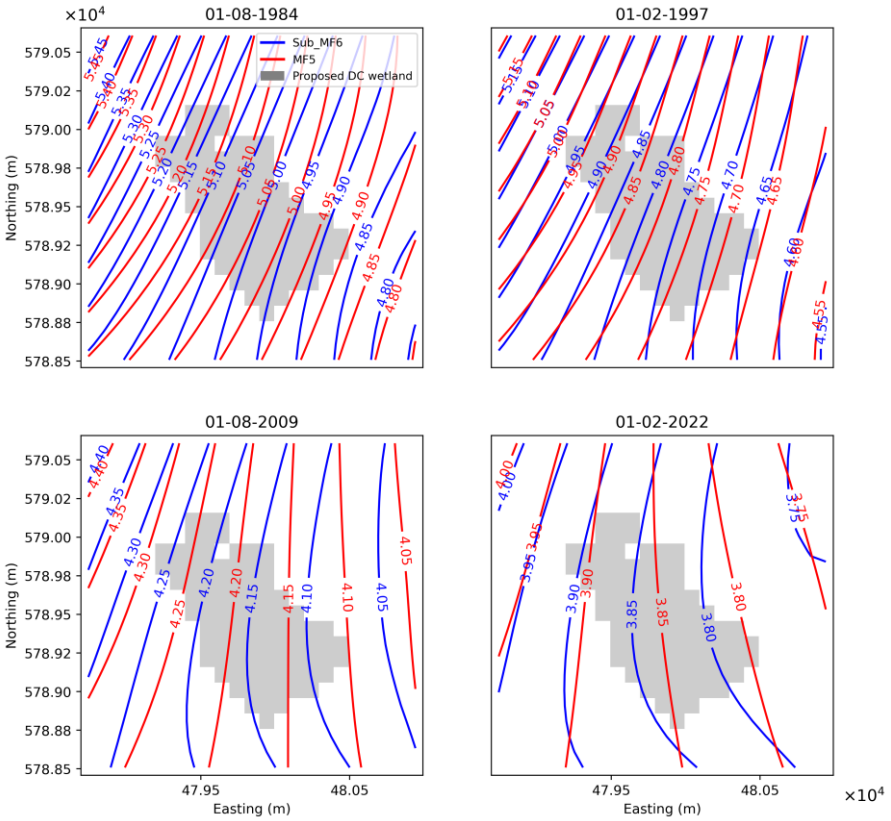

Figure 28. Comparison of head contours between the MODFLOW 2005 parent model ("MF5") and the sub-model of the Karst Springs Restoration site ("Sub_MF6"), developed in MODFLOW 6, at four different times (layer 3). The grey area indicates the location of the Karst Springs Restoration (i.e., Deep Creek; DC) site.

Figures 26 to 28 show significant differences between the MODFLOW 6 sub-model of the Karst Springs Restoration site and the parent MODFLOW 2005 (with the SWI2 package invoked). In all cases, the heads at the northern, eastern and western boundary are well matched. This occurs because the heads around those boundaries in the MODFLOW 6 sub-model were extracted from the parent model and applied as boundary conditions. Heads in the south and central parts of the study area differ between the models to varying degrees across the three layers. In layer 1 (Figure 26), the heads of the MODFLOW 6 model are generally higher than those of the parent model. The opposite occurs in layers 2 and 3 (Figures 27 and 28), with MODFLOW 6 model heads being lower than the parent model. A region of near-constant heads surrounded by a steep gradient is apparent in layer 2. This coincides with the occurrence of seawater in that layer, and is associated with the conversion from seawater heads to equivalent freshwater heads as discussed earlier.

5.3 Wetland simulation

Following construction of sub-models, as presented in the previous sub-section, the Lake package of MODFLOW 6 was added to each sub-model, with adjustments made to account for the explicit representation of the Bool Lagoon Complex and the Karst Springs Restoration wetlands. The following describes the results obtained from that endeavour.

5.3.1 Bool Lagoon Complex

Figure 29 compares the head contours of the sub-model (Bool Lagoon Complex) with the Lake package to those of the original MODFLOW 2005 parent model at four different times. The figure demonstrates that the

inclusion of the Lake package in the sub-model results in simulated heads that align closely with the original MODFLOW 2005 model. The consistency in contour patterns and head values validates the method for implementing the Lake package, and confirms that the modifications were implemented correctly. By effectively capturing interactions between surface water and groundwater, the Lake package maintains fidelity to the original model's outputs. These results indicate that the MODFLOW 6 sub-models with the Lake package applied are a reasonable reproduction of the groundwater hydrology of the original model of DEW (2023a).

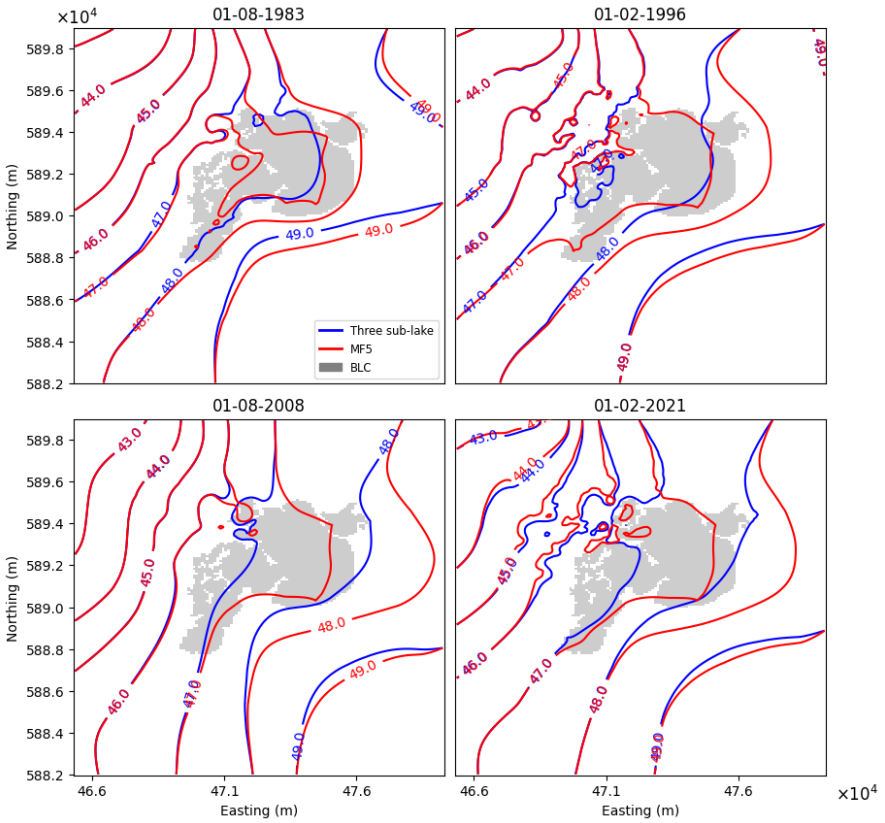

Figure 29. Comparison of head contours between MODFLOW 2005 ("MF5") and sub-models of Bool Lagoon Complex with the Lake package ("Three sub-lake") added using MODFLOW 6, at four different times. The grey area represents the location of Bool Lagoon Complex (BLC).

The sensitivity analysis of the lakebed leakance that was undertaken on the prototype MODFLOW 6 model involved applying multipliers of 0.1 and 2 to the base value of the lakebed's hydraulic conductivity. This was meant to cover the broad range of values obtained by the field testing of Taylor et al. (2015). The resulting variations in groundwater and surface water levels at observation wells and at wetland stage monitoring sites (locations shown in Figure 14) for different values of the lakebed hydraulic conductivity are presented in Appendix B. The findings indicate that variations in the lakebed hydraulic conductivity had only a small influence on groundwater heads at most observation wells, although the groundwater heads at observation wells ROB023 and ROB025 for the condition where the hydraulic conductivity is multiplied by 0.1 were lower compared to models adopting higher values of the lakebed hydraulic conductivity. Comparison of observation data and simulated surface water levels shows that when the hydraulic conductivity multiplier is set to 0.1, the match between observed and simulated data weakens, particularly at gauging stations A2391066 and A2391067. The match with the prototype lakebed hydraulic conductivity and double this value produced approximately the same match to field data.

5.3.2 Karst Springs Restoration site

Figure 30-32 shows comparisons between the MODFLOW 6 Karst Springs Restoration sub-model with the Lake package added (shown for layers 1 to 3, respectively) and the MODFLOW 2005 parent model (DEW, 2023b).

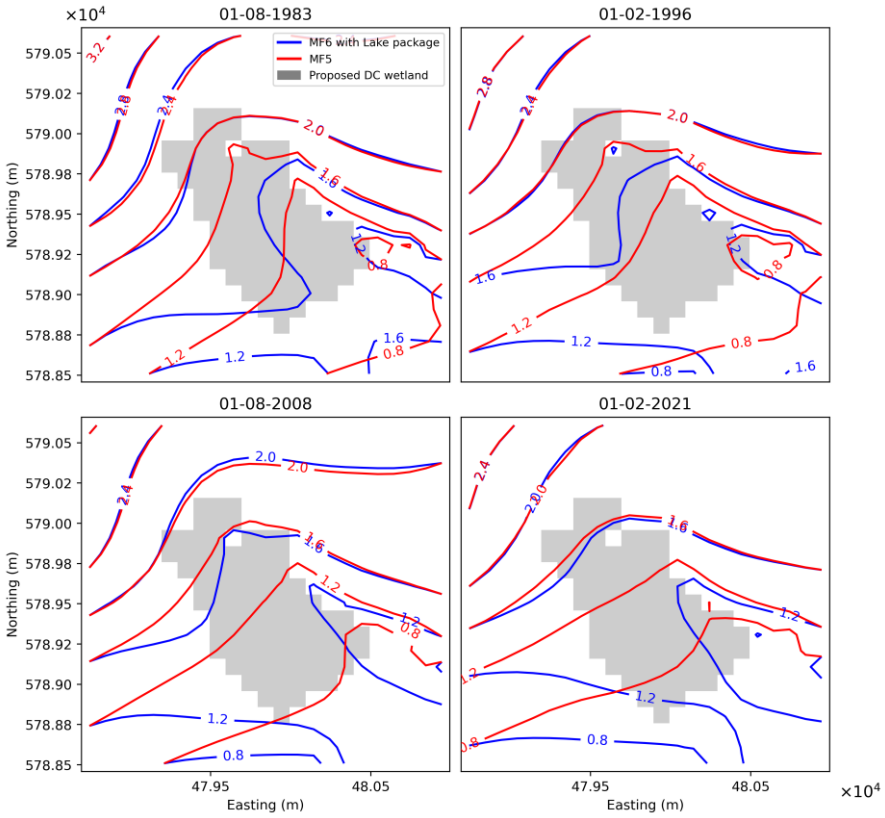

Figure 30. Comparison of head contours between MODFLOW 2005 ("MF5") and sub-model of the Karst Springs Restoration site with added Lake package ("MF6 with Lake package"), developed in MODFLOW 6, at four different times (layer 1). The grey area indicates the location of the Karst Springs Restoration (i.e., Deep Creek; DC) site.

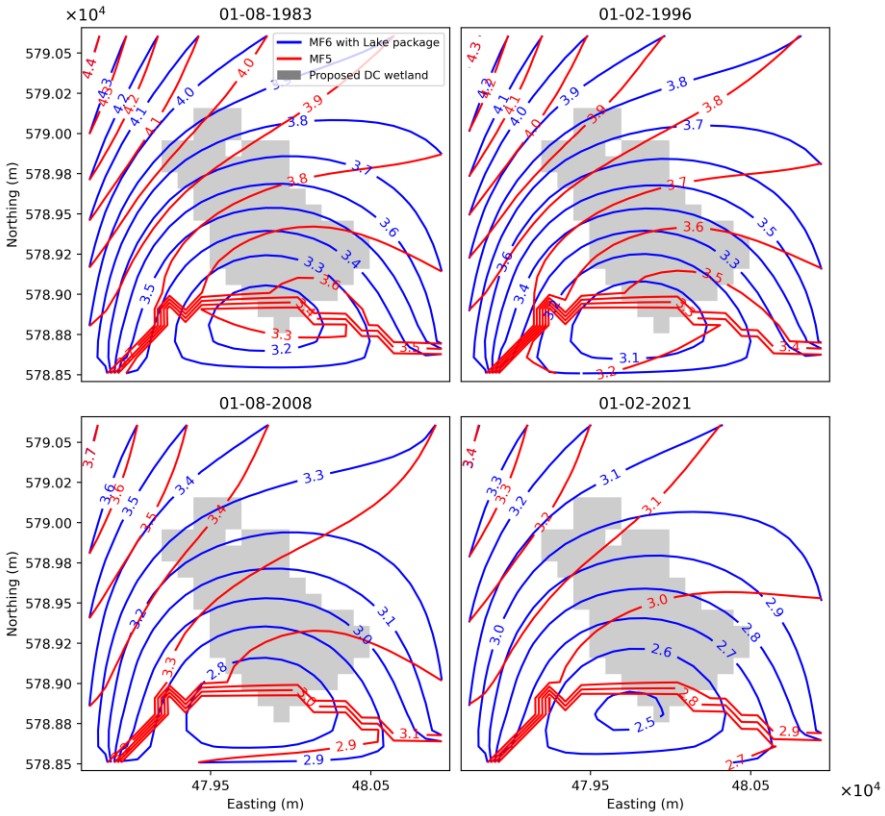

Figure 31. Comparison of head contours between MODFLOW 2005 ("MF5") and sub-model of the Karst Springs Restoration site with added Lake package ("MF6 with Lake package"), developed in MODFLOW 6, at four different times (layer 2). The grey area indicates the location of the Karst Springs Restoration (i.e., Deep Creek; DC) site.

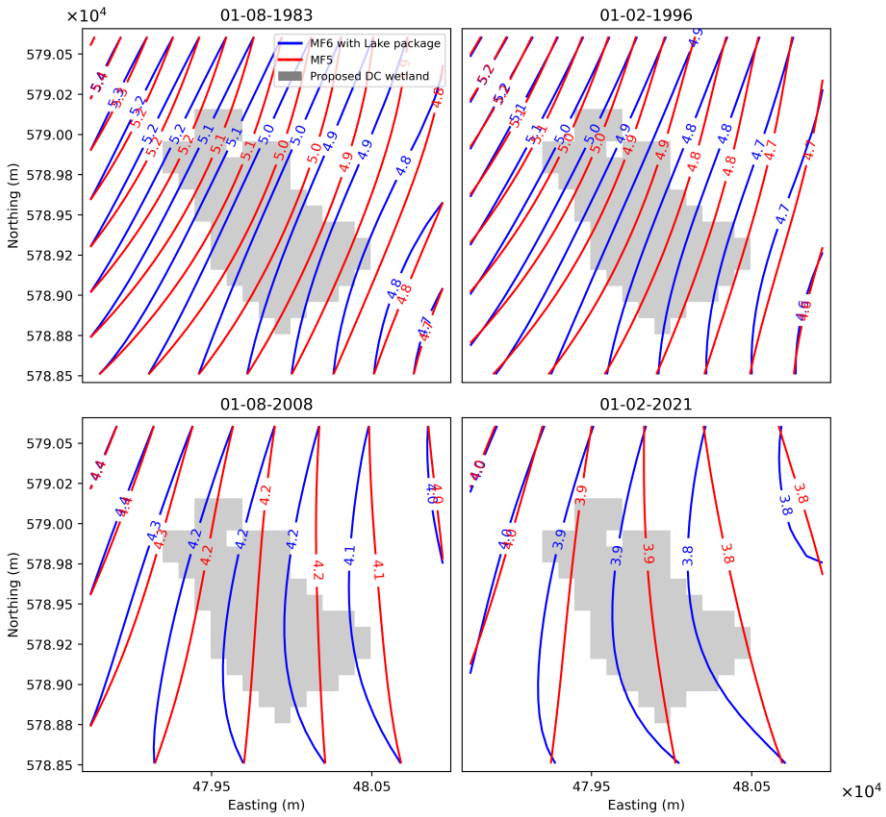

Figure 32. Comparison of head contours between MODFLOW 2005 ("MF5") and sub-model of the Karst Springs Restoration site with added Lake package ("MF6 with Lake package"), developed in MODFLOW 6, at four different times (layer 3). The grey area indicates the location of the Karst Springs Restoration (i.e., Deep Creek; DC) site.

Figures 30 to 32 illustrate significant differences between the MODFLOW 6 sub-model of the Karst Springs Restoration site, which incorporates the Lake package, and the parent MODFLOW-2005 model with the SWI2 Package. The reasons for these discrepancies are explained in Sections 5.1 and 5.2.

The sensitivity analysis of the lakebed leakance involved applying multipliers of 0.2 and 5 to the base value of the lakebed's hydraulic conductivity. The results of the variation in groundwater levels at selected cells (locations shown in Figure 33) for different values of the lakebed's hydraulic conductivity, are presented in Appendix B. The findings indicate that these variations in the lakebed's hydraulic conductivity did not significantly affect groundwater heads.

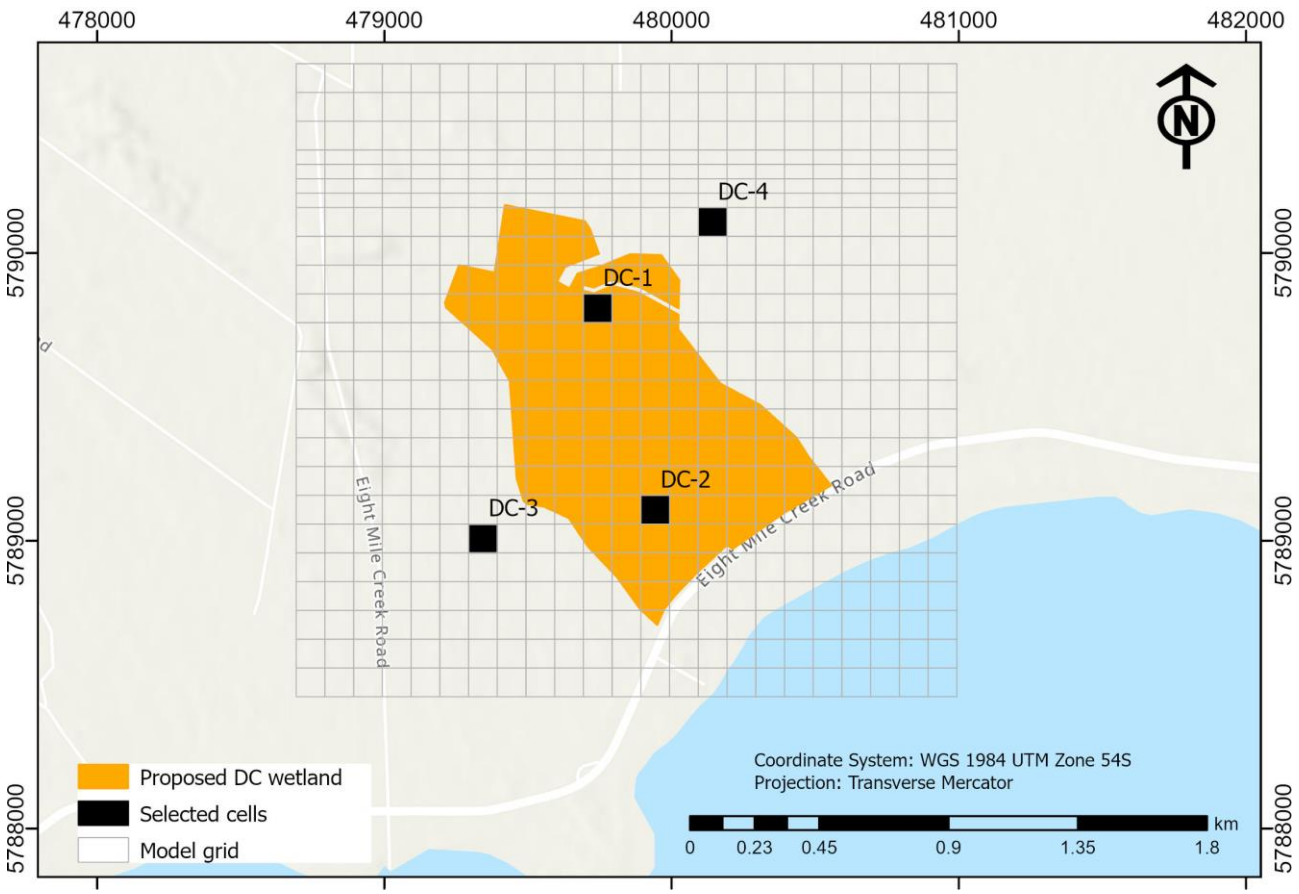

Figure 33. Locality map of the proposed Karst Springs Restoration (i.e., Deep Creek; DC) wetland, showing the model grid of the Karst Springs Restoration sub-model and selected cells used for groundwater head sensitivity analysis.

5.3.3 Comparison between modelled and remotely sensed water surface

After applying the cloud filter to all available WOfS images, 726 images remained for further analysis, including 528 images acquired after the failure of the scan-line corrector in May 2003. For illustrative purposes, a comparison between lake surface extent on selected dates, as derived from the lake-groundwater coupled model and WOfS, is presented in Figure 34. Visual inspection reveals that the modelled inundation area is by-and-large reasonably consistent with that derived from WOfS. However, the current MODFLOW 6 model adopts a 3-part separation from north to south, which limits its ability to accurately simulate the hydrological processes of wetlands. This simplification leads to variations in the distribution of the water body compared to the WOfS data, further exacerbated by the differences in resolution between the model cells (100 m x 100 m) and WOfS pixels (30 m x 30 m). The inundated area of MODFLOW 6 aligns more closely with those derived from WOfS during wet periods, when the lake stage is high (e.g., 22 August 1988 and 27 January 2011, as shown in Figure 34). During other periods, however, Bool Lagoon is characterised by a mixture of wetland vegetation and water, with portions of the water body obscured by vegetation. This complexity challenges the WOfS classification algorithm, making it difficult to accurately distinguish between water and vegetation. Perhaps the most significant difference between MODFLOW 6 outputs and WOfS was that the MODFLOW 6 model failed to capture the complete dryness of Bool Lagoon that is apparent in WOfS data during some drought periods (e.g., 25 April 2020, as shown in Figure 34). However, the classification algorithm of WOfS is limited in distinguishing shallow water from vegetation, as discussed above, and therefore, it remains unclear as to whether WOfS or MODFLOW 6 is in error during drought periods.

Constraints in the conceptual model of the Bool Lagoon Complex, used in the Lake package, likely contribute to differences between WOfS and MODFLOW 6, given that a uniform lake surface is assumed in MODFLOW 6 for each sub-lake, which oversimplifies the variability in surface water conditions. Despite these limitations,

the proposed model framework should be considered as a reasonable modelling tool for further investigating lake-groundwater interactions in the Bool Lagoon Complex and other key wetlands, although care is needed when interpreting the wetland hydrology predicted by MODFLOW 6 during drought periods.

1988-08-22

(a)

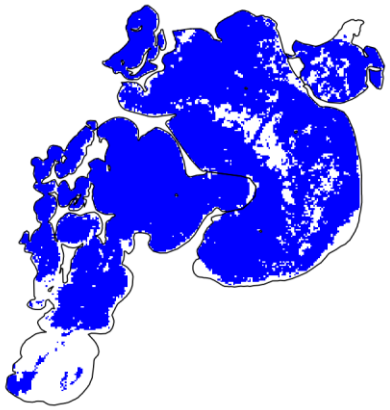

Area of water surface : 20.32 km^2

(b)

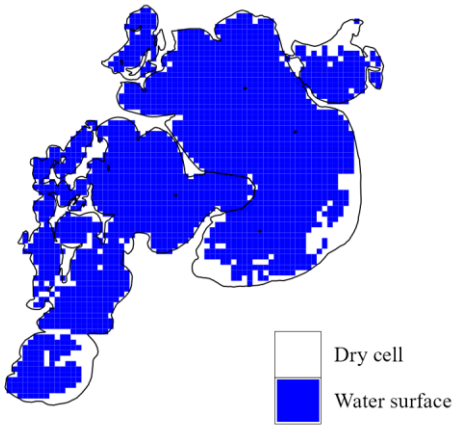

Area of water surface : 22.6 km^2

1996-02-18

(a)

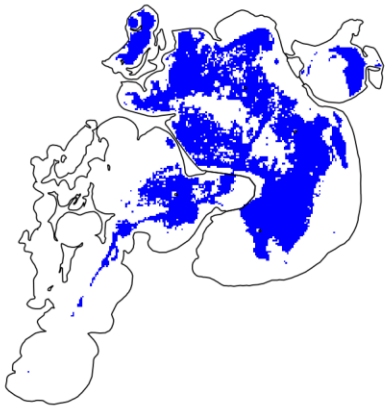

Area of water surface : 7.99 km^2

(b)

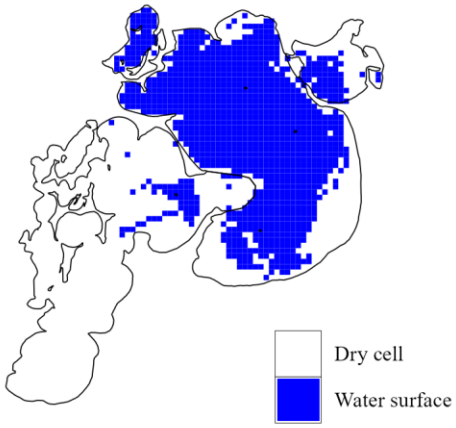

Area of water surface : 11.55 km^2

2011-01-27

(a)

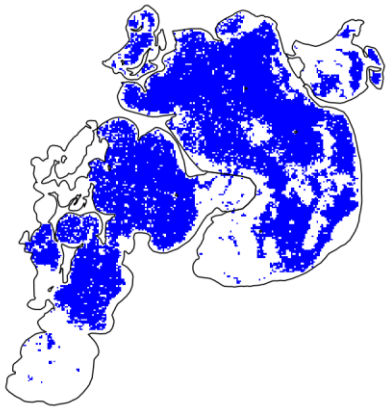

Area of water surface : 13.75 km^2

(b)

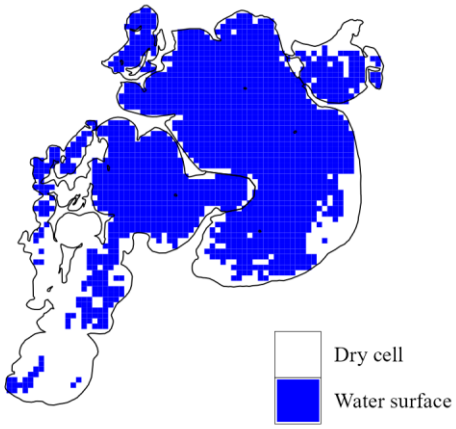

Area of water surface : 18.36 km^2

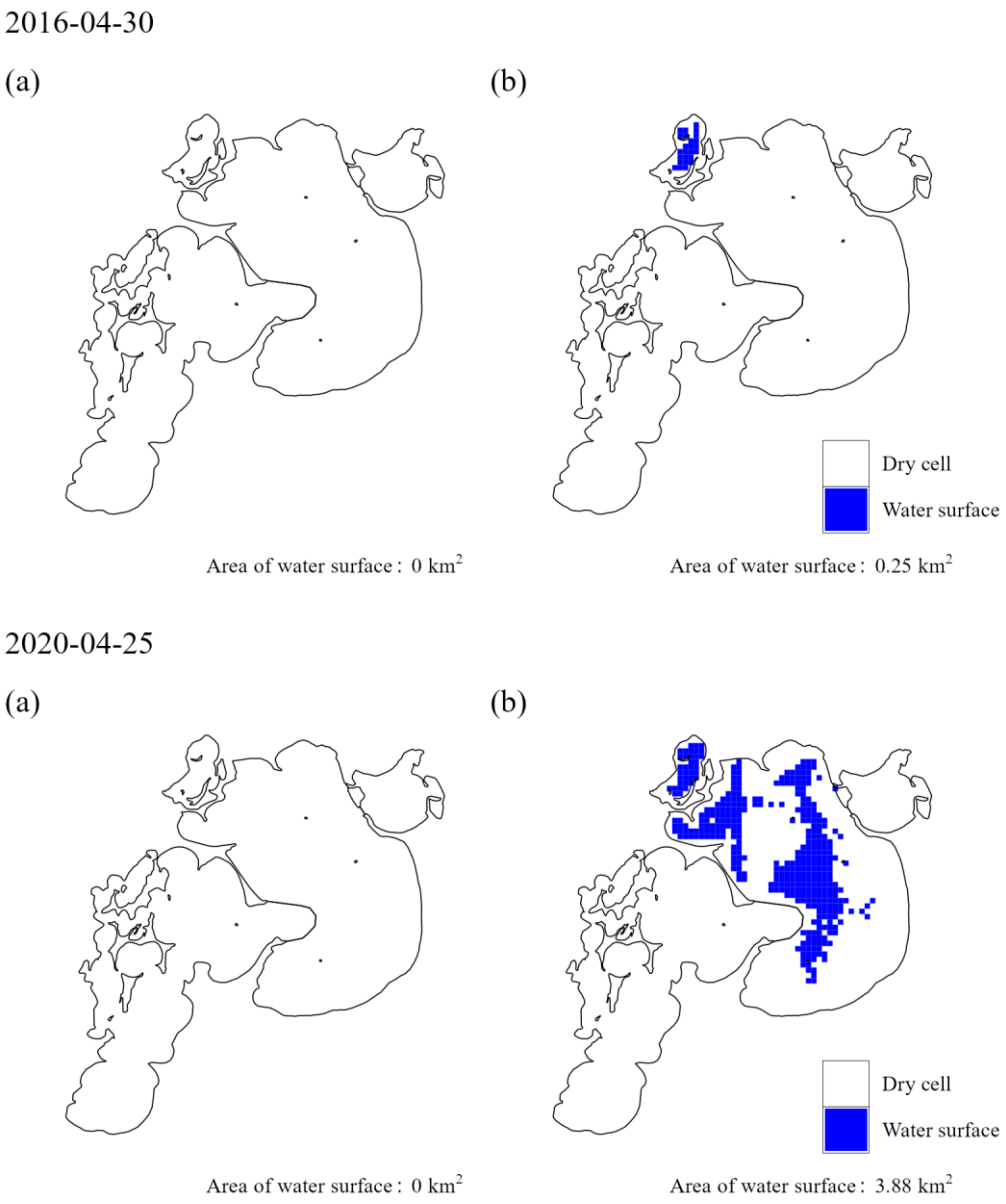

Figure 34. Comparison between (a) WOfS-derived inundated area of Bool Lagoon, and (b) Bool Lagoon inundated area (from the Lake package) in MODFLOW 6. Images (from top to bottom) apply to specific dates in 1988, 1996, 2011, 2016 and 2020.

5.4 Results of modelling scenarios

5.4.1 Bool Lagoon Complex

At the time of writing this report, the Bool Lagoon Complex sub-model was used to run seven predictive scenarios aimed at exploring various options for improving ecosystem health in Bool Lagoon. These scenarios were designed to assess the implications of specific changes (see Section 4.4.3) in water management practices on both surface water and groundwater systems.

The first scenario (BLC-S1) simulates a 20% decrease in inflow from Mosquito Creek, representing drought conditions or upstream water abstractions that could limit inflow. Similarly, the second scenario (BLC-S2) examines a 20% increase in inflow from Mosquito Creek, reflecting potential upstream water management

interventions to enhance water availability. Both scenarios applied uniform adjustments to inflow rates across all time steps in the simulation.

The third and fourth scenarios (BLC-S3 and BLC-S4) focused on the impacts of restricting groundwater pumping near BL. The third scenario proposed ceasing all groundwater pumping within a 2-km radius of the Bool Lagoon Complex, while the fourth scenario extended this restriction to a 5-km radius. For the 2-km radius case, this involved the cessation of approximately 0.78 ML/d (time-averaged) of extraction, while the 5-km case, 3.42 ML/d (time-averaged) were removed from the model. These scenarios aimed to evaluate the potential benefits of reduced groundwater extraction for alleviating stress on the hydrological system and improving the lagoon's ecological health.

Despite these varied configurations, the results from the first four scenarios indicate no significant changes in groundwater head and surface water levels at local groundwater monitoring wells and surface water monitoring sites, respectively (see Figure 14 for their locations). Additionally, the results show no significant changes in the inundation area of Bool Lagoon in these scenarios. Appendix C shows a comprehensive comparison of results between the base model and the predictive scenarios modelled. The comparisons include key hydrological parameters such as groundwater levels, surface water levels, inundation area, and water volume.

In the fifth scenario (BLC-S5), we examined the effects of blocking the downstream regulator (of the Bool Lagoon Complex) to Drain M. Our first attempt to simulate this utilised the Bool Lagoon Complex sub-model configured as a single lake. The model predicts that this scenario would lead to a significant increase in water levels within the Bool Lagoon Complex, an improvement in groundwater levels, and an expansion of the inundation area of the Bool Lagoon Complex (see Appendix C), although the water levels in the Bool Lagoon Complex rose to unrealistic values at times of highest inflows.

The sixth and seventh scenarios (BLC-S6 and BLC-S7) examined the impact of increasing the elevation of the levee between the Main Basin (including Little Bool Lagoon) and the Central Basin (including Western Basin), with the levee raised by 0.20 m and 0.40 m in BLC-S6 and BLC-S7, respectively. These scenarios aimed to assess the potential benefits of modifying the levee elevation to improve the lagoon's ecological health. The model predicts that raising the levee elevation between the Main and Central Basins increases water levels in the Main Basin (upstream of the levee), with the time-averaged water level rising from 47.87 m in the base scenario (BLC-S0) to 48.01 m in BLC-S6 and 48.14 m in BLC-S7. The largest water level rise over the time series produced by the model was 0.20 m in BLC-S6 and 0.40 m in BLC-S7. The simulation results show an increase in surface water levels in Hacks Lagoon during dry conditions, with the time-averaged water level increasing from 48.10 m in the base scenario (BLC-S0) to 48.12 m in BLC-S6 and 48.14 m in BLC-S7. The largest increase in the water levels of Hacks Lagoon over the simulation period (1970–2021), caused by the levee raising, was 0.11 m in BLC-S6 and 0.20 m in BLC-S7, which occurred under dry conditions.

Raising the levee had a complicated effect on the downstream Central Basin (including Western Basin). For example, water levels in the Central Basin (including Western Basin) were higher during dry conditions and lower during wet conditions once the levee was raised. The time-averaged Central Basin (including Western Basin) water level increased from 47.64 m in the base scenario (BLC-S0) to 47.69 m in BLC-S6 and 47.71 m in BLC-S7. This increase was mainly caused by higher water levels (by up to 0.68 m and 1.12 m (maxima across the 51-year simulation) for BLC-S6 and BLC-S7, respectively, during dry conditions. Water levels were lower during wet conditions; by up to 0.21 m and 0.28 m, respectively. The higher water levels in the Central Basin (including Western Basin) are attributable to groundwater level increases with the levees in place, whereby groundwater levels were higher by up to 0.24 m and 0.38 m, respectively, at monitoring well ROB25 (see Figure 14 for its location). Evaluation of the inundation area indicates that an expansion of the areal extent of the water body resulted from raising the levee, consistent with the higher water levels, with BLC-S7 causing a greater expansion than BLC-S6, as expected.

5.4.2 Karst Springs Restoration site

Six predictive scenarios were implemented to examine the hydrological implications of modifying the downstream control weir crest and reducing water inputs at the proposed Karst Springs Restoration wetland.

As summarised in Table 6, these scenarios involved adjusting the weir crest height and decreasing either rainfall or surface water inflow. Four selected groundwater monitoring cells (Figure 33) were used to evaluate changes in groundwater head, while variations in surface water levels, water volumes, and inundation areas were also assessed. The results are presented in Appendix D.

- DC-S1: Lowering the weir crest by 0.50 m (from the initial crest elevation of 2.0 m AHD) produced an average decrease of approximately 0.50 m in the wetland's surface water level over the 1970–2022 simulation period – as expected. Concurrently, the volume of water stored in the wetland, on average, declined from 9.59×10^4 m³ (95.9 ML) to 0.54 m³, effectively eliminating the wetland's storage capacity. Despite these changes in surface water conditions, only small differences in the groundwater heads (between scenarios) were observed at the four monitoring cells.
- DC-S2: Lowering the weir crest height by 0.30 m (from the initial elevation of 2.0 m AHD) resulted in an average decrease of approximately 0.30 m in surface water levels across the wetland during the 1970–2022 simulation period – again, as expected. This change also led to a sharp reduction in the time-averaged water volume – from 9.59×10^4 m³ to 1.85×10^4 m³ —creating a significantly reduced wetland water body. Groundwater levels at the four monitoring locations again showed only minor differences between cases.
- DC-S3: Raising the weir crest by 0.20 m led to an average increase of approximately 0.20 m in the wetland's surface water level over the simulation period. Correspondingly, the time-averaged water volume in the wetland was increased from 9.59×10^4 m³ to 17.31×10^4 m³, accompanied by a noticeable expansion in the inundation area. As with the cases above, only small changes in groundwater heads were detected in the model, indicating that groundwater levels are not strongly linked to the wetland conditions, at least at wells that we assessed in the model.
- DC-S4: A further increase in the weir crest elevation (raised to 0.50 m) caused the wetland water levels to increase from 2.08 m AHD to 2.58 m AHD (averaged over the 52-year simulation). This resulted in a significantly greater wetland volume, from 9.59×10^4 m³ to 33.84×10^4 m³ (time-averaged values), and a notable increase of the inundation area. As in the other weir-adjustment scenarios, groundwater heads at the four monitoring cells showed only small differences with the base case simulation, suggesting that higher weir crests do not appreciably affect the shallow groundwater system at this site.
- DC-S5: A 20% reduction in rainfall (applied to the wetland – noting that the aquifer recharge doesn't change from the base case) yielded only small changes in surface water levels (i.e., the water level was lower by 0.0001 m), water volumes, and inundation extents relative to the baseline. Groundwater heads were almost unchanged at the monitored sites.
- DC-S6: Reducing surface water inflow by 20% resulted in only a minimal reduction in surface water levels (0.01 m on average) and a small decrease in wetland volume (compared to the base model, DC-S0). The inundation area also decreased minimally, and there were only very small changes in groundwater heads at the four monitoring cells.

The scenario results highlight the dominant role of weir-crest modifications in influencing surface water dynamics (levels, volume, and inundation) at the proposed Karst Springs Restoration wetland, while groundwater heads at the monitoring cells exhibit weak connectivity to the wetland conditions in terms of the weir elevation, inputs, storage volume, etc.

6 Discussion

This study aimed to evaluate various intervention measures to improve the hydrological conditions, benefiting ecosystem health, at the Bool Lagoon Complex and at the Karst Springs Restoration site. For the Bool Lagoon Complex, the comparison between field measurements of wetland water levels (Figures A1 to A5, and A13 to A17) and outflows to Drain M (Figures A11 to A12, and A23 to A24) indicates that the models developed in this study provide an acceptable match with observation data. This was the case whether the Bool Lagoon Complex was considered as a single lake or divided into three lakes. We undertook very limited calibration steps to obtained an improved match to field measurements, mainly focussing on the outlet boundary condition.

Discrepancies between observed and simulated surface water levels for the Bool Lagoon Complex arise most likely due to simplifications in the treatment of the surface water domain in MODFLOW 6, which is primarily a groundwater modelling program. For example, water movement within each of the lake water bodies (the Bool Lagoon Complex was simulated using up to three water bodies) is not simulated by the Lake package. Water moving from upstream to downstream in the Bool Lagoon Complex was simulated by partitioning the system into sub-lakes, with each having a horizontal water surface, whereas in reality, the shallow water of Bool Lagoon probably creates complex flow patterns and spatially varying water surface elevations that are not simulated in MODFLOW 6's Lake package. That is, the Lake package assumes a uniform water surface elevation for each lake or sub-lake, and even though this varies between time steps depending on inputs and outputs, flow dynamics within each sub-lake is reduced to a simple water balance calculation. We attempted to partly account for this by dividing the Bool Lagoon Complex into three sub-lakes, although the connection between the sub-lakes is approximate and whether the division into three lakes optimally represents the effects of natural restrictions to flow within the system has not been tested. Another source of approximation in the model is that the lake bottom was discretised at the same resolution as the underlying groundwater model, which has a cell size of 100 m x 100 m, potentially oversimplifying local-scale topography features that influence flow patterns in the Bool Lagoon Complex, and contributing to the discrepancies in water levels between simulated outputs and field data.

As an extension to the original expectations for this project, we compared the simulated inundated area of the Bool Lagoon Complex with remote sensing data. This aligns with recommendations by Turnadge and Lamontagne (2015) to use remote sensing data to evaluate the hydrology of Limestone Coast wetlands. The comparison demonstrated a reasonable match, although there are challenges in applying the interpretations of WOfS due to the vegetation cover in the Bool Lagoon Complex and other shortcomings in the remotely sensed data. Additionally, the spatial resolution of WOfS and the MODFLOW 6 model are different, with model cells being 100 m x 100 m and the WOfS pixels being 30 m x 30 m. Nevertheless, we concluded from this comparison that the model reasonably simulated the spatial extent of wetland inundation as a function of time. A more rigorous comparison between MODFLOW 6 and WOfS is recommended for subsequent investigations to more closely scrutinise the performance of the wetland-groundwater model. This would probably allow for the Bool Lagoon Complex to be subdivided into a larger number of distinct water bodies, and capture more of the complexity of the system.

The Karst Springs Restoration model adopted only a single lake because of its smaller size, and we are unable to evaluate whether the predicted inundated areas are correct, because the model represents a new situation, for which there is not historical data (i.e., surface water levels for the simulated conditions) to assess the model performance.

A sensitivity analysis of lakebed leakance was undertaken for both case study sites because the knowledge of lakebed sediments and the hydraulic conductivity thereof is limited. In the sensitivity analysis of lakebed leakance, the prototype model values were multiplied by 0.1 and 2 for the Bool Lagoon Complex (Figures B1 to B10) and 0.2 and 5 for the Karst Springs Restoration site (Figures B11 to B15). The higher multiplier values for the Karst Springs Restoration site were adopted because the base case value for the lakebed leakance produced only small changes in the groundwater system between scenarios. Given the greater uncertainty in the lakebed sediments at that site, it was considered necessary to explore more conductive lakebed options to determine whether the surrounding aquifer might respond to the wetland restoration of the site. The effect of changing the lakebed leakance was assessed by considering the surface water levels (at sites

where observations are available), and the groundwater heads at five observation well locations near the Bool Lagoon Complex (Figure 14) and at four locations near the Karst Springs Restoration site (Figure 33) (noting that there is a lack of groundwater monitoring wells in close proximity to the Karst Springs Restoration site).

Based on the sensitivity analysis of lakebed hydraulic conductivity across Bool Lagoon Complex, applying a 0.1 multiplier decreased the agreement between observed and simulated surface water levels—particularly at gauging stations A2391066 and A2391067 (Figures B1 to B5)—and groundwater levels, especially at observation wells within the lagoon (ROB23 and ROB25) (Figures B6 to B10). It appears from this result that the lakebed leakance is not lower than the value adopted in the base case scenario. Also, this seems to indicate water exchange between the wetland and the surrounding aquifer, whereby discrepancies arise between field data and the model if a lower lakebed leakance is adopted that limits the interaction between surface water and groundwater.

Results of the sensitivity analysis of lakebed leakance for the Karst Springs Restoration site indicates that variations had minimal impact on surface water levels (Figure B11) and groundwater heads (Figures B12 to B15). The reason behind this is that inflows into the wetland are high relative to the wetland size, creating fairly stable surface water levels regardless of changes in the rates of leakage to groundwater, at least within the parameter ranges tested here. The lack of observation wells near the Karst Springs Restoration wetland site makes it challenging to assess the nearby groundwater response to lakebed leakance changes.

The results presented in Figures D7, D14, D21, D28, and D35 indicate that discharge from the proposed wetland at the Karst Springs Restoration site remains consistent across scenarios with identical inflow values. This suggests that wetland outflow is only slightly affected by variations in the groundwater system. Such limited sensitivity is likely due to the relatively low connectivity between the wetland and the underlying aquifers. Furthermore, any changes in groundwater inflows or outflows are buffered by the hydraulic control at the outlet: as the wetland water level rises (e.g., due to increased groundwater inflow), outflow increases accordingly, helping to maintain a relatively stable surface water level. As a result, although MODFLOW 6 underestimates groundwater heads compared to MODFLOW 2005—due to the absence of the SWI2 package during model conversion—this discrepancy appears to have minimal impact on the simulated wetland surface water levels.

The predictive scenarios indicate that adjustments to inflow rates from Mosquito Creek (±20%) and restrictions on groundwater pumping (within 2-km and 5-km radii) resulted in only small changes to the conditions at the Bool Lagoon Complex in terms of groundwater heads (Figures C4 to C8, C16 to C20, C28 to C32, and C40 to C44), surface water levels (Figures C1 to C3, C13 to C15, C25 to C27, and C37 to C39), water volumes (Figures C9 to C11, C21 to C23, C33 to C35, and C45 to C47), and the inundated area (Figures C80 to C83). The small impact from groundwater pumping restrictions on surface water levels and groundwater heads can be attributed to the relatively modest groundwater extraction rates proximal to the Bool Lagoon Complex (relative to other outflows), whereby pumping accounts for only 1.6% of total outflows within the model. The analysis of the influence of pumping neglected wells outside the model domain, which may affect wetland–aquifer interactions in ways that have not been assessed.The reason behind the minimal effect of changing inflow rates from Mosquito Creek (±20%) on surface water levels in the Bool Lagoon Complex is that during the periods of greatest inflow, the lake discharges to Drain M, and any changes to the Mosquito Creek inflow causes modified outflows to Drain M (Figures C12 and C24), which buffers the effect (on the stored water volume) of changing the inflow. Otherwise, changes to the inflows from Mosquito Creek at times of lower flow also have only small effects because of the large area of the Bool Lagoon Complex over which these inflows are distributed. The interactions with groundwater also act to mute to a minor degree that effects of changing surface water inflow rates.

In contrast, blocking the downstream Bool Lagoon Complex regulator to Drain M led to a significant increase in water levels (Figure C49), higher groundwater heads (Figures C50 to C54) and water volumes (Figure C55), and a larger inundated area (Figures C80 to C83). This scenario was assessed using the single-lake version of the Bool Lagoon Complex model. An attempt to block the downstream regulator using the three-lake version of the model led to unrealistic heads at the most-downstream sub-lake. This occurred because there is presently no mechanism in MODFLOW 6 to allow backwater effects, i.e., downstream surface water bodies do not affect upstream water bodies in MODFLOW 6, with the exception of groundwater pathways that connect sub-lakes.

Raising the levee elevation between the Main Basin and Central Basin (in the Bool Lagoon Complex) by 0.20 m and 0.40 m resulted in increased surface water levels in the Main Basin (Figures C57 and C69). It also led to higher surface water levels in Hacks Lagoon and the Central Basin (including Western Basin) during dry conditions (Figures C56, C58, C68, and C70). However, during wet conditions, the raised levee caused a decrease in surface water levels in the Central Basin (Figures C58 and C70). The increase in surface water levels in Hacks Lagoon and the Central Basin (including Western Basin) during dry periods is attributed the rise in groundwater levels that was caused by water retention in the Main Basin (including Little Bool Lagoon). That is, groundwater rise in the aquifers underlying the wetland affected groundwater-wetland exchange rates, causing higher surface water levels in both Hacks Lagoon and the Central Basin (including Western Basin) during dry conditions. The increase in groundwater levels under these scenarios is evident at observation well ROB25, located in the Central Basin (Figures C63 and C75). The decrease in surface water levels in the Central Basin (including Western Basin) during wet conditions is the expected consequence of the elevated levee restricting the flow of water from the Main Basin (including Little Bool Lagoon) to the Central Basin (including Western Basin).

The predictive scenarios implemented for the proposed Karst Springs Restoration wetland highlight the significant role of weir-crest modifications in influencing surface water. As expected, lowering the weir crest to 1.5 m AHD (Scenario DC-S1) and to 1.7 m (Scenario DC-S2) led to reduced surface water levels (Figures D1 and D8), water volumes (Figures D7 and D13), and inundated areas (Figures D43 to D46), while raising the crest to 2.2 m (Scenario DC-S3) and to 2.5 m (Scenario DC-S4) increased surface water levels (Figures D15 and D22), water volumes (Figures D20 and D27), and inundated areas (Figures D43 to D46). Higher weir crests reduced the discharge from the wetland, with the reduced discharge allowing a greater volume of storage. This has the effect of increasing the mean residence time (equal to the average wetland volume divided by the average outflow rate) of water in the wetland from 2.89 days to 5.78 days (for weir crest heights of 2.2 m and 2.5 m, respectively). In contrast, scenarios involving a 20% reduction in either rainfall (DC-S5) or surface water inflows (DC-S6) resulted in only small changes to surface water levels (Figures D29 and D36), wetland volumes (Figures D34 and D41), and the inundated area (Figures D43 and D46). This occurred because direct rainfall to the wetland is a small component of the wetland water balance (around 1%). The 20% reduction in surface water inflows mainly caused a corresponding change in the outflow, without significantly affecting the stored volume or inundated area of the wetland (Figure D42). None of the scenarios described above had a significant effect on groundwater heads at the observation sites within the Karst Springs Restoration model (Figures D2 to D5, D9 to D12, D16 to D19, D23 to D26, D30 to D33, and D37 to D40).

7 Conclusions and Recommendations

This report presents the development and application of numerical models to assess the impacts of various intervention measures on the ecohydrological systems of the Bool Lagoon Complex and the Karst Springs Restoration site in the South East of South Australia. This work was conducted as part of Task 3 (*Groundwater and wetland modelling*) of the Goyder Project: *Adaptation of the South-Eastern Drainage System under a Changing Climate*. The main findings of this project are summarised as:

1. The methodology for converting the regional-scale groundwater flow models from MODFLOW 2005 to MODFLOW 6 and extracting sub-models was validated by comparing groundwater levels from both versions. Close agreement was obtained for the groundwater heads in the Bool Lagoon Complex model, between the original MODFLOW 2005 and the MODFLOW 6 models used in the current study. Discrepancies occurred in the Karst Springs Restoration model that were attributed to the use of the SWI2 package in MODFLOW 2005.
2. Bool Lagoon Complex and Karst Springs Restoration sub-models were extracted from larger parent models, with good agreement between the parent models and the sub-models in terms of groundwater heads. Again, the Karst Springs Restoration sub-model was affected by the SWI2 package applied in the MODFLOW 2005 model.
3. Comparisons between historical surface water behaviour at the Bool Lagoon Complex, in terms of the inundated area, surface water levels, and discharge rates, indicate that the MODFLOW 6 model and its simulation of the Bool Lagoon Complex using the Lake package provided a reasonable representation of the wetland system, albeit it was challenging to accurately simulate the downstream regulator due to complexities in its historical operation. Remote sensing analysis of the inundated area of the Bool Lagoon Complex, and comparison with model outputs, seems to indicate that at high water levels, the match between remotely sensed inundated areas and those of the model is reasonable. However, there appear to be times when the Bool Lagoon Complex is virtually dry in remotely sensed images, but the model shows stored water in the Bool Lagoon Complex.
4. The proposed methodology for constructing wetland-aquifer interaction models was considered to be validated and allowed for scenario testing of alternative management actions and their effect on the hydrology of the Bool Lagoon Complex and the Karst Springs Restoration sites to be undertaken with reasonable confidence in the predictions.
5. Sensitivity analysis of lakebed leakance for the Bool Lagoon Complex model indicates that surface water and groundwater levels are sensitive to an order-of-magnitude lowering of the lakebed leakance, but otherwise, changes to the lakebed leakance produced only modest changes to groundwater and surface water levels in the model. Variations to the lakebed leakance in the Karst Springs Restoration model caused only minor changes.
6. The results of scenario testing, including changes in Mosquito Creek inflows, groundwater pumping near the Bool Lagoon Complex (which accounts for only 1.6% of all model outflows), levee elevation adjustments, and the outflow regulator, showed that adjustments to Mosquito Creek inflows (±20%) and restrictions to proximal groundwater pumping caused only minor changes to surface water and groundwater levels in and around the Bool Lagoon Complex. Raising the levee between the Main and Central Basins in the Bool Lagoon Complex by 0.20 m and 0.40 m resulted in higher surface water levels in the Main Basin (including Little Bool Lagoon). Surprisingly, raising the levee caused higher surface water levels in the downstream wetland (Central Basin (including Western Basin)) and in Hacks Lagoon, which both benefited during dry periods. This was attributed to the effects of raising the levee on the groundwater system beneath the wetland. Surface water levels in the Central Basin (including Western Basin) decreased during wet conditions with the levee in place due to lower inputs from floodwaters. Blocking the downstream regulator of the Bool Lagoon Complex resulted in significantly increased surface water levels, greater inundated areas, and higher groundwater levels, highlighting the critical role of the regulator in the hydrology of the system. It is noteworthy that Bool Lagoon Complex water levels exceed thresholds for the integrity of downstream structures when the regulator was blocked in the model, and therefore, the scenarios involving reduced flow to Drain M

are not realistic. Further simulations are needed to explore in more detail potential regulator operations that store water in the Bool Lagoon Complex at environmentally optimal volumes that maintain the flood mitigation properties of the wetland.

7. Scenario testing at the Karst Springs Restoration site demonstrated that raising the downstream weir crest significantly increased surface water levels, water volumes, and the inundation area, while lowering the crest had the opposite effect. Other changes caused only minor changes to the surface water extent at the Karst Springs Restoration site. Therefore, as with the Bool Lagoon Complex, the downstream control appears to be the most important factor in modifying the hydrology of the Karst Springs Restoration wetland.

The modelling described above represents the first attempts to model explicitly wetlands of the South East, rather than implicit representations in previous modelling attempts. The selection of scenarios reported here is intended to provide a baseline of modelling outcomes to foster engagement with stakeholders regarding the capability of the models and initial feedback on the effects of a small number of wetland modification measures. It is expected that a broader set of modelling analyses will be established in the future to evaluate in more detail the likely behaviour of the Bool Lagoon Complex and the Karst Springs Restoration wetlands under modified conditions, seeking to optimise the health of the ecosystems within those wetlands. This requires engagement with ecohydrological experts to assess in converting hydrological changes within these wetlands to modified ecological health indicators.

Additional simulations to further explore the potential to enhance the hydrology of the Bool Lagoon Complex are recommended, including: (a) levee construction scenarios in Bool Lagoon, such as modifications to the existing connection between Hacks Lagoon and Bool Lagoon, the construction of a levee through the middle of Bool Lagoon, and a third levee within the lower part of Bool Lagoon (this latter option requires the Bool Lagoon Complex to be subdivided into four sub-lakes); (b) pumping of groundwater into Bool Lagoon; (c) implementation of Aquifer Storage and Recovery schemes; and (d) land-surface lowering scenarios. These scenarios are envisaged as part of further work, to be described in subsequent short reports/memos and on the basis of continuing engagement with the Limestone Coast Landscape Board.

References

ANCA, 2001. A directory of important wetlands in Australia. ANCA, Canberra. http://www.environment.gov.au/resource/directory-important-wetlands-australia-third-edition

Andrefouet, S., Bindschadler, R., Brown de Colstoun, E., Choate, M., Chomentowski, W., Christopherson, J., Doorn, B., Hall, D.K., Holifield, C., Howard, S., and Kranenburg, C., 2003. Preliminary assessment of the value of Landsat-7 ETM+ data following scan line corrector malfunction. US Geological Survey, EROS Data Center: Sioux Falls, SD, USA. https://d9-wret.s3.us-west-2.amazonaws.com/assets/palladium/production/s3fs-public/atoms/files/SLC_off_Scientific_Usability.pdf (Accessed: 12 May 2025).

Bachmann, M.R., Dickson, C.R., and Sweeney, O. 2015. Karst rising springs wetland community regional action plan in the South East of South Australia: 2015–2025. Report to the Department of Environment. https://natureglenelg.org.au/wp-content/uploads/2022/02/RAP-1-Karst-Rising-Springs-RAP-FINAL-2016-12-02-updated-map-on-p-17.pdf (Accessed: 12 May 2025).

Banta, E.R., 2000. MODFLOW-2000, the U.S. Geological Survey Modular Ground-Water Model – Documentation of packages for simulating evapotranspiration with a segmented function (ETS1) and drains with return flow (DRT1), U.S. Geological Survey Open–File Report 00–466, U.S. Geological Survey, Denver, Colorado. https://pubs.usgs.gov/of/2000/0466/report.pdf (Accessed: 12 May 2025).

Barnett, S., Lawson, J., Li, C., Morgan, L., Wright, S., Skewes, M., Harrington, N., Woods, J., Werner, A., and Plush, B., 2015. A hydrostratigraphic model for the shallow aquifer systems of the Gambier Basin and South Western Murray Basin, Goyder Institute for Water Research Technical Report Series No. 15/15. https://goyderinstitute.org/wp-content/uploads/2023/04/goyder_trs_15-15_hydrostratigraphic_model_gambier_murray_basin.pdf (Accessed: 12 May 2025).

Benyon, R.G., and Doody, T.M., 2004. Water use by tree plantations in the south east South Australia. CSIRO, Australia. https://doi.org/10.4225/08/585eb80e79dcd

Brinson, M.M., and Malvárez, A.I., 2002. Temperate freshwater wetlands: Types, status, and threats. Environmental Conservation, 29, 115–133. https://doi.org/10.1017/S0376892902000085

Brown, C.M., and Stephenson, A.E., 1991. Geology of the Murray Basin, Southeastern Australia. Bureau of Mineral Resources, Australia, Bulletin 235, 430 p.

Brownlow, M.D., 1997 Water regime and the aquatic vegetation of Bool Lagoon, South Australia, PhD Thesis, University of Adelaide, 252 p.

CDM Smith, 2017. Technical review of groundwater resources Province 2 - Groundwater Modelling, report prepared for Department of Environment, Land, Water and Planning, Victoria.

Chaudhry, M.H., 2007, Open-channel flow (2nd ed.): New York, Springer Science & Business Media, 523 p. https://doi.org/10.1007/978-0-387-68648-6

Cobb, M.A., and Barnett, S.R., 1994. Naracoorte hydrogeological map (1:250000 scale). Australian Geological Survey Organisation, Canberra.

Colvin, S.A.R., Sullivan, S.M.P., Shirey, P.D., Colvin, R.W., Winemiller, K.O, Hughes, R.M., Fausch, K.D., Infante, D.M., Olden, J.D., Bestgen, K.R., Danehy, R.J., Eby, L., 2019. Headwater streams and wetlands are critical for sustaining fish, Fisheries, and Ecosystem Services. Fisheries, 44, 73–91. https://doi.org/10.1002/fsh.10229

Cook, P., Wood, C., White, T., Simmons, C., Fass, T., and Brunner, P., 2008. Groundwater inflow to a shallow, poorly-mixed wetland estimated from a mass balance of radon. Journal of Hydrology 354, 213–226. https://doi.org/10.1016/j.jhydrol.2008.03.016

Cramer, S., 1990. Naracoorte Ranges proclaimed region point source recharge to the unconfined aquifer, Australian Hydrographers Association Workshop 1990 Darwin, Australian Hydrographers Association.

Cranswick, R.H., and Herpich, D., 2018. Groundwater–surface water exchange in the South East: 30 years of change. DEW Technical report 2018/09, Government of South Australia, Department for Environment and Water, Adelaide. https://www.waterconnect.sa.gov.au/Content/Publications/DEW/Groundwater%E2%80%93surface%20water%20exchange%20in%20the%20South%20East%2030%20years%20of%20change.pdf (Accessed on 5 June 2025).

Crosbie, R., and Davies, P., 2013. Recharge estimation, in: Framework for a regional water balance model for the South Australian Limestone Coast Region (eds N. Harrington and S. Lamontagne), Goyder Institute for Water Research Technical Report Series No. 13/14, Adelaide.

Crosbie, R., Pickett, T., Mpelasoka, F.S., Hodgson, G., Charles, S.P., and Barron, O.V., 2013. An assessment of the climate change impacts on groundwater recharge at a continental scale using a probabilistic approach with an ensemble of GCMs. Climatic Change,117, 41–53. https://doi.org/10.1007/s10584-012-0558-6

DCCEEW, 2021a. Department of climate change, energy, the environment and water. Directory of Important Wetlands in Australia. Available at: https://www.dcceew.gov.au/water/wetlands/australian-wetlands-database/directory-important-wetlands (Accessed: 13 December 2022).

DEH and DWLB, 2003. Department for environment and Heritage and the Department of Water, Land and Biodiversity. Wetlands Strategy For South Australia. Department for Environment and Heritage, South Australia.

DEH, 2006. Bool Lagoon Game Reserve and Hacks Lagoon Conservation Park Management and Ramsar Plan, Department for Environment and Heritage, Adelaide, South Australia, 102 p.

DELWP, 2020. South Australian–Victorian Border Groundwaters Agreement Review Committee - Thirty-Fifth Annual Report, Authorised and published by the Victorian Government, Department for Environment, Land, Water and Planning (Melbourne), and by the South Australian Government, Department for Environment and Water (Adelaide) https://cdn.environment.sa.gov.au/environment/docs/groundwaters-agreement-35-annual-report-2020-rep.pdf (Accessed: 13 October 2020).

DEW, 2020. ELVIS Digital Elevation Model Imagery Catalog, Government of South Australia, Department for Environment and Water, Adelaide. https://data.sa.gov.au/data/dataset/elvis-digital-elevation-model-imagery-catalog (Accessed: 13 October 2020).

DEW, 2021. Hydrogeological conceptualisation in the area south of Mount Gambier, DEW Technical report 2021/22, Government of South Australia, Department for Environment and Water, Adelaide.

DEW, 2023a. Lower Limestone Coast sub-regional modelling: mid-South East, DEW Technical report 2023/xx, Government of South Australia, Department for Environment and Water, Adelaide.

DEW, 2023b. Lower Limestone Coast subregional model: coastal areas south of Mount Gambier, DEW Technical report 2023/81, Government of South Australia, Department for Environment and Water, Adelaide. https://www.waterconnect.sa.gov.au/Content/Publications/DEW/DEW_TR_2023_81.pdf (Accessed: 12 May 2025).

Dhu, T., Dunn, B., Lewis, B., Lymburner, L., Mueller, N., Telfer, E., Lewis, A., McIntyre, A., Minchin, A., and Phillips, C., 2017. Digital earth Australia–unlocking new value from earth observation data. Big Earth Data, 1, 64-74. https://doi.org/10.1080/20964471.2017.1402490

Doherty, J.E., Fienen, M.N., and Hunt, R.J., 2010, Approaches to highly parameterized inversion: Pilot-point theory, guidelines, and research directions: U.S. Geological Survey Scientific Investigations Report 2010–5168, 36 p. https://pubs.usgs.gov/sir/2010/5168/pdf/sir20105168.pdf (Accessed: 12 May 2025).

ESA, 2015. Sentinel-2 User Handbook; European Commission: Paris, France, 2015; Volume 1.2.

Fass, T., and Cook, P.G., 2005. Reconnaissance survey of groundwater dependence of wetlands, South East, South Australia, Using a Mass balance of Radon and Chloride. Unpublished.

FGDC, 2013. Federal geographic data committee. Classification of wetlands and deepwater habitats of the United States. FGDC-STD-004-2013. Second Edition. Wetlands Subcommittee, Federal Geographic Data Committee and U.S. Fish and Wildlife Service, Washington, DC. https://www.fgdc.gov/standards/projects/wetlands/nwcs-2013 (Accessed: 12 May 2025).

Fu, G., Crosbie, R.S., Barron, O., Charles, S.P., Dawes, W., Shi, X., Van Niel, T., and Li, C., 2019. Attributing variations of temporal and spatial groundwater recharge: a statistical analysis of climatic and non-climatic factors. Journal of Hydrology, 568, 816–834. https://doi.org/10.1016/j.jhydrol.2018.11.022

Gehrig, S, Harding, C, Turner, D, Nicol, J, Clarke, K, Clark, M, Deane, D, Aldridge, K, Brookes, J, Ostendorf, B., and Lewis, M., 2015. 'Developing ecological response models and determining water requirements for wetlands in the South-East of South Australia: Task 1: Data review and methodological framework.' Goyder Institute for Water Research Technical Report Series No. 15/23, Adelaide, South Australia.

GSA, 2000. Government of South Australia. State Water Plan 2000. Department for Water Resources. Three volumes.

Hammera, M., Wedderburna, S., and Weenenb, J.V., 2009. Action Plan for south Australian Freshwater Fishes. https://cdn.environment.sa.gov.au/environment/docs/saff-action-plan-sec1.pdf (Accessed: 12 May 2025).

Harding, C., Herpich, D., and Cranswick, R.H., 2018. Examining temporal and spatial changes in surface water hydrology of groundwater dependent ecosystems using WOfS (Water Observations from Space): southern Border Groundwaters Agreement area, South East South Australia, DEW Technical report 2018/08, Government of South Australia, Department for Environment and Water, Adelaide. https://www.waterconnect.sa.gov.au/Content/Publications/DEW/Temporal%20changes%20in%20wetland%20hydrology%20using%20WOfS.pdf (Accessed on 5 June 2025).

Harding, C., and O'Connor, P., 2012. Delivering a strategic approach for identifying water-dependent ecosystems at risk: A preliminary assessment of risk to water-dependent ecosystems in South Australia from groundwater extraction, DFW Technical Report 2012/03, Government of South Australia, through Department for Water, Adelaide. https://www.waterconnect.sa.gov.au/Content/Publications/DEW/DFW_TR_2012_03.pdf (Accessed: 12 May 2025).

Harrington, G.A., Walker, G.R., Love, A.J., and Narayan, K.A., 1999. A compartmental mixing-cell approach for the quantitative assessment of groundwater dynamics in the Otway Basin, South Australia. Journal of Hydrology, 214, 49–63. https://doi.org/10.1016/S0022-1694(98)00243-1

Harrington, N., and Lamontagne, S., 2013. Framework for a regional water balance model for the South Australian Limestone Coast region, Goyder Institute for Water Research Technical Report Series No. 13/14. https://goyderinstitute.org/wp-content/uploads/2023/06/goyder_trs_13-14_framework_regional_water_balance_model.pdf (Accessed: 12 May 2025).

Harrington, N., and Li, C., 2015. Development of a groundwater extraction dataset for the South East of SA: 1970–2013, Goyder Institute for Water Research Technical Report Series No. 15/17, Adelaide. https://goyderinstitute.org/wp-content/uploads/2023/06/goyder_trs_15-17_groundwater_extraction_dataset_1970-2013.pdf (Accessed: 12 May 2025).

Harrington, N.M., Chambers, K., and Lawson, J., 2008. Primary production to mitigate water quality threats project. zone 1A numerical modelling study: Conceptual model development, DWLBC Report 2008/12, Government of South Australia, through Department of Water, Land and Biodiversity Conservation, Adelaide. https://www.waterconnect.sa.gov.au/Content/Publications/DEW/dwlbc_report_2008_12.pdf (Accessed: 12 May 2025).

Harvey, D., 2009, Accounting for plantation forest groundwater impacts in the lower South East of South Australia. DWLBC Report 2009/13, Government of South Australia, through Department of Water, Land and Biodiversity Conservation, Adelaide. https://www.waterconnect.sa.gov.au/Content/Publications/DEW/DWLBC_Technical_Report_2009_13.pdf (Accessed: 12 May 2025).

Henderson, F.M., 1966. Open channel flow. Macmillan Publishing Co., Inc. New York.

Heneker, T.M., 2006. Additional hydrological investigations for the diversion of flow from the lower to the upper south east: Potential impact of forestry and climate change on water resource availability, DWLBC Technical Note 2006/06, Government of South Australia, through Department of Water, Land and Biodiversity Conservation, Adelaide. https://www.waterconnect.sa.gov.au/Content/Publications/DEW/ki_dwlbc_technote_2006_06_final_2007.pdf (Accessed: 12 May 2025).

Herczeg, A.L., Leaney, F.W.J., Stadler, M.F., Allan, G.L., and Fifield, L.K., 1997. Chemical and isotopic indicators of point-source recharge to a karst aquifer, South Australia. Journal of Hydrology, 192, 271–299. https://doi.org/10.1016/S0022-1694(96)03100-9

Holmes, J.W., and Waterhouse, J.D., 1983. Hydrology. in 'natural history of the South East'. Royal Society of South Australia: Adelaide. https://www.rssa.org.au/wp-content/uploads/2022/07/nhstheast.pdf (Accessed: 12 May 2025).

Keddy, P.A., 2010. Wetland ecology: principles and conservation (2nd ed.). New York: Cambridge University Press.

Knight, A.C., Werner, A.D., Irvine, D.J., 2019. Combined geophysical and analytical methods to estimate offshore freshwater extent. Journal of Hydrology, 576, 529–540. https://doi.org/10.1016/j.jhydrol.2019.06.059

Langevin, C.D., Hughes, J.D., Banta, E.R., Niswonger, R.G., Panday, S., and Provost, A.M., 2017. Documentation for the MODFLOW 6 Groundwater Flow Model: U.S. Geological Survey Techniques and Methods, book 6, chap. A55, 197 p., https://doi.org/10.3133/tm6A55

Lawson, J.S, 2013. Water quality and movement of the unconfined and confined aquifers in the capture zone of the Blue Lake, Mount Gambier, South Australia and implications for their Management, Masters thesis, University of South Australia, South Australia.

Lawson, J., Mustafa, S., and Wood, C., 2009. Field investigations into the influence of faulting on groundwater flow and recharge of the Tertiary Limestone Aquifer, Lower South East, South Australia. South Australian Department for Water.

LCLB, 2021. Exploring water in our landscape through the Mosquito Creek Catchment and Bool Lagoon. Landscape South Australia Limestone Coast. 79p . https://cdn.environment.sa.gov.au/landscape/docs/lc/Bool_Resource_FINAL.pdf (Accessed: 6 May 2025).

Leibowitz, S.G., Wigington, P.J., Schofield, K.A., Alexander, L.C., Vanderhoof, M.K., Golden, H.E., 2018. Connectivity of streams and wetlands to downstream waters: An integrated systems framework. Journal of the American Water Resources Association, 54, 298–322. https://doi.org/10.1111/1752-1688.12631

Lewis, A., Oliver, S., Lymburner, L., Evans, B., Wyborn, L., Mueller, N., Raevksi, G., Hooke, J., Woodcock, R., Sixsmith, J., Wu, W., Tan, P., Li, F., Killough, B., Minchin, S., Roberts, D., Ayers, D., Bala, B., Dwyer, J., Dekker, A., Dhu, T., Hicks, A., Ip, A., Purss, M., Richards, C., Sagar, S., Trenham, C., Wang, P., and Wang, L.-W., 2017. The Australian geoscience data cube—foundations and lessons learned. Remote Sensing of Environment, 202, 276–292. https://doi.org/10.1016/j.rse.2017.03.015

Love, A.J., Herczeg, A.L., Armstrong, D., Stadter, F., and Mazor, E., 1993. Groundwater flow regime within the Gambier Embayment of the Otway Basin, Australia: evidence from hydraulics and hydrochemistry. Journal of Hydrology, 143, 297–338. https://doi.org/10.1016/0022-1694(93)90197-H

Loveland, T.R., and Dwyer, J.L., 2012. Landsat: Building a strong future. Remote Sensing of Environment, 122, 22–29. https://doi.org/10.1016/j.rse.2011.09.022

MBWSR, 2019. Minnesota board of water and soil resources. Minnesota Wetland Restoration Guide. Available at https://bwsr.state.mn.us/wetland-restoration-0 (Accessed on 17 November 2024).

MGA, 2018. Minnesota Groundwater Association. Drain tiles and groundwater resources: Understanding the relations. Available at

https://www.mgwa.org/documents/whitepapers/Drain_Tiles_and_Groundwater_Resources.pdf (Accessed on 12 March 2025).

Morgan, L.K., Harrington, N., Werner, A.D., Hutson, J.L., Woods, J., and Knowling, M.J., 2015. South East Regional Water Balance Project – Phase 2. Development of a Regional Groundwater Flow Model, Goyder Institute for Water Research Technical Report Series No. 15/38. https://goyderinstitute.org/wp-content/uploads/2023/06/goyder_trs_15-38_south_east_regional_water_balance_phase_2.pdf (Accessed on 9 May 2025).

Mueller, N., Lewis, A., Roberts, D., Ring, S., Melrose, R., Sixsmith, J., Lymburner, L., McIntyre, A., Tan, P., Curnow, S., and Ip, A., 2016. Water observations from space: Mapping surface water from 25 years of Landsat imagery across Australia. Remote Sensing of Environment, 174, 341–352. https://doi.org/10.1016/j.rse.2015.11.003

Mustafa, S., Slater, S., and Barnett, S., 2012. Preliminary investigation of seawater intrusion into a freshwater coastal aquifer-lower south east. Science, Monitoring and Information Division Department of Environment, Water and Natural Resources. Technical Report DEWNR 2012/01, 68p. https://www.waterconnect.sa.gov.au/Content/Publications/DEW/DEWNR_TR_2012_01.pdf (Accessed on 17 November 2024).

Nguyen, T., and Plush, B., 2024. Technical Memo: Eight Mile Creek Wetland Restoration. Water Science and Monitoring. Department of environment and science, 8 p.

Nitschke, J.E., 1984. Guidelines for the operation of Bool Lagoon and Drain M regulators for flood mitigation purposes, South Eastern Drainage Board.

Peterson, T.J., and Western, A.W., 2018. Statistical interpolation of groundwater hydrographs. Water Resources Research, 54, 4663–4680. https://doi.org/10.1029/2017WR021838

SAVBGARC, 2023. Management Review Province 2 of the Designated Area. South Australian – Victorian Border Groundwaters Agreement Review Committee, Melbourn and Adelaide. https://cdn.environment.sa.gov.au/environment/docs/Management-Review-Province-2-of-the-Designated-Area-March-2023.pdf (Accessed: 9 May 2025).

SENRMB, 2013. Water allocation plan for the Lower Limestone Coast prescribed wells area, Government of South Australia, South East Natural Resources Management Board, Mount Gambier.

SENRMB, 2019. https://lc.landscape.sa.gov.au/files/documents/Strategies-plans-and-reports/2019_se_drainage_wetlands_strategy.pdf (Accessed: 9 May 2025).

SKM, 2009a. Classification of groundwater surface water interactions for water dependent ecosystems in the South East, South Australia. Department of Water, Land and Biodiversity.

Slater, S., and Farrington, L., 2010. Lower South East drainage network adaptive management: preliminary scoping study. Department of Environment and Natural Resources, South East region. 116 p.

Smith, S.D., Lamontagne, S., Taylor, A.R., Cook, P.G., 2015. Evaluation of groundwater – surface water interactions at Bool Lagoon and Lake Robe using environmental tracers, Goyder Institute for Water Research Technical Report Series No. 15/14.

Solórzano-Rivas, S.C., and Werner, A.D., 2018. On the representation of subsea aquitards in models of offshore fresh groundwater. Advances in Water Resources, 112, 283–294. https://doi.org/10.1016/j.advwatres.2017.11.025

Taylor, A., Lamontagne, S., Turnadge, C., Smith, S., and Davies, P., 2015. Groundwater – surface water interactions at Bool Lagoon, Lake Robe and Deadmans Swamp (Limestone Coast, SA): A review of monitoring data. https://goyderinstitute.org/wp-content/uploads/2023/04/goyder_trs_15-13_groundwater_interactions_bool_lagoon_data_review-1.pdf (Accessed: 12 May 2025).

Taylor, B., 2006. Wetland inventory – Lower South East. Department for Environment and Heritage, South East. https://cdn.environment.sa.gov.au/environment/docs/lower_southeast.pdf (Accessed: 12 May 2025).

Turnadge, C.J., and Lamontagne, S., 2015, A MODFLOW-based approach to simulating wetland–groundwater interactions in the Lower Limestone Coast Prescribed Wells Area, Goyder Institute for Water Research Technical Report Series No. 15/12, Adelaide, South Australia. https://goyderinstitute.org/wp-content/uploads/2023/04/goyder_trs_15-12_modflow_lower_limestone_coast-1.pdf (Accessed: 12 May 2025).

US EPA, 2021. US Environmental Protection Agency. Threats to Wetlands. https://www.epa.gov/sites/default/files/2021-01/documents/threats_to_wetlands.pdf (Accessed: 13 December 2022).

Valnet Inc, 2022. What are the major threats to wetland ecosystems around the world? https://www.worldatlas.com/articles/what-are-the-major-threats-to-wetland-ecosystems-around-the-world.html (Accessed: 13 December 2022).

Whiteway, T., 2009. Australian bathymetry and topography grid, June 2009. Record 2009/021. Geoscience Australia, Canberra. http://dx.doi.org/10.4225/25/53D99B6581B9A

Wood, C., 2017. Lower Limestone Coast forest water accounting groundwater model, DEWNR Technical report 2017/14, Government of South Australia, Department of Environment, Water and Natural Resources, Adelaide. https://www.waterconnect.sa.gov.au/Content/Publications/DEW/DEWNR_2017-14_pdf_final_2.pdf (Accessed: 12 May 2025).

The Goyder Institute for Water Research is a research alliance between the South Australian Government through the Department for Environment and Water, CSIRO, Flinders University, the University of Adelaide and the University of South Australia.

Appendix A – Simulation and validation of different model configurations

A.1 Simulation and validation of the single-lake model

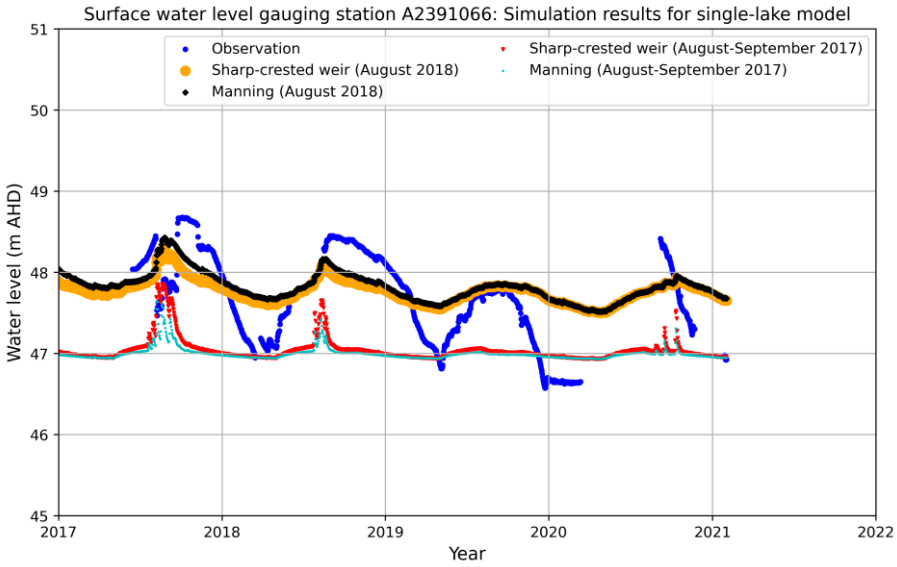

Figure A1. Comparison of observed surface water level at observation gauging station A2391066 with simulated results. The simulations were conducted using the single-lake model, testing outlet equations (i.e., Sharp-crested weir and Manning) for the periods of August–September 2017 and August 2018.

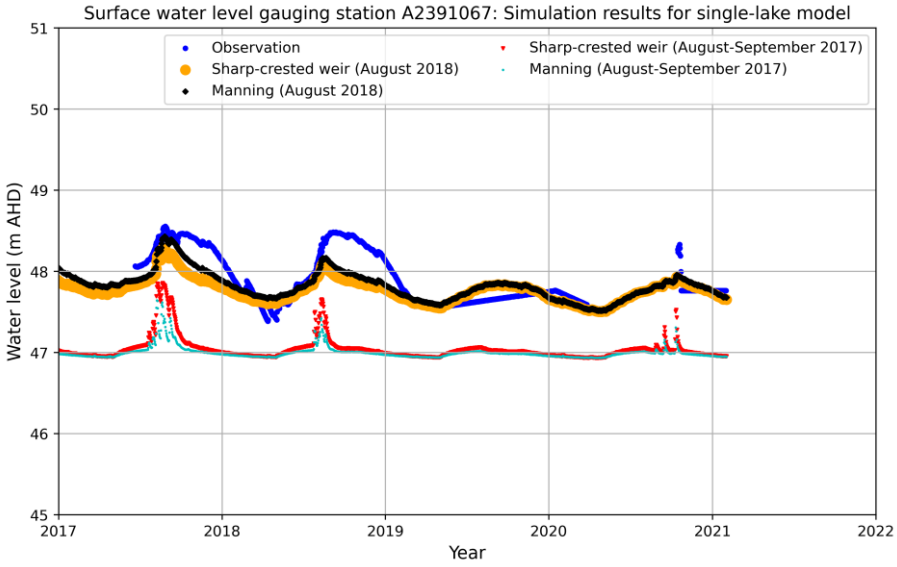

Figure A2. Comparison of observed surface water level at observation gauging station A2391067 with simulated results. The simulations were conducted using the single-lake model, testing outlet equations (i.e., Sharp-crested weir and Manning) for the periods of August–September 2017 and August 2018.

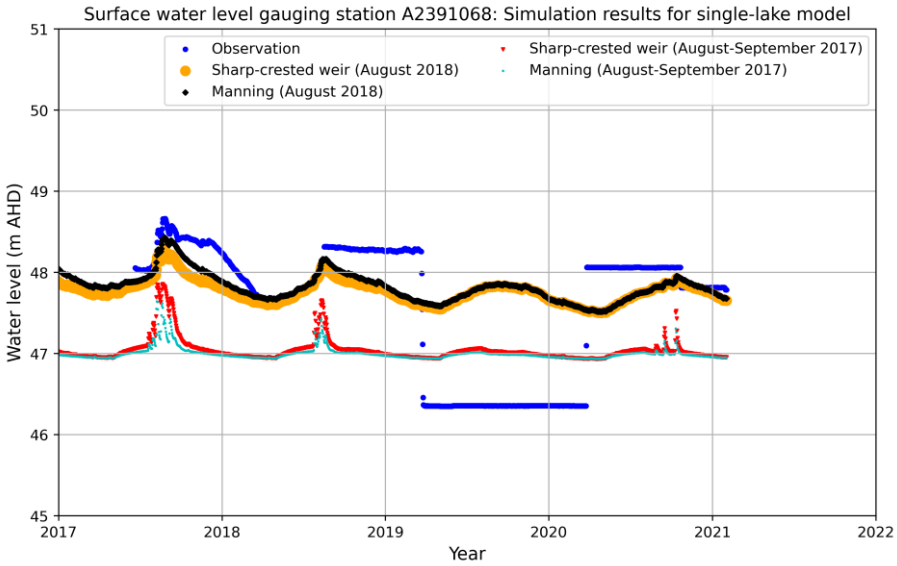

Figure A3. Comparison of observed surface water level at observation gauging station A2391068 with simulated results. The simulations were conducted using the single-lake model, testing outlet equations (i.e., Sharp-crested weir and Manning) for the periods of August–September 2017 and August 2018.

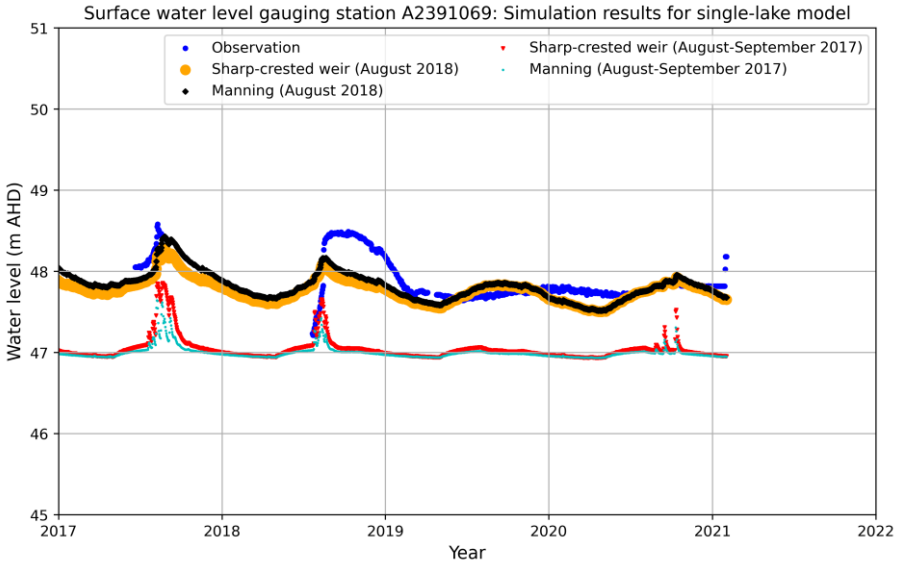

Figure A4. Comparison of observed surface water level at observation gauging station A2391069 with simulated results. The simulations were conducted using the single-lake model, testing outlet equations (i.e., Sharp-crested weir and Manning) for the periods of August–September 2017 and August 2018.

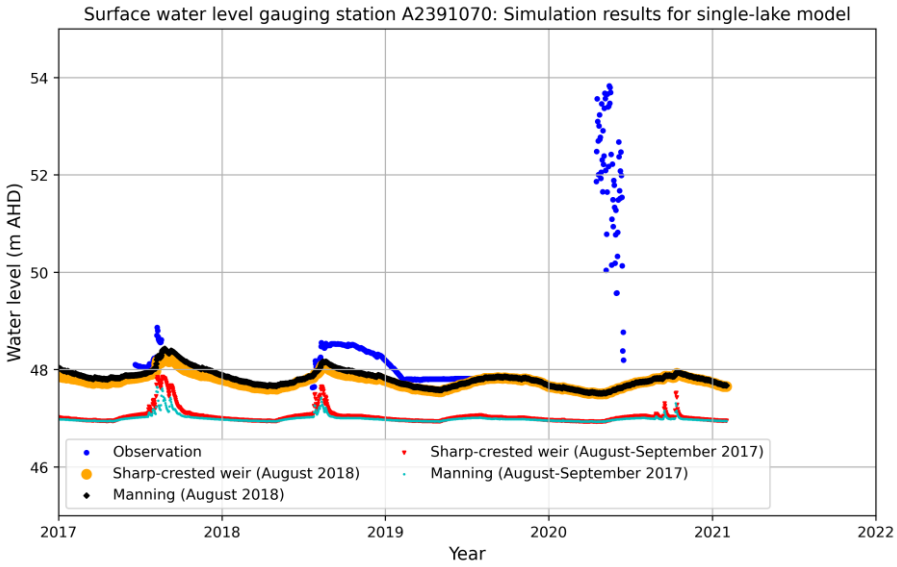

Figure A5. Comparison of observed surface water level at observation gauging station A2391070 with simulated results. The simulations were conducted using the single-lake model, testing outlet equations (i.e., Sharp-crested weir and Manning) for the periods of August–September 2017 and August 2018.

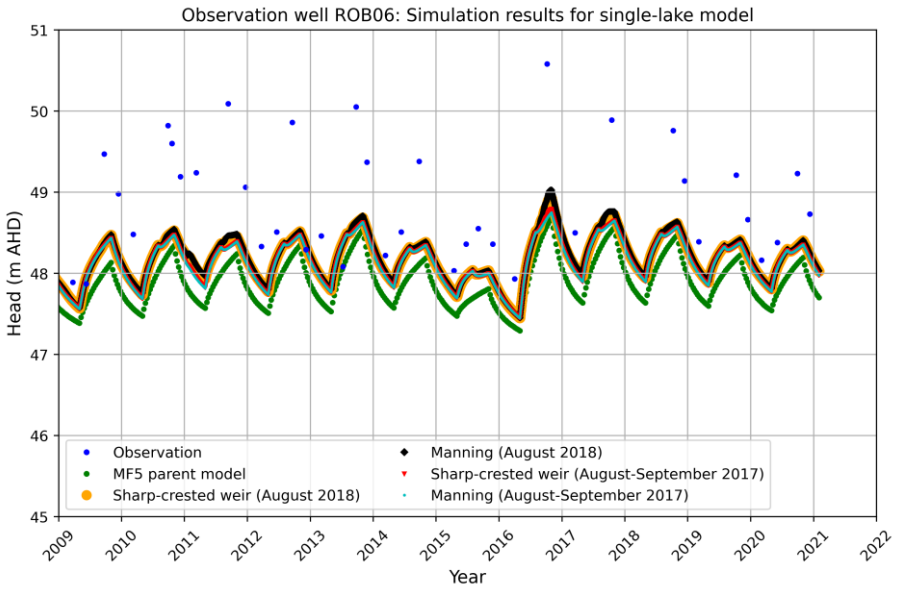

Figure A6. Comparison of observed groundwater head at observation well ROB06 with simulated results. The simulations were conducted using the single-lake model and compared to the MF5 parent model, testing outlet equations (i.e., Sharp-crested weir and Manning) for the periods of August–September 2017 and August 2018.

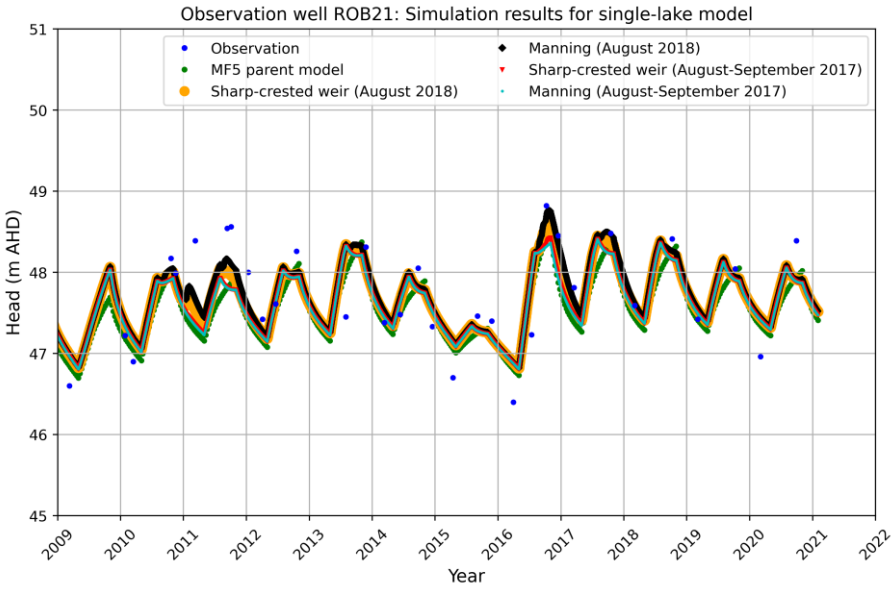

Figure A7. Comparison of observed groundwater head at observation well ROB21 with simulated results. The simulations were conducted using the single-lake model and compared to the MF5 parent model, testing outlet equations (i.e., Sharp-crested weir and Manning) for the periods of August–September 2017 and August 2018.

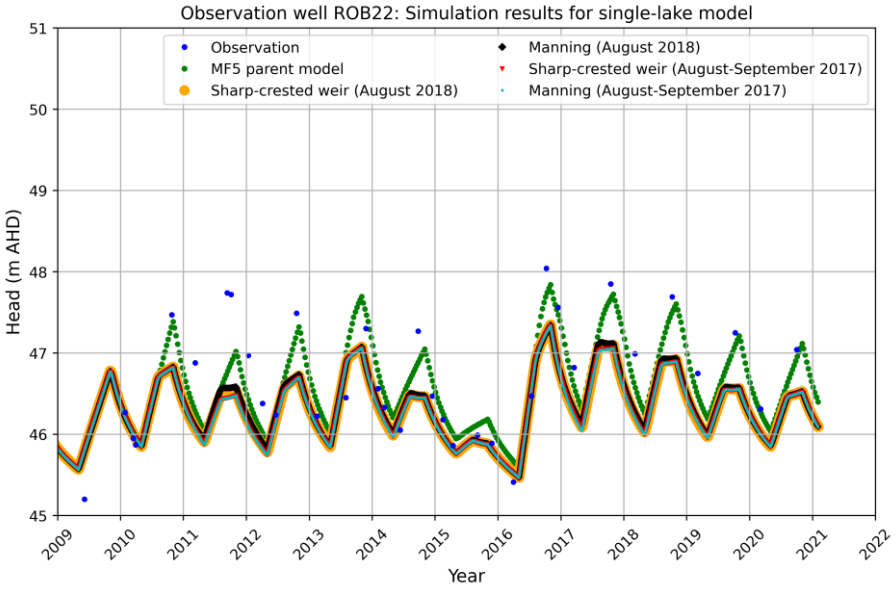

Figure A8. Comparison of observed groundwater head at observation well ROB22 with simulated results. The simulations were conducted using the single-lake model and compared to the MF5 parent model, testing outlet equations (i.e., Sharp-crested weir and Manning) for the periods of August–September 2017 and August 2018.

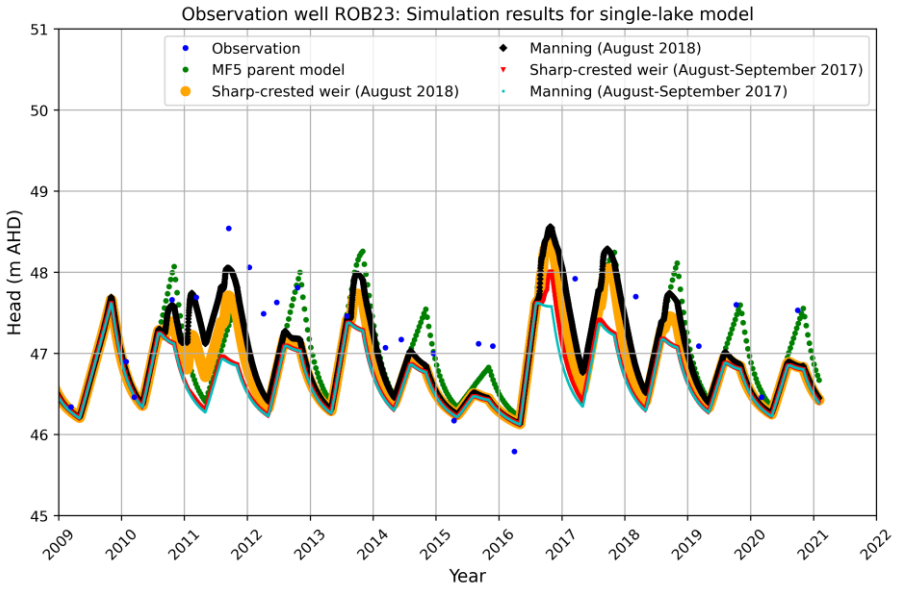

Figure A9. Comparison of observed groundwater head at observation well ROB23 with simulated results. The simulations were conducted using the single-lake model and compared to the MF5 parent model, testing outlet equations (i.e., Sharp-crested weir and Manning) for the periods of August–September 2017 and August 2018.

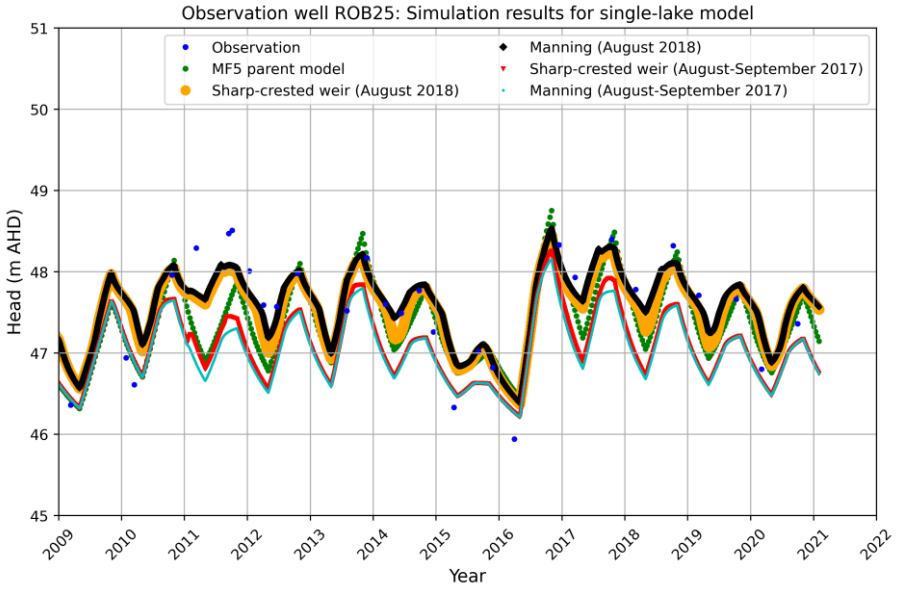

Figure A10. Comparison of observed groundwater head at observation well ROB25 with simulated results. The simulations were conducted using the single-lake model and compared to the MF5 parent model, testing outlet equations (i.e., Sharp-crested weir and Manning) for the periods of August–September 2017 and August 2018.

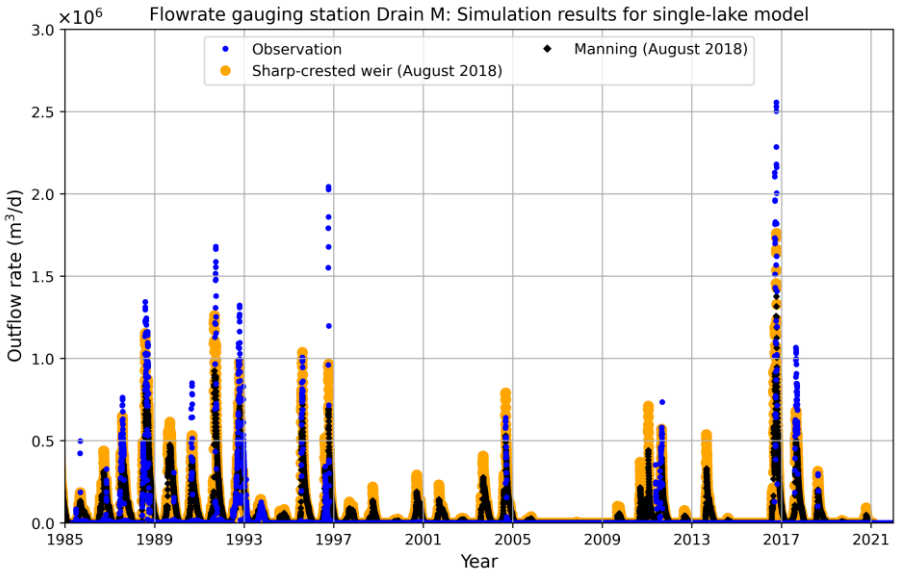

Figure A11. Comparison between observed outflow rates at Drain M and simulated results using the single-lake model is presented, with sharp-crested weir and Manning equations adapted for the period of August 2018.

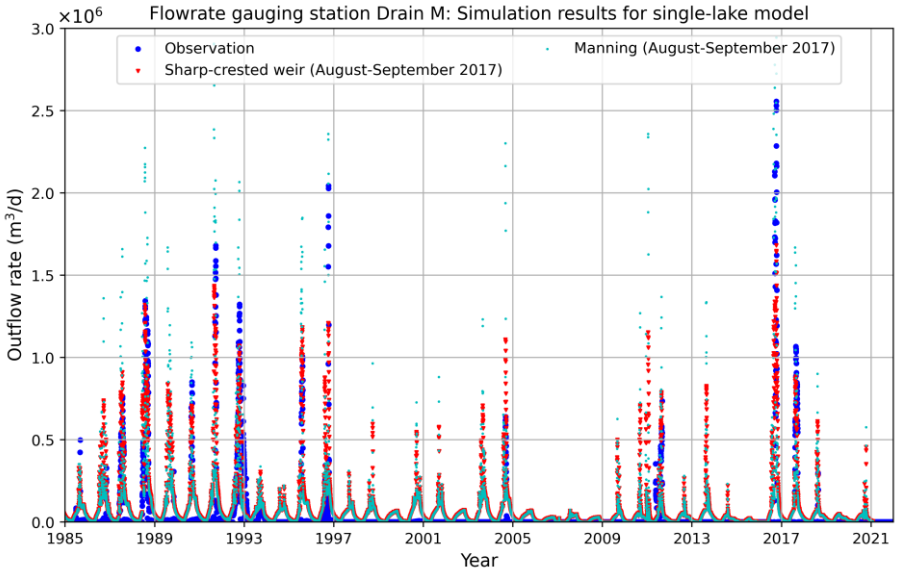

Figure A12. Comparison between observed outflow rates at Drain M and simulated results using the single-lake model is presented, with sharp-crested weir and Manning equations adapted for the period of August–September 2017.

A.2 Simulation and validation of the three sub-lake model

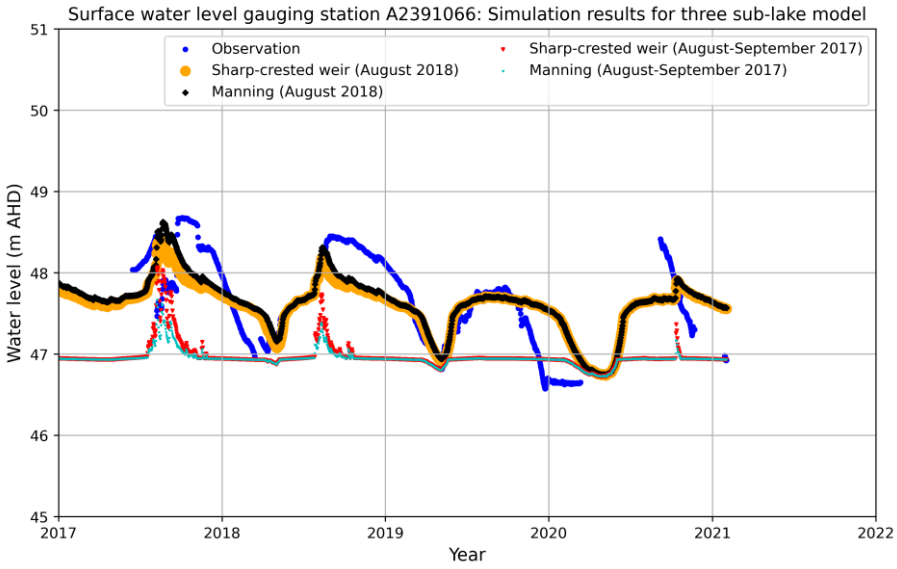

Figure A13. Comparison of observed surface water level at observation gauging station A2391066 with simulated results. The simulations were conducted using the three sub-lake model, testing outlet equations (i.e., Sharp-crested weir and Manning) for the periods of August–September 2017 and August 2018.

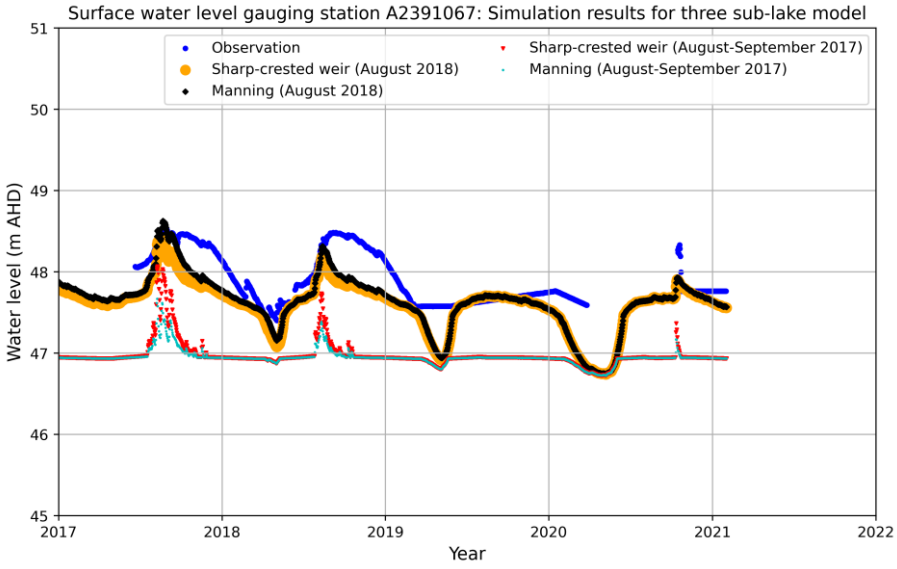

Figure A14. Comparison of observed surface water level at observation gauging station A2391067 with simulated results. The simulations were conducted using the three sub-lake model, testing outlet equations (i.e., Sharp-crested weir and Manning) for the periods of August–September 2017 and August 2018.

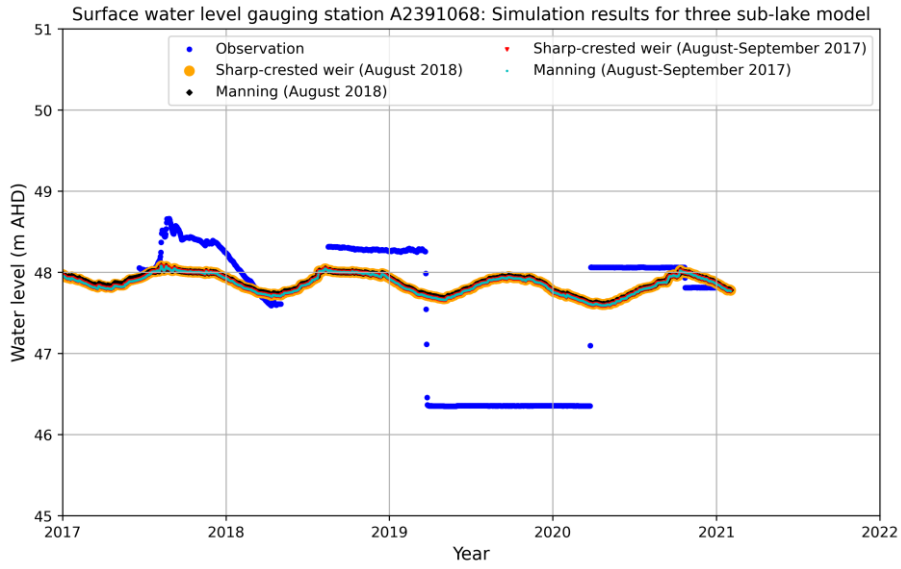

Figure A15. Comparison of observed surface water level at observation gauging station A2391068 with simulated results. The simulations were conducted using the three sub-lake model, testing outlet equations (i.e., Sharp-crested weir and Manning) for the periods of August–September 2017 and August 2018.

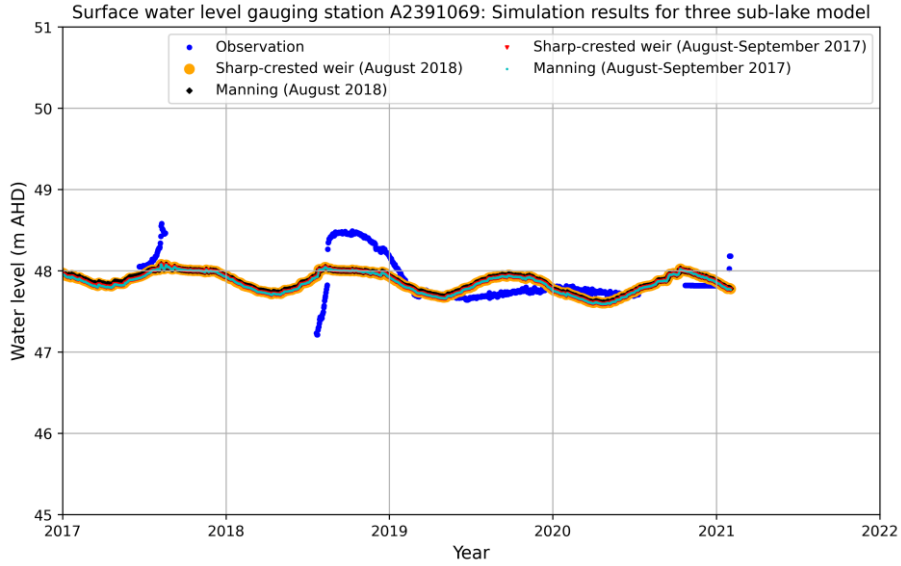

Figure A16. Comparison of observed surface water level at observation gauging station A2391069 with simulated results. The simulations were conducted using the three sub-lake model, testing outlet equations (i.e., Sharp-crested weir and Manning) for the periods of August–September 2017 and August 2018.

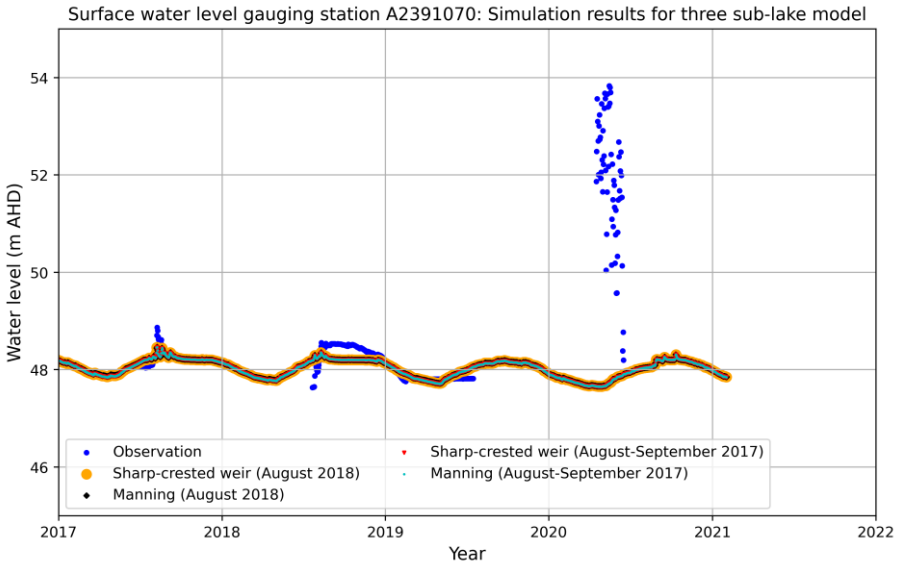

Figure A17. Comparison of observed surface water level at observation gauging station A2391070 with simulated results. Simulations include the three sub-lake model, which incorporates sharp-crested weir and Manning-type outlet equations for the August-September 2017 and August 2018 scenarios.

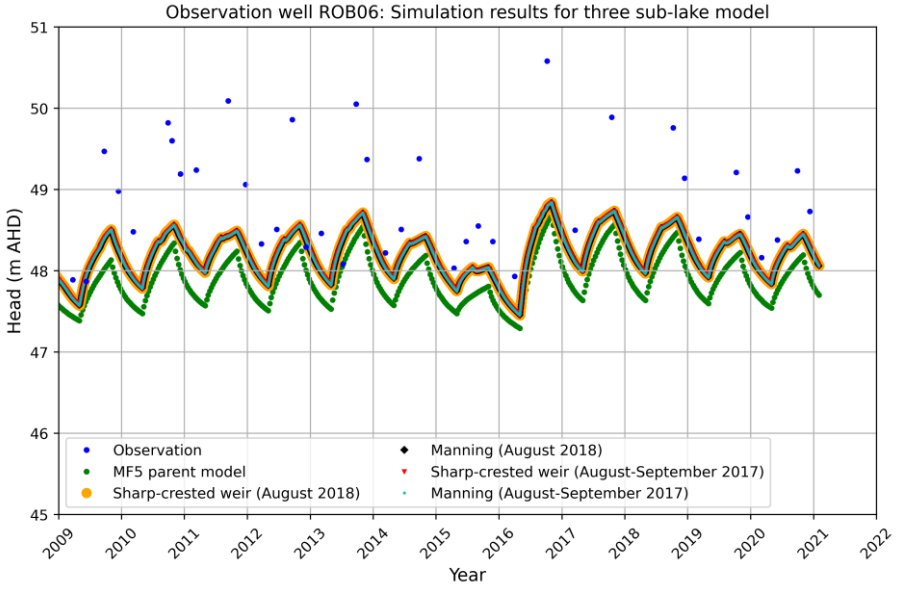

Figure A18. Comparison of observed groundwater head at observation well ROB06 with simulated results. The simulations were conducted using the three sub-lake model and compared to the MF5 parent model, testing outlet equations (i.e., Sharp-crested weir and Manning) for the periods of August–September 2017 and August 2018.

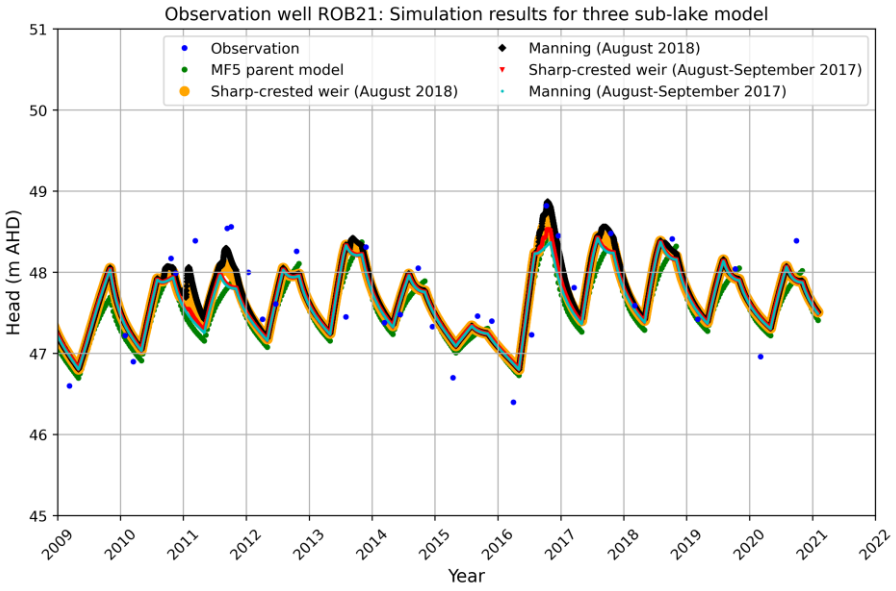

Figure A19. Comparison of observed groundwater head at observation well ROB21 with simulated results. The simulations were conducted using the three sub-lake model and compared to the MF5 parent model, testing outlet equations (i.e., Sharp-crested weir and Manning) for the periods of August–September 2017 and August 2018.

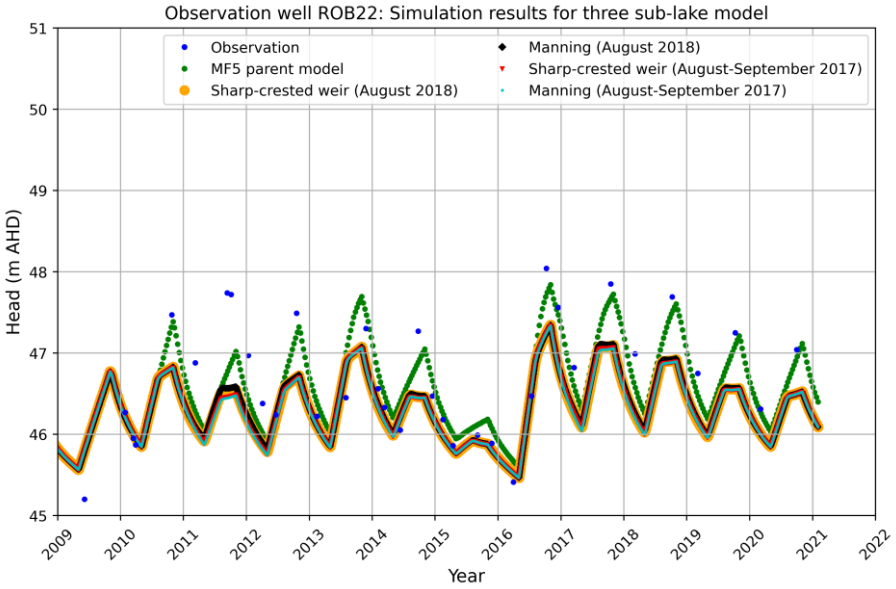

Figure A20. Comparison of observed groundwater head at observation well ROB22 with simulated results. The simulations were conducted using the three sub-lake model and compared to the MF5 parent model, testing outlet equations (i.e., Sharp-crested weir and Manning) for the periods of August–September 2017 and August 2018.

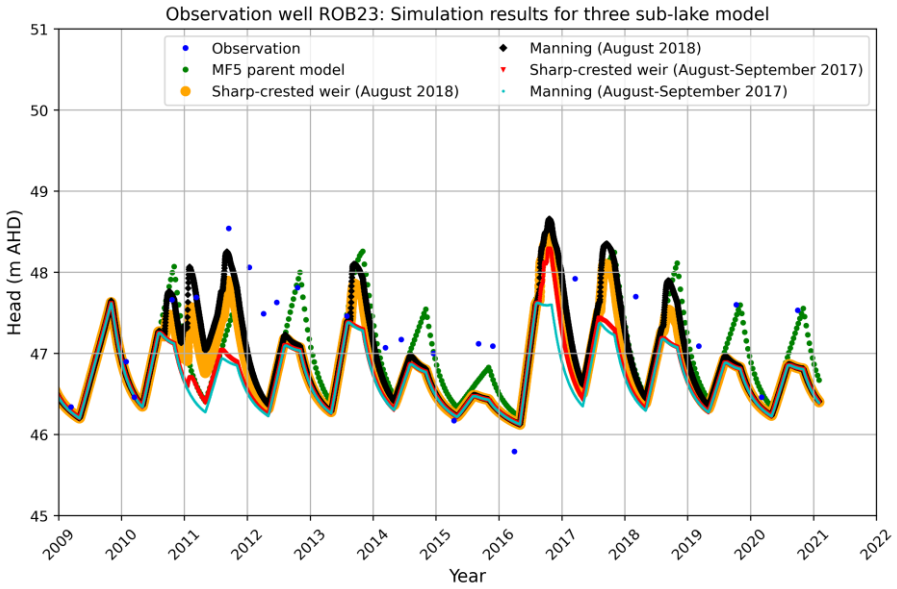

Figure A21. Comparison of observed groundwater head at observation well ROB23 with simulated results. The simulations were conducted using the three sub-lake model and compared to the MF5 parent model, testing outlet equations (i.e., Sharp-crested weir and Manning) for the periods of August–September 2017 and August 2018.

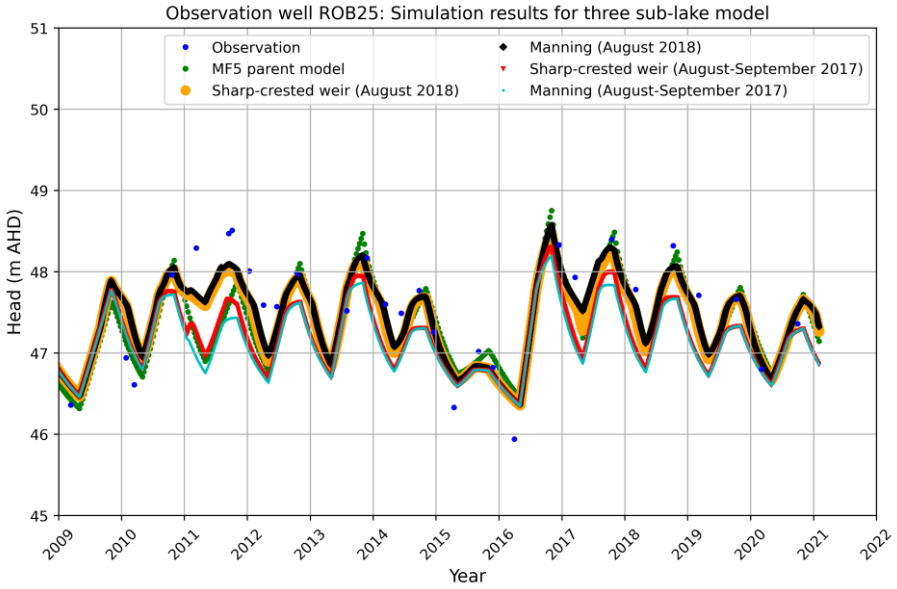

Figure A22. Comparison of observed groundwater head at observation well ROB25 with simulated results. The simulations were conducted using the three sub-lake model and compared to the MF5 parent model, testing outlet equations (i.e., Sharp-crested weir and Manning) for the periods of August–September 2017 and August 2018.

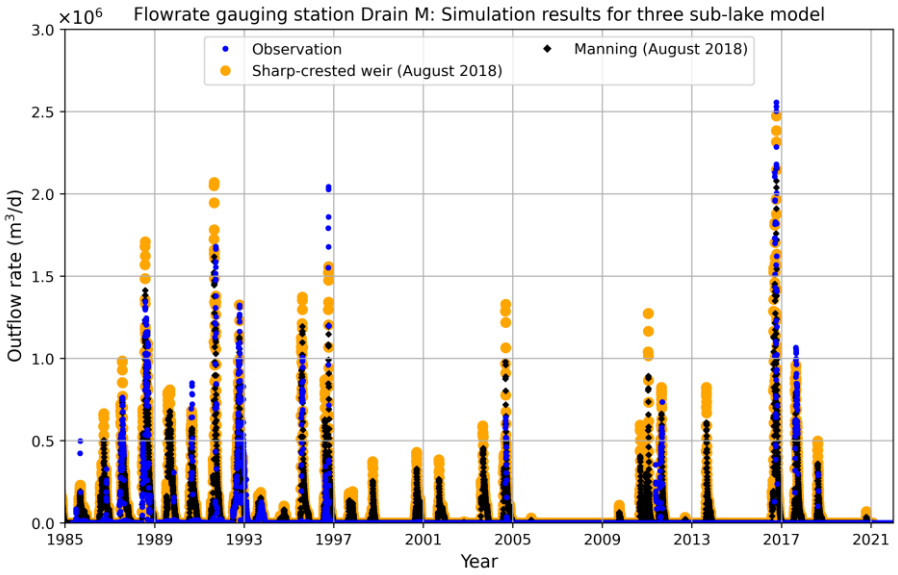

Figure A23. Comparison between observed outflow rates at Drain M and simulated results using the three sub-lake model is presented, with sharp-crested weir and Manning equations adapted for the period of August 2018.

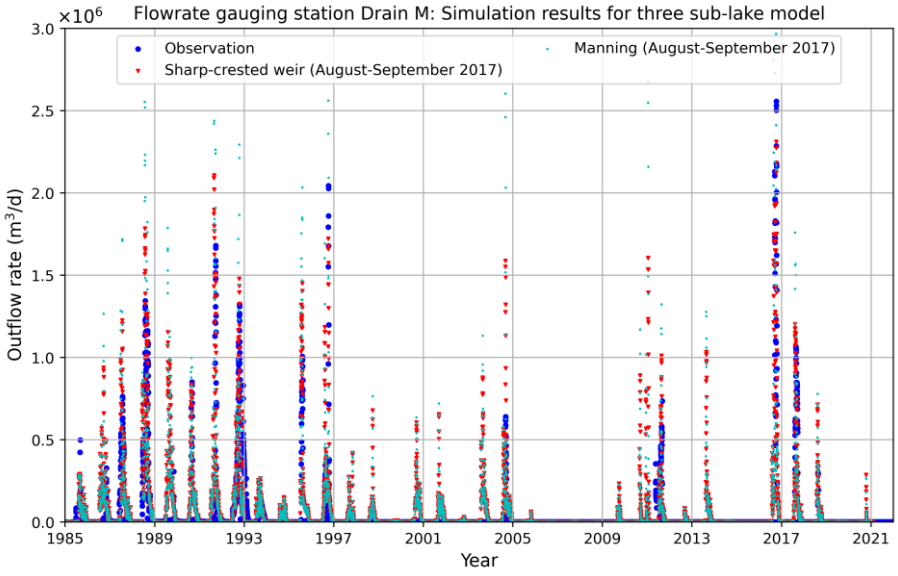

Figure A24. Comparison between observed outflow rates at Drain M and simulated results using the three sub-lake model is presented, with Sharp-crested weir and Manning equations adapted for the period of August–September 2017.

Appendix B – Sensitivity analysis of lakebed leakance

B.1 Bool Lagoon Complex

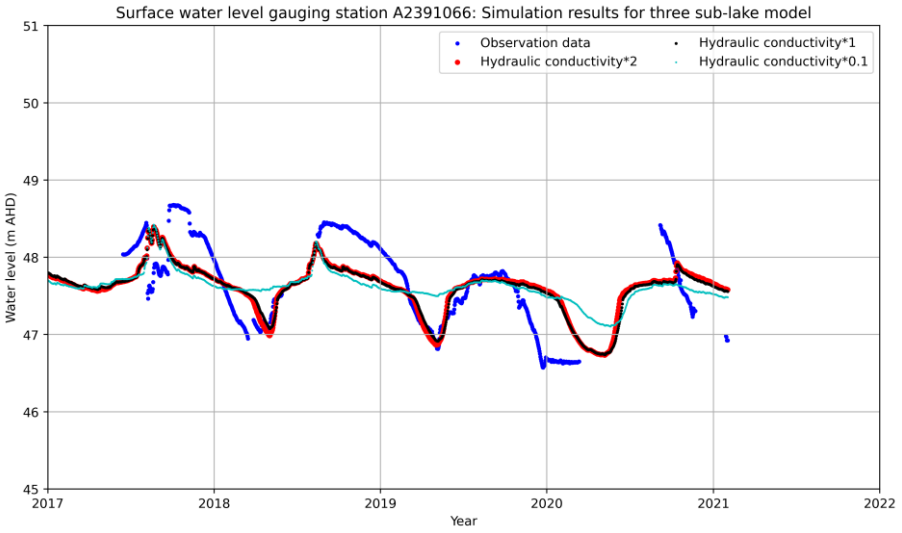

Figure B1. Comparison of observed surface water level at observation gauging station A2391066 with simulated results. The simulations were conducted using the three sub-lake models, testing lakebed leakance by applying two multipliers (0.1 and 2) to the lakebed's hydraulic conductivity.

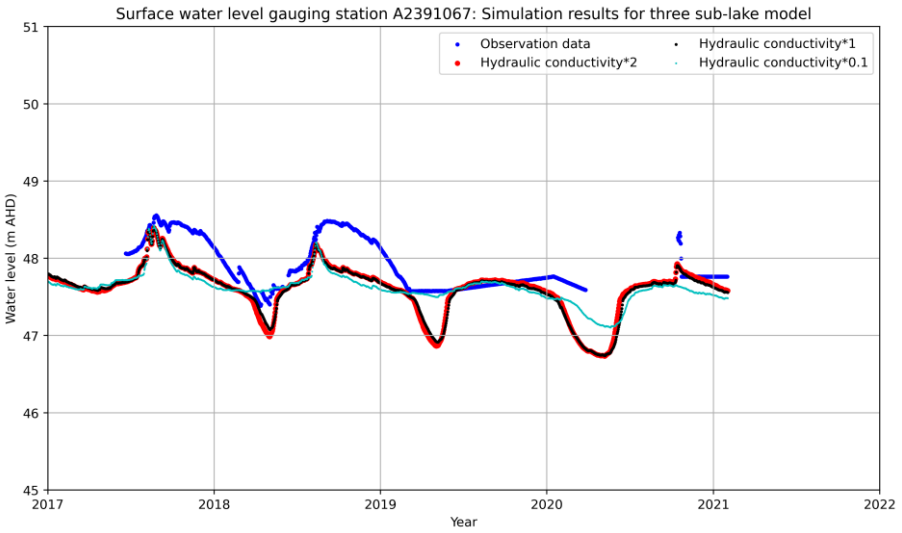

Figure B2. Comparison of observed surface water level at observation gauging station A2391067 with simulated results. The simulations were conducted using the three sub-lake models, testing lakebed leakance by applying two multipliers (0.1 and 2) to the lakebed's hydraulic conductivity.

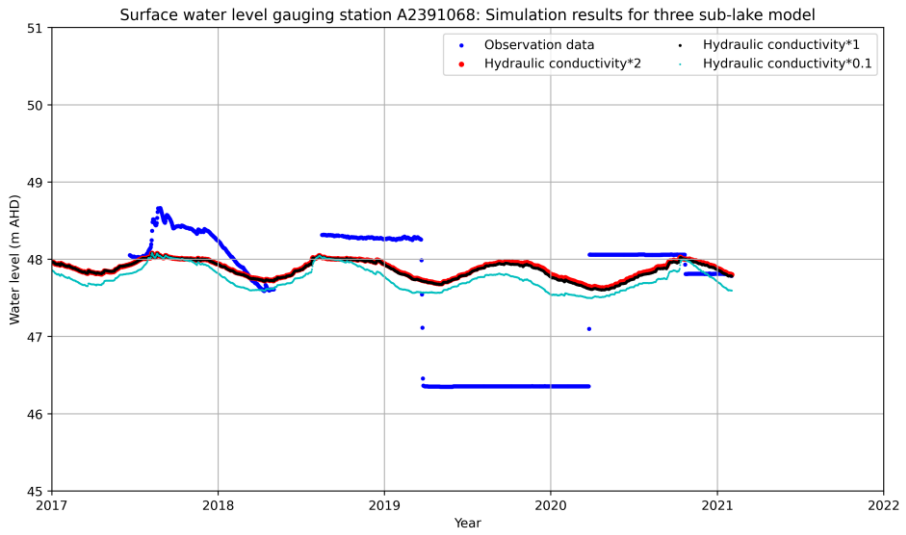

Figure B3. Comparison of observed surface water level at observation gauging station A2391068 with simulated results. The simulations were conducted using the three sub-lake models, testing lakebed leakance by applying two multipliers (0.1 and 2) to the lakebed's hydraulic conductivity.

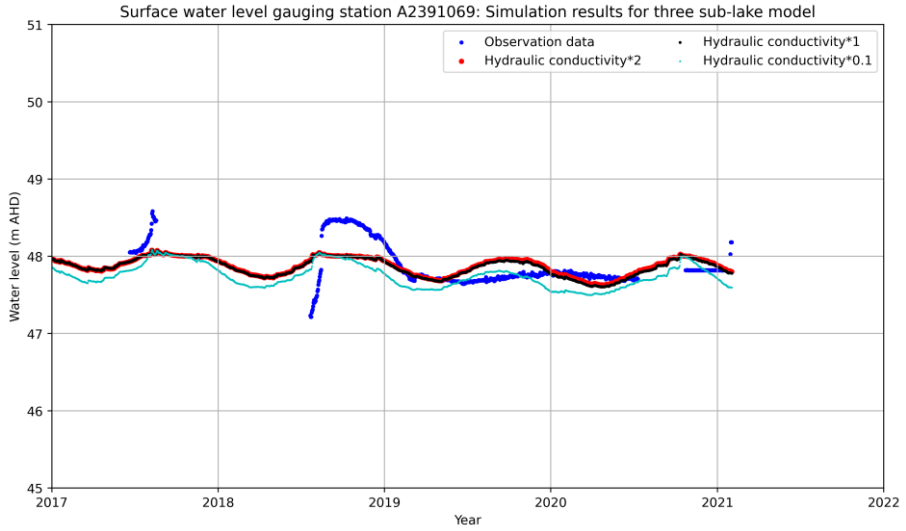

Figure B4. Comparison of observed surface water level at observation gauging station A2391069 with simulated results. The simulations were conducted using the three sub-lake models, testing lakebed leakance by applying two multipliers (0.1 and 2) to the lakebed's hydraulic conductivity.

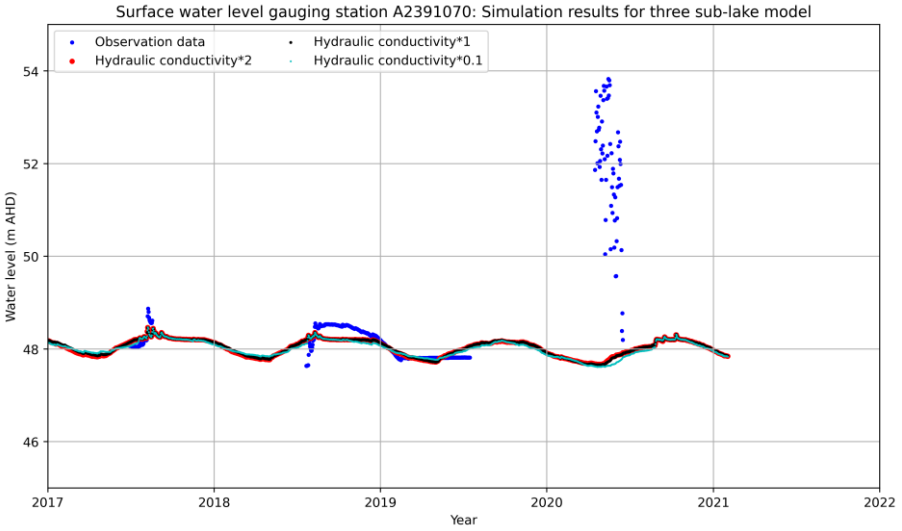

Figure B5. Comparison of observed surface water level at observation gauging station A2391070 with simulated results. The simulations were conducted using the three sub-lake models, testing lakebed leakance by applying two multipliers (0.1 and 2) to the lakebed's hydraulic conductivity.

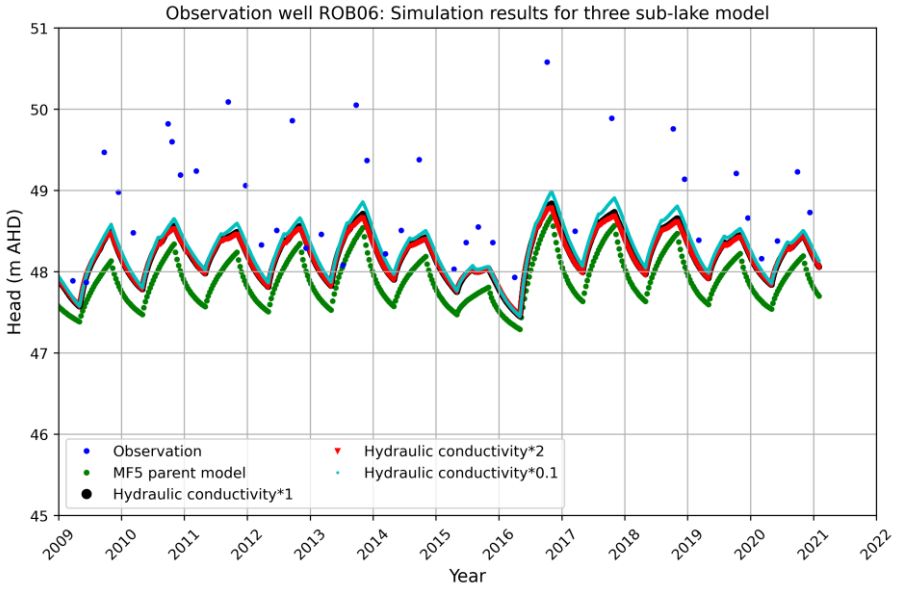

Figure B6. Comparison of observed groundwater head at observation well ROB06 with simulated results. The simulations were conducted using the three sub-lake models and compared to the MF5 parent model, testing lakebed leakance by applying two multipliers (0.1 and 2) to the lakebed's hydraulic conductivity.

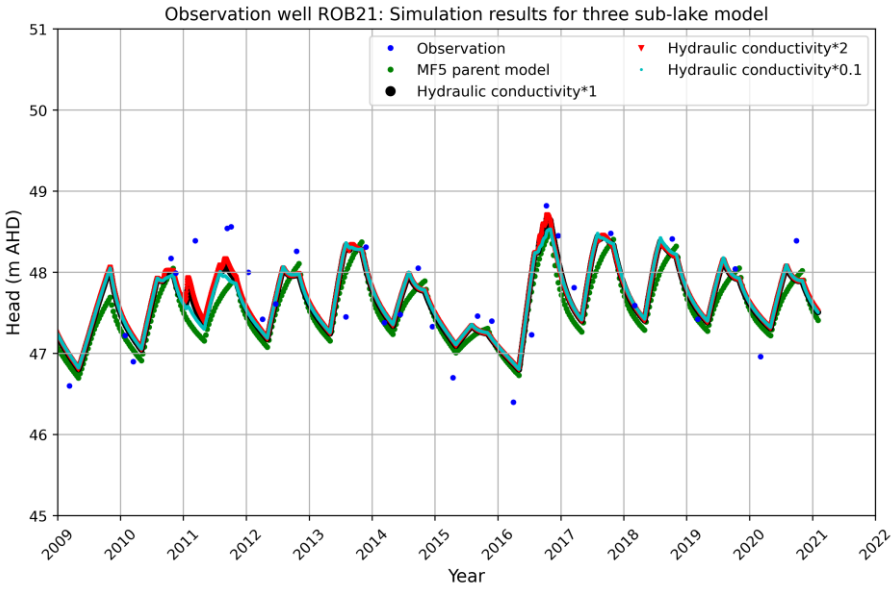

Figure B7. Comparison of observed groundwater head at observation well ROB21 with simulated results. The simulations were conducted using the three sub-lake models and compared to the MF5 parent model, testing lakebed leakance by applying two multipliers (0.1 and 2) to the lakebed's hydraulic conductivity.

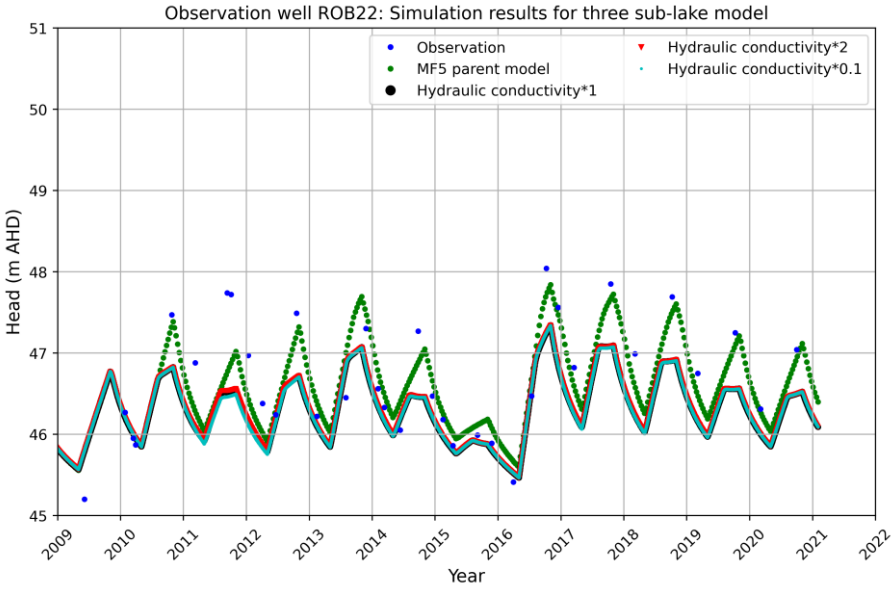

Figure B8. Comparison of observed groundwater head at observation well ROB22 with simulated results. The simulations were conducted using the three sub-lake models and compared to the MF5 parent model, testing lakebed leakance by applying two multipliers (0.1 and 2) to the lakebed's hydraulic conductivity.

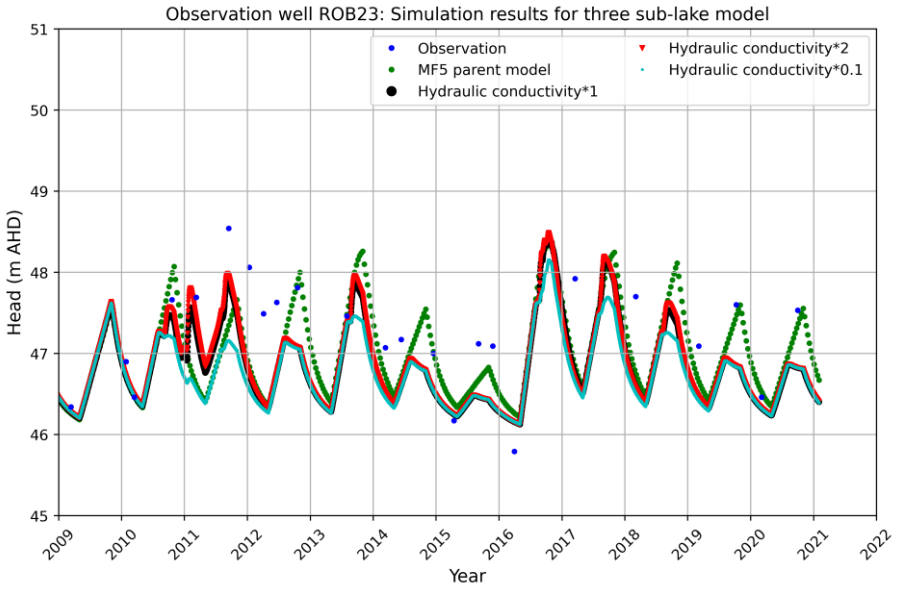

Figure B9. Comparison of observed groundwater head at observation well ROB23 with simulated results. The simulations were conducted using the three sub-lake models and compared to the MF5 parent model, testing lakebed leakance by applying two multipliers (0.1 and 2) to the lakebed's hydraulic conductivity.

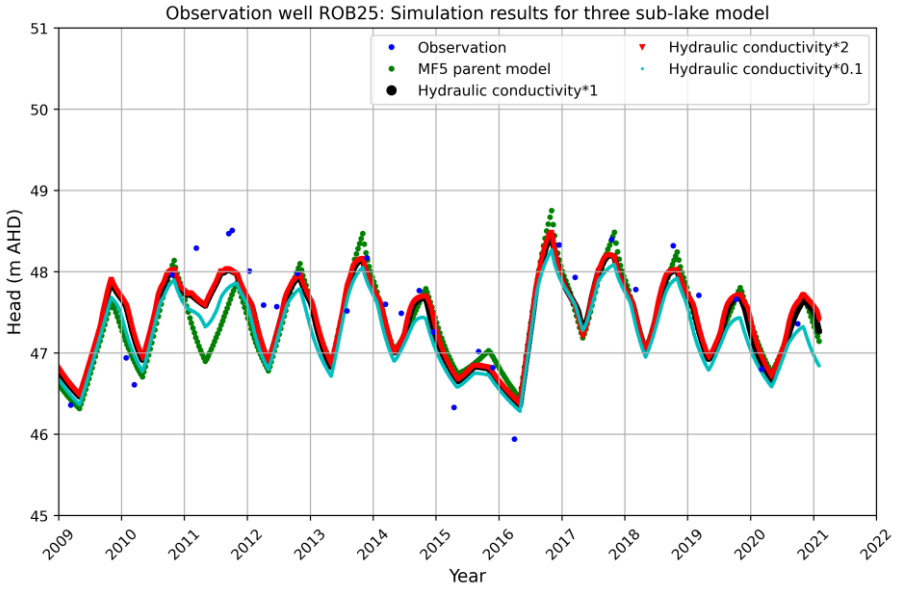

Figure B10. Comparison of observed groundwater head at observation well ROB25 with simulated results. The simulations were conducted using the three sub-lake models and compared to the MF5 parent model, testing lakebed leakance by applying two multipliers (0.1 and 2) to the lakebed's hydraulic conductivity.

B.2 Karst Springs Restoration site

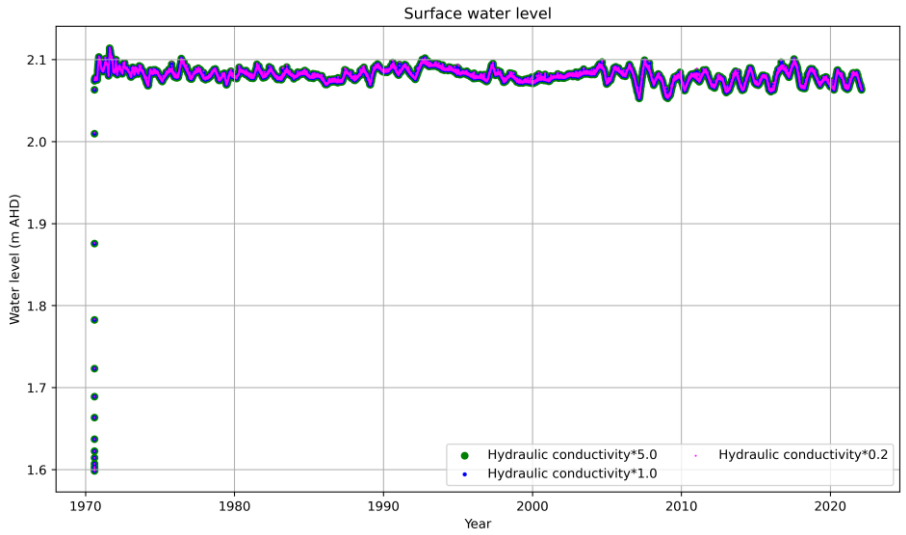

Figure B11. Comparison of observed surface water level for testing lakebed leakance by applying two multipliers (0.2 and 5) to the lakebed's hydraulic conductivity.

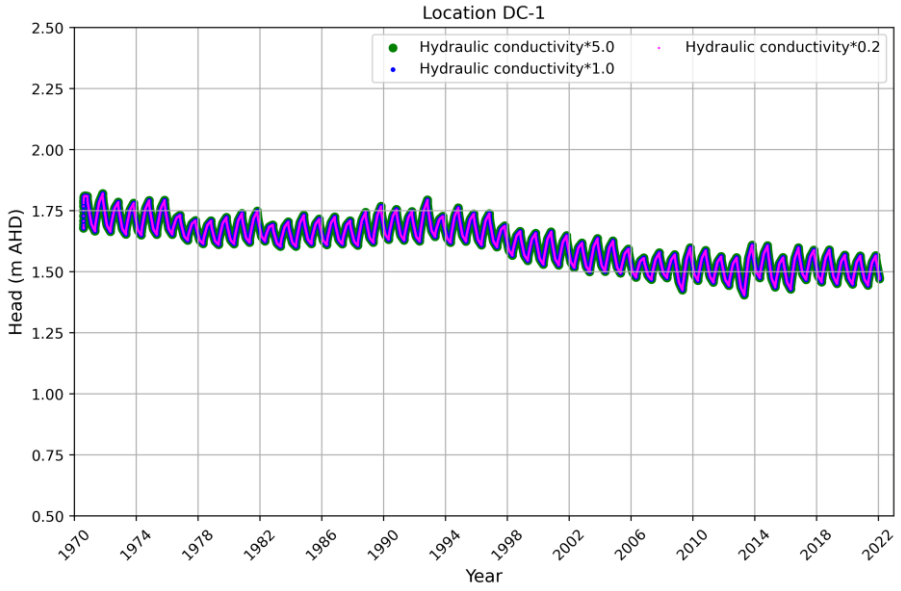

Figure B12. Comparison of simulated groundwater heads at selected cell DC-1 under varying lakebed hydraulic conductivity options. The DC sub-model with the Lake package (base model: "Hydraulic conductivity*1.0") is compared against simulations applying multipliers of 0.2 and 5 to the lakebed's hydraulic conductivity.

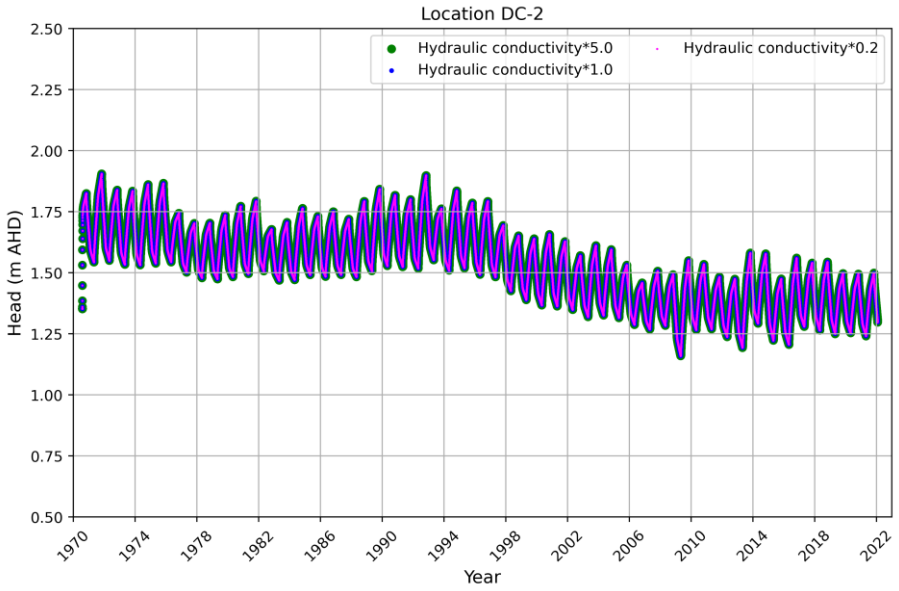

Figure B13. Comparison of simulated groundwater heads at selected cell DC-2 under varying lakebed hydraulic conductivity options. The DC sub-model with the Lake package (base model: "Hydraulic conductivity*1.0") is compared against simulations applying multipliers of 0.2 and 5 to the lakebed's hydraulic conductivity.

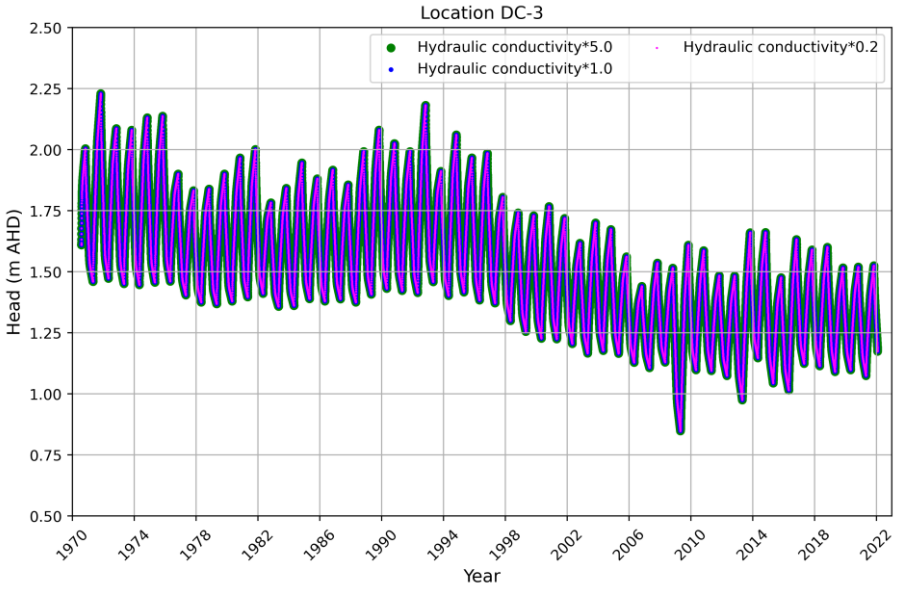

Figure B14. Comparison of simulated groundwater heads at selected cell DC-3 under varying lakebed hydraulic conductivity options. The DC sub-model with the Lake package (base model: "Hydraulic conductivity*1.0") is compared against simulations applying multipliers of 0.2 and 5 to the lakebed's hydraulic conductivity.

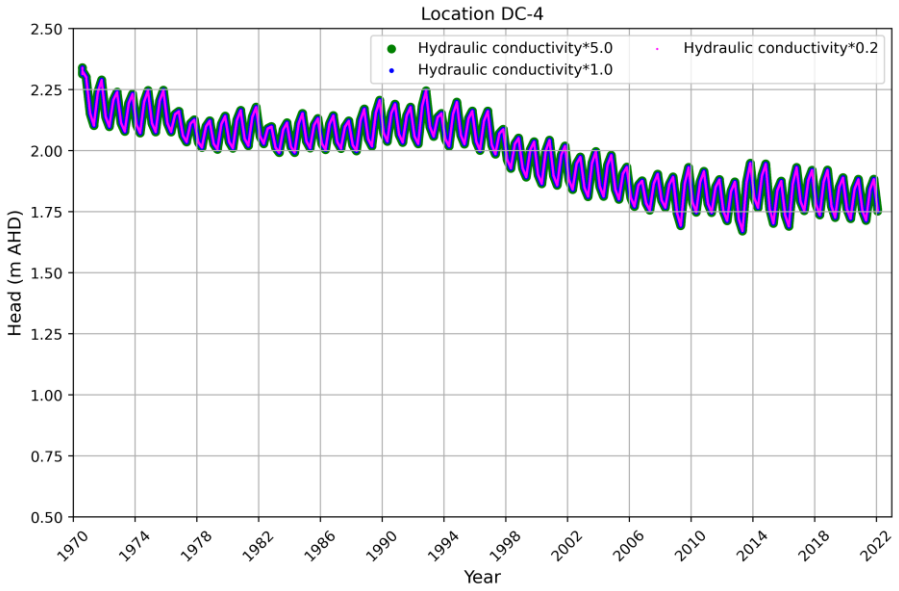

Figure B15. Comparison of simulated groundwater heads at selected cell DC-4 under varying lakebed hydraulic conductivity options. The DC sub-model with the Lake package (base model: “Hydraulic conductivity*1.0”) is compared against simulations applying multipliers of 0.2 and 5 to the lakebed's hydraulic conductivity.

Appendix C – Comparative analysis of hydrological results from predictive scenarios for Bool Lagoon Complex

C.1 Hydrological outcomes of BLC-S1 simulation

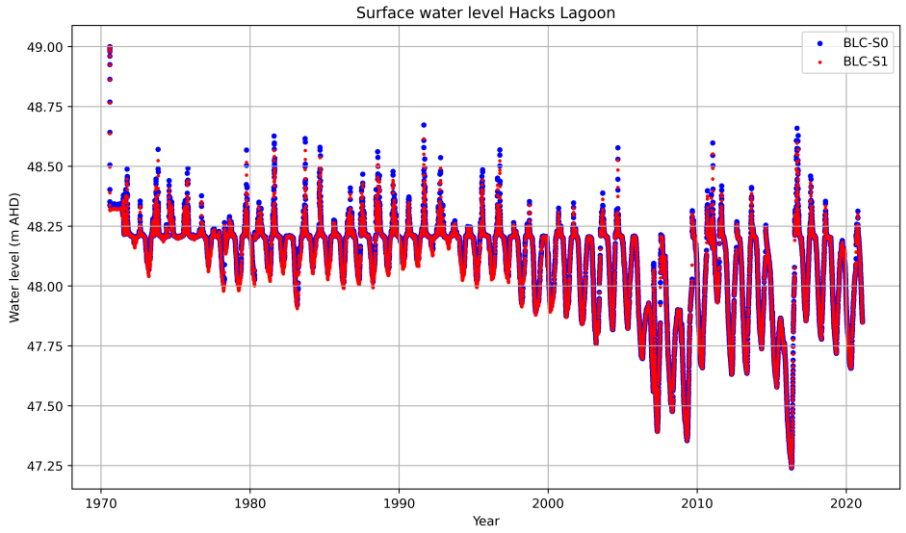

Figure C1. Comparison of surface water level between the base model (BLC-S0) and simulated results of BLC-S1 in Hacks Lagoon for the period 1970–2021.

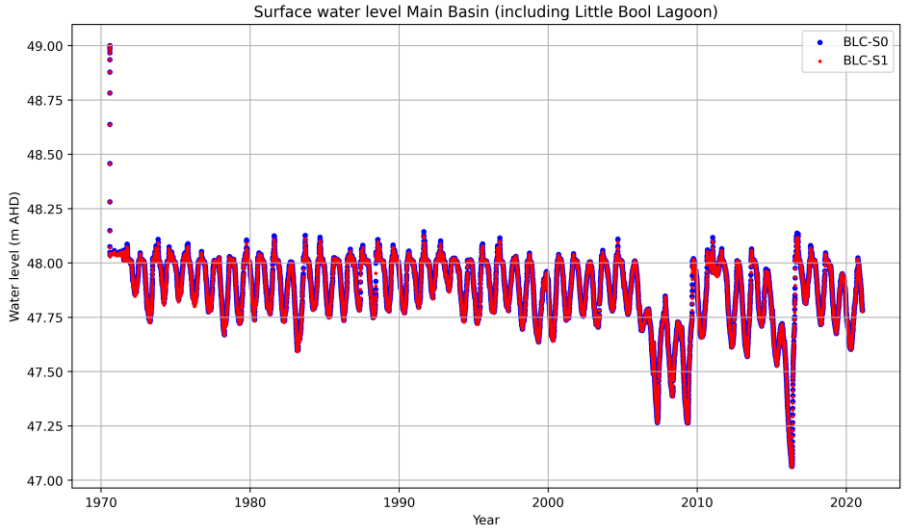

Figure C2. Comparison of surface water level between the base model (BLC-S0) and simulated results of BLC-S1 in Main Basin (including Little Bool Lagoon) for the period 1970–2021.

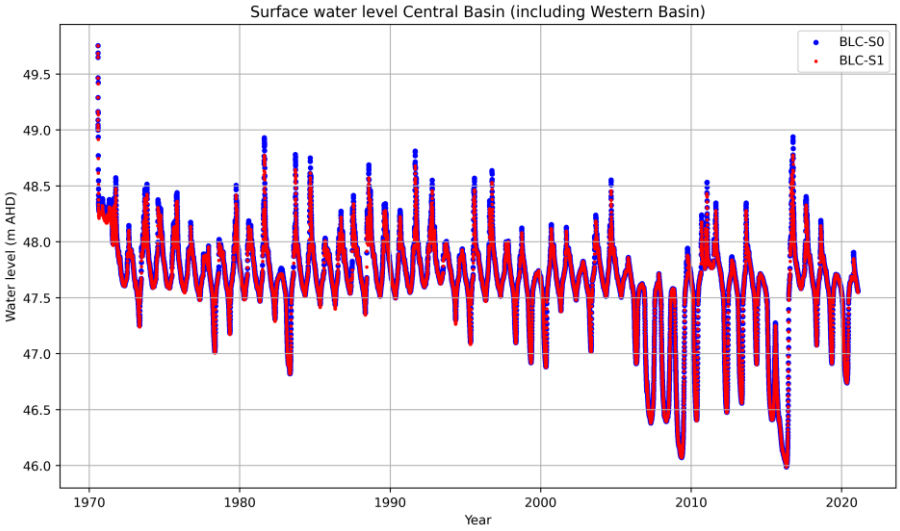

Figure C3. Comparison of surface water level between the base model (BLC-S0) and simulated results of BLC-S1 in Central Basin (including Western Basin) for the period 1970–2021.

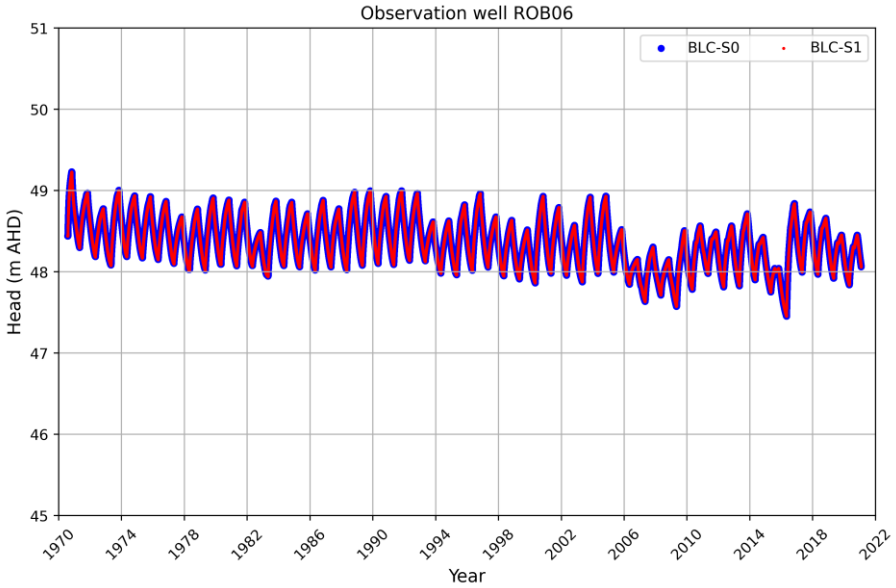

Figure C4. Comparison of groundwater head between the base model (BLC-S0) and simulated results of BLC-S1 at observation well ROB06 for the period 1970–2021.

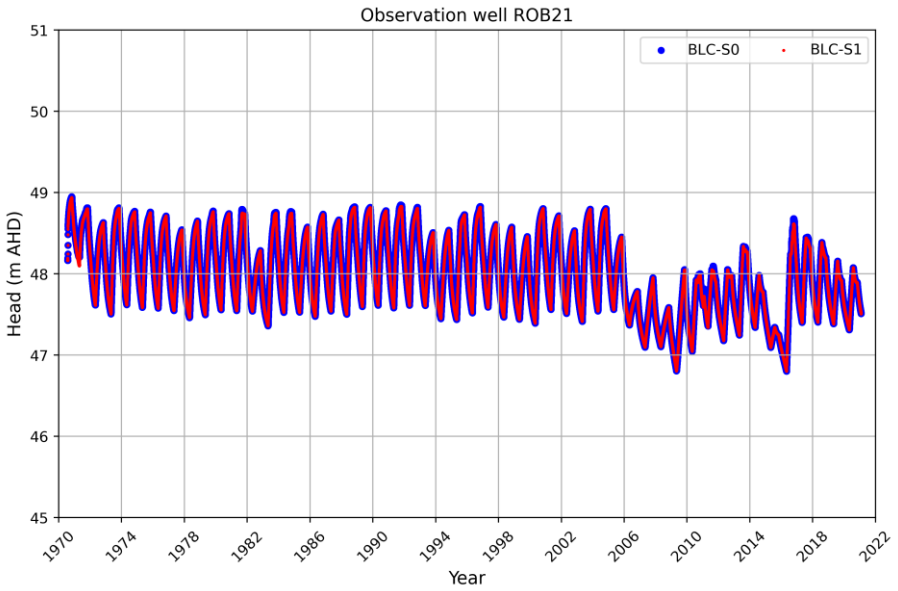

Figure C5. Comparison of groundwater head between the base model (BLC-S0) and simulated results of BLC-S1 at observation well ROB021 for the period 1970–2021.

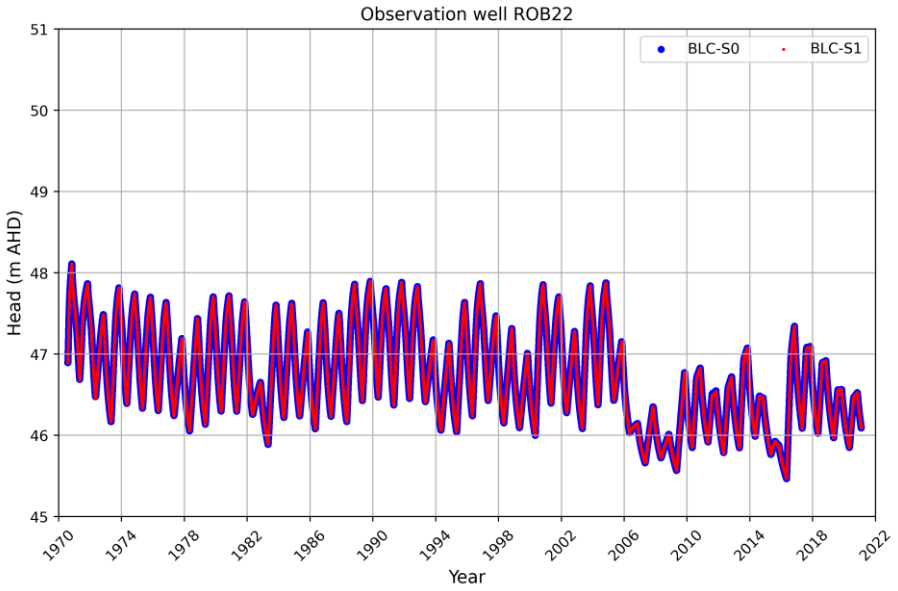

Figure C6. Comparison of groundwater head between the base model (BLC-S0) and simulated results of BLC-S1 at observation well ROB22 for the period 1970–2021.

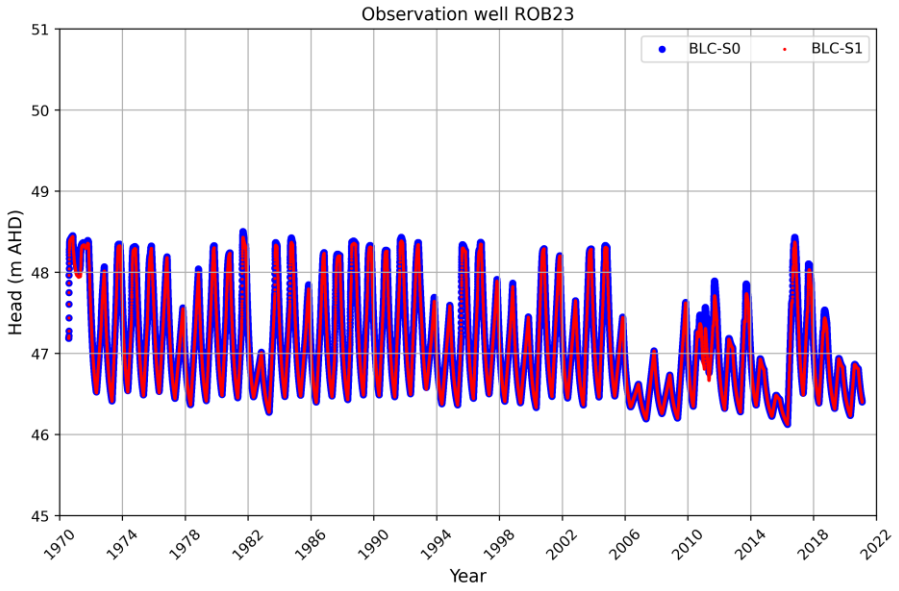

Figure C7. Comparison of groundwater head between the base model (BLC-S0) and simulated results of BLC-S1 at observation well ROB23 for the period 1970–2021.

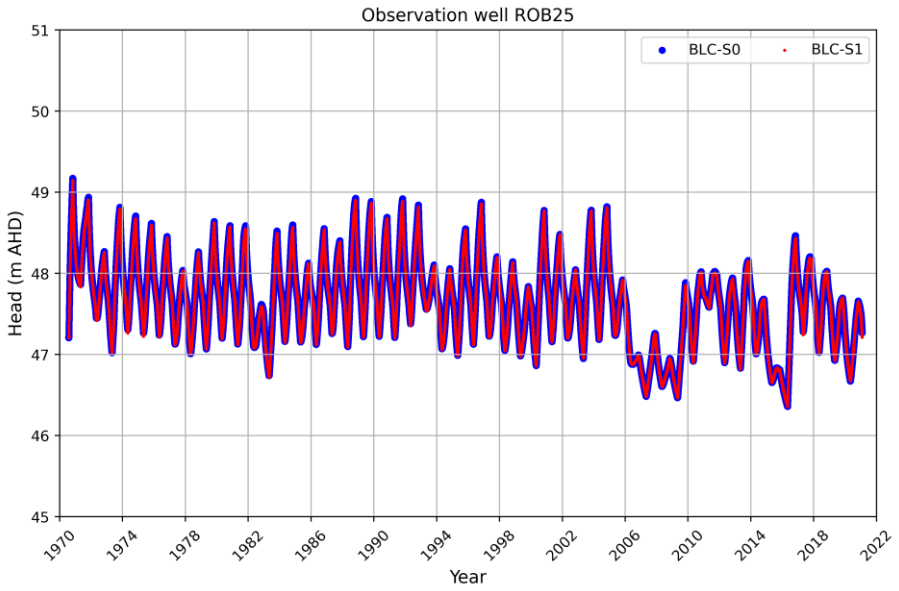

Figure C8. Comparison of groundwater head between the base model (BLC-S0) and simulated results of BLC-S1 at observation well ROB25 for the period 1970–2021.

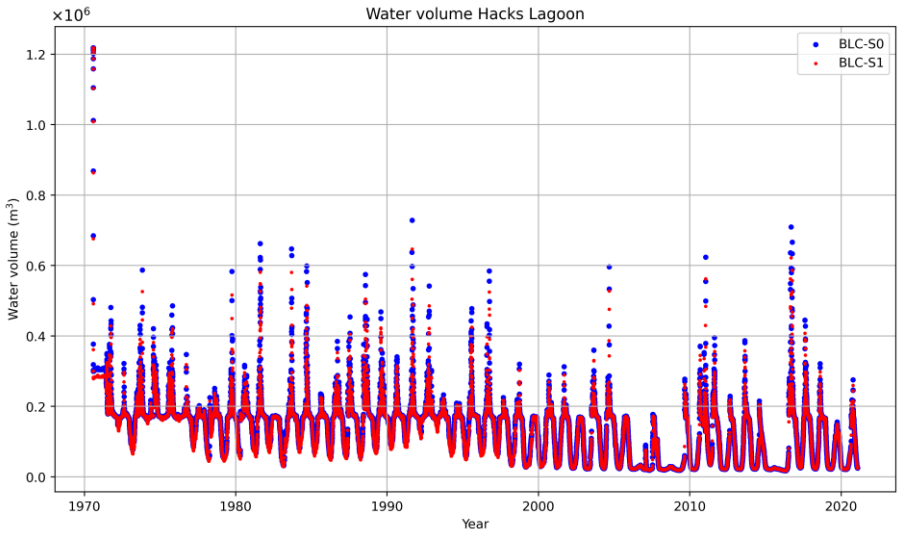

Figure C9. Comparison of water volume between the base model (BLC-S0) and simulated results of BLC-S1 in Hacks Lagoon for the period 1970–2021.

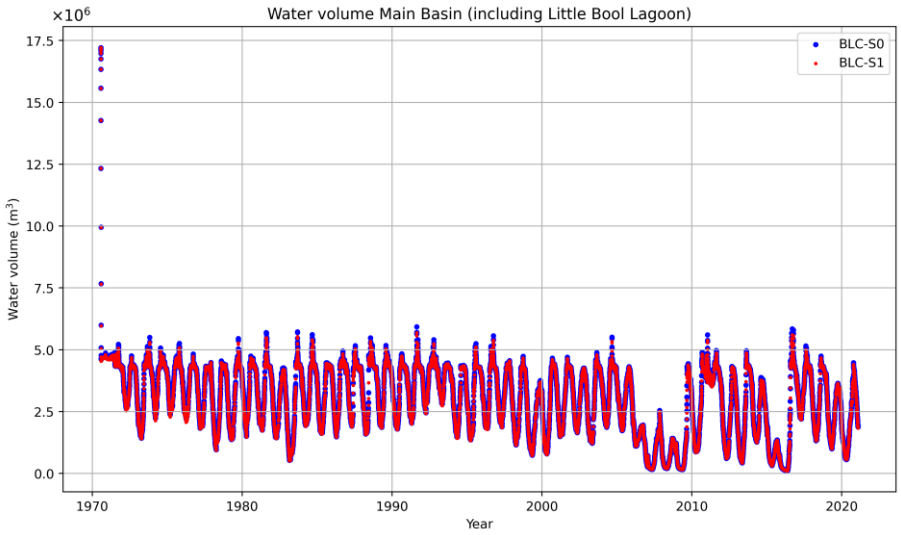

Figure C10. Comparison of water volume between the base model (BLC-S0) and simulated results of BLC-S1 in Main Basin (including Little Bool Lagoon) for the period 1970–2021.

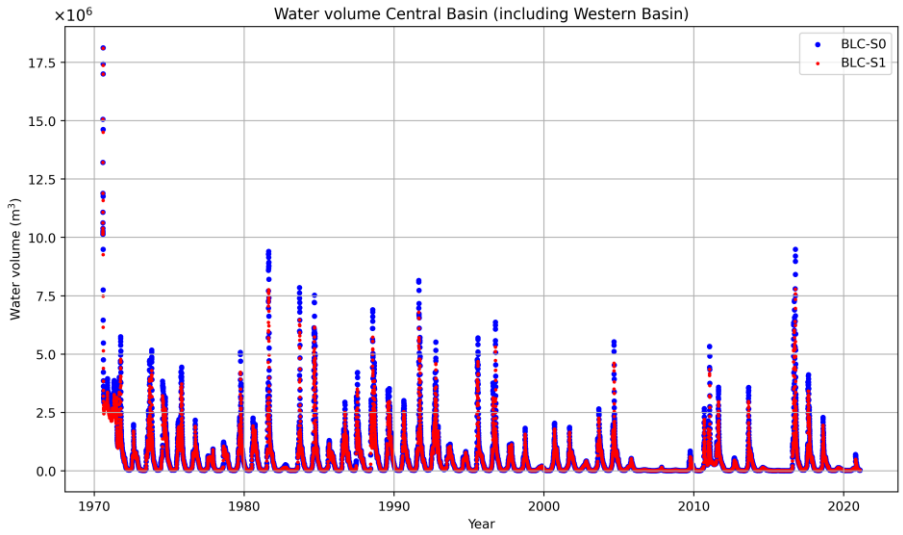

Figure C11. Comparison of water volume between the base model (BLC-S0) and simulated results of BLC-S1 in Central Basin (including Western Basin) for the period 1970–2021.

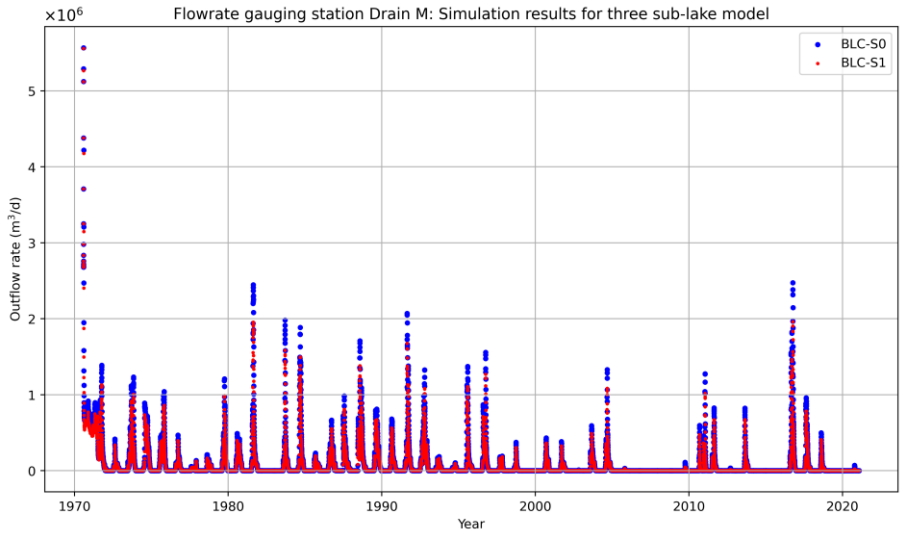

Figure C12. Comparison of outflow rates at Drain M between the base model (BLC-S0) and simulated results of BLC-S1 for the period 1970–2021.

C.2 Hydrological outcomes of BLC-S2 simulation

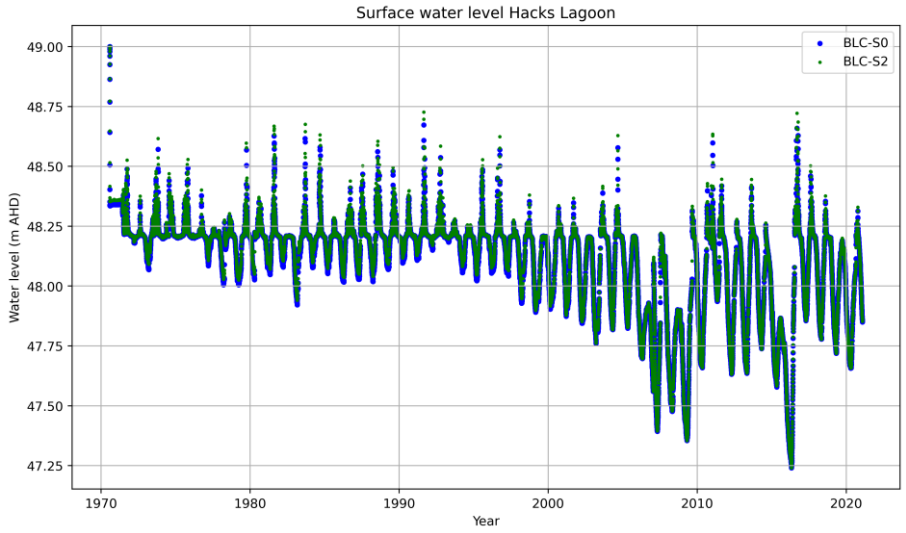

Figure C13. Comparison of surface water level between the base model (BLC-S0) and simulated results of BLC-S2 in Hacks Lagoon for the period 1970–2021.

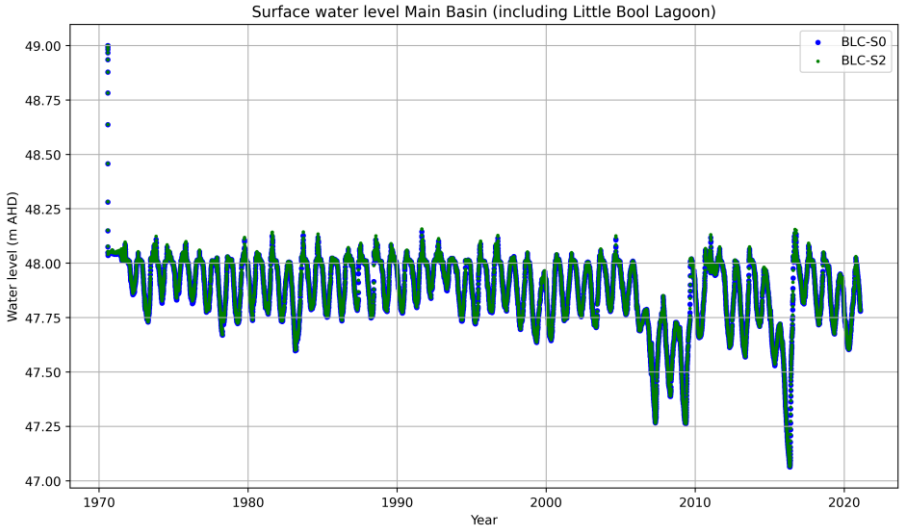

Figure C14. Comparison of surface water level between the base model (BLC-S0) and simulated results of BLC-S2 in Main Basin (including Little Bool Lagoon) for the period 1970–2021.

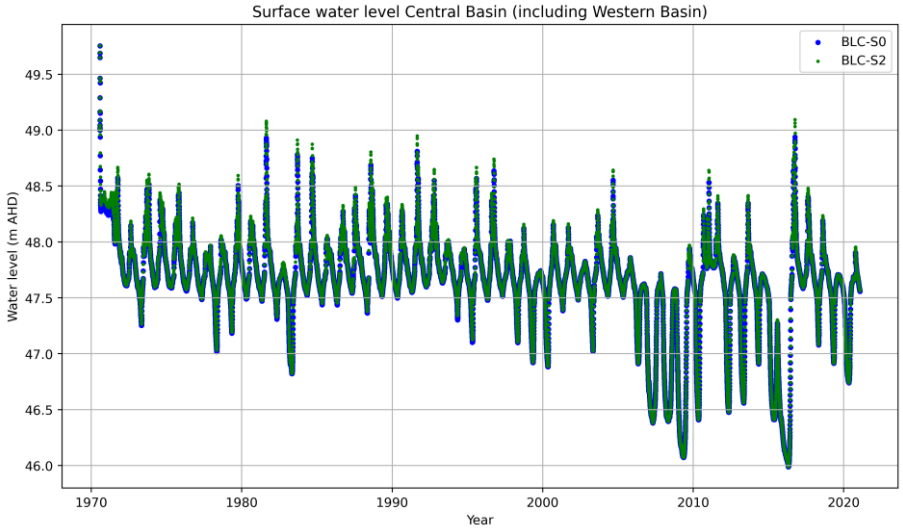

Figure C15. Comparison of surface water level between the base model (BLC-S0) and simulated results of BLC-S2 in Central Basin (including Western Basin) for the period 1970–2021.

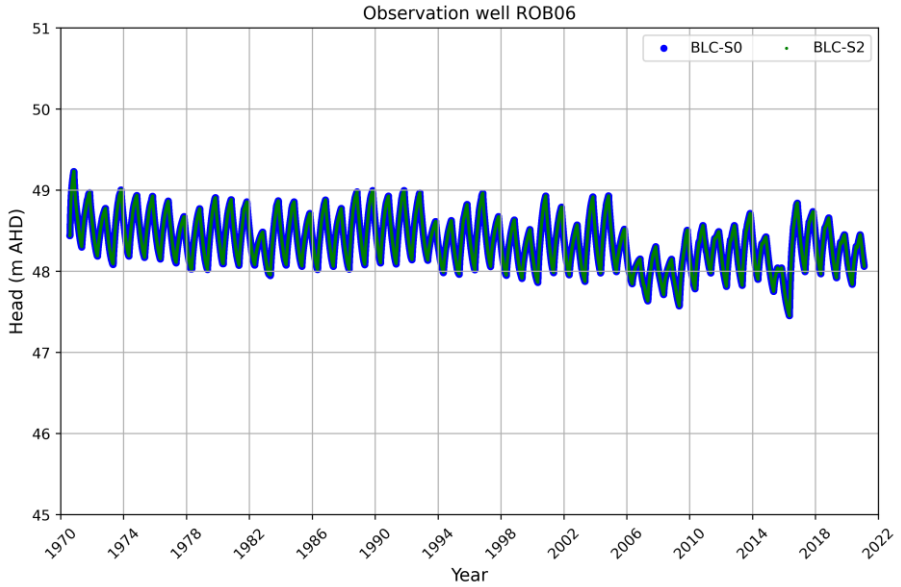

Figure C16. Comparison of groundwater head between the base model (BLC-S0) and simulated results of BLC-S2 at observation well ROB06 for the period 1970–2021.

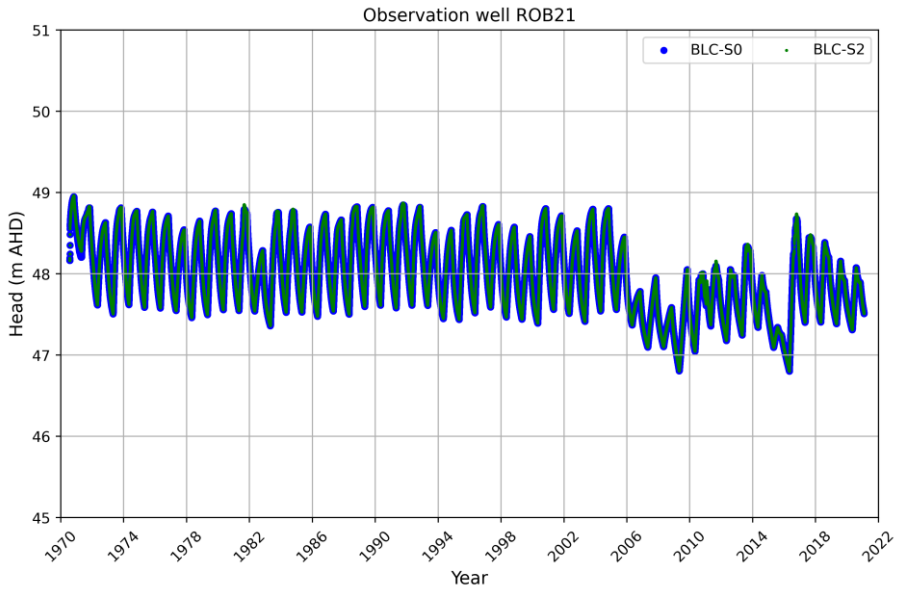

Figure C17. Comparison of groundwater head between the base model (BLC-S0) and simulated results of BLC-S2 at observation well ROB021 for the period 1970–2021.

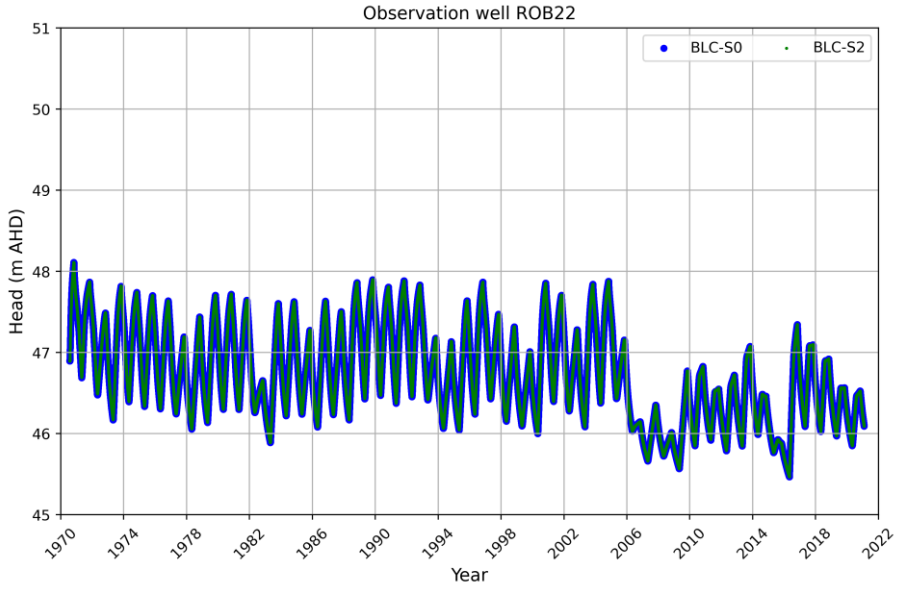

Figure C18. Comparison of groundwater head between the base model (BLC-S0) and simulated results of BLC-S2 at observation well ROB22 for the period 1970–2021.

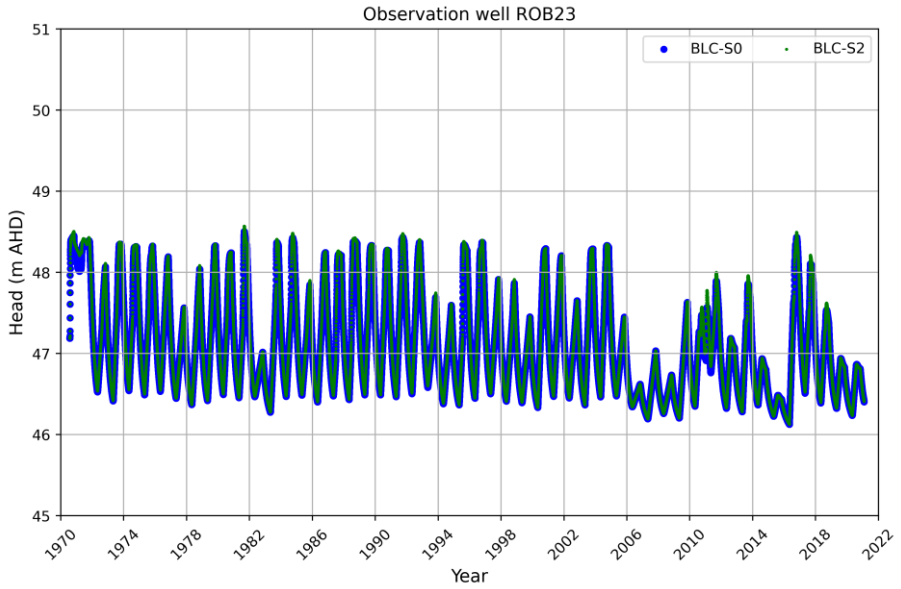

Figure C19. Comparison of groundwater head between the base model (BLC-S0) and simulated results of BLC-S2 at observation well ROB23 for the period 1970–2021.

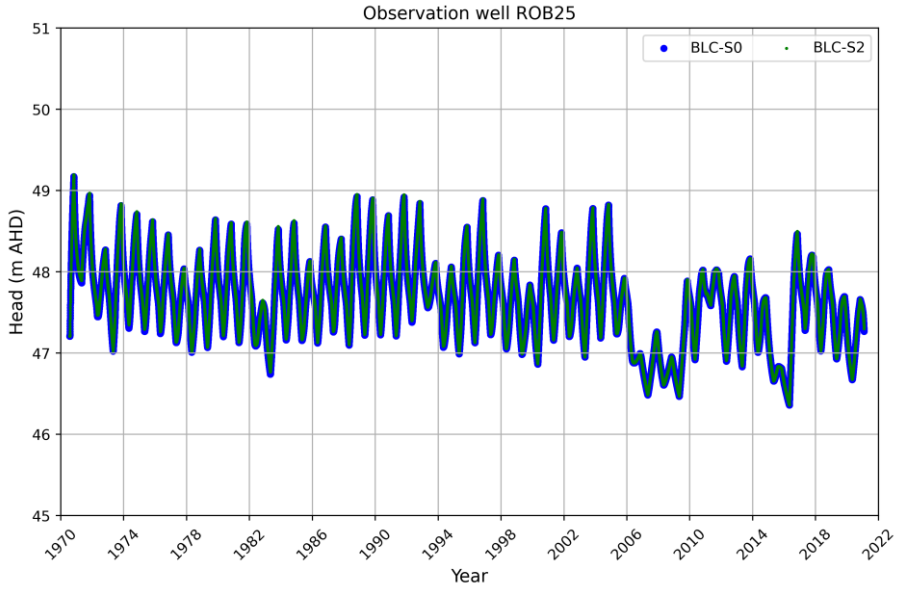

Figure C20. Comparison of groundwater head between the base model (BLC-S0) and simulated results of BLC-S2 at observation well ROB25 for the period 1970–2021.

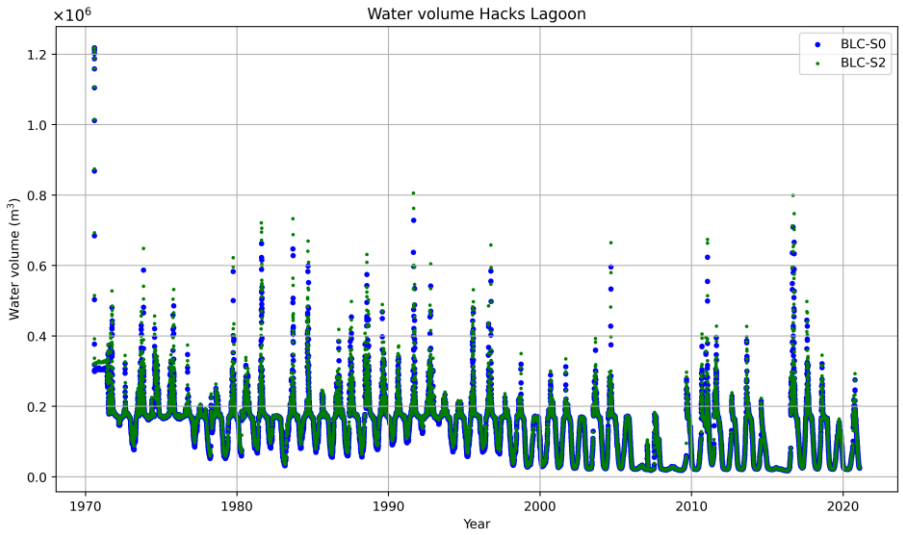

Figure C21. Comparison of water volume between the base model (BLC-S0) and simulated results of BLC-S2 in Hacks Lagoon for the period 1970–2021.

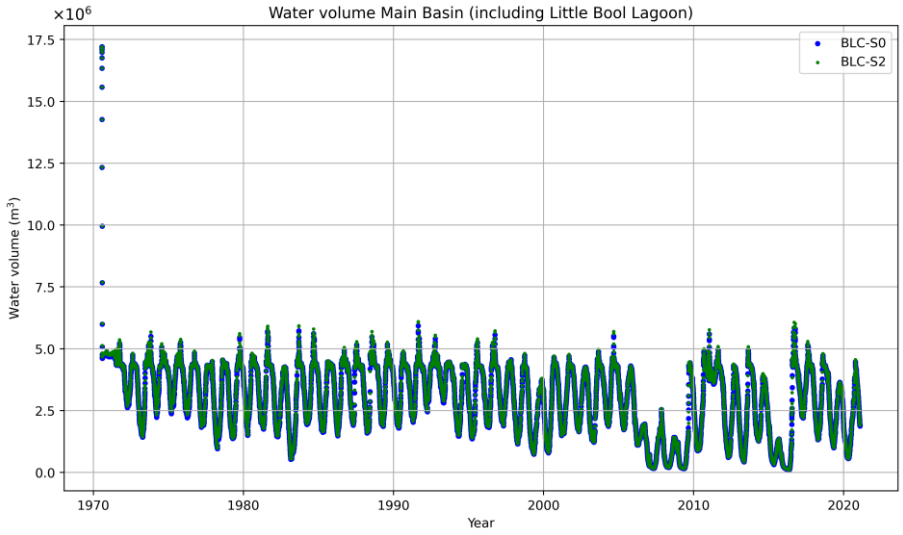

Figure C22. Comparison of water volume between the base model (BLC-S0) and simulated results of BLC-S2 in Main Basin (including Little Bool Lagoon) for the period 1970–2021.

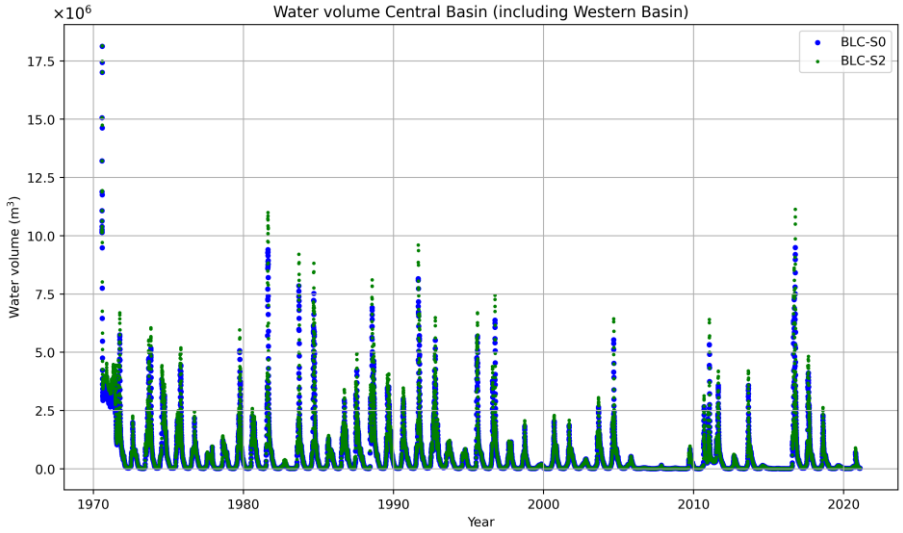

Figure C23. Comparison of water volume between the base model (BLC-S0) and simulated results of BLC-S2 in Central Basin (including Western Basin) for the period 1970–2021.

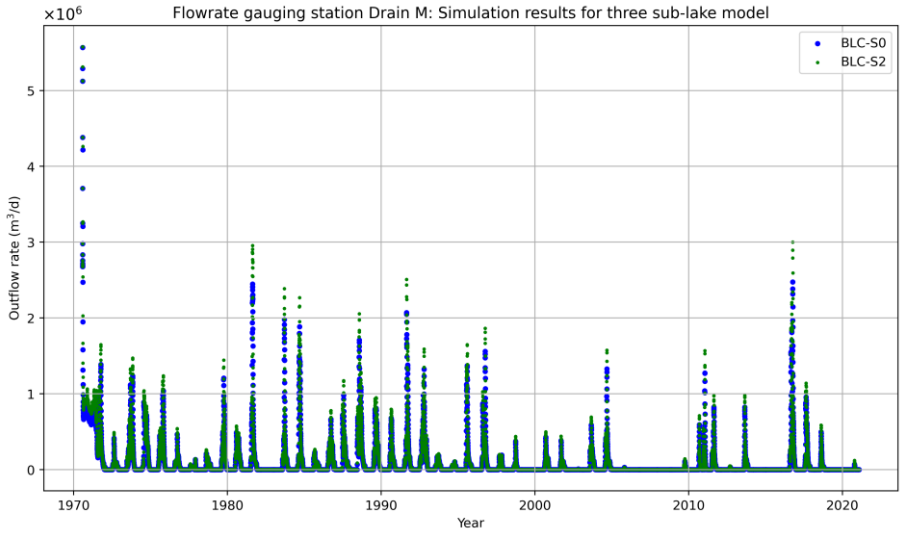

Figure C24. Comparison of outflow rates at Drain M between the base model (BLC-S0) and simulated results of BLC-S2 for the period 1970–2021.

C.3 Hydrological outcomes of BLC-S3 simulation

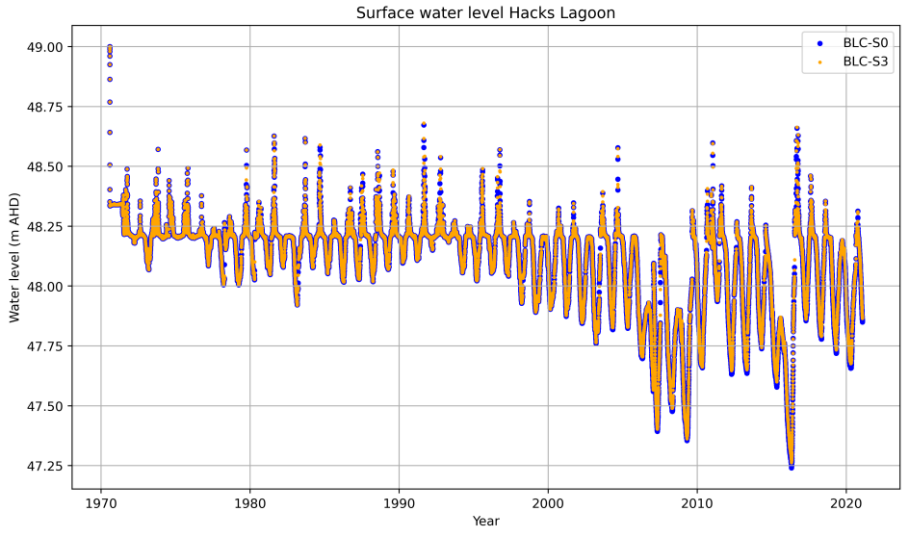

Figure C25. Comparison of surface water level between the base model (BLC-S0) and simulated results of BLC-S3 in Hacks Lagoon for the period 1970–2021.

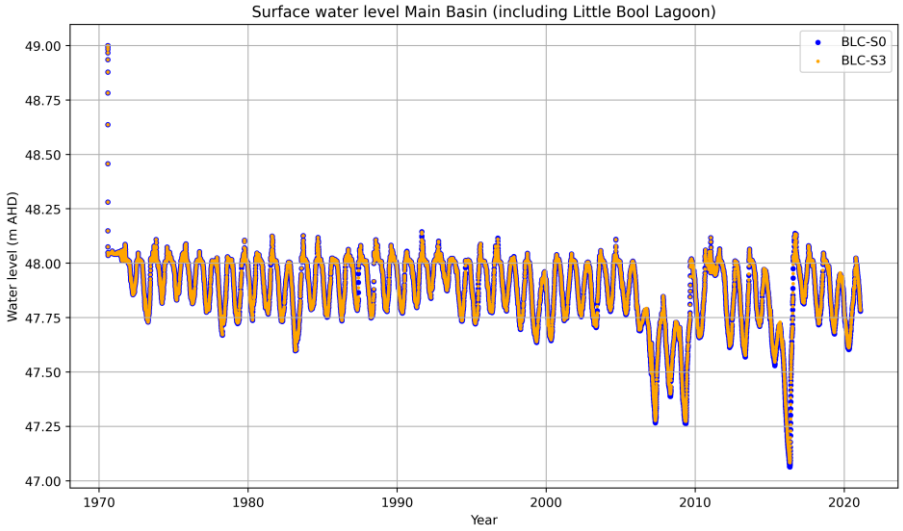

Figure C26. Comparison of surface water level between the base model (BLC-S0) and simulated results of BLC-S3 in Main Basin (including Little Bool Lagoon) for the period 1970–2021.

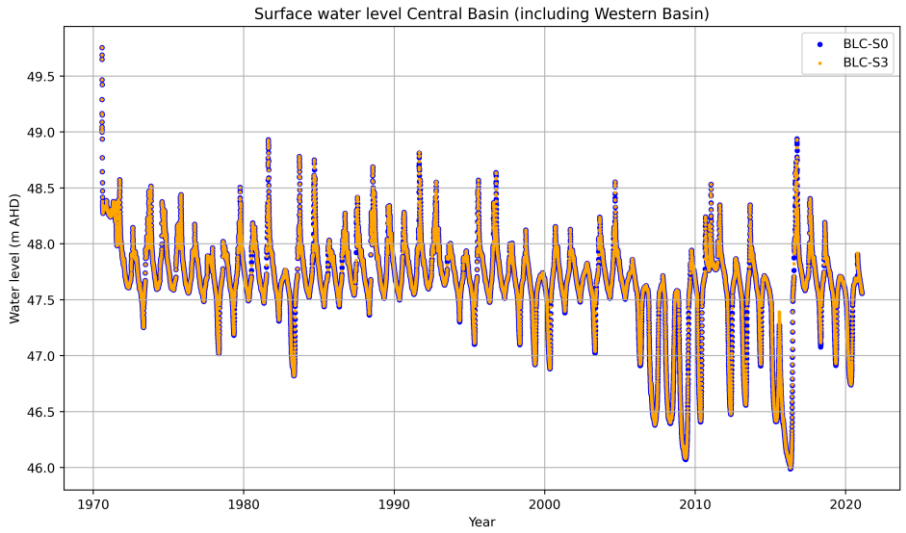

Figure C27. Comparison of surface water level between the base model (BLC-S0) and simulated results of BLC-S3 in Central Basin (including Western Basin) for the period 1970–2021.

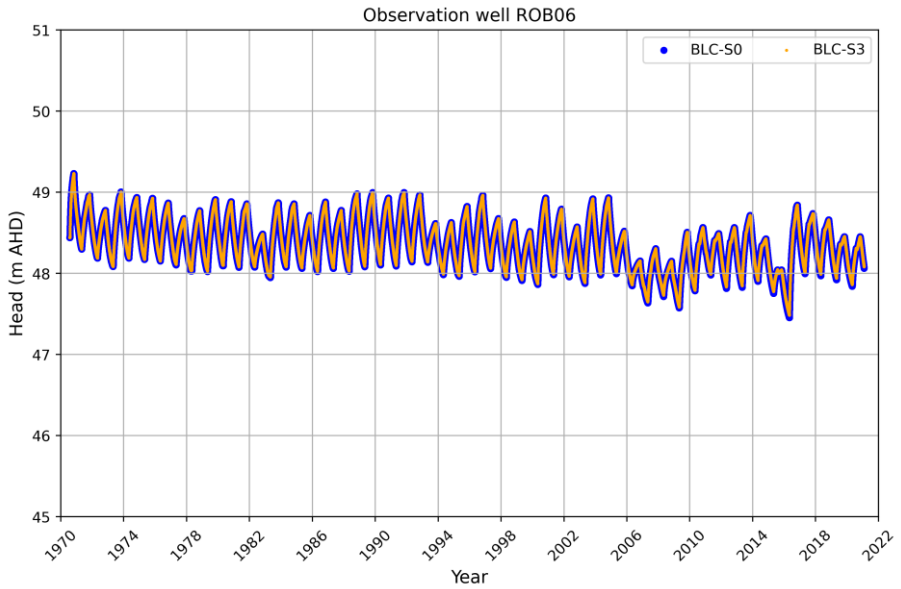

Figure C28. Comparison of groundwater head between the base model (BLC-S0) and simulated results of BLC-S3 at observation well ROB06 for the period 1970–2021.

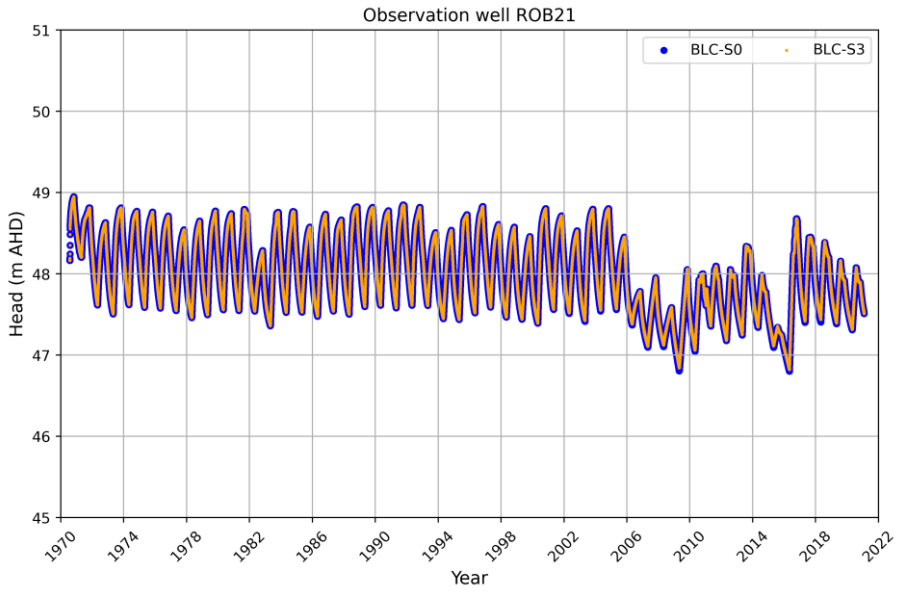

Figure C29. Comparison of groundwater head between the base model (BLC-S0) and simulated results of BLC-S3 at observation well ROB021 for the period 1970–2021.

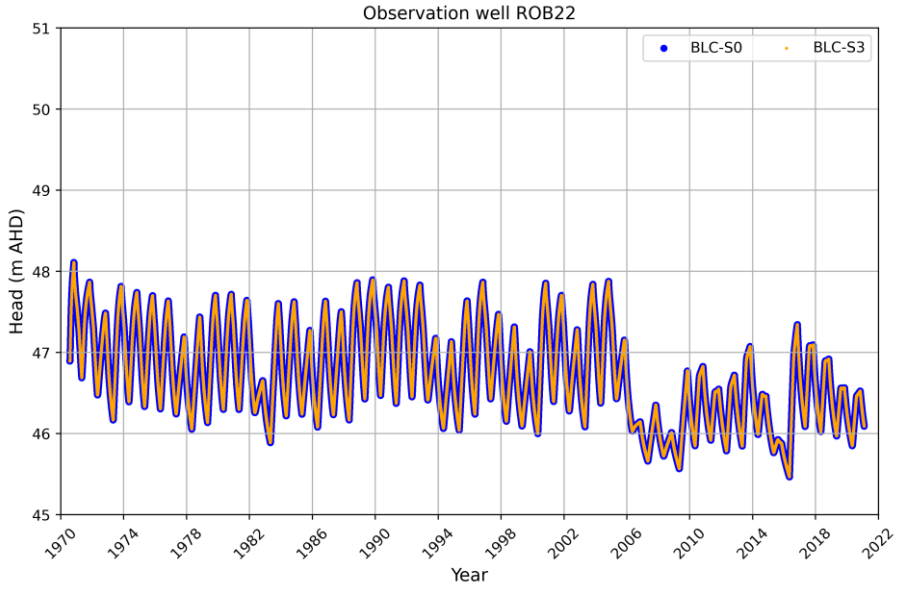

Figure C30. Comparison of groundwater head between the base model (BLC-S0) and simulated results of BLC-S3 at observation well ROB22 for the period 1970–2021.

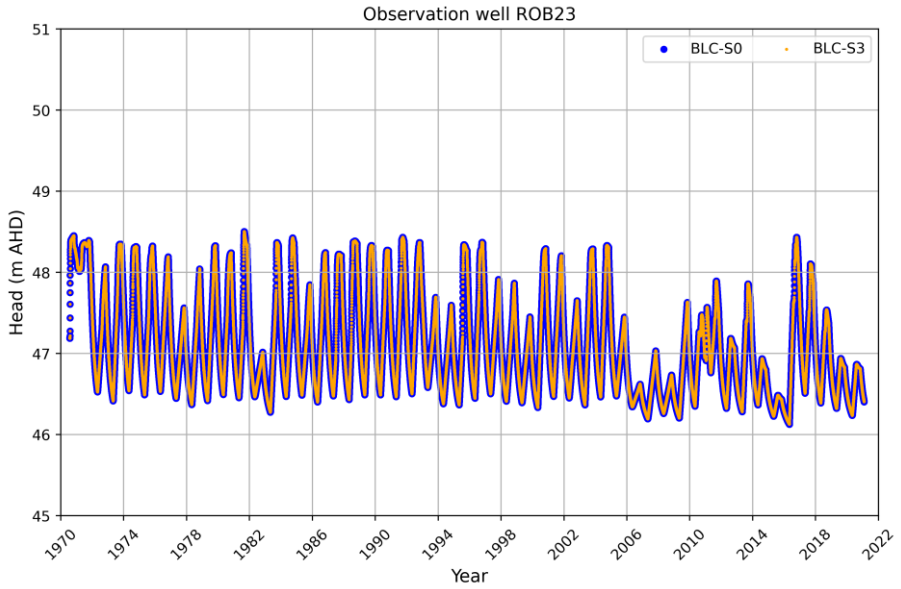

Figure C31. Comparison of groundwater head between the base model (BLC-S0) and simulated results of BLC-S3 at observation well ROB23 for the period 1970–2021.

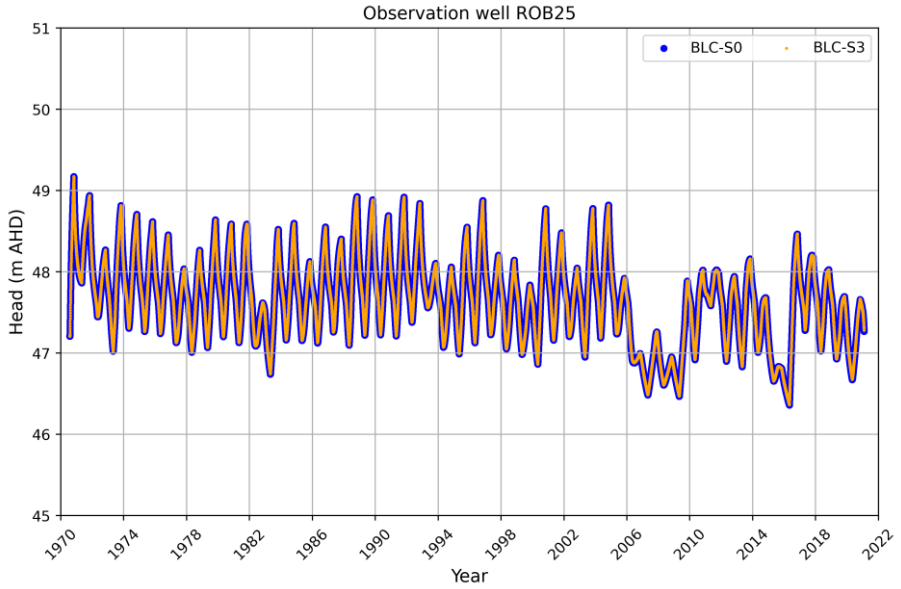

Figure C32. Comparison of groundwater head between the base model (BLC-S0) and simulated results of BLC-S3 at observation well ROB25 for the period 1970–2021.

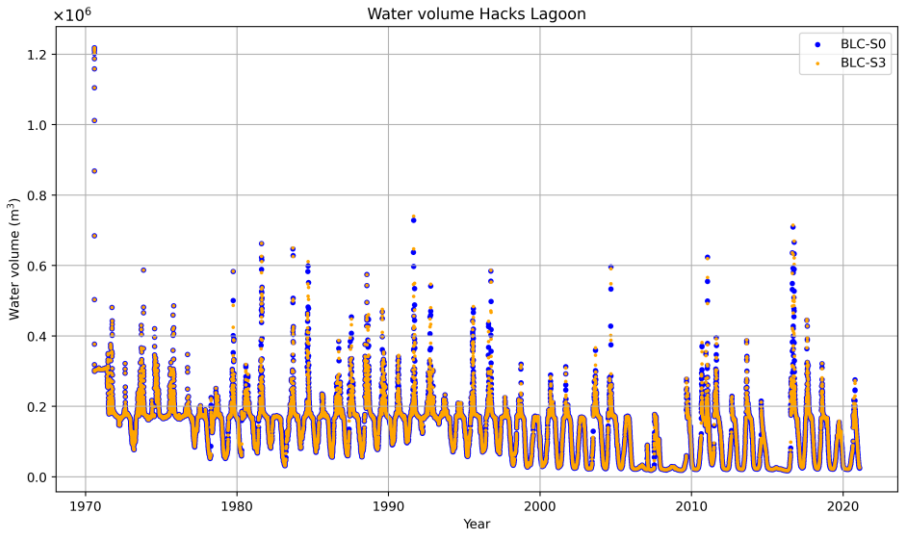

Figure C33. Comparison of water volume between the base model (BLC-S0) and simulated results of BLC-S3 in Hacks Lagoon for the period 1970–2021.

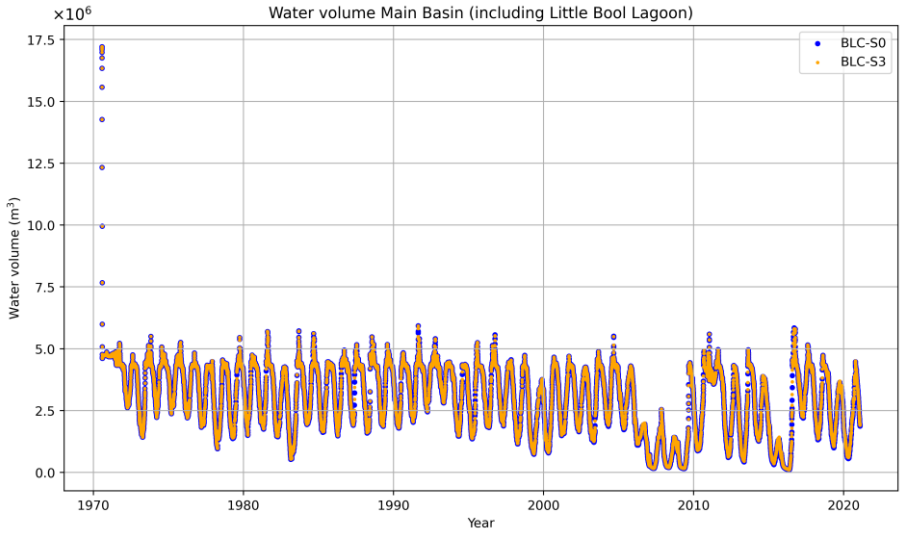

Figure C34. Comparison of water volume between the base model (BLC-S0) and simulated results of BLC-S3 in Main Basin (including Little Bool Lagoon) for the period 1970–2021.

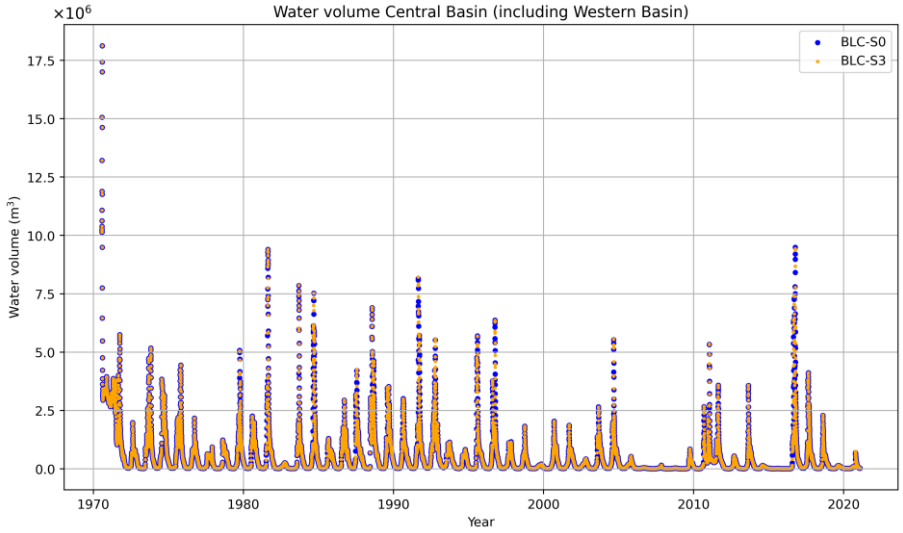

Figure C35. Comparison of water volume between the base model (BLC-S0) and simulated results of BLC-S3 in Central Basin (including Western Basin) for the period 1970–2021.

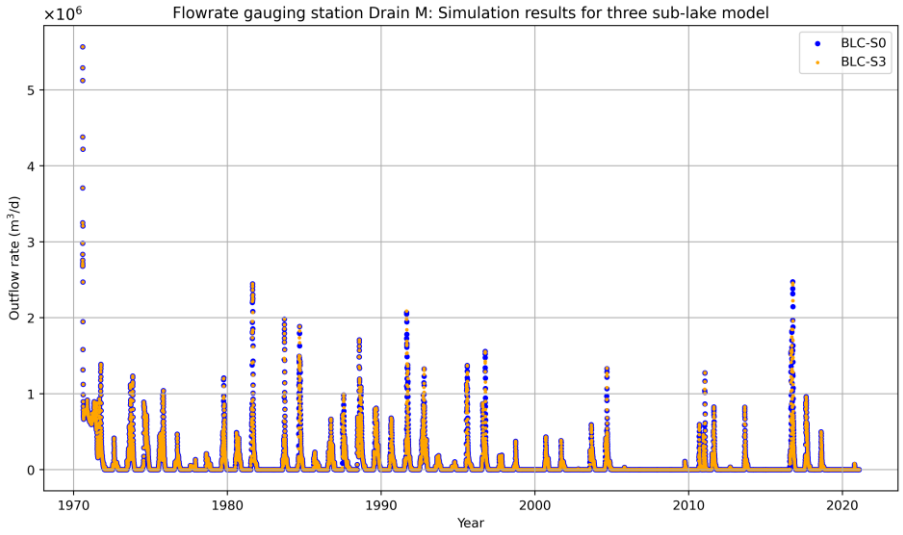

Figure C36. Comparison of outflow rates at Drain M between the base model (BLC-S0) and simulated results of BLC-S3 for the period 1970–2021.

C.4 Hydrological outcomes of BLC-S4 simulation

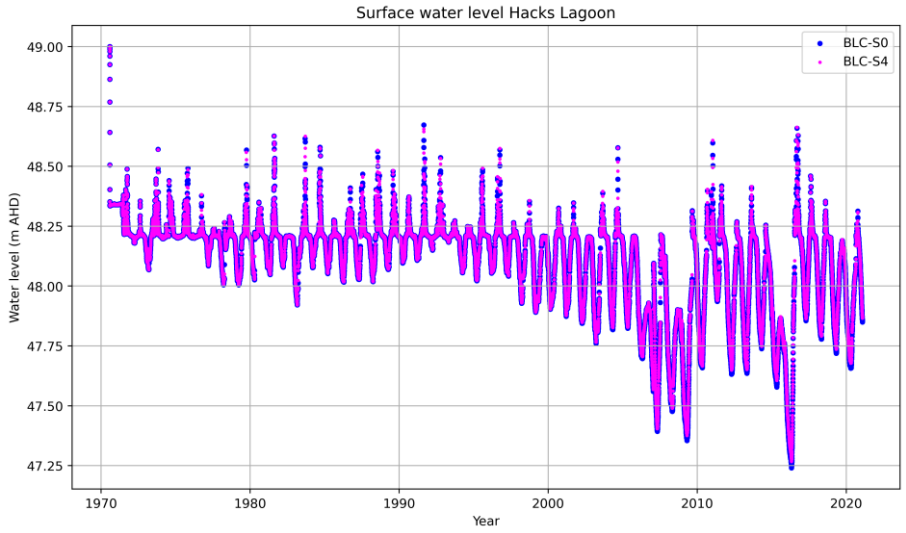

Figure C37. Comparison of surface water level between the base model (BLC-S0) and simulated results of BLC-S4 in Hacks Lagoon for the period 1970–2021.

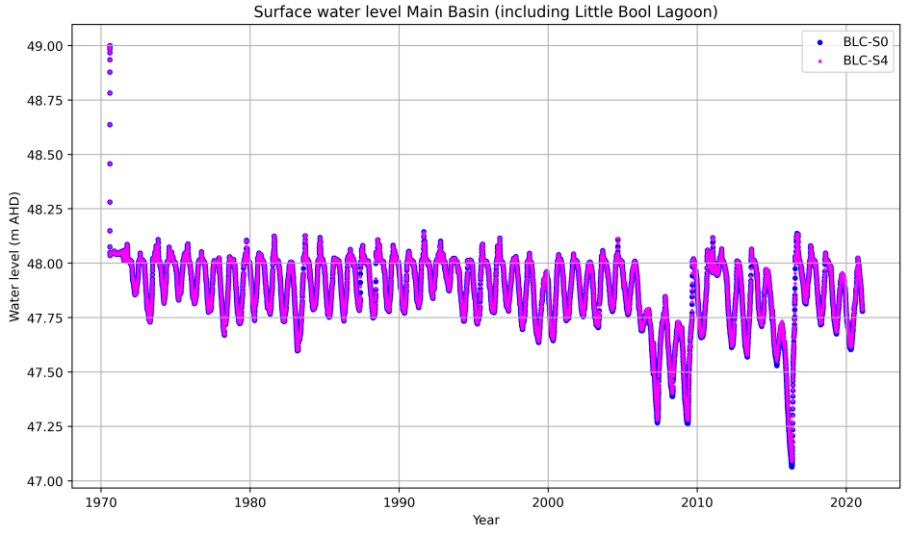

Figure C38. Comparison of surface water level between the base model (BLC-S0) and simulated results of BLC-S4 in Main Basin (including Little Bool Lagoon) for the period 1970–2021.

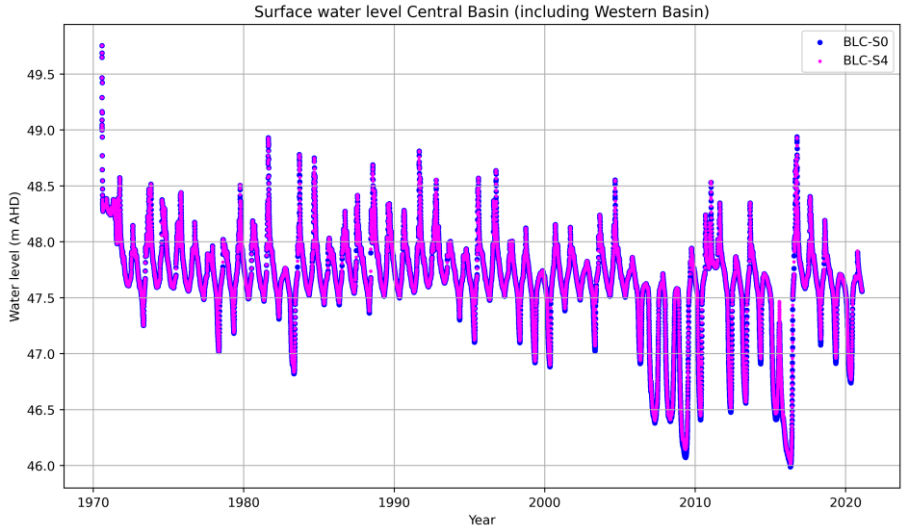

Figure C39. Comparison of surface water level between the base model (BLC-S0) and simulated results of BLC-S4 in Central Basin (including Western Basin) for the period 1970–2021.

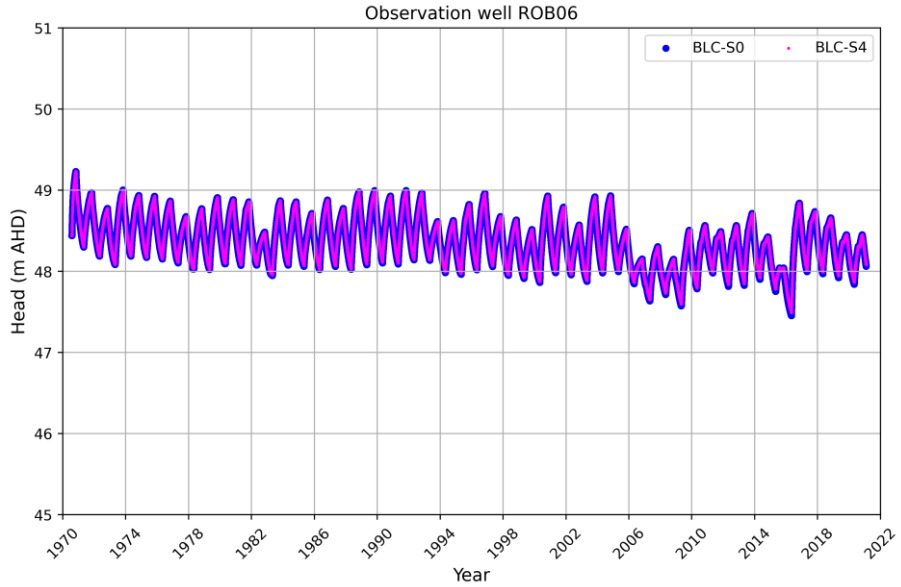

Figure C40. Comparison of groundwater head between the base model (BLC-S0) and simulated results of BLC-S4 at observation well ROB06 for the period 1970–2021.

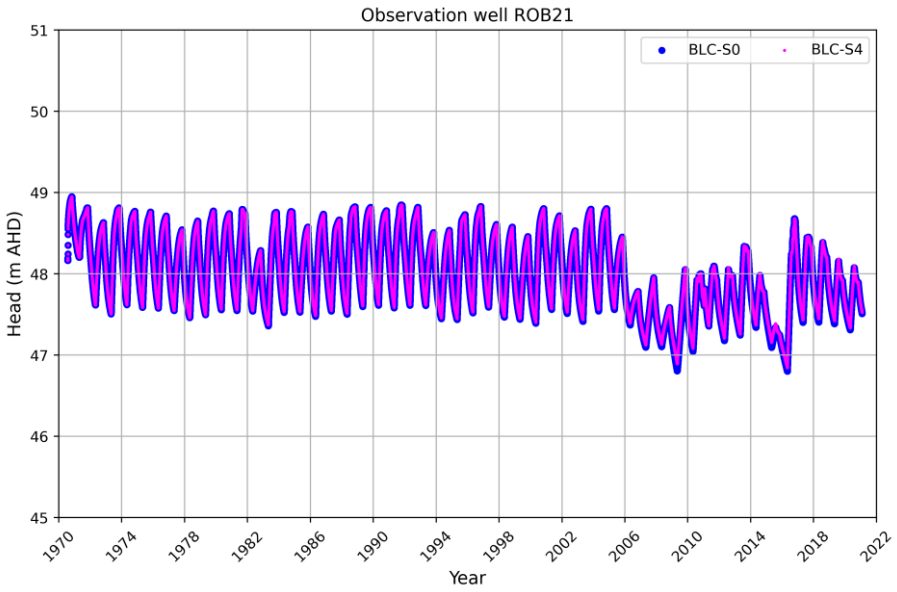

Figure C41. Comparison of groundwater head between the base model (BLC-S0) and simulated results of BLC-S4 at observation well ROB021 for the period 1970–2021.

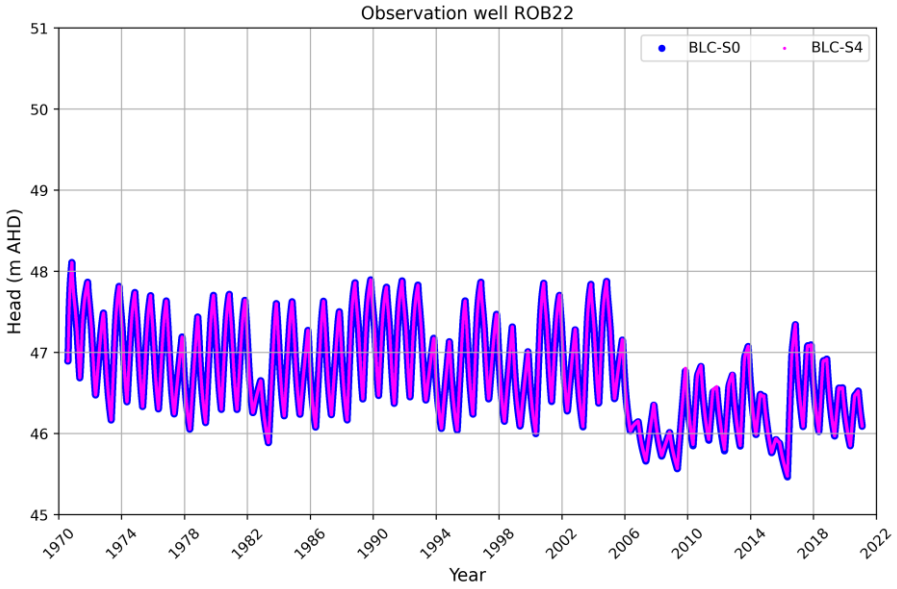

Figure C42. Comparison of groundwater head between the base model (BLC-S0) and simulated results of BLC-S4 at observation well ROB22 for the period 1970–2021.

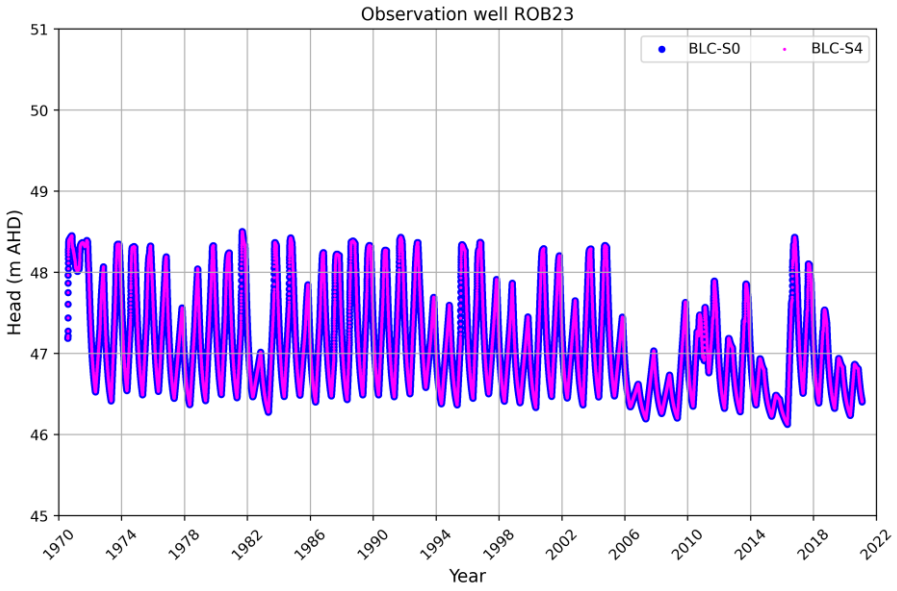

Figure C43. Comparison of groundwater head between the base model (BLC-S0) and simulated results of BLC-S4 at observation well ROB23 for the period 1970–2021.

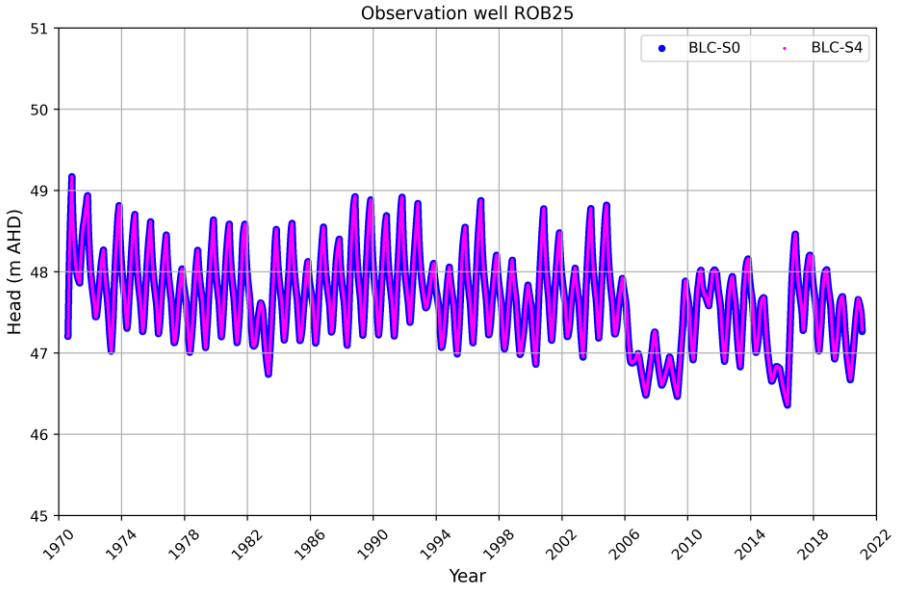

Figure C44. Comparison of groundwater head between the base model (BLC-S0) and simulated results of BLC-S4 at observation well ROB25 for the period 1970–2021.

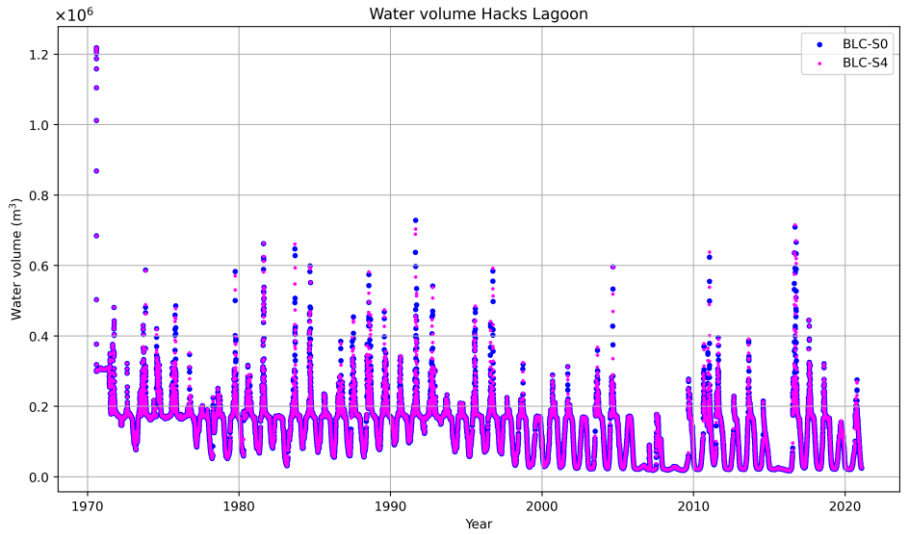

Figure C45. Comparison of water volume between the base model (BLC-S0) and simulated results of BLC-S4 in Hacks Lagoon for the period 1970–2021.

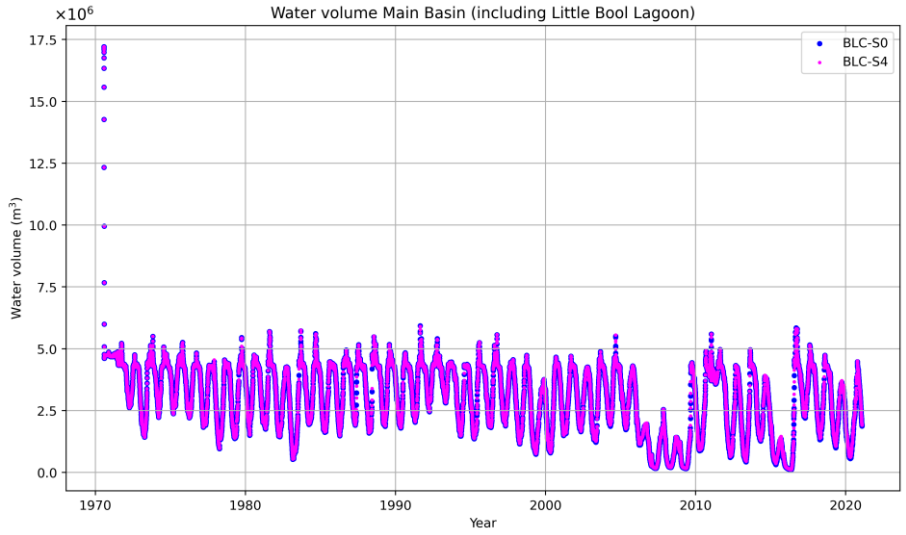

Figure C46. Comparison of water volume between the base model (BLC-S0) and simulated results of BLC-S4 in Main Basin (including Little Bool Lagoon) for the period 1970–2021.

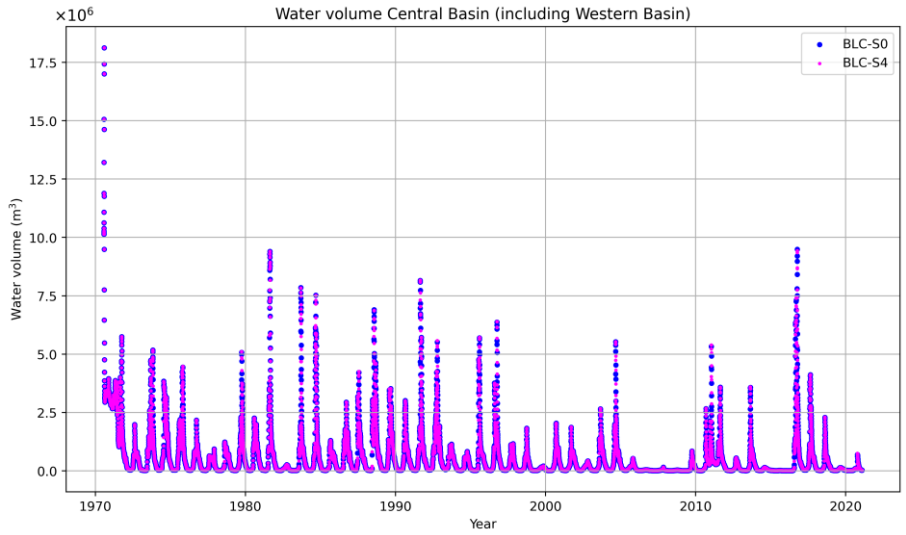

Figure C47. Comparison of water volume between the base model (BLC-S0) and simulated results of BLC-S4 in Central Basin (including Western Basin) for the period 1970–2021.

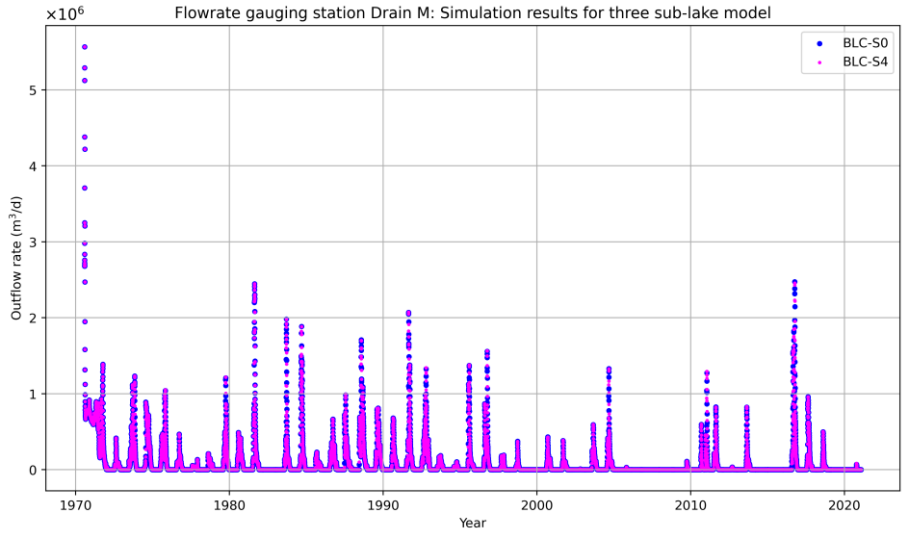

Figure C48. Comparison of outflow rates at Drain M between the base model (BLC-S0) and simulated results of BLC-S4 for the period 1970–2021.

C.5 Hydrological outcomes of BLC-S5 simulation

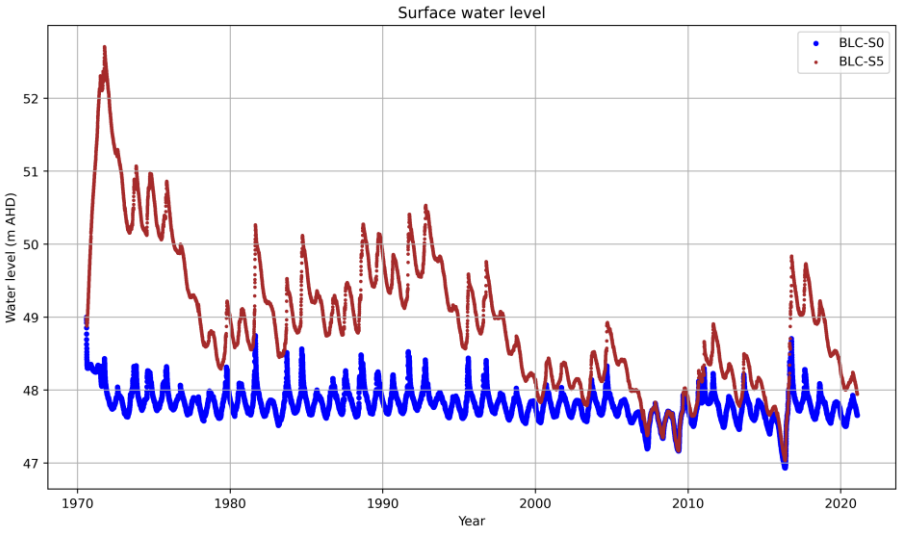

Figure C49. Comparison of surface water level between the base model (BLC-S0) with a single lake and simulated results of BLC-S5 for the period 1970–2021.

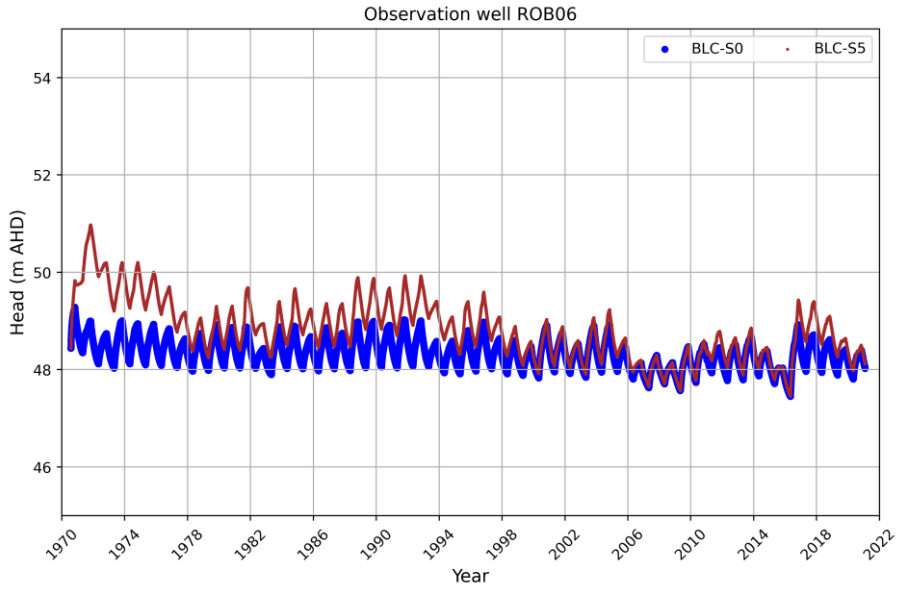

Figure C50. Comparison of groundwater head between the base model (BLC-S0) with a single lake and simulated results of BLC-S5 at observation well ROB06 for the period 1970–2021.

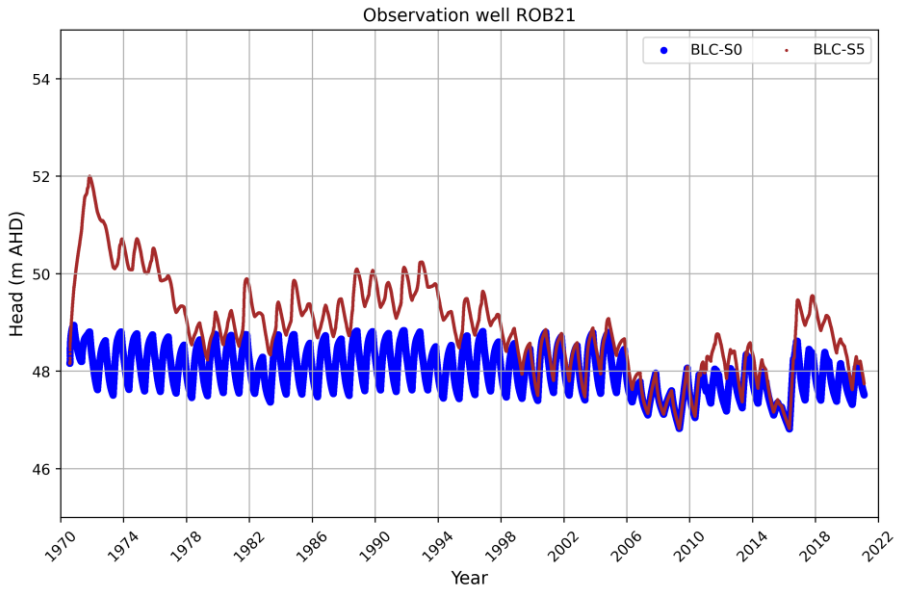

Figure C51. Comparison of groundwater head between the base model (BLC-S0) with a single lake and simulated results of BLC-S5 at observation well ROB021 for the period 1970–2021.

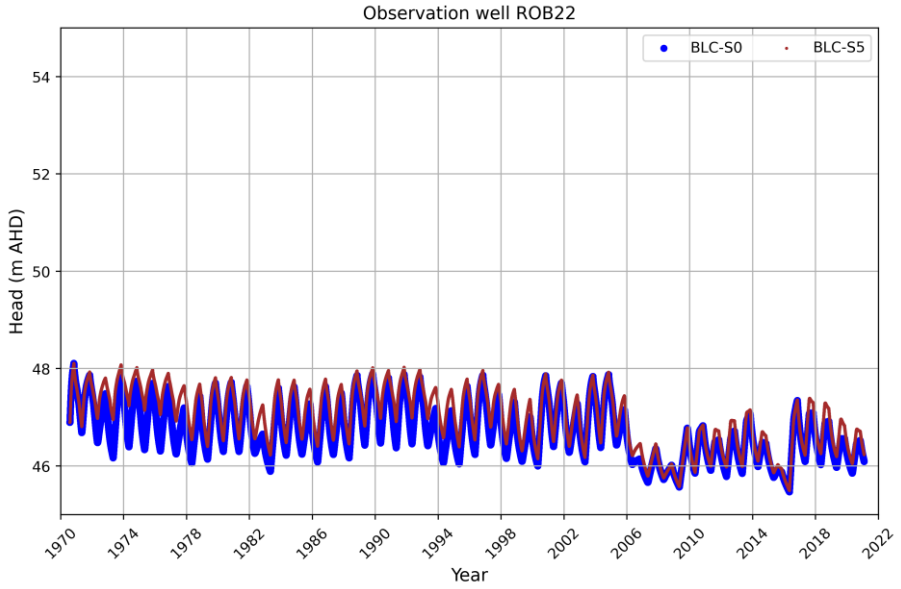

Figure C52. Comparison of groundwater head between the base model (BLC-S0) with a single lake and simulated results of BLC-S5 at observation well ROB22 for the period 1970–2021.

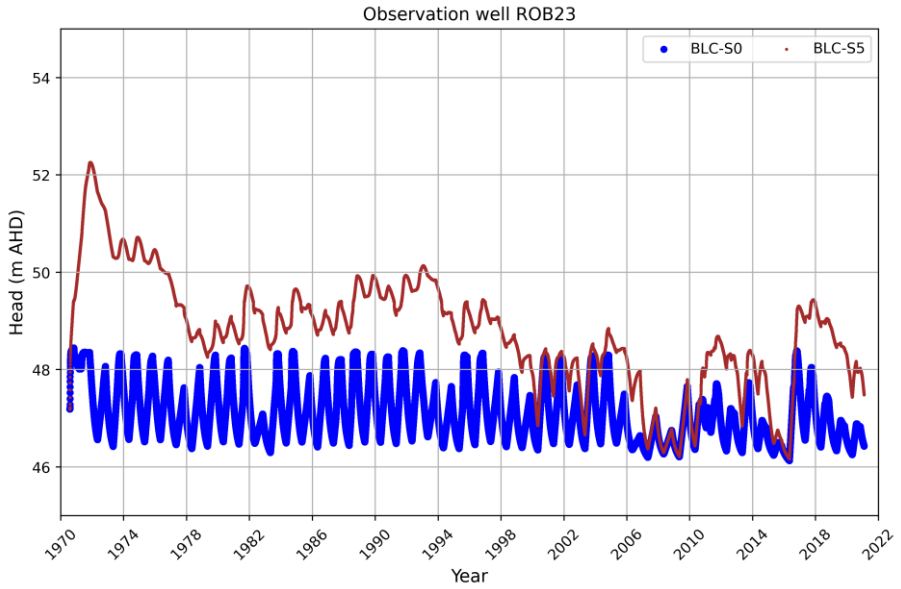

Figure C53. Comparison of groundwater head between the base model (BLC-S0) with a single lake and simulated results of BLC-S5 at observation well ROB23 for the period 1970–2021.

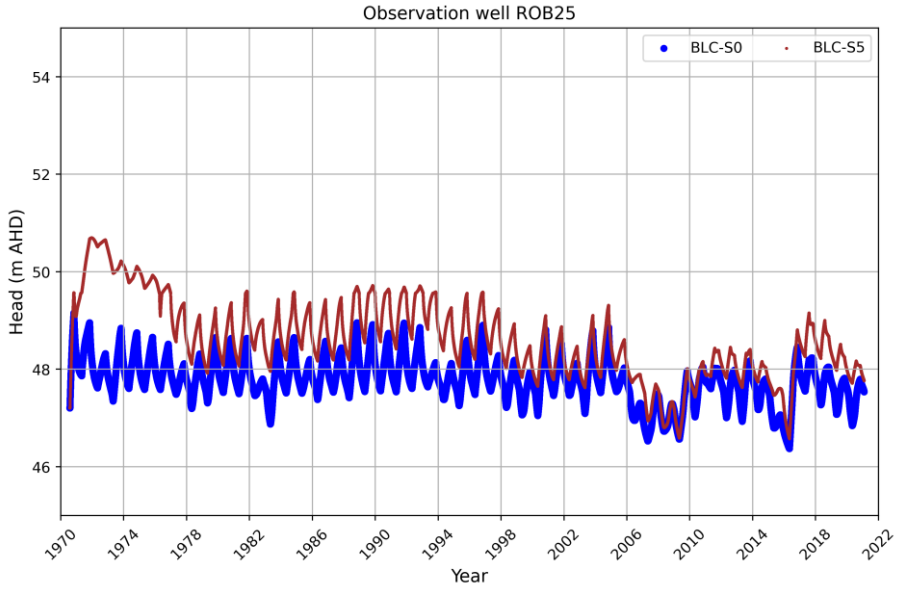

Figure C54. Comparison of groundwater head between the base model (BLC-S0) with a single lake and simulated results of BLC-S5 at observation well ROB25 for the period 1970–2021.

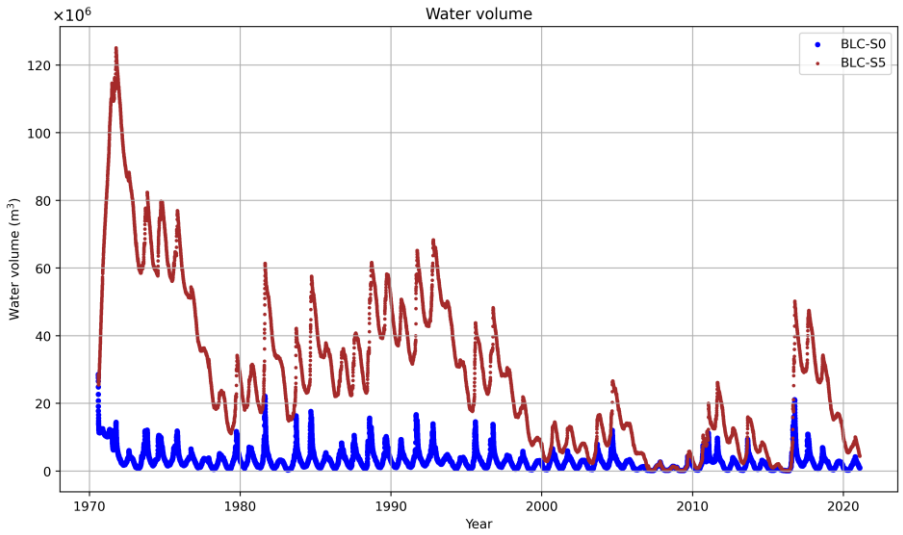

Figure C55. Comparison of water volume between the base model (BLC-S0) with a single lake and simulated results of BLC-S5 for the period 1970–2021.

C.6 Hydrological outcomes of BLC-S6 simulation

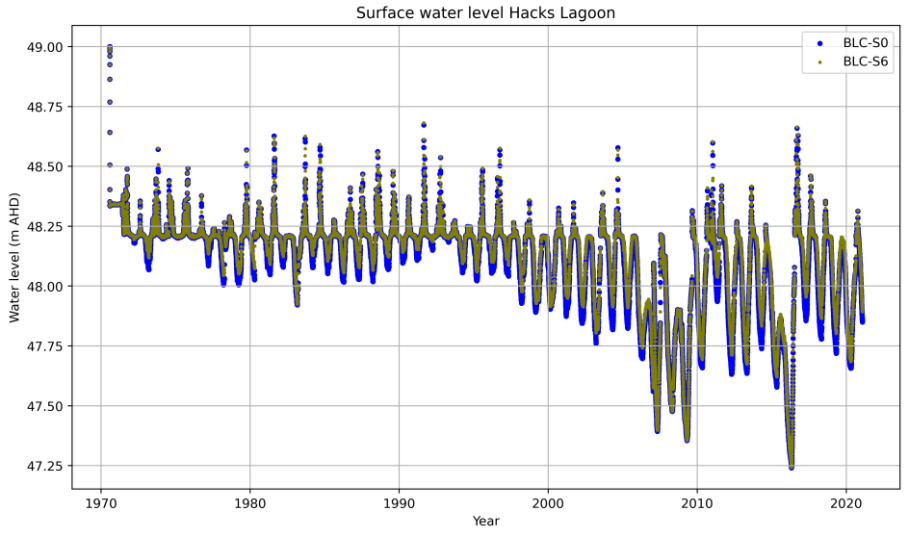

Figure C56. Comparison of surface water level between the base model (BLC-S0) and simulated results of BLC-S6 in Hacks Lagoon for the period 1970–2021.

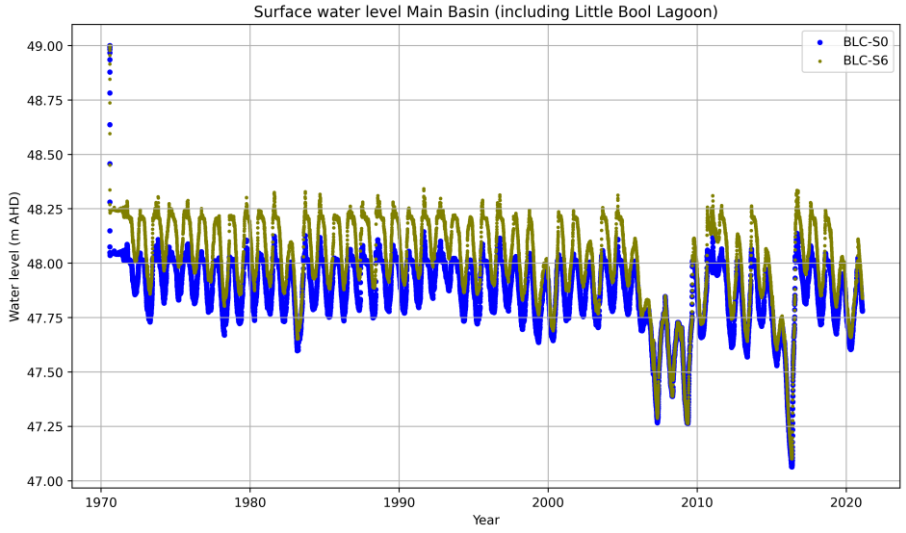

Figure C57. Comparison of surface water level between the base model (BLC-S0) and simulated results of BLC-S6 in Main Basin (including Little Bool Lagoon) for the period 1970–2021.

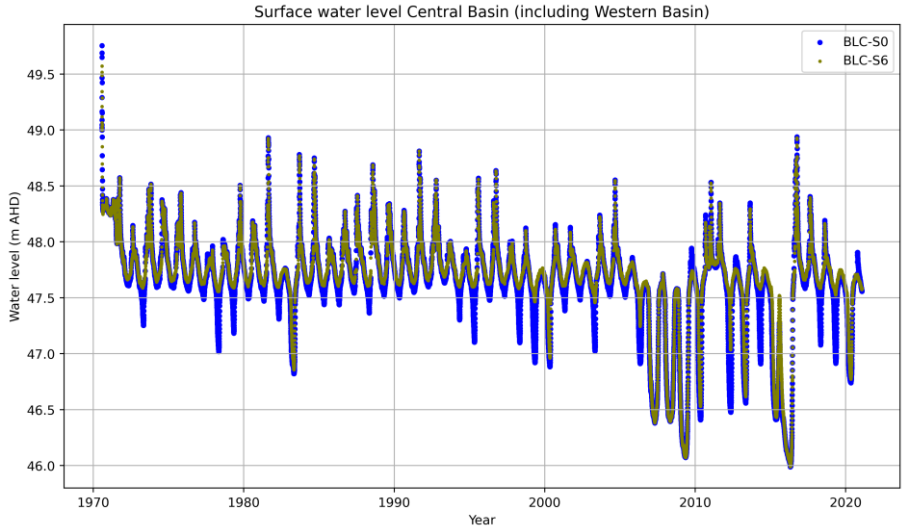

Figure C58. Comparison of surface water level between the base model (BLC-S0) and simulated results of BLC-S6 in Central Basin (including Western Basin) for the period 1970–2021.

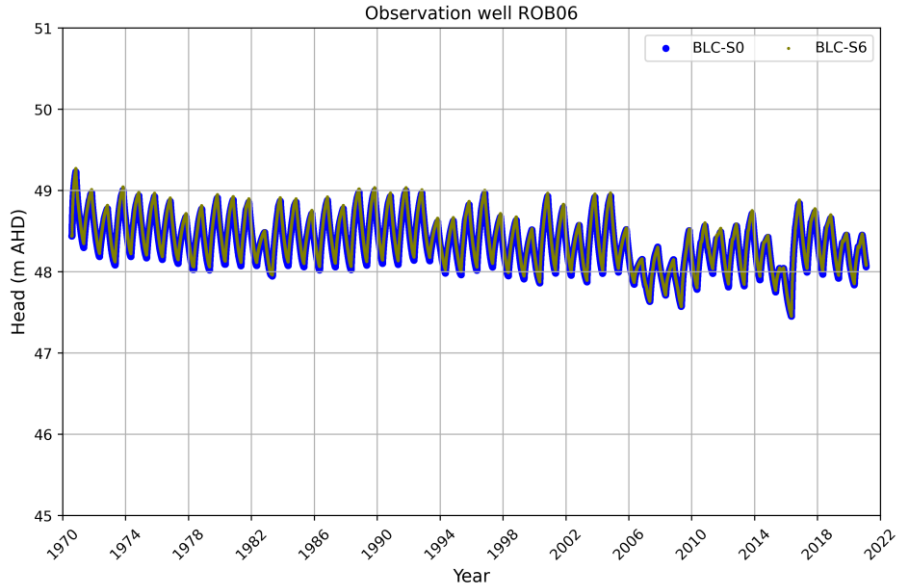

Figure C59. Comparison of groundwater head between the base model (BLC-S0) and simulated results of BLC-S6 at observation well ROB06 for the period 1970–2021.

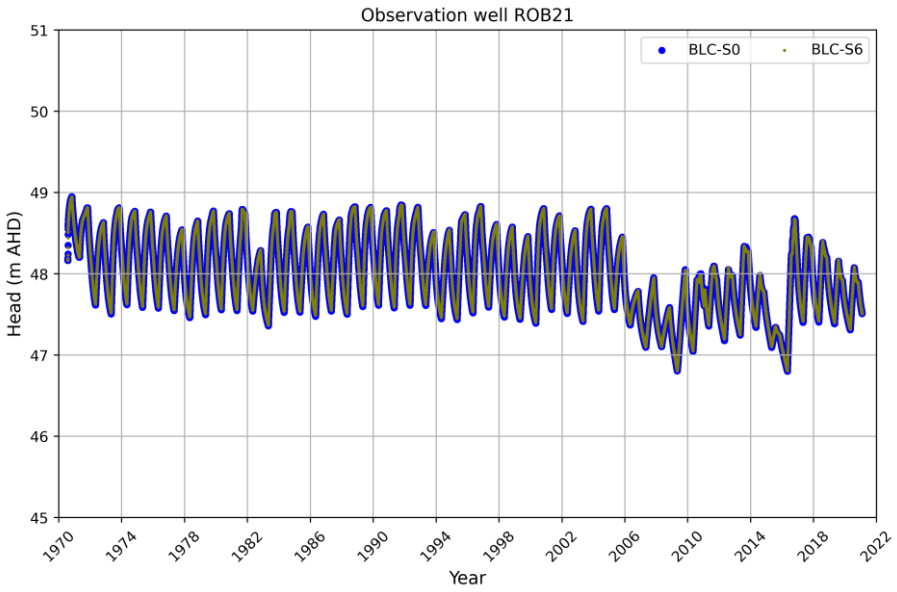

Figure C60. Comparison of groundwater head between the base model (BLC-S0) and simulated results of BLC-S6 at observation well ROB021 for the period 1970–2021.

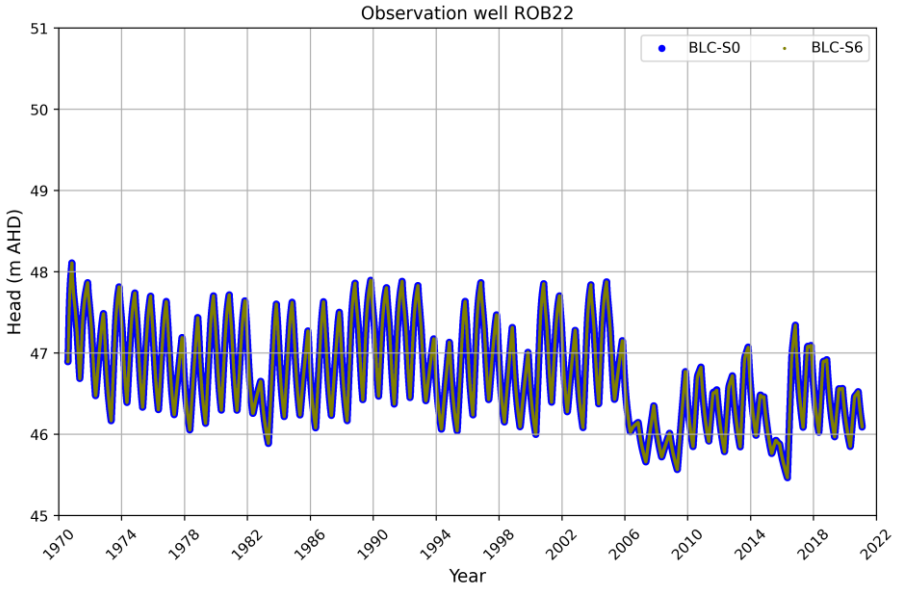

Figure C61. Comparison of groundwater head between the base model (BLC-S0) and simulated results of BLC-S6 at observation well ROB22 for the period 1970–2021.

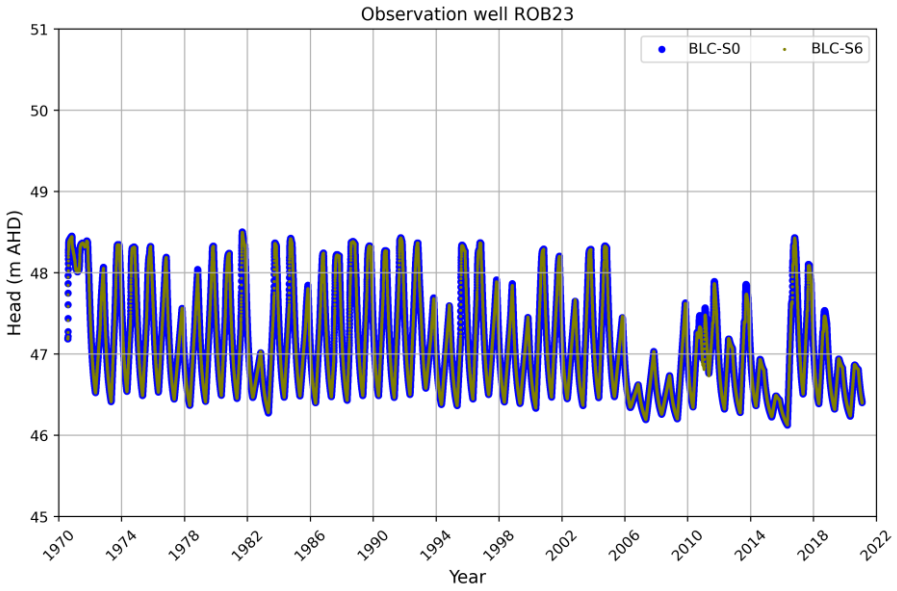

Figure C62. Comparison of groundwater head between the base model (BLC-S0) and simulated results of BLC-S6 at observation well ROB23 for the period 1970–2021.

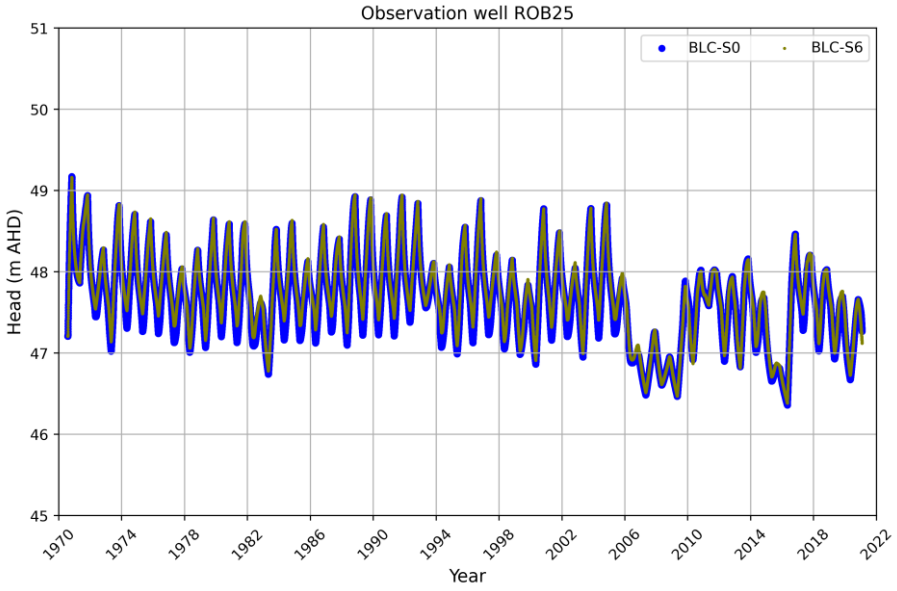

Figure C63. Comparison of groundwater head between the base model (BLC-S0) and simulated results of BLC-S6 at observation well ROB25 for the period 1970–2021.

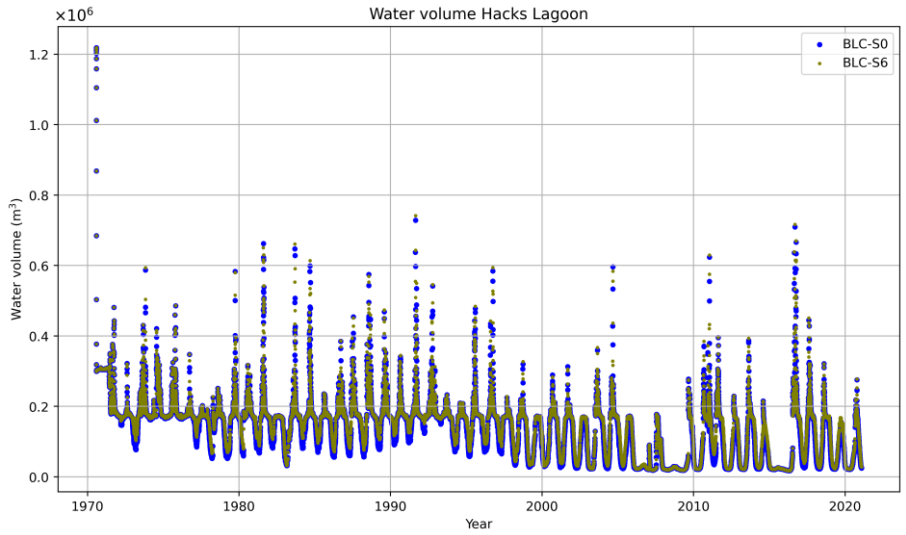

Figure C64. Comparison of water volume between the base model (BLC-S0) and simulated results of BLC-S6 in Hacks Lagoon for the period 1970–2021.

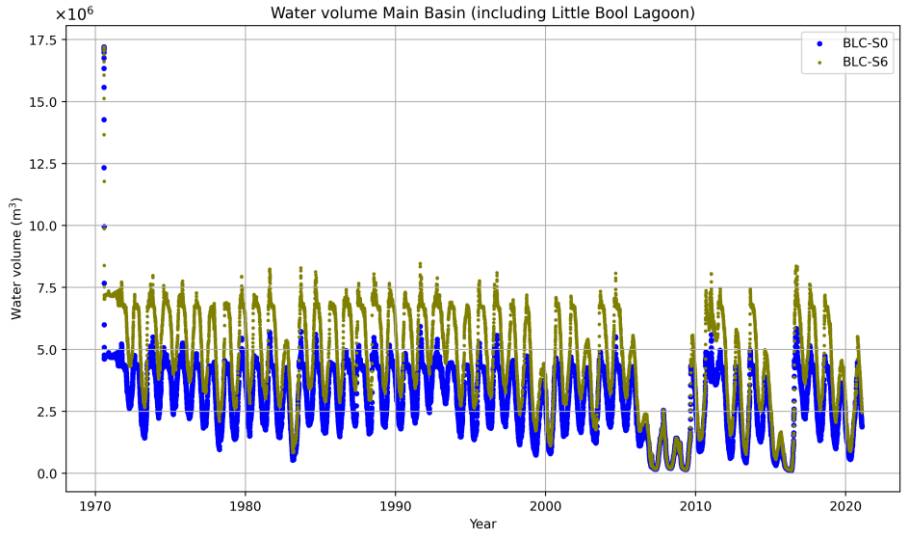

Figure C65. Comparison of water volume between the base model (BLC-S0) and simulated results of BLC-S6 in Main Basin (including Little Bool Lagoon) for the period 1970–2021.

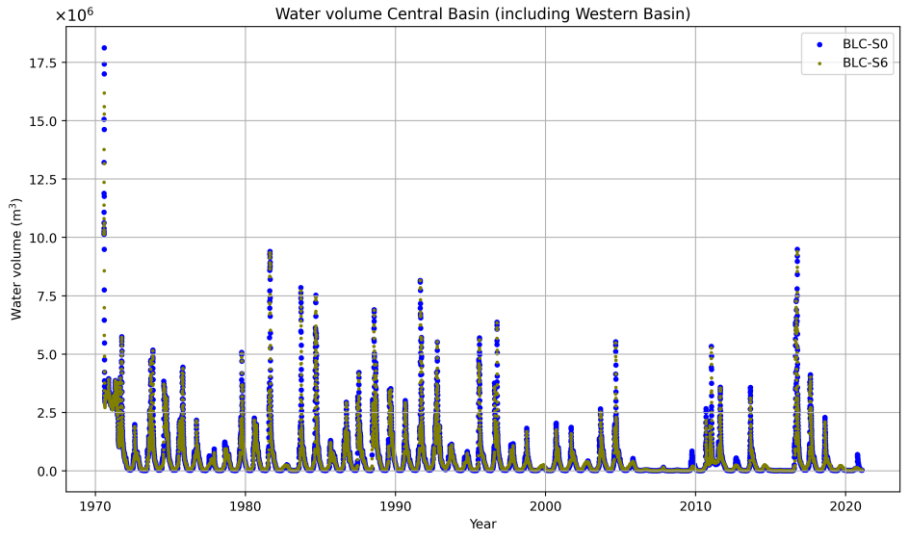

Figure C66. Comparison of water volume between the base model (BLC-S0) and simulated results of BLC-S6 in Central Basin (including Western Basin) for the period 1970–2021.

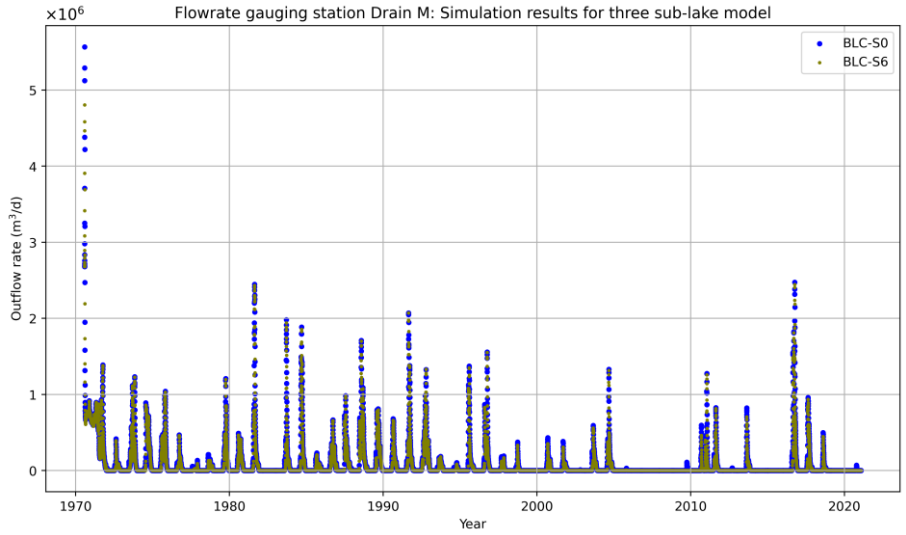

Figure C67. Comparison of outflow rates at Drain M between the base model (BLC-S0) and simulated results of BLC-S6 for the period 1970–2021.

C.7 Hydrological outcomes of BLC-S7 simulation

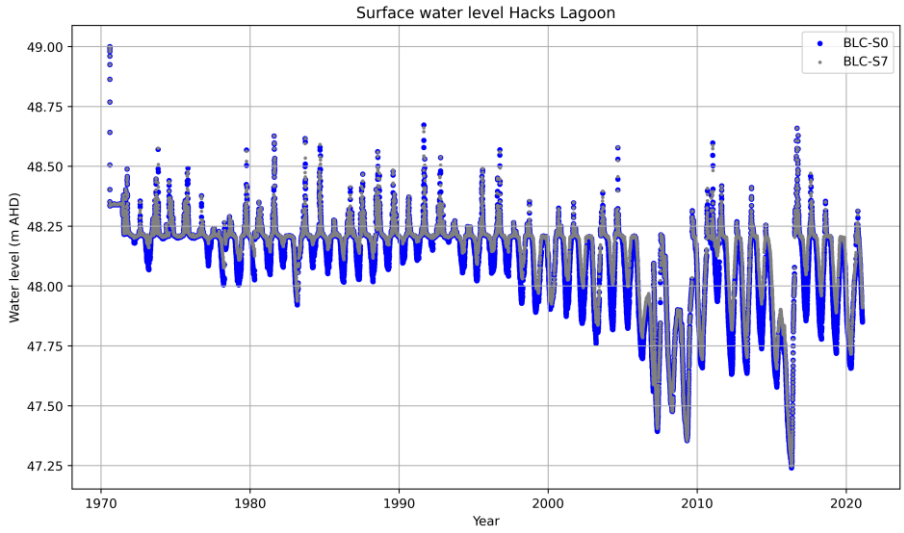

Figure C68. Comparison of surface water level between the base model (BLC-S0) and simulated results of BLC-S7 in Hacks Lagoon for the period 1970–2021.

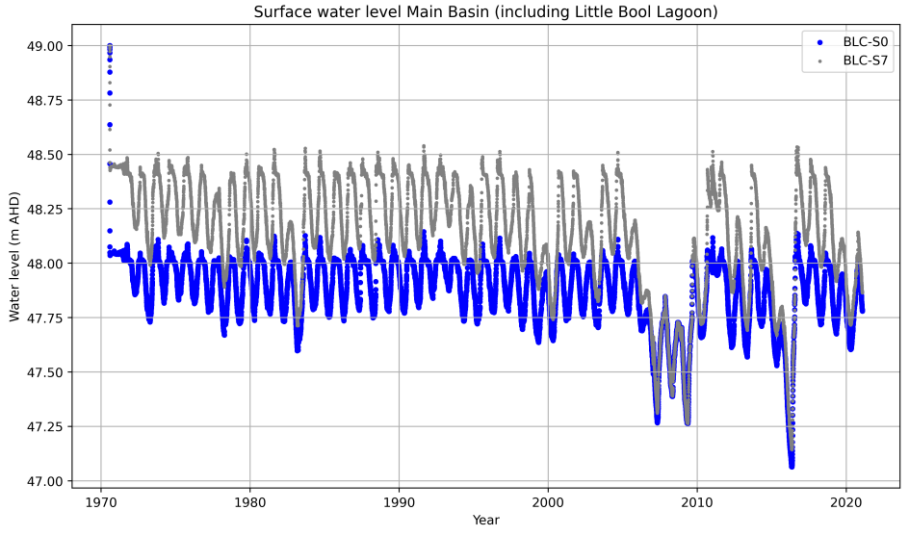

Figure C69. Comparison of surface water level between the base model (BLC-S0) and simulated results of BLC-S4 in Main Basin (including Little Bool Lagoon) for the period 1970–2021.

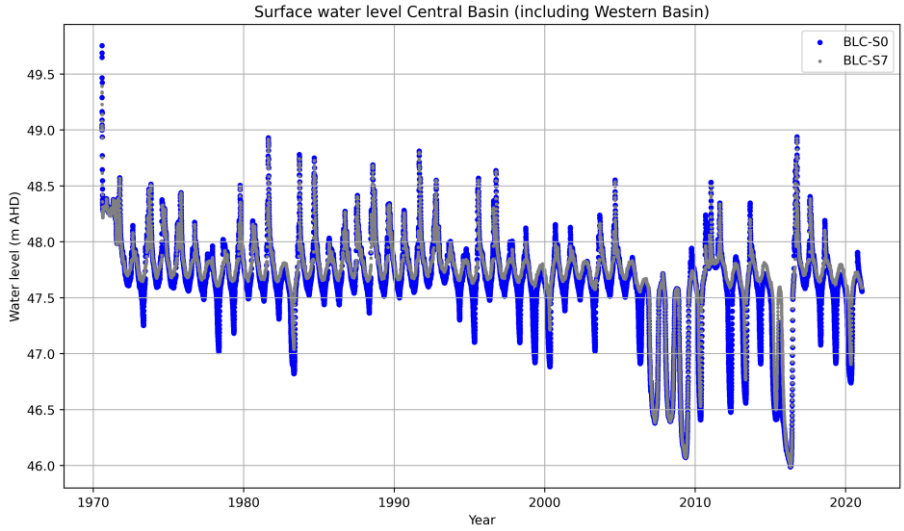

Figure C70. Comparison of surface water level between the base model (BLC-S0) and simulated results of BLC-S7 in Central Basin (including Western Basin) for the period 1970–2021.

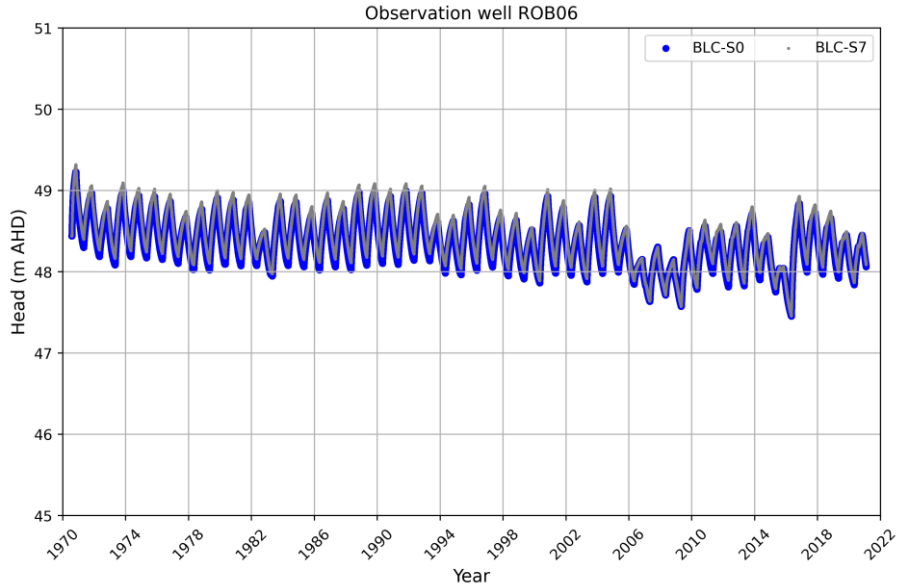

Figure C71. Comparison of groundwater head between the base model (BLC-S0) and simulated results of BLC-S7 at observation well ROB06 for the period 1970–2021.

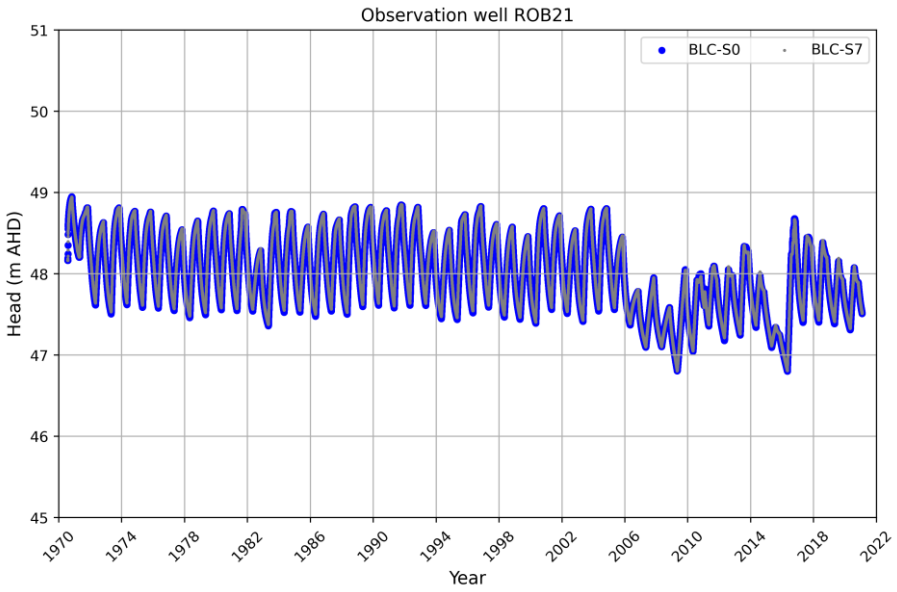

Figure C72. Comparison of groundwater head between the base model (BLC-S0) and simulated results of BLC-S7 at observation well ROB021 for the period 1970–2021.

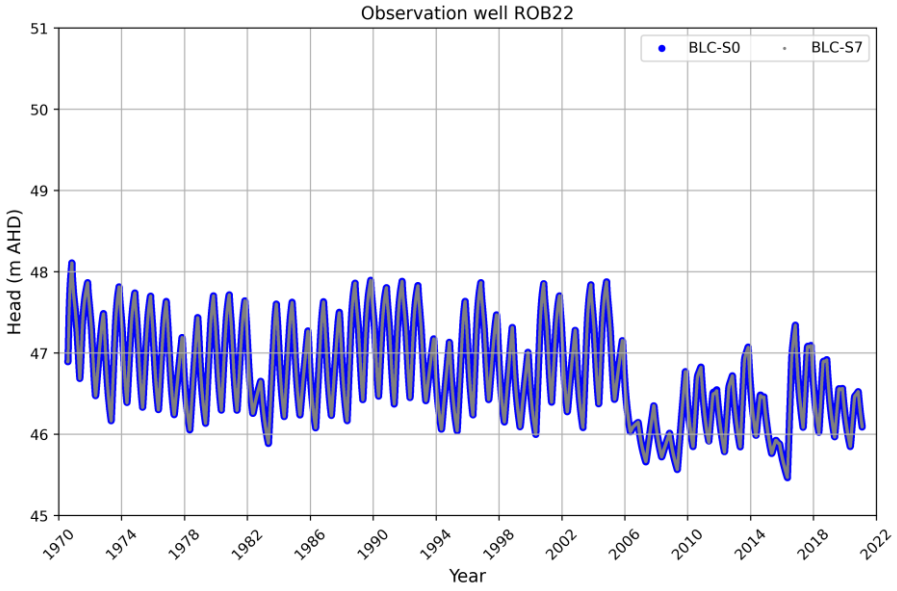

Figure C73. Comparison of groundwater head between the base model (BLC-S0) and simulated results of BLC-S7 at observation well ROB22 for the period 1970–2021.

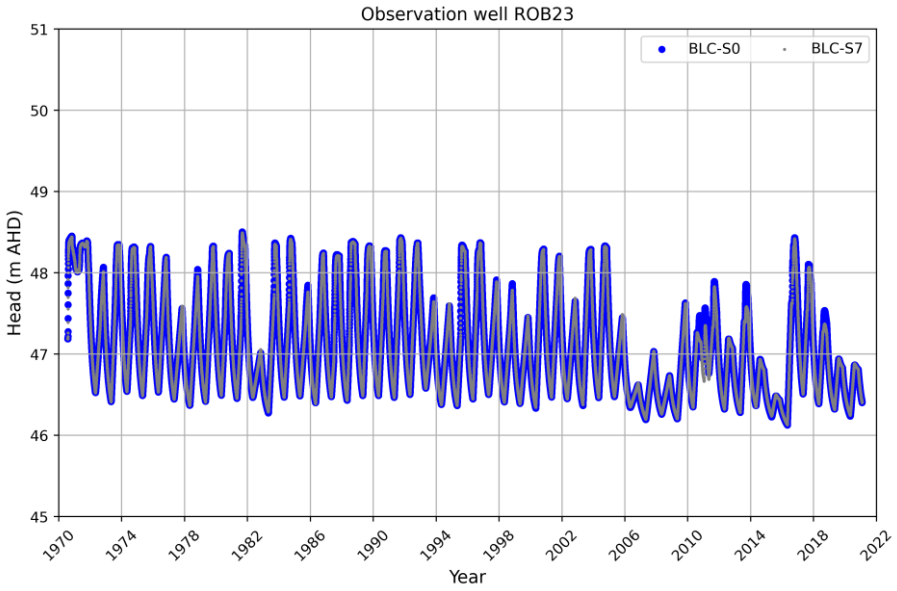

Figure C74. Comparison of groundwater head between the base model (BLC-S0) and simulated results of BLC-S7 at observation well ROB23 for the period 1970–2021.

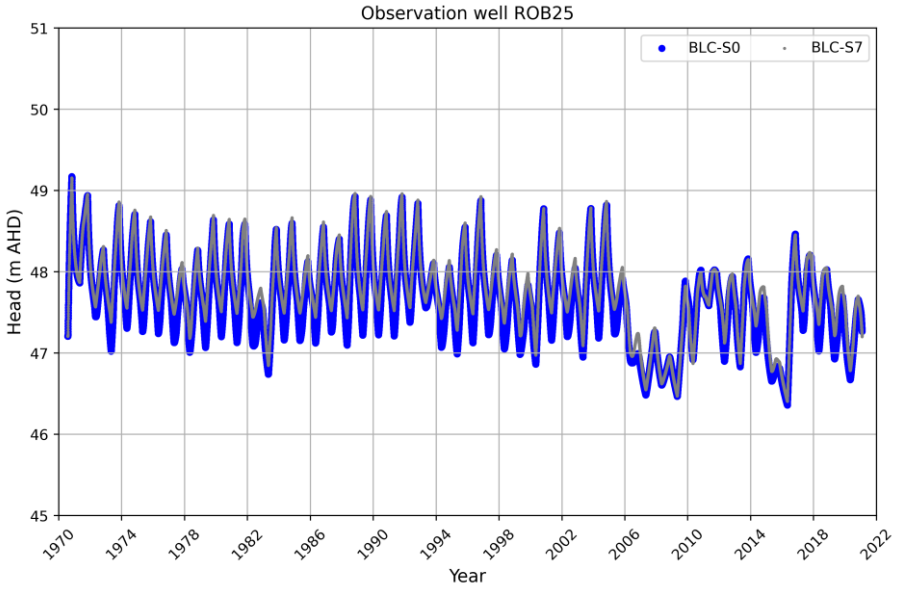

Figure C75. Comparison of groundwater head between the base model (BLC-S0) and simulated results of BLC-S7 at observation well ROB25 for the period 1970–2021.

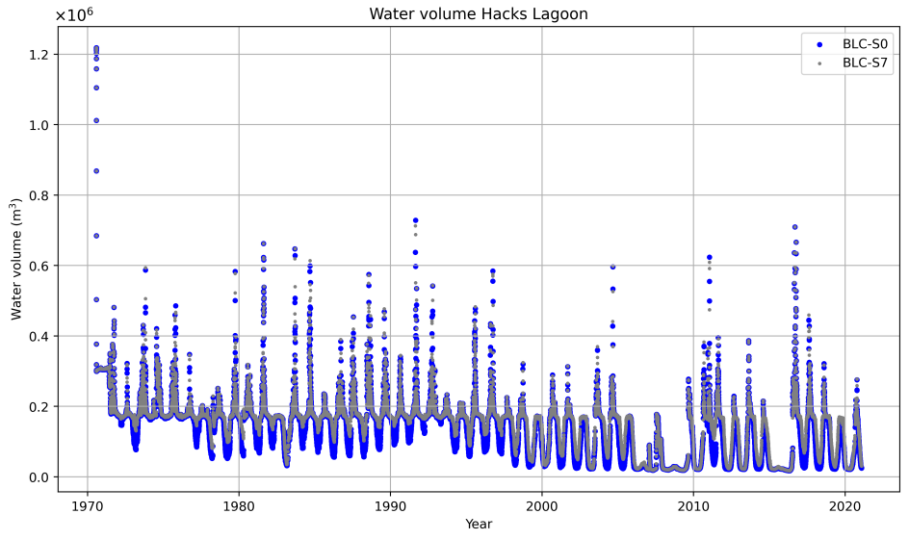

Figure C76. Comparison of water volume between the base model (BLC-S0) and simulated results of BLC-S7 in Hacks Lagoon for the period 1970–2021.

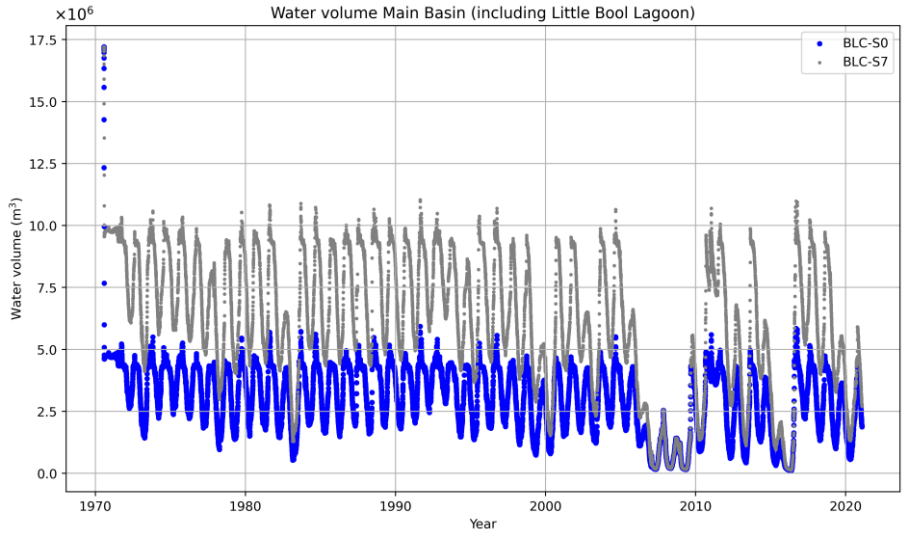

Figure C77. Comparison of water volume between the base model (BLC-S0) and simulated results of BLC-S7 in Main Basin (including Little Bool Lagoon) for the period 1970–2021.

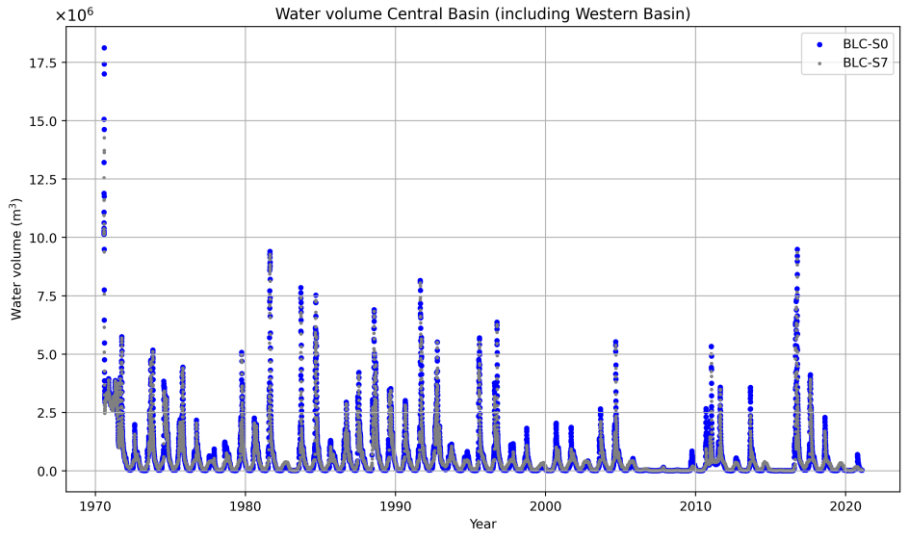

Figure C78. Comparison of water volume between the base model (BLC-S0) and simulated results of BLC-S7 in Central Basin (including Western Basin) for the period 1970–2021.

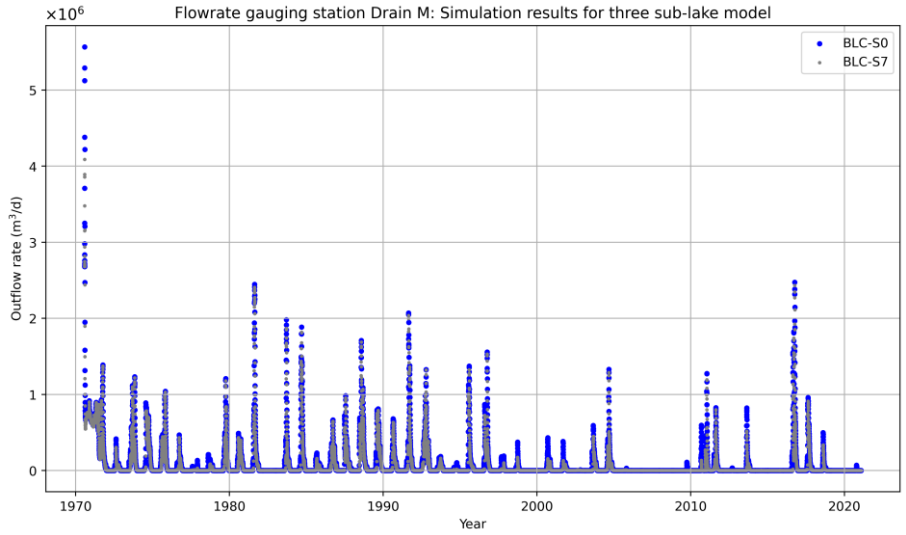

Figure C79. Comparison of outflow rates at Drain M between the base model (BLC-S0) and simulated results of BLC-S7 for the period 1970–2021.

C.8 Inundation areas of Bool Lagoon under base model and scenarios

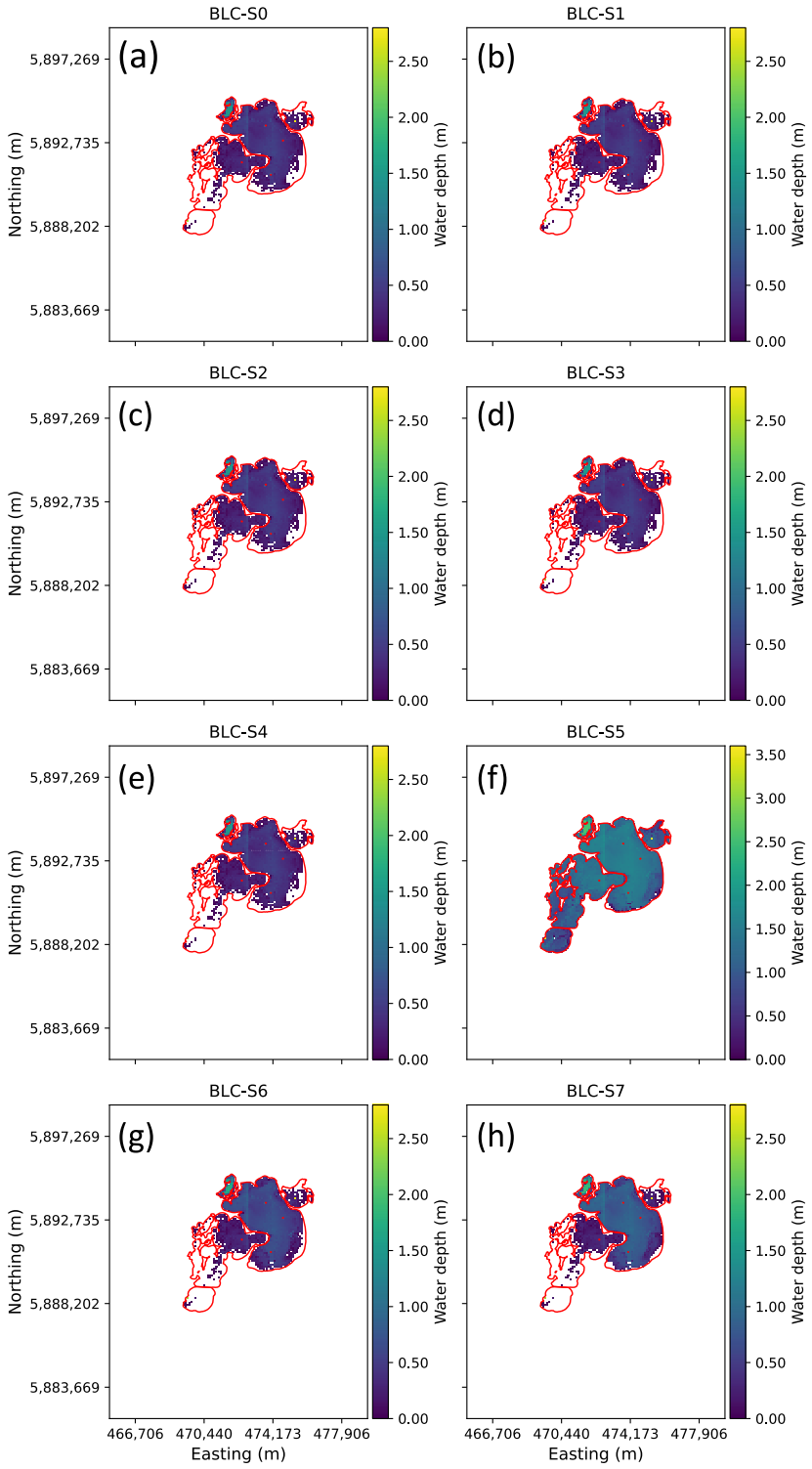

Figure C80. Inundation area of Bool Lagoon in November 1980 under base model and seven scenarios: (a) Base model (BLC-S0), (b) BLC-S1, (c) BLC-S2, (d) BLC-S3, (e) BLC-S4, (f) BLC-S5, (g) BLC-S6, and (f) BLC-S7. Each subplot illustrates the water depth distribution for the respective scenario. Note: For BLC-S5, a single-lake model was used, whereas for other scenarios, a model with three sub-lakes was employed.

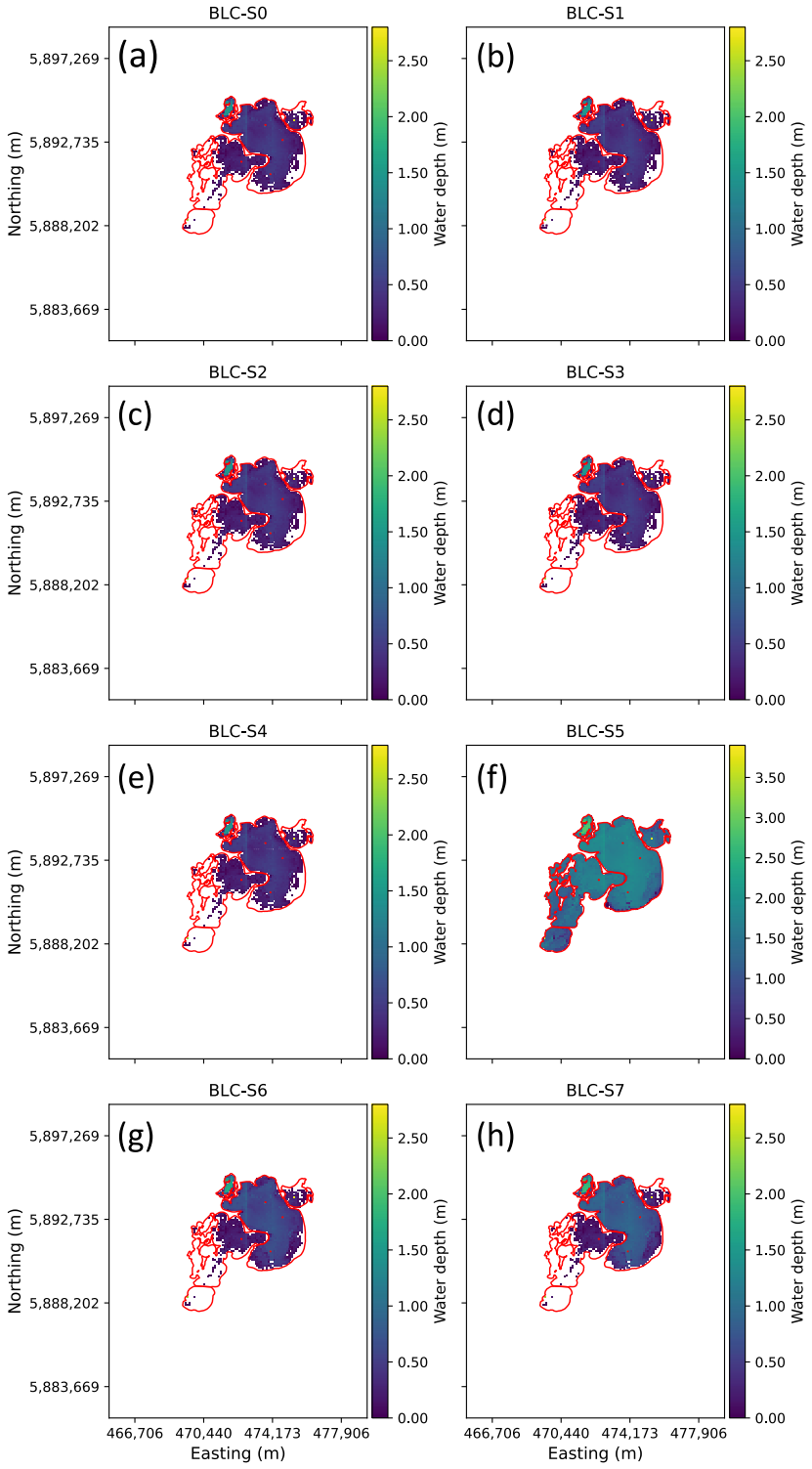

Figure C81. Inundation area of Bool Lagoon in November 1995 under base model and seven scenarios: (a) Base model (BLC-S0), (b) BLC-S1, (c) BLC-S2, (d) BLC-S3, (e) BLC-S4, (f) BLC-S5, (g) BLC-S6, and (f) BLC-S7. Each subplot illustrates the water depth distribution for the respective scenario. Note: For BLC-S5, a single-lake model was used, whereas for other scenarios, a model with three sub-lakes was employed.

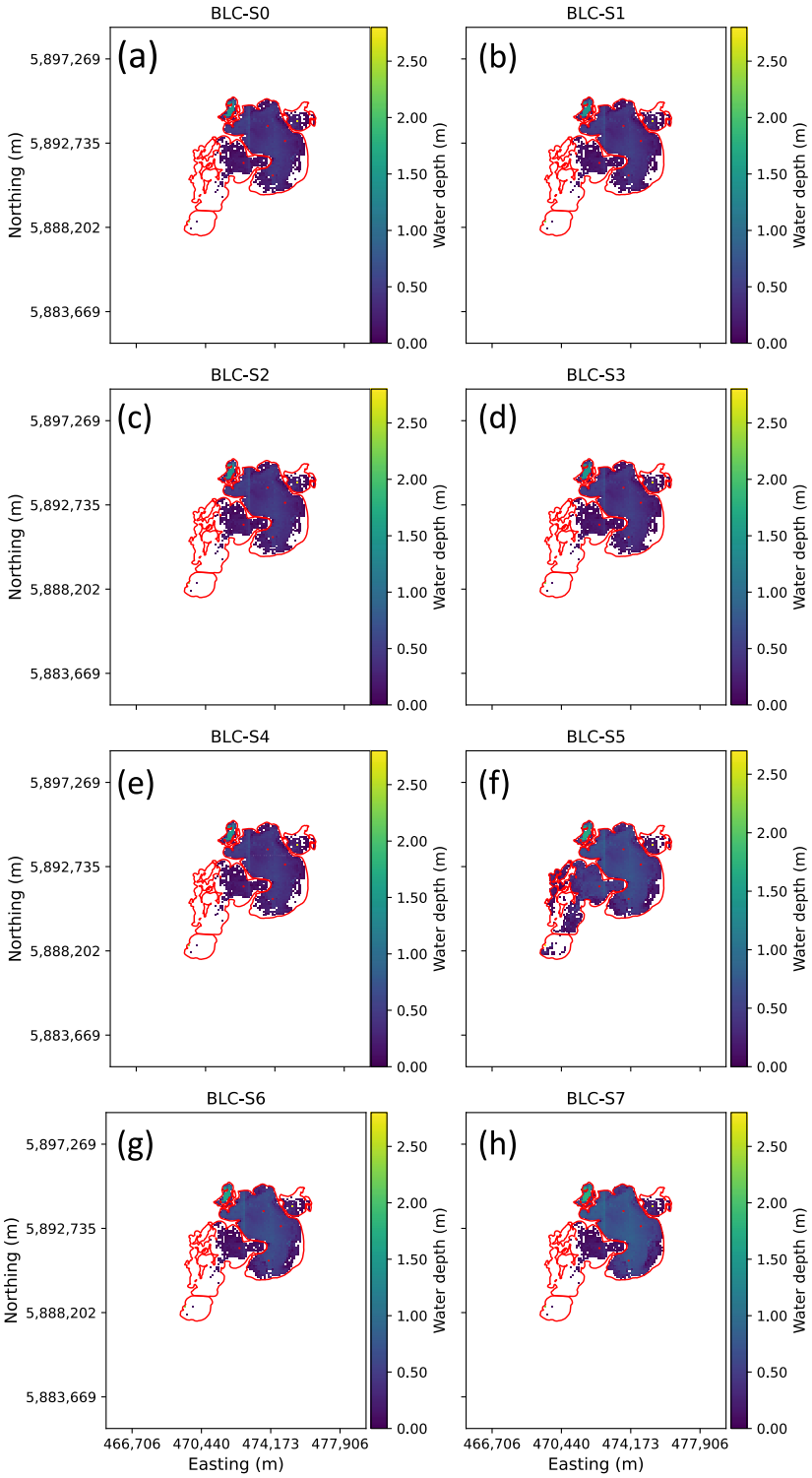

Figure C82. Inundation area of Bool Lagoon in November 2010 under base model and seven scenarios: (a) Base model (BLC-S0), (b) BLC-S1, (c) BLC-S2, (d) BLC-S3, (e) BLC-S4, (f) BLC-S5, (g) BLC-S6, and (f) BLC-S7. Each subplot illustrates the water depth distribution for the respective scenario. Note: For BLC-S5, a single-lake model was used, whereas for other scenarios, a model with three sub-lakes was employed.

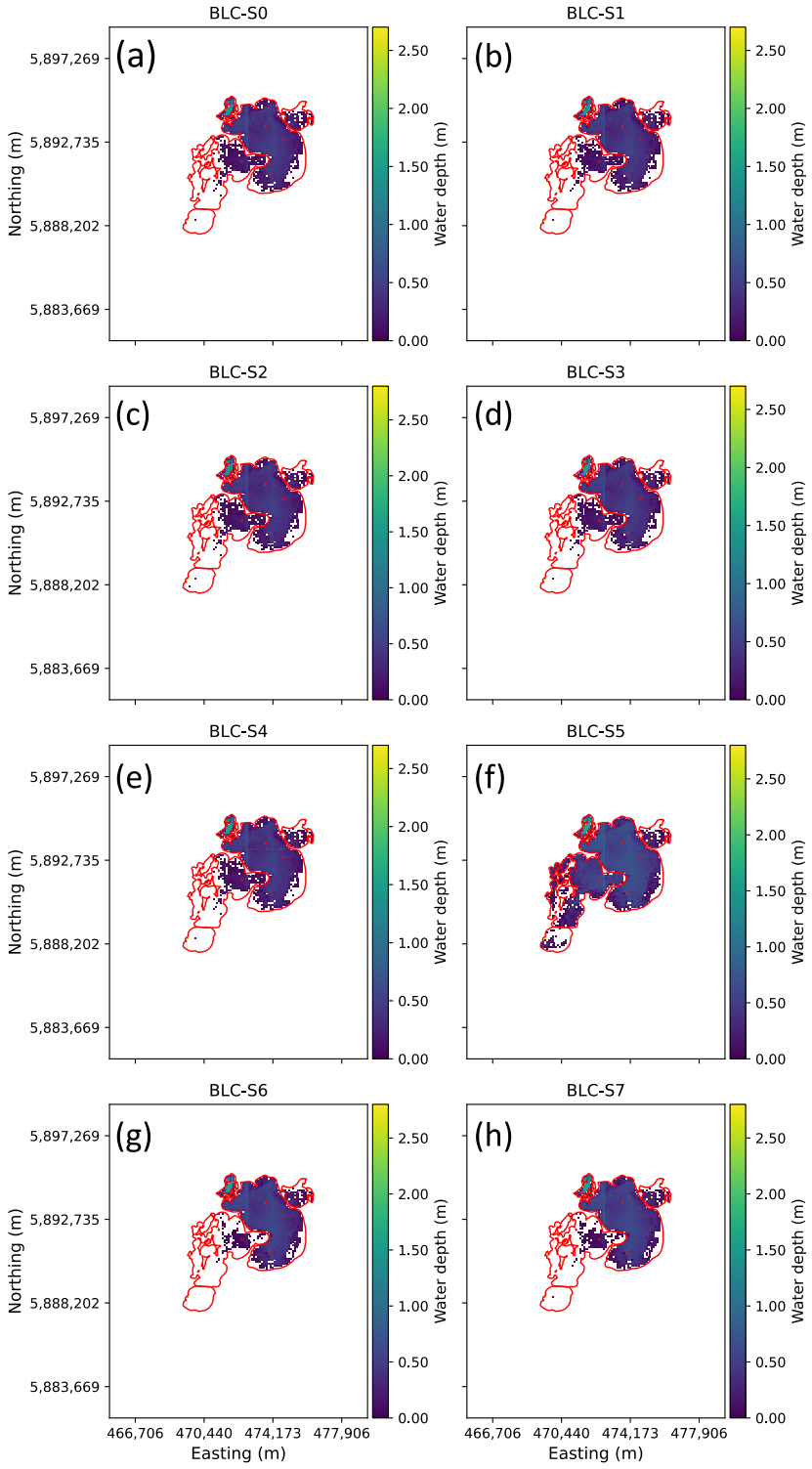

Figure C83. Inundation area of Bool Lagoon in November 2020 under base model and seven scenarios: (a) Base model (BLC-S0), (b) BLC-S1, (c) BLC-S2, (d) BLC-S3, (e) BLC-S4, (f) BLC-S5, (g) BLC-S6, and (f) BLC-S7. Each subplot illustrates the water depth distribution for the respective scenario. Note: For BLC-S5, a single-lake model was used, whereas for other scenarios, a model with three sub-lakes was employed.

Appendix D – Comparative analysis of hydrological results from predictive scenarios for Karst Springs Restoration site

D.1 Hydrological outcomes of DC-S1 simulation

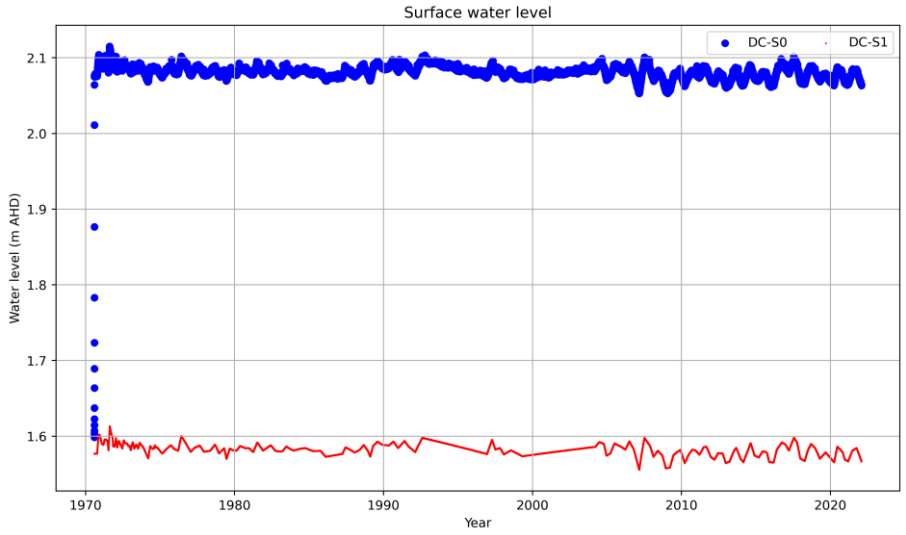

Figure D1. Comparison of surface water level between the base model (DC-S0) and simulated results of DC-S1 in proposed DC wetland for the period 1970–2022.

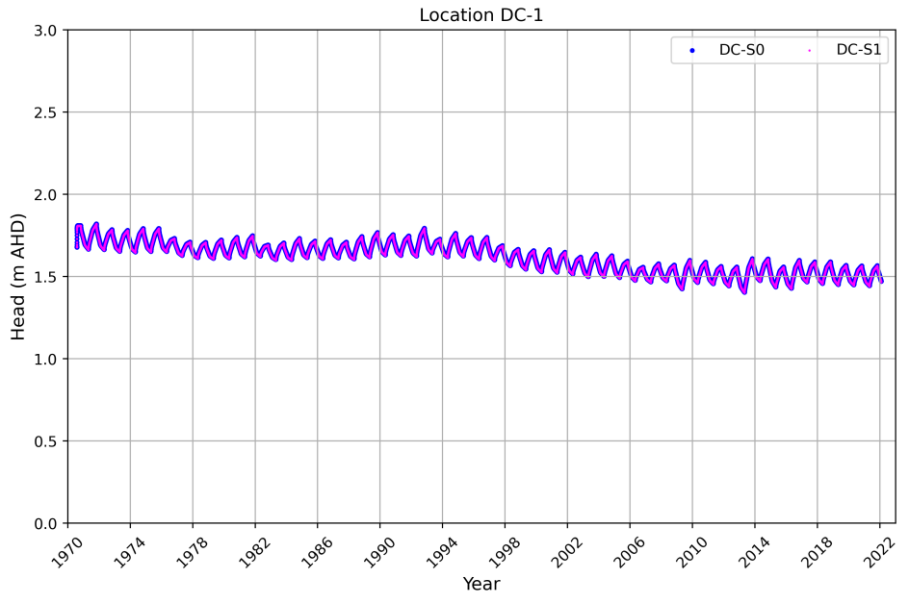

Figure D2. Comparison of groundwater head between the base model (DC-S0) and simulated results of DC-S1 at selected cell DC-1 for the period 1970–2022.

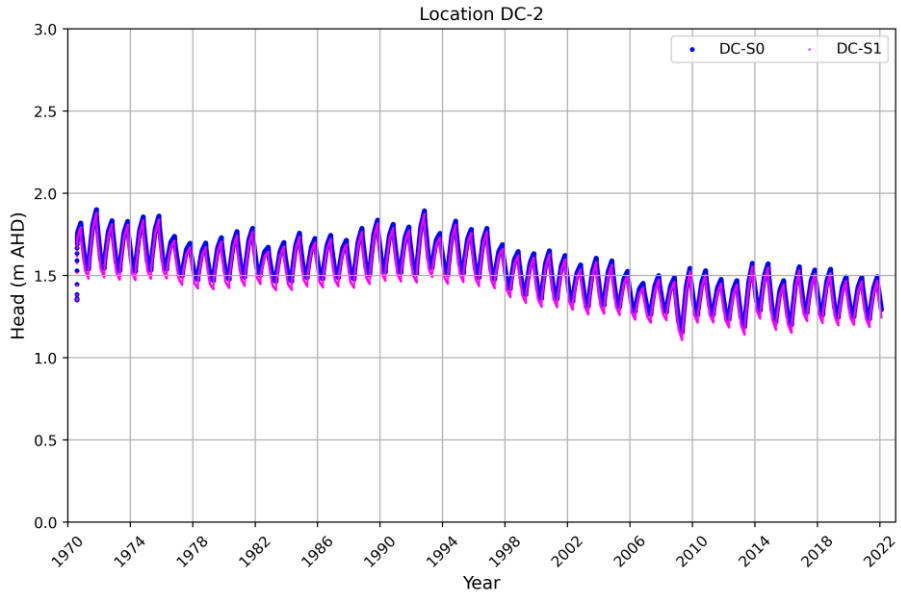

Figure D3. Comparison of groundwater head between the base model (DC-S0) and simulated results of DC-S1 at selected cell DC-2 for the period 1970–2022.

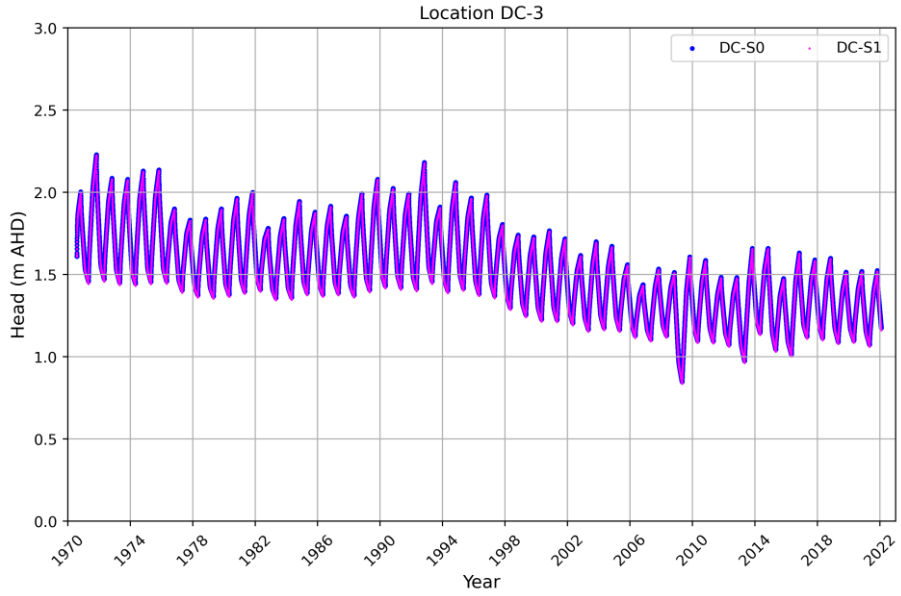

Figure D4. Comparison of groundwater head between the base model (DC-S0) and simulated results of DC-S1 at selected cell DC-3 for the period 1970–2022.

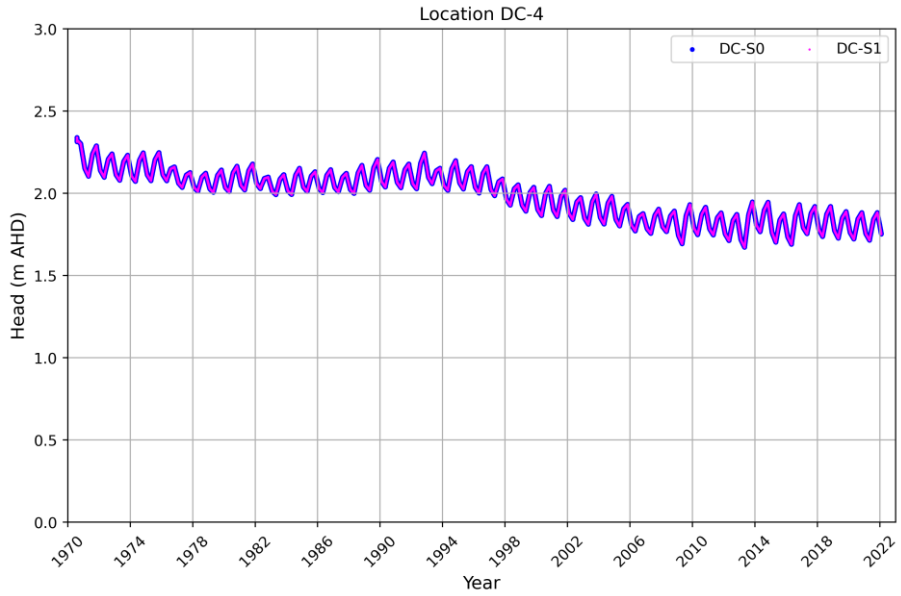

Figure D5. Comparison of groundwater head between the base model (DC-S0) and simulated results of DC-S1 at selected cell DC-4 for the period 1970–2022.

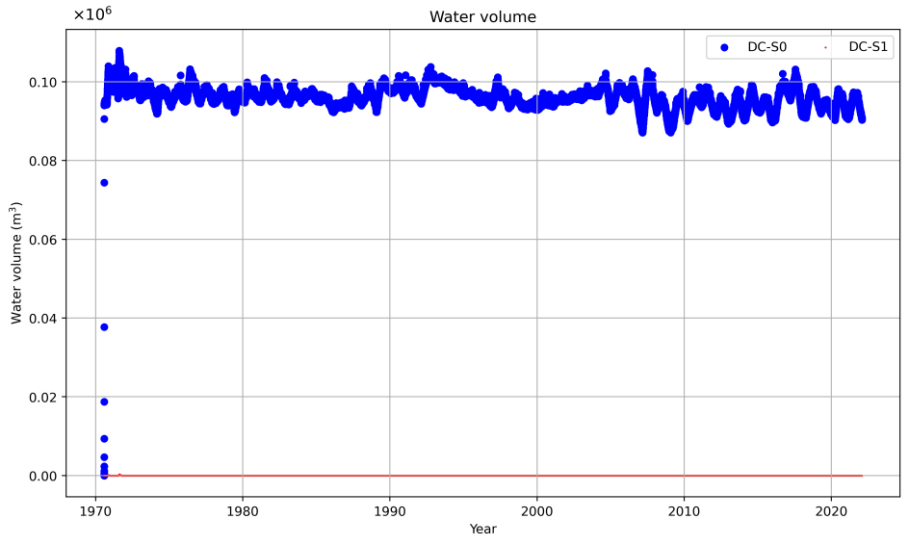

Figure D6. Comparison of water volume between the base model (DC-S0) with a single lake and simulated results of DC-S1 for the period 1970–2022.

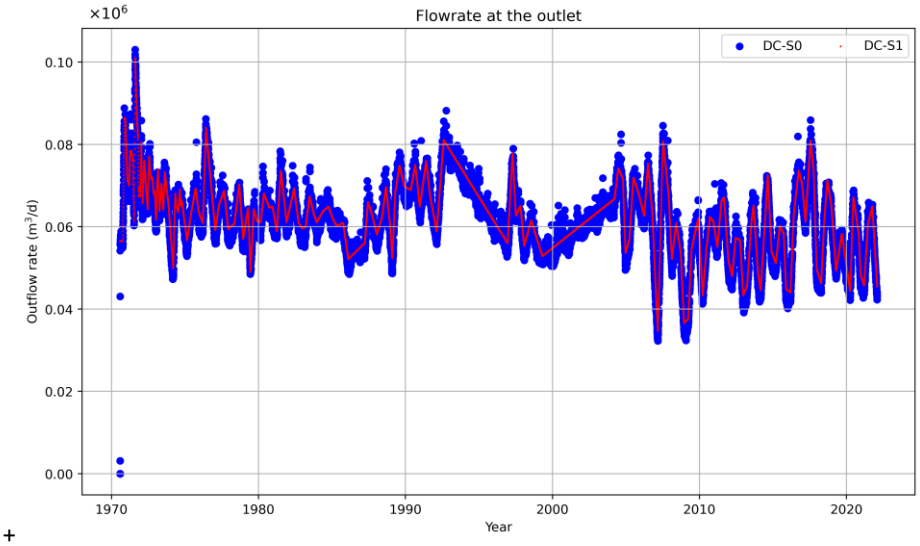

Figure D7. Comparison of outflow rates at outlet between the base model (DC-S0) and simulated results of DC-S1 for the period 1970–2022.

D.2 Hydrological outcomes of DC-S2 simulation

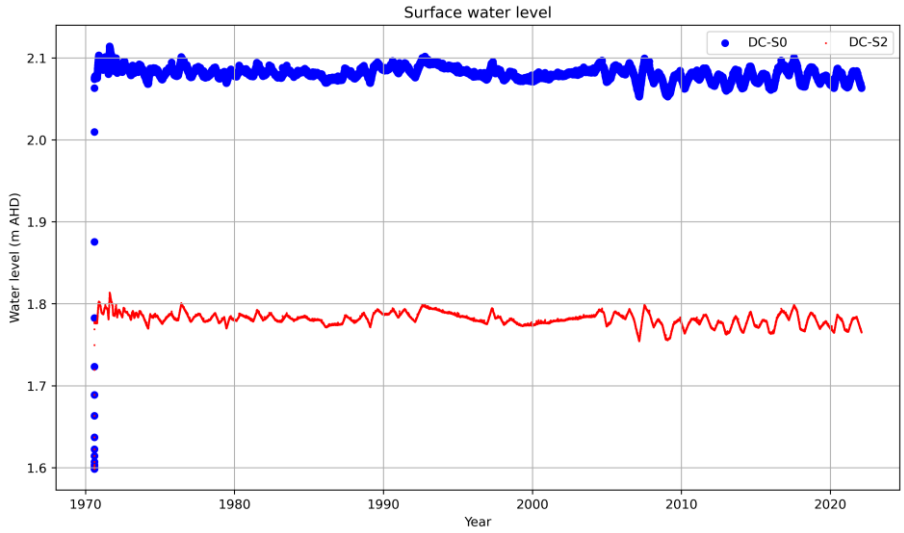

Figure D8. Comparison of surface water level between the base model (DC-S0) and simulated results of DC-S2 in proposed DC wetland for the period 1970–2022.

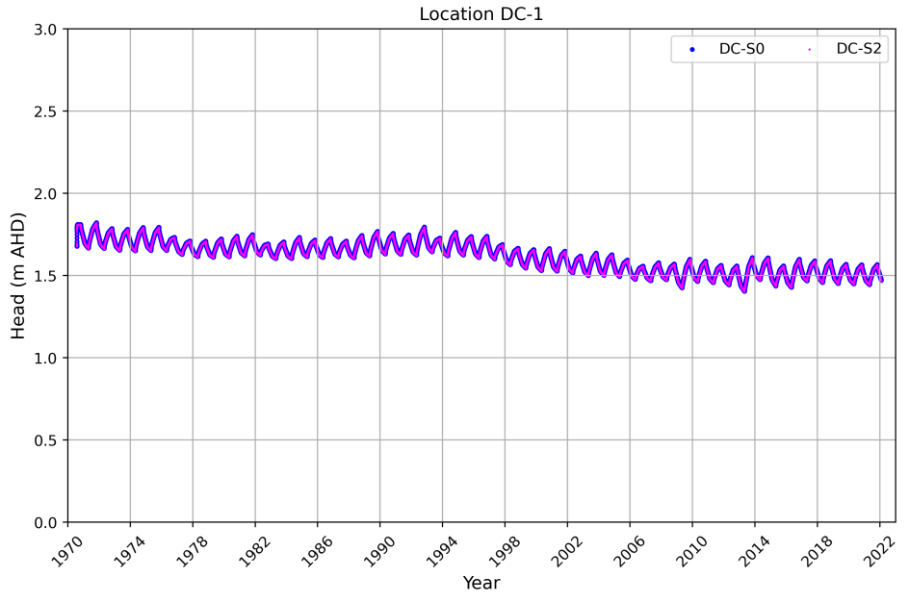

Figure D9. Comparison of groundwater head between the base model (DC-S0) and simulated results of DC-S2 at selected cell DC-1 for the period 1970–2022.

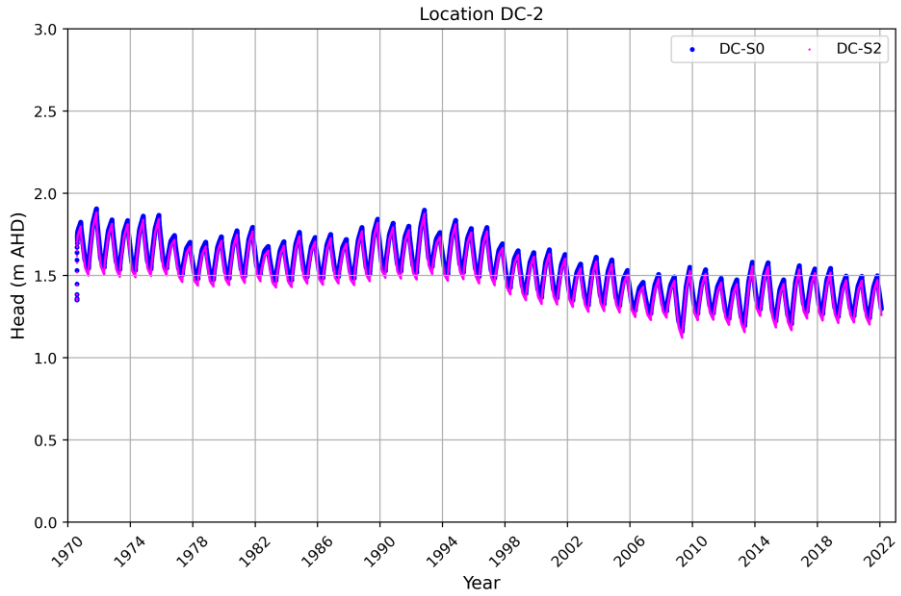

Figure D10. Comparison of groundwater head between the base model (DC-S0) and simulated results of DC-S2 at selected cell DC-2 for the period 1970–2022.

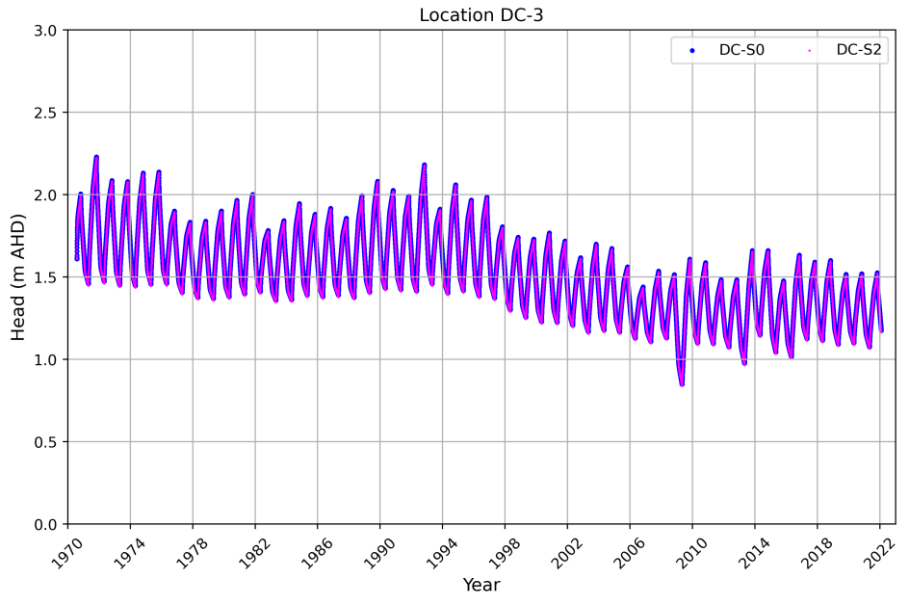

Figure D11. Comparison of groundwater head between the base model (DC-S0) and simulated results of DC-S2 at selected cell DC-3 for the period 1970–2022.

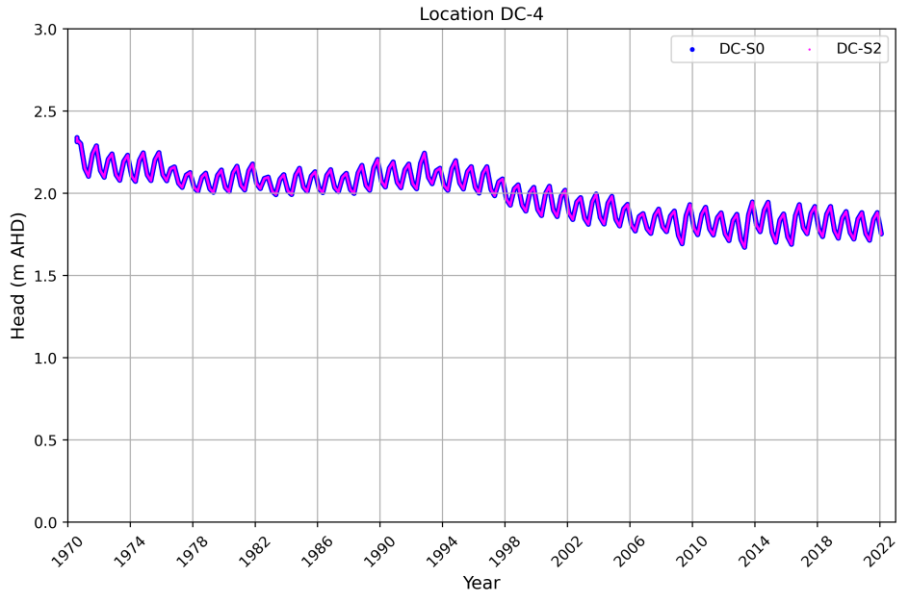

Figure D12. Comparison of groundwater head between the base model (DC-S0) and simulated results of DC-S2 at selected cell DC-4 for the period 1970–2022.

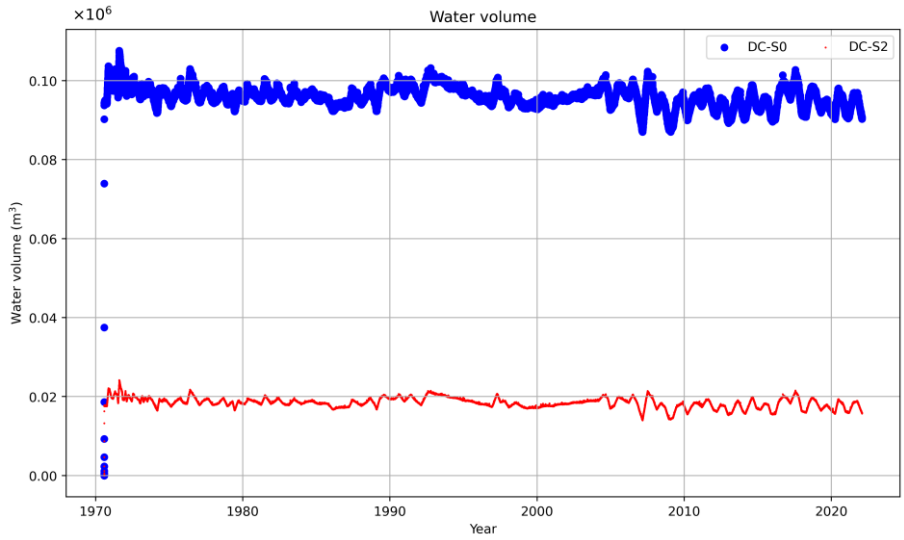

Figure D13. Comparison of water volume between the base model (DC-S0) with a single lake and simulated results of DC-S2 for the period 1970–2022.

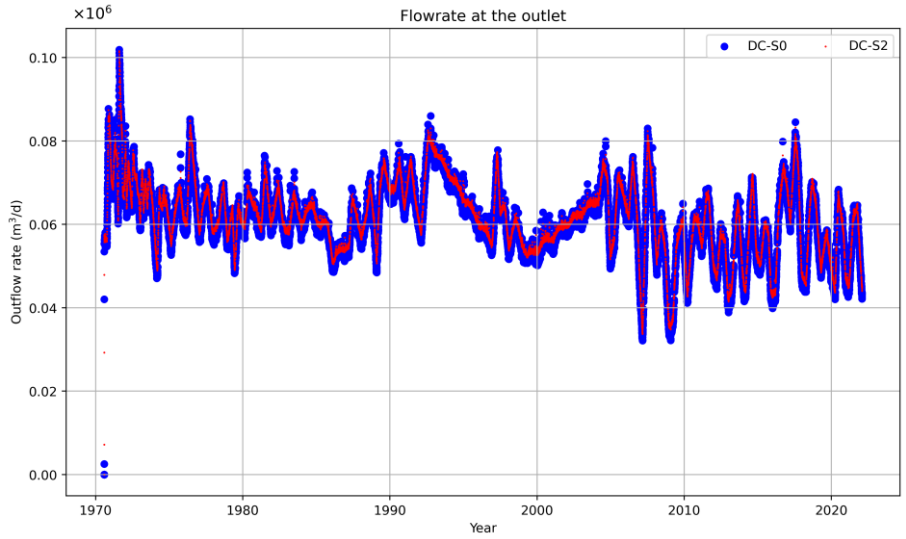

Figure D14. Comparison of outflow rates at outlet between the base model (DC-S0) and simulated results of DC-S2 for the period 1970–2022.

D.3 Hydrological outcomes of DC-S3 simulation

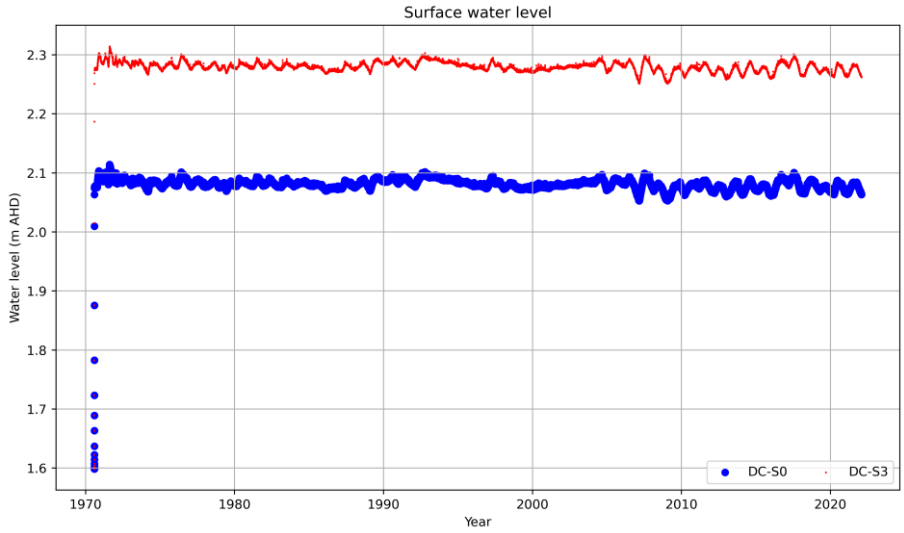

Figure D15. Comparison of surface water level between the base model (DC-S0) and simulated results of DC-S3 in proposed DC wetland for the period 1970–2022.

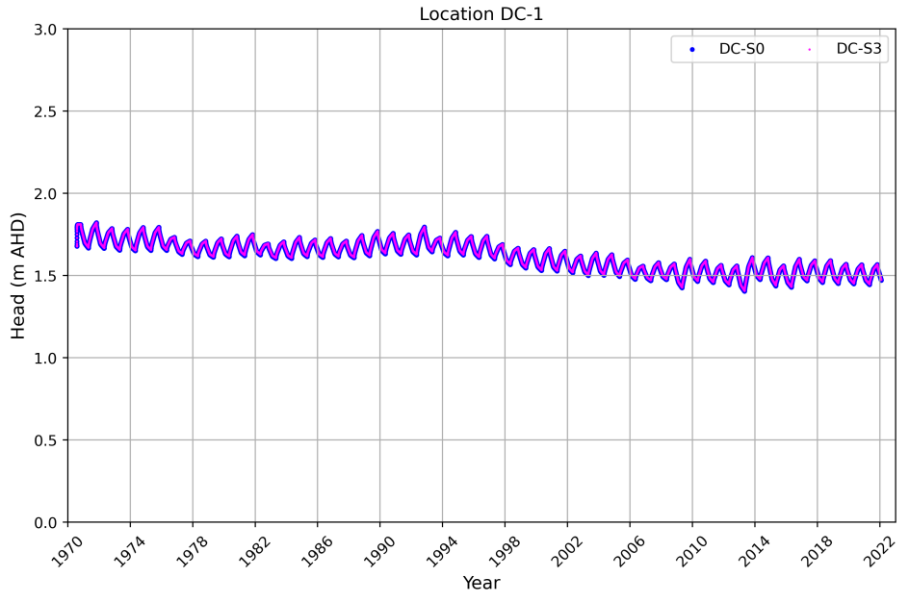

Figure D16. Comparison of groundwater head between the base model (DC-S0) and simulated results of DC-S3 at selected cell DC-1 for the period 1970–2022.

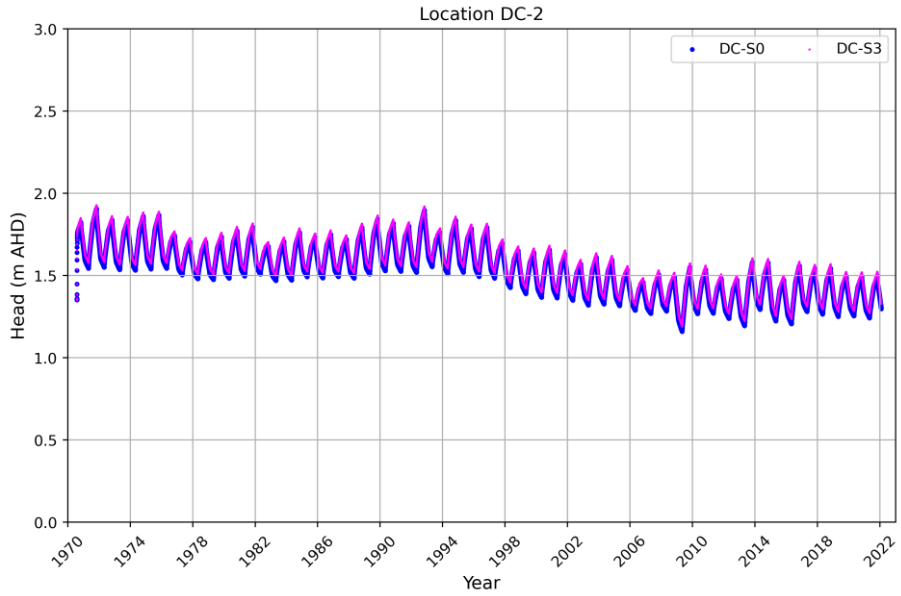

Figure D17. Comparison of groundwater head between the base model (DC-S0) and simulated results of DC-S3 at selected cell DC-2 for the period 1970–2022.

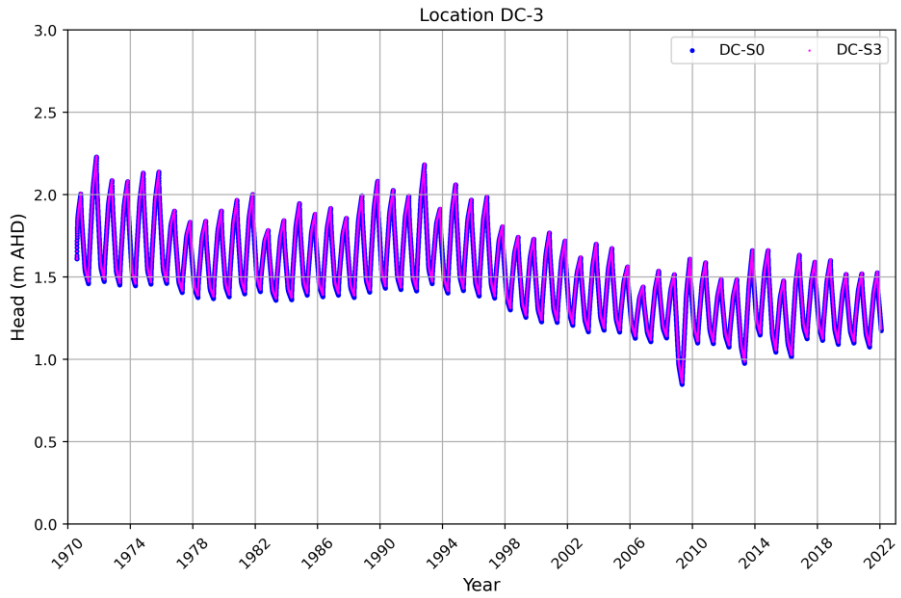

Figure D18. Comparison of groundwater head between the base model (DC-S0) and simulated results of DC-S3 at selected cell DC-3 for the period 1970–2022.

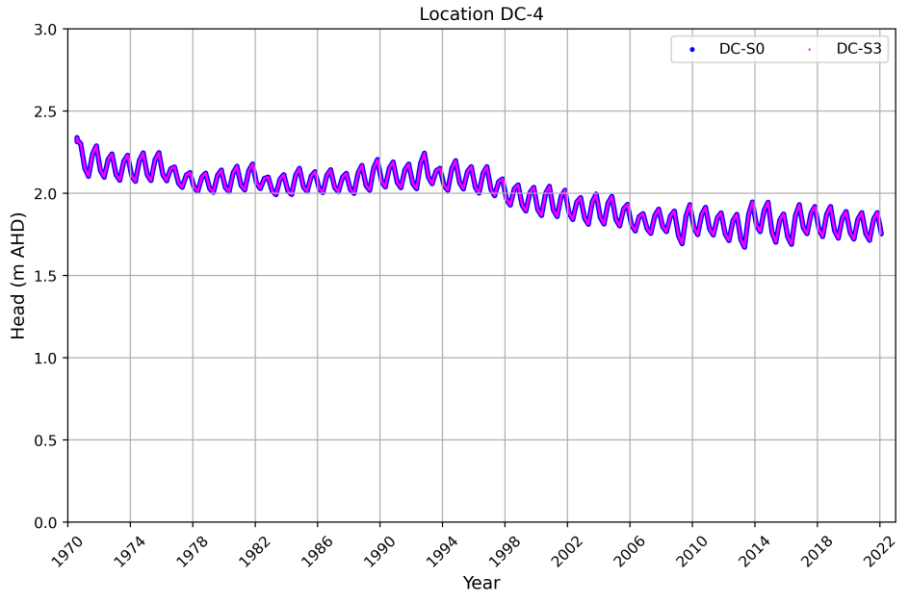

Figure D19. Comparison of groundwater head between the base model (DC-S0) and simulated results of DC-S3 at selected cell DC-4 for the period 1970–2022.

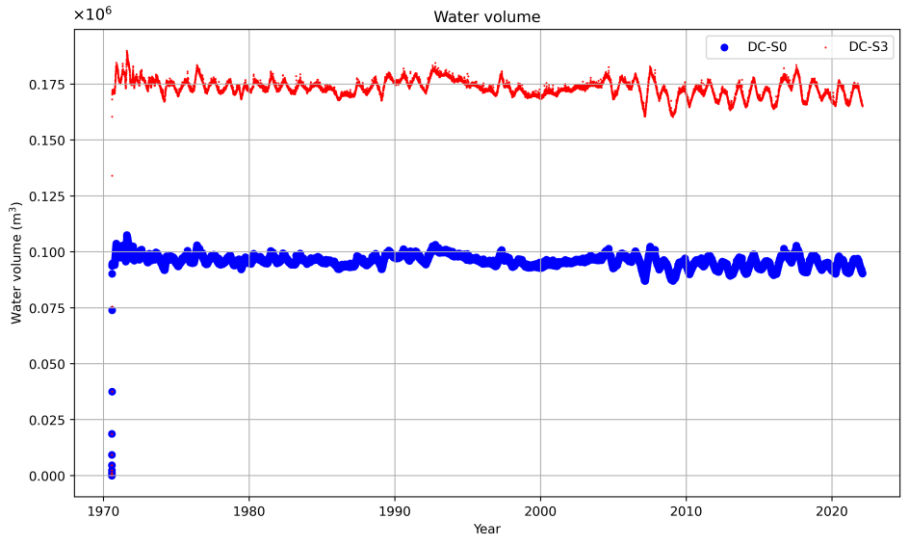

Figure D20. Comparison of water volume between the base model (DC-S0) with a single lake and simulated results of DC-S3 for the period 1970–2022.

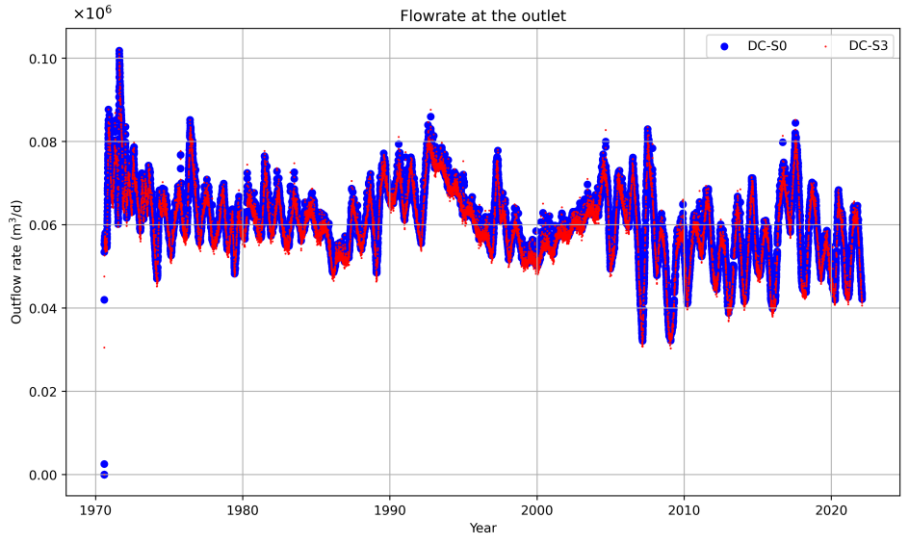

Figure D21. Comparison of outflow rates at outlet between the base model (DC-S0) and simulated results of DC-S3 for the period 1970–2022.

D.4 Hydrological outcomes of DC-S4 simulation

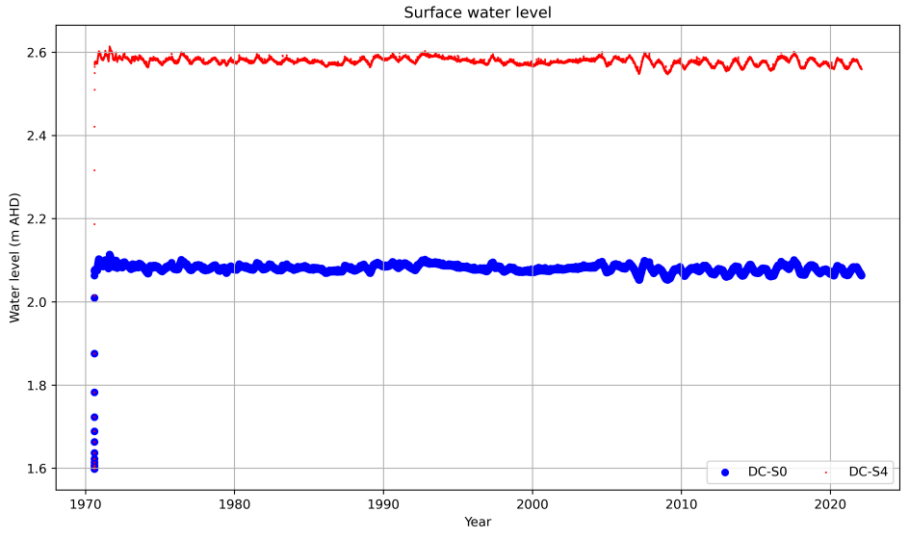

Figure D22. Comparison of surface water level between the base model (DC-S0) and simulated results of DC-S4 in proposed DC wetland for the period 1970–2022.

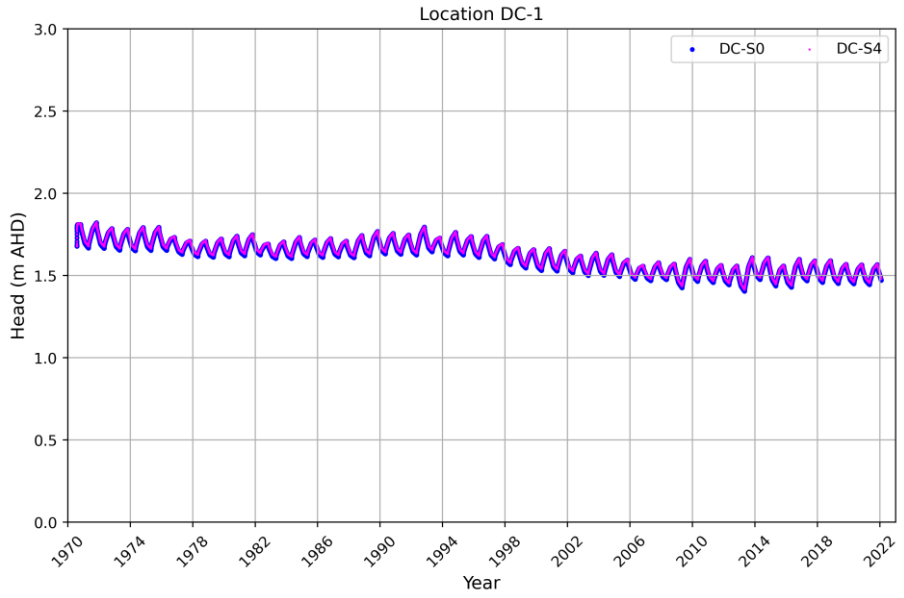

Figure D23. Comparison of groundwater head between the base model (DC-S0) and simulated results of DC-S4 at selected cell DC-1 for the period 1970–2022.

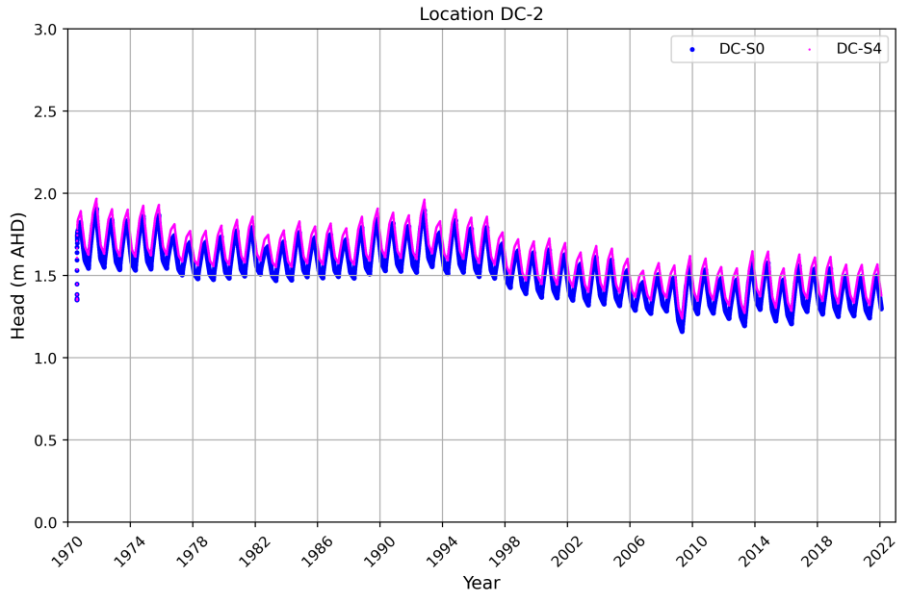

Figure D24. Comparison of groundwater head between the base model (DC-S0) and simulated results of DC-S4 at selected cell DC-2 for the period 1970–2022.

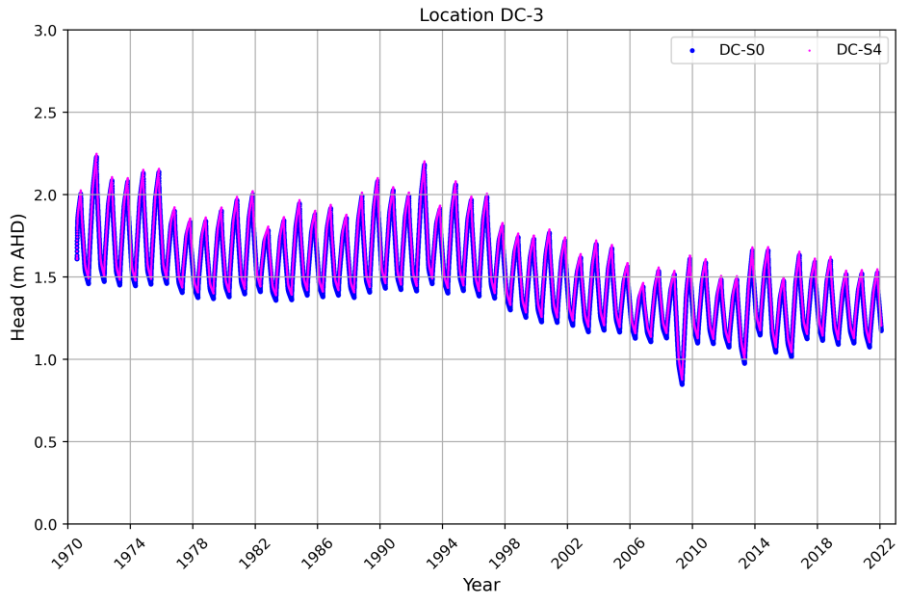

Figure D25. Comparison of groundwater head between the base model (DC-S0) and simulated results of DC-S4 at selected cell DC-3 for the period 1970–2022.

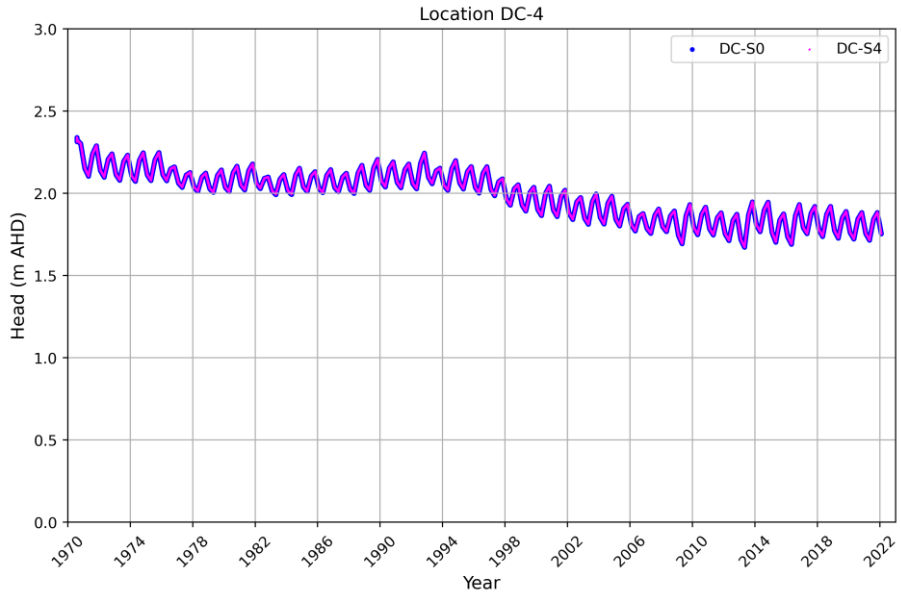

Figure D26. Comparison of groundwater head between the base model (DC-S0) and simulated results of DC-S4 at selected cell DC-4 for the period 1970–2022.

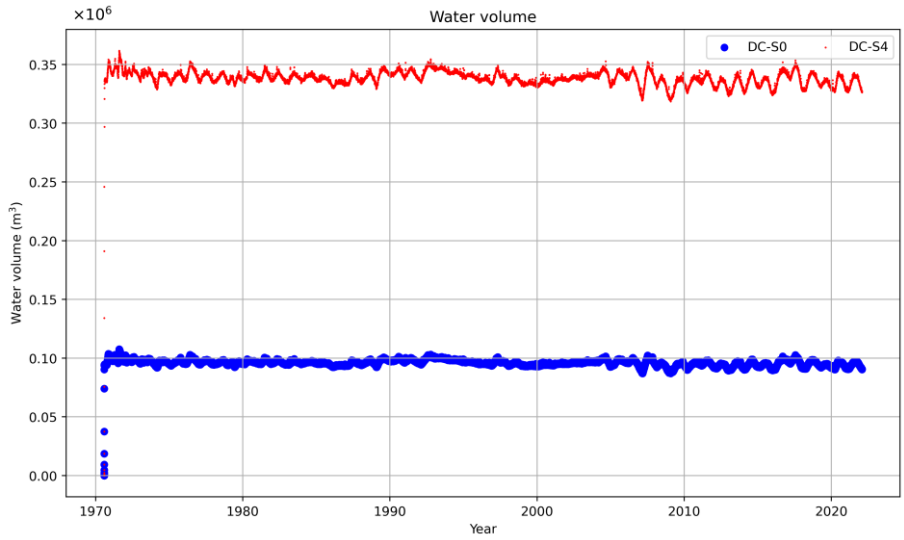

Figure D27. Comparison of water volume between the base model (DC-S0) with a single lake and simulated results of DC-S4 for the period 1970–2022.

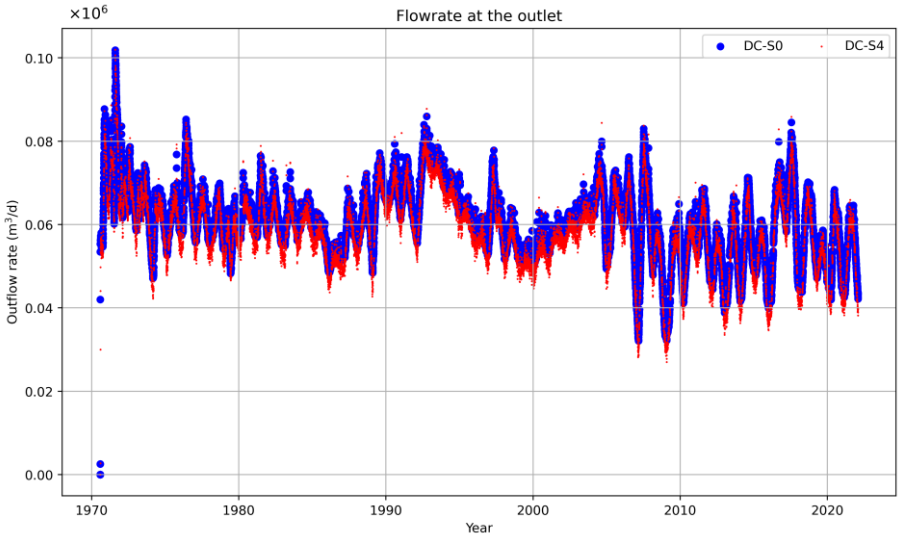

Figure D28. Comparison of outflow rates at outlet between the base model (DC-S0) and simulated results of DC-S4 for the period 1970–2022.

D.5 Hydrological outcomes of DC-S5 simulation

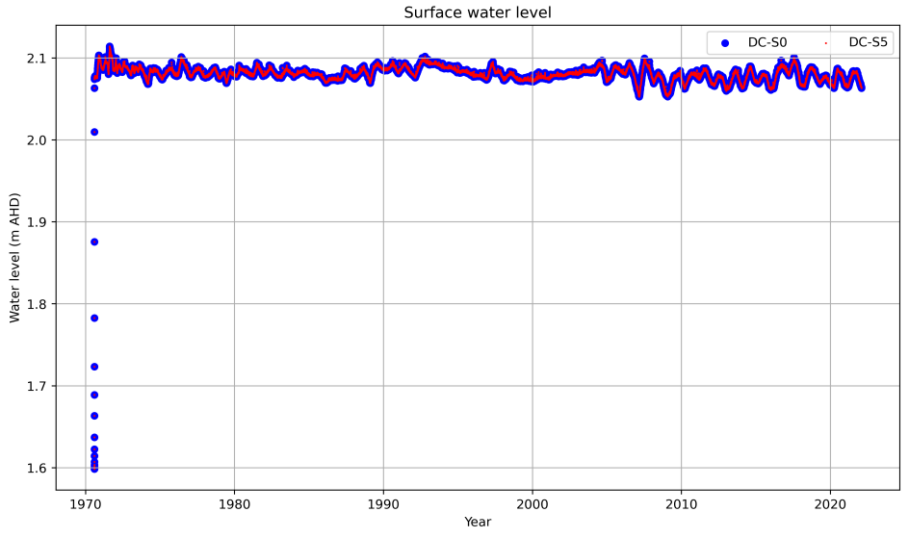

Figure D29. Comparison of surface water level between the base model (DC-S0) and simulated results of DC-S5 in proposed DC wetland for the period 1970–2022.

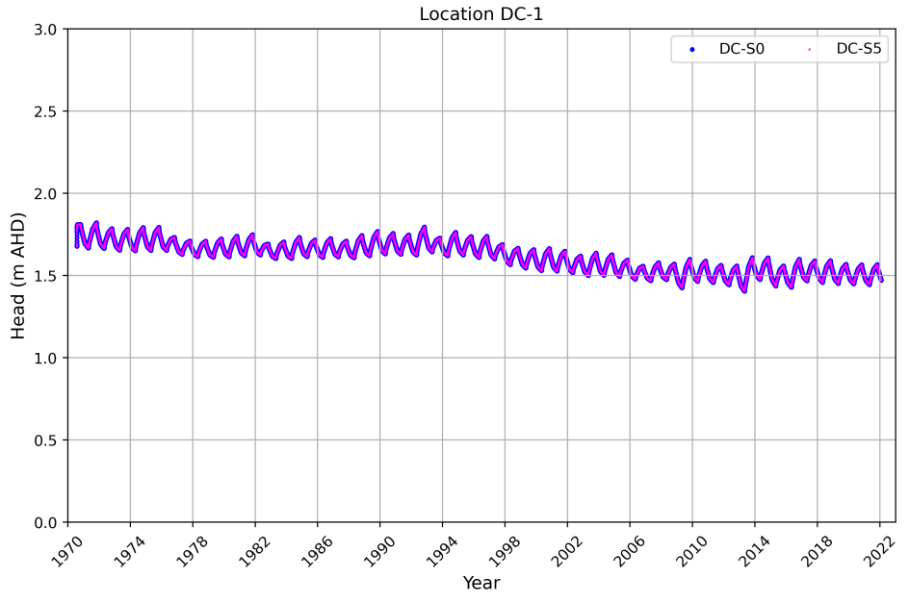

Figure D30. Comparison of groundwater head between the base model (DC-S0) and simulated results of DC-S5 at selected cell DC-1 for the period 1970–2022.

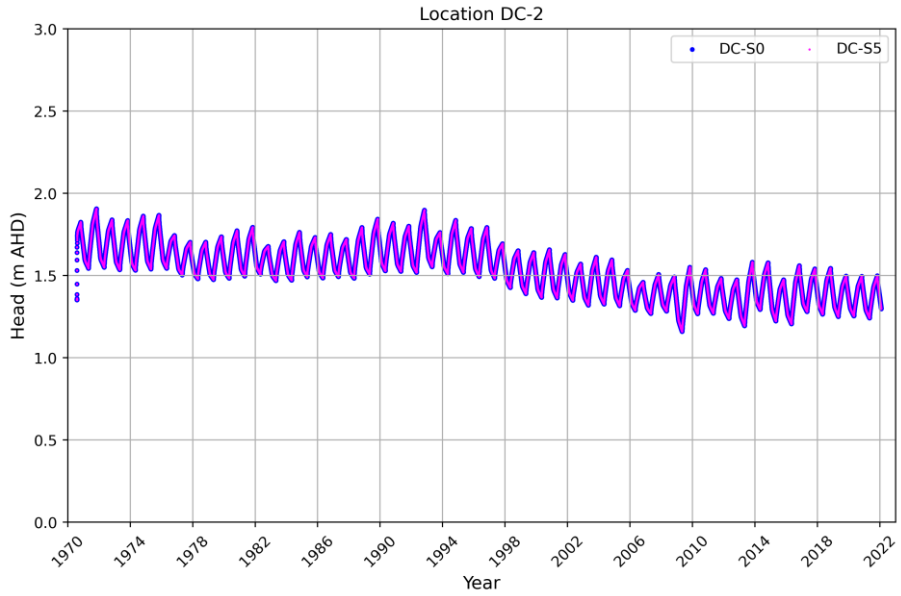

Figure D31. Comparison of groundwater head between the base model (DC-S0) and simulated results of DC-S5 at selected cell DC-2 for the period 1970–2022.

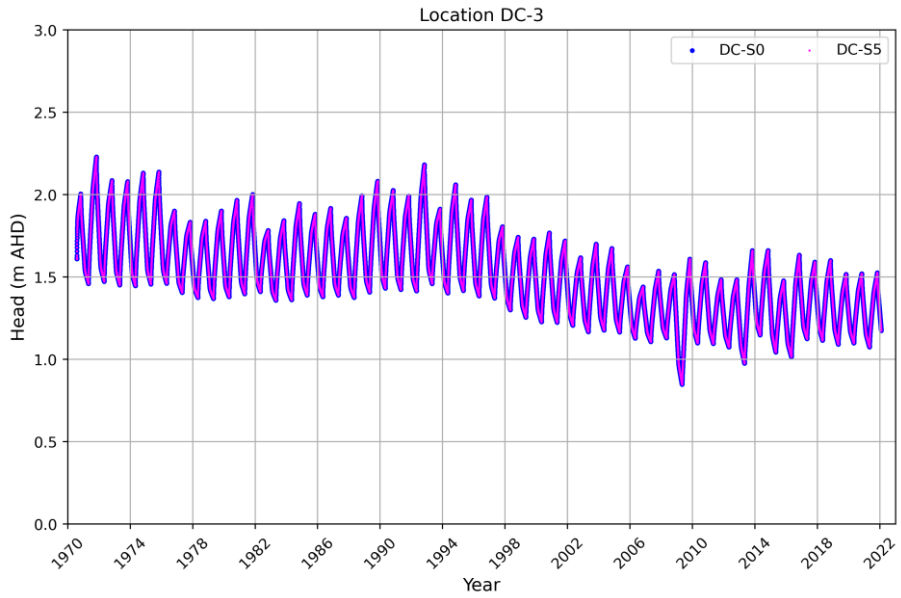

Figure D32. Comparison of groundwater head between the base model (DC-S0) and simulated results of DC-S5 at selected cell DC-3 for the period 1970–2022.

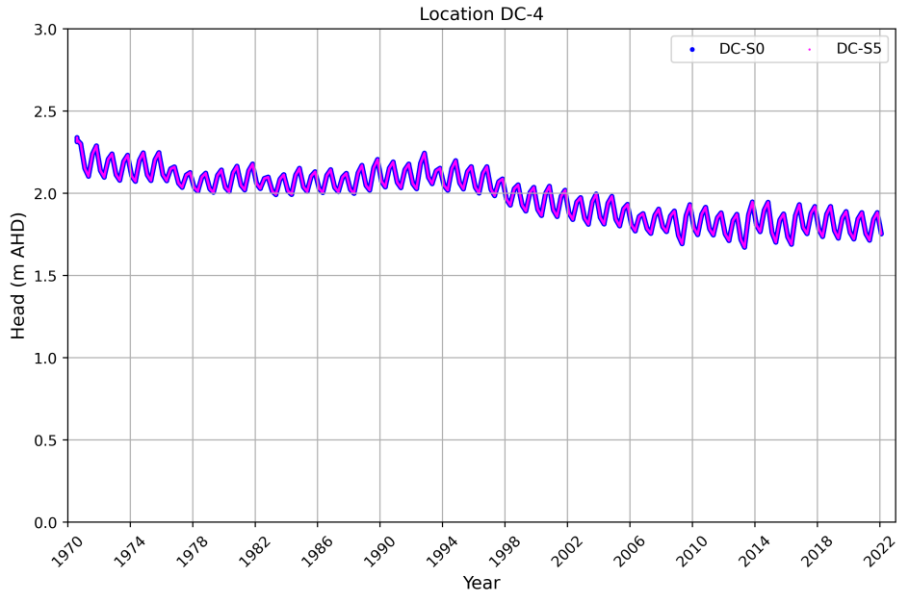

Figure D33. Comparison of groundwater head between the base model (DC-S0) and simulated results of DC-S5 at selected cell DC-4 for the period 1970–2022.

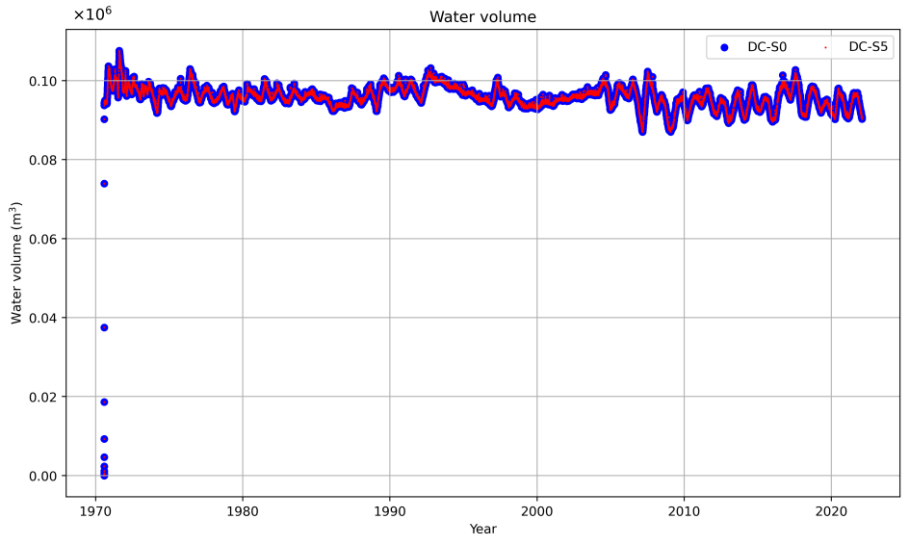

Figure D34. Comparison of water volume between the base model (DC-S0) with a single lake and simulated results of DC-S5 for the period 1970–2022.

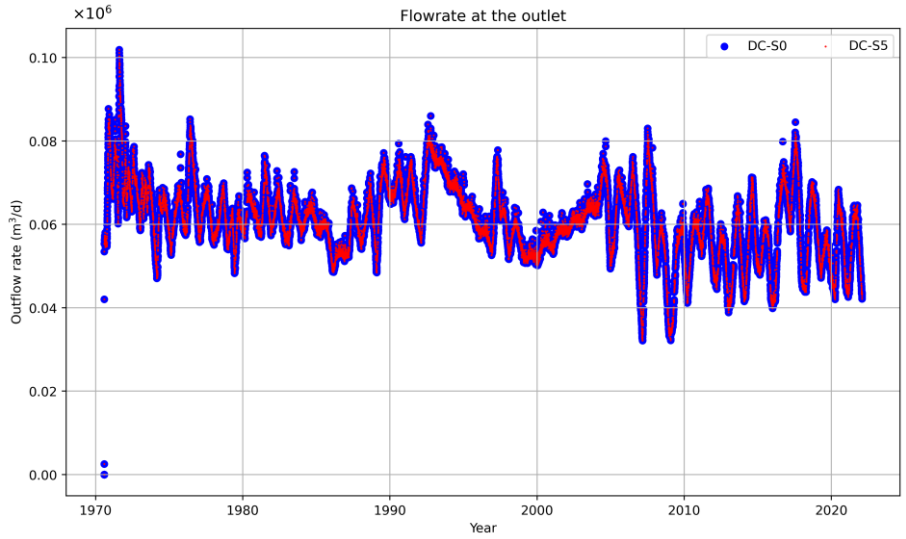

Figure D35. Comparison of outflow rates at outlet between the base model (DC-S0) and simulated results of DC-S5 for the period 1970–2022.

D.6 Hydrological outcomes of DC-S6 simulation

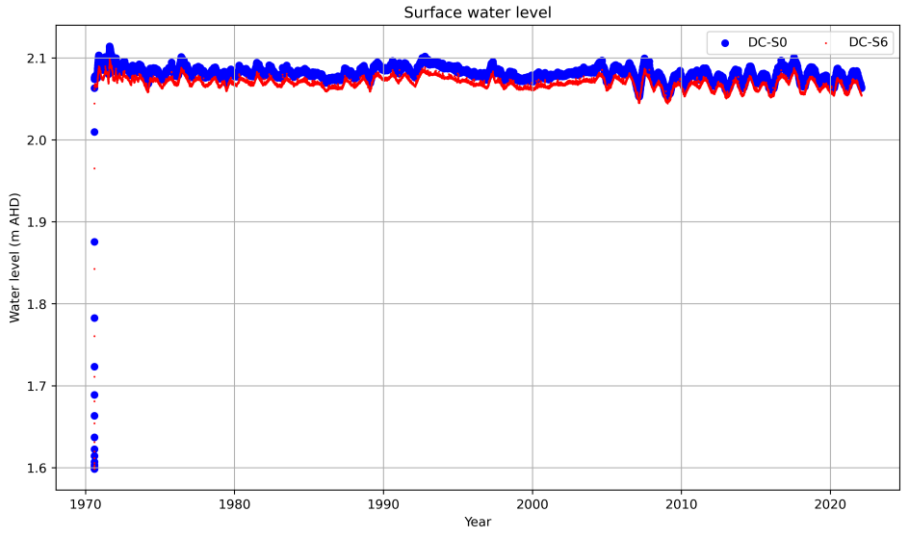

Figure D36. Comparison of surface water level between the base model (DC-S0) and simulated results of DC-S6 in proposed DC wetland for the period 1970–2022.

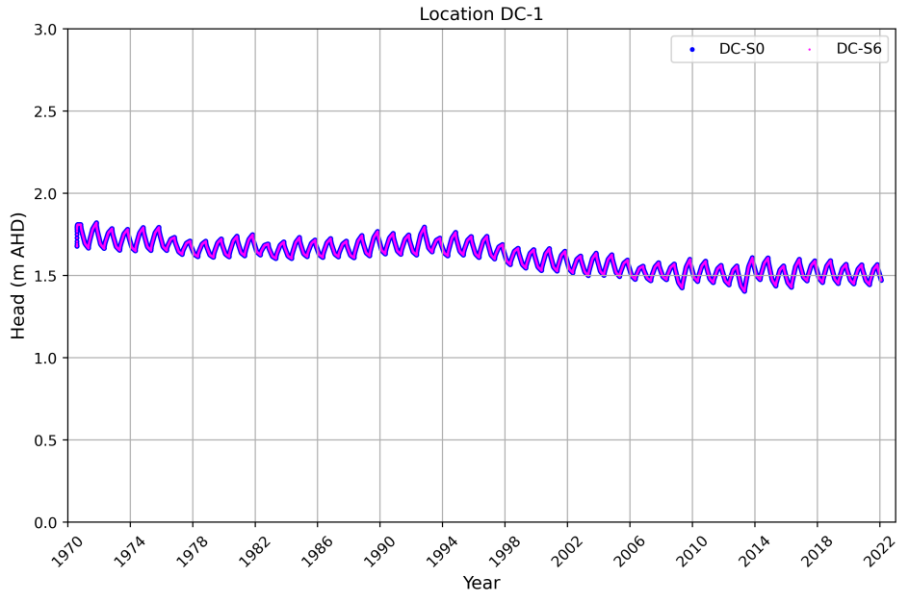

Figure D37. Comparison of groundwater head between the base model (DC-S0) and simulated results of DC-S6 at selected cell DC-1 for the period 1970–2022.

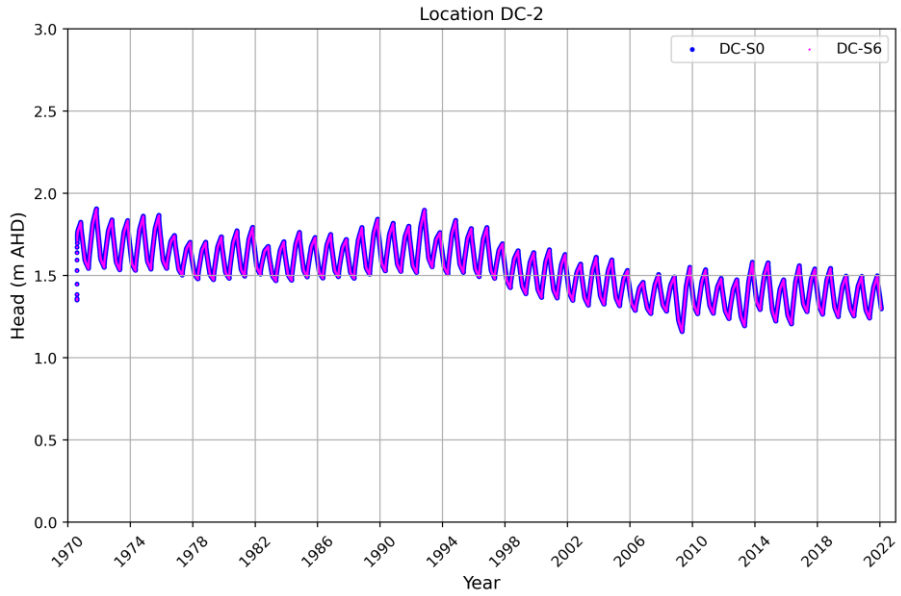

Figure D38. Comparison of groundwater head between the base model (DC-S0) and simulated results of DC-S6 at selected cell DC-2 for the period 1970–2022.

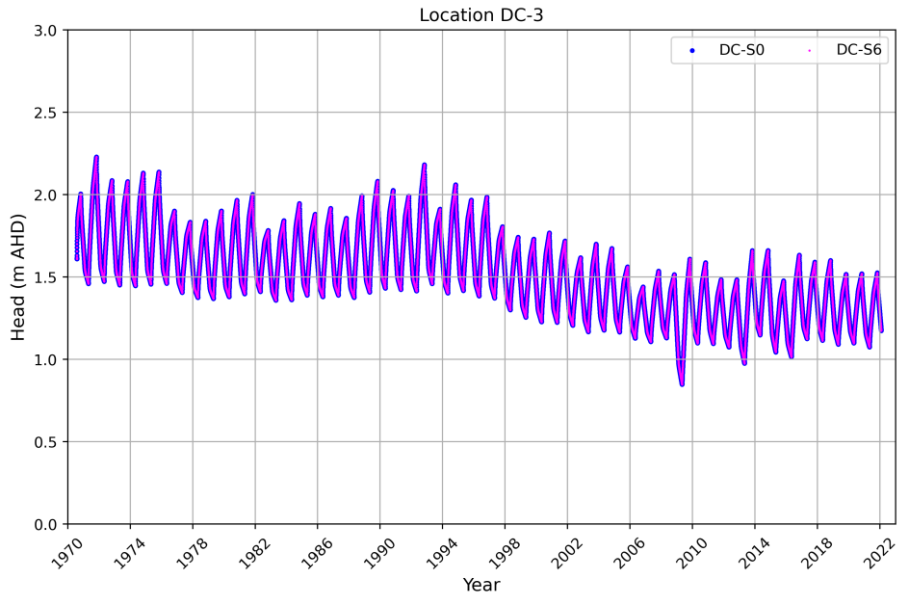

Figure D39. Comparison of groundwater head between the base model (DC-S0) and simulated results of DC-S6 at selected cell DC-3 for the period 1970–2022.

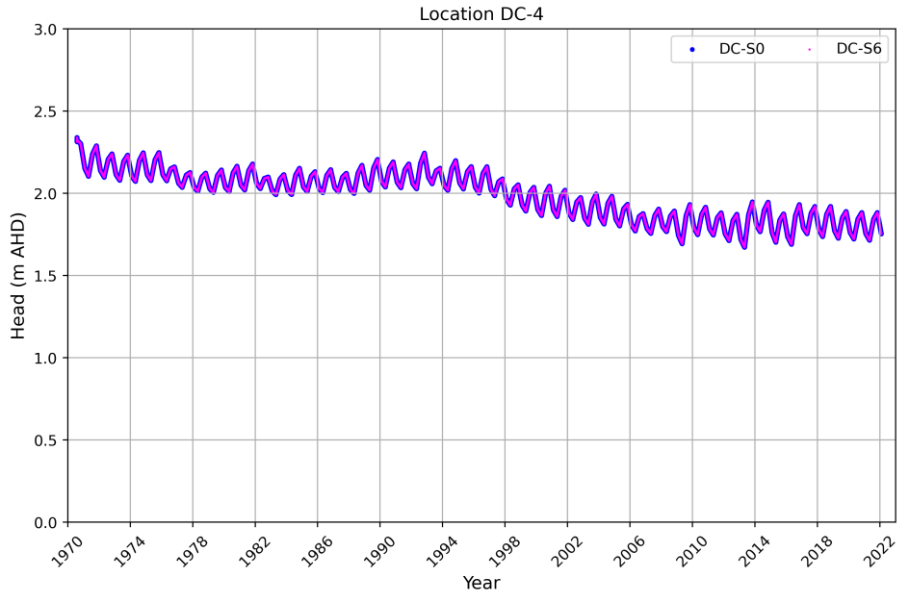

Figure D40. Comparison of groundwater head between the base model (DC-S0) and simulated results of DC-S6 at selected cell DC-4 for the period 1970–2022.

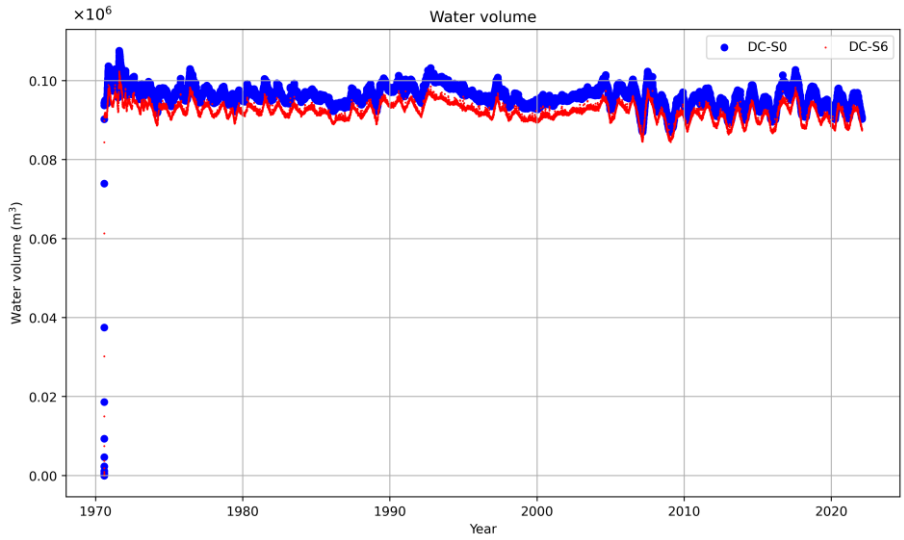

Figure D41. Comparison of water volume between the base model (DC-S0) with a single lake and simulated results of DC-S6 for the period 1970–2022.

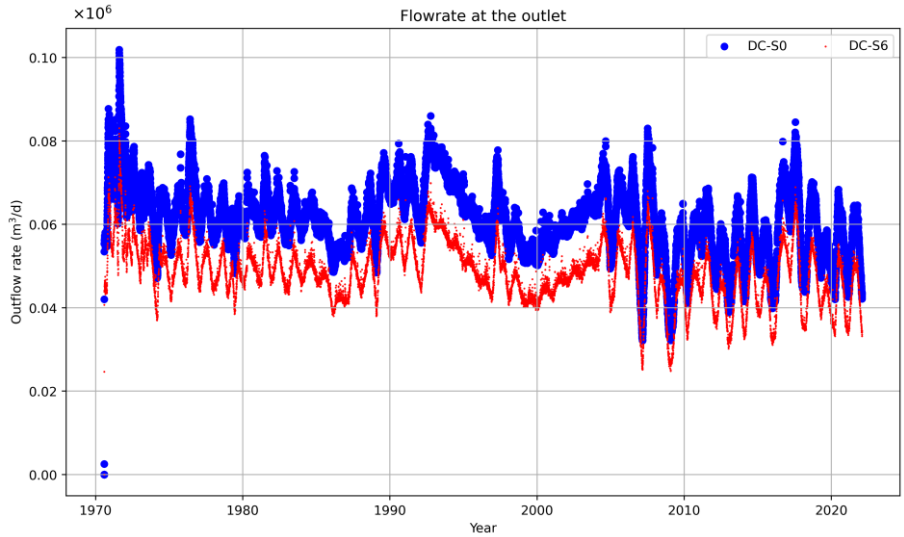

Figure D42. Comparison of outflow rates at outlet between the base model (DC-S0) and simulated results of DC-S6 for the period 1970–2022.

D.7 Inundation areas of proposed DC wetland under base model and scenarios

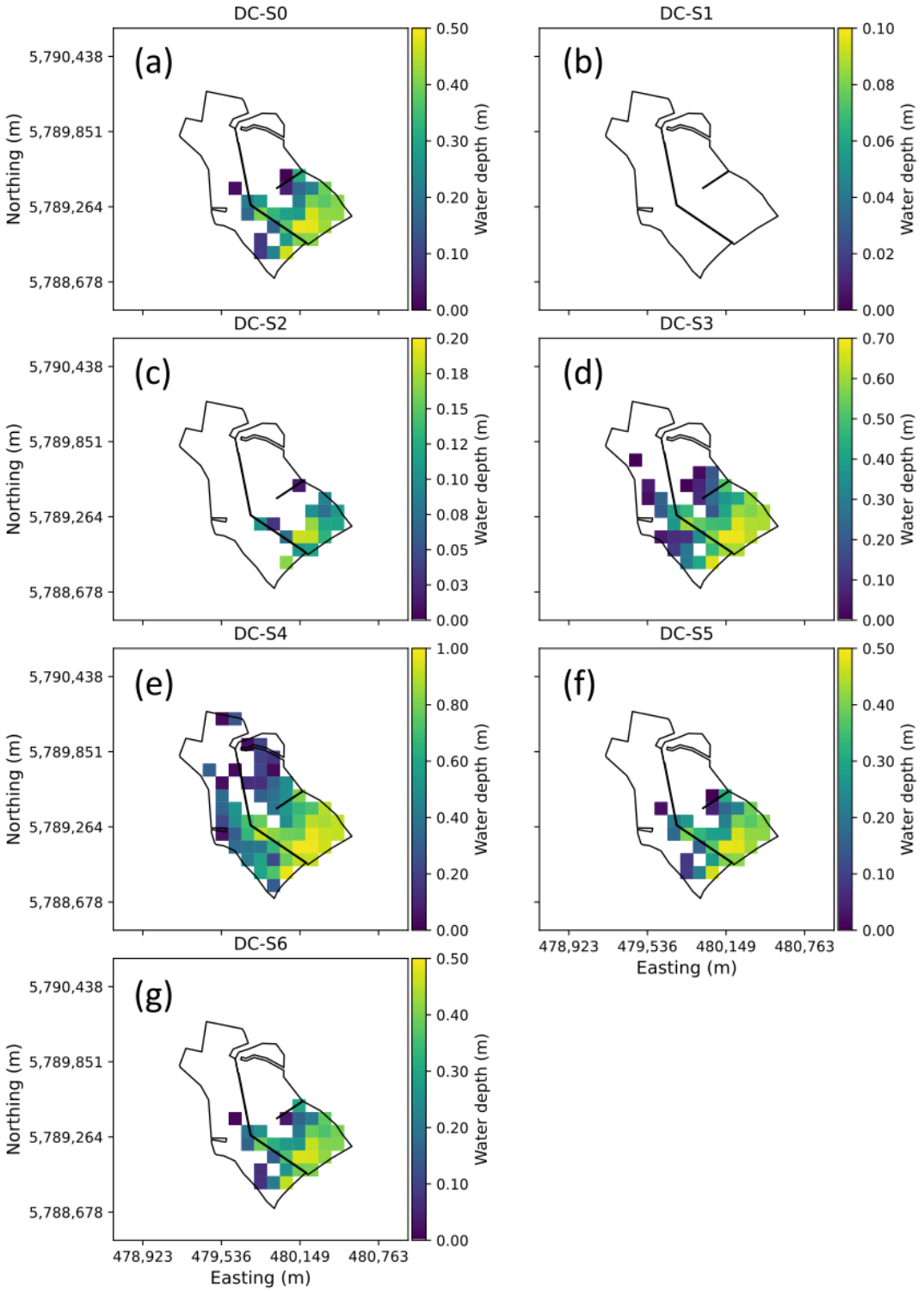

Figure D43. Inundation area of proposed DC wetland in May 1983 under base model and six scenarios: (a) Base model (DC-S0), (b) DC-S1, (c) DC-S2, (d) DC-S3, (e) DC-S4, (f) DC-S5, and (g) DC-S6. Each subplot illustrates the water depth distribution for the respective scenario.

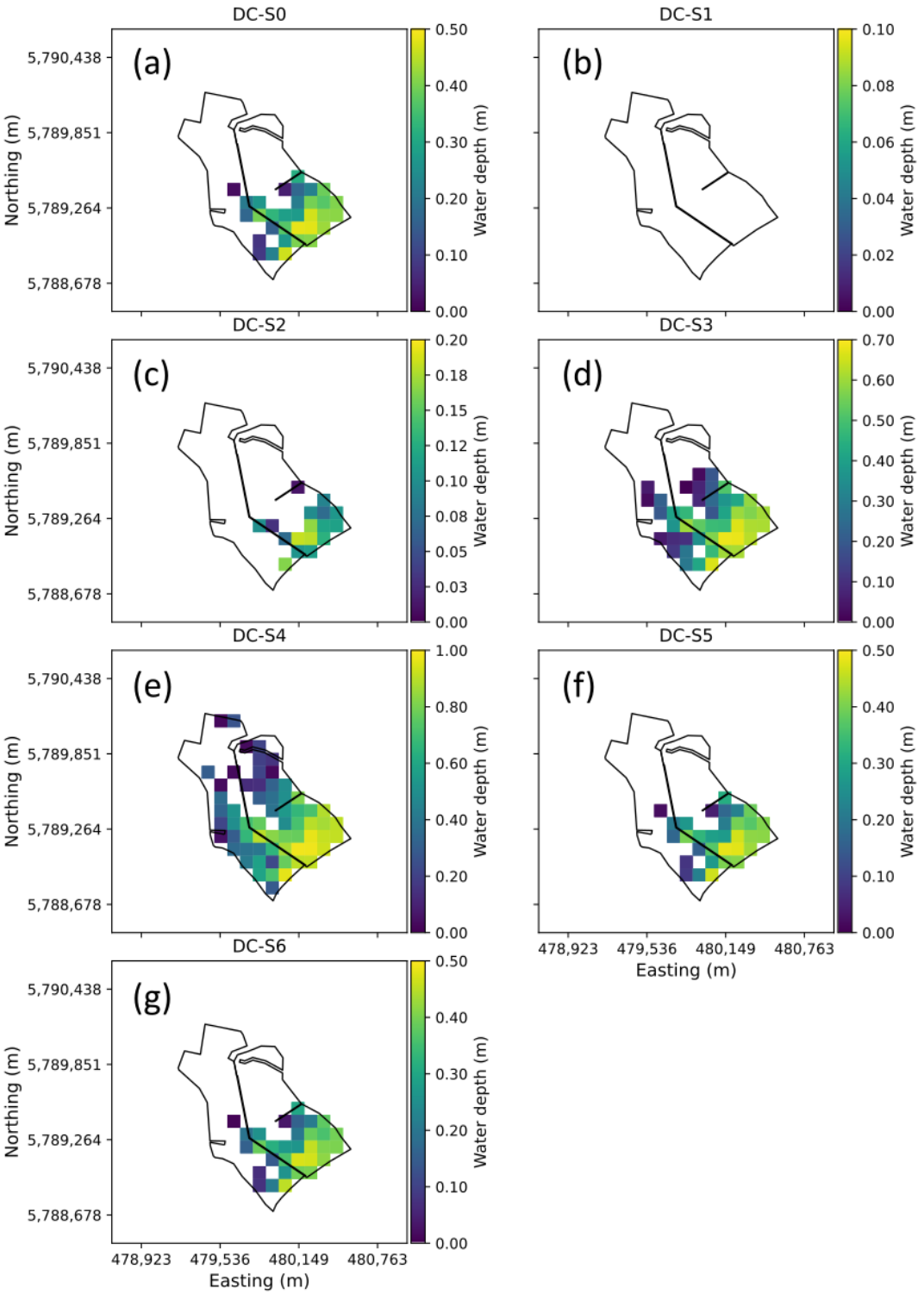

Figure D44. Inundation area of proposed DC wetland in November 1995 under base model and six scenarios: (a) Base model (DC-S0), (b) DC-S1, (c) DC-S2, (d) DC-S3, (e) DC-S4, (f) DC-S5, and (g) DC-S6. Each subplot illustrates the water depth distribution for the respective scenario.

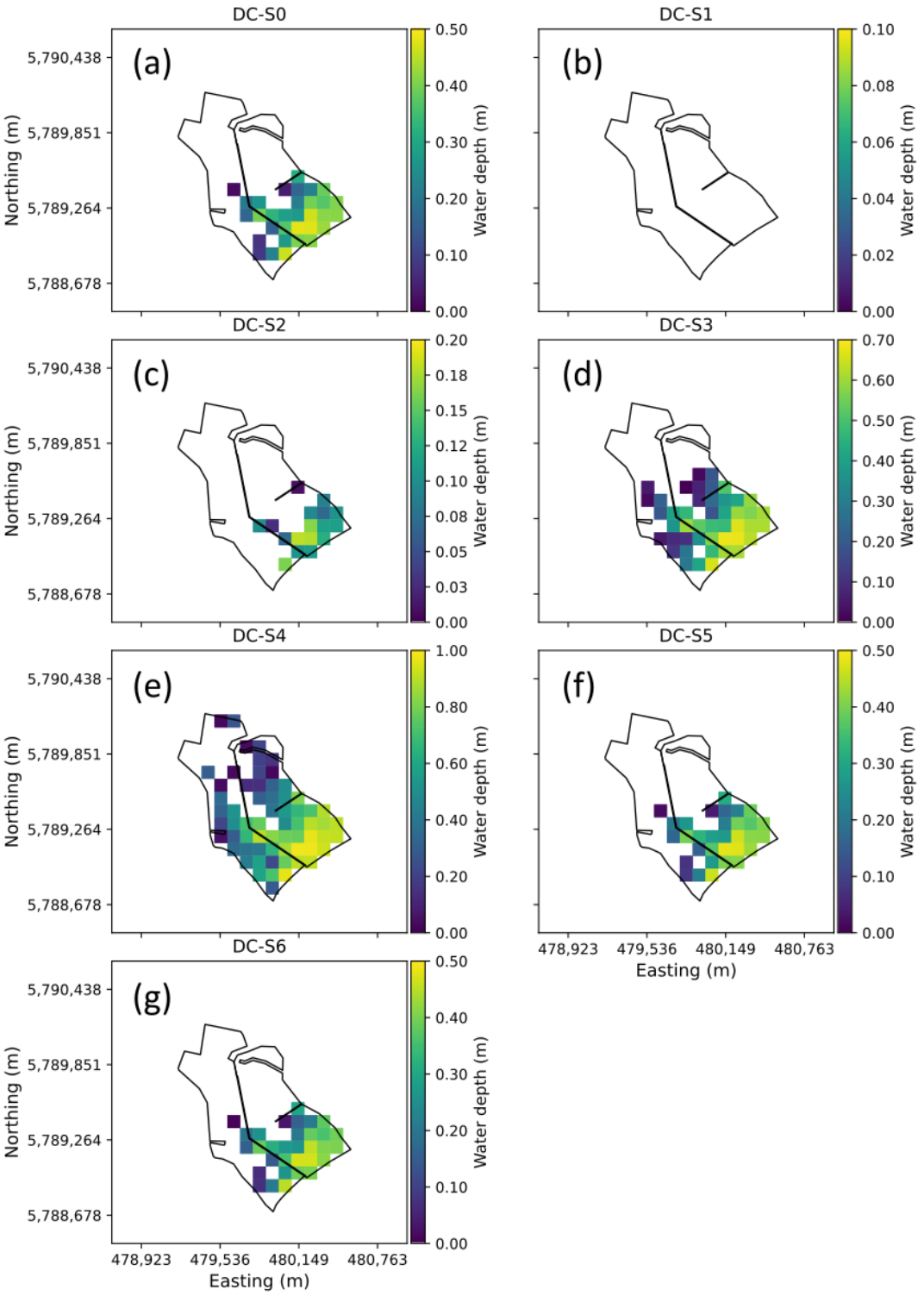

Figure D45. Inundation area of proposed DC wetland in May 2008 under base model and six scenarios: (a) Base model (DC-S0), (b) DC-S1, (c) DC-S2, (d) DC-S3, (e) DC-S4, (f) DC-S5, and (g) DC-S6. Each subplot illustrates the water depth distribution for the respective scenario.

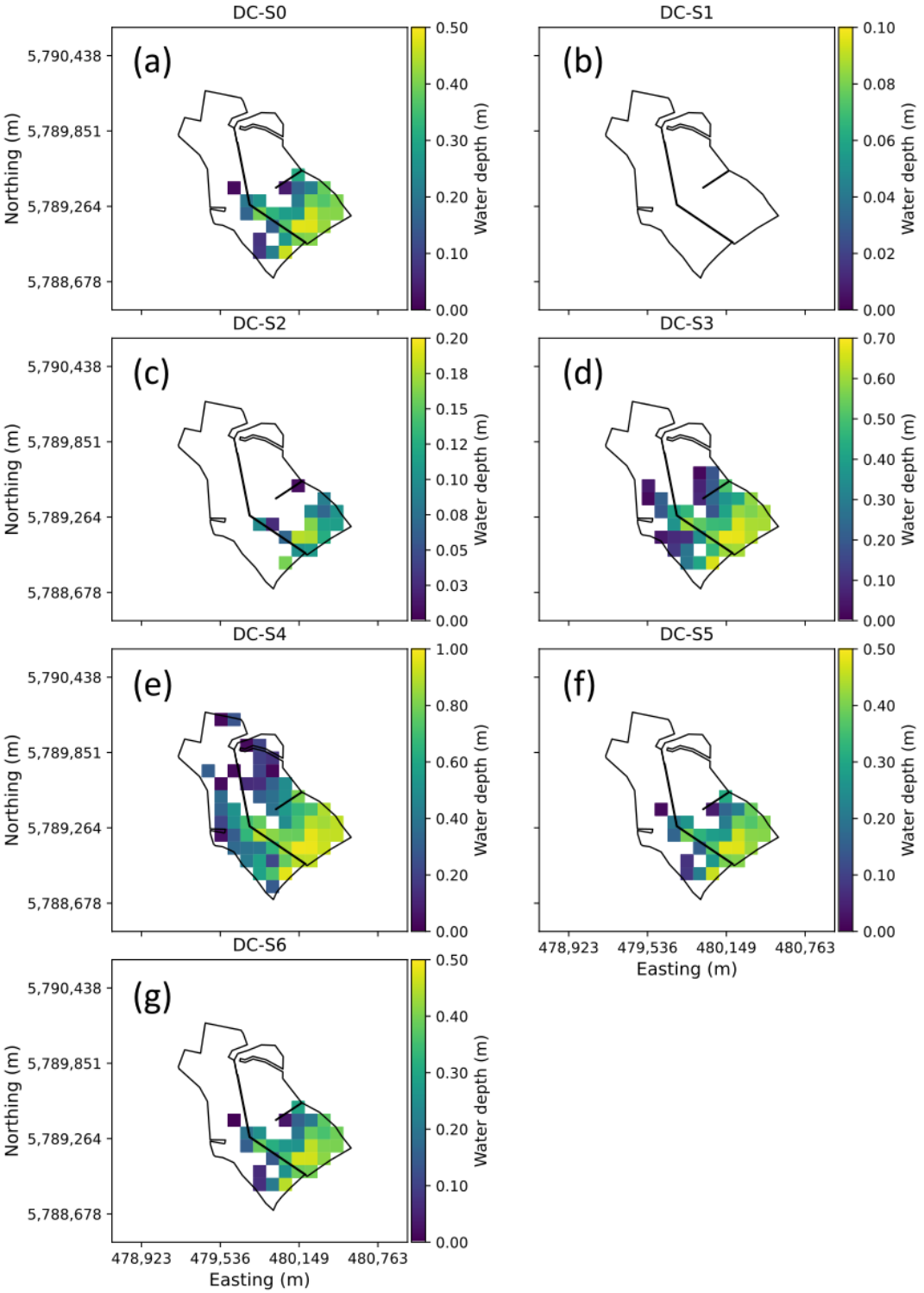

Figure D46. Inundation area of proposed DC wetland in November 2020 under base model and six scenarios: (a) Base model (DC-S0), (b) DC-S1, (c) DC-S2, (d) DC-S3, (e) DC-S4, (f) DC-S5, and (g) DC-S6. Each subplot illustrates the water depth distribution for the respective scenario.